



**Universiteit  
Leiden**  
The Netherlands

## **Aged human osteochondral explants as biomimetic osteoarthritis model: towards a druggable target in osteoarthritis**

Houtman, E.

### **Citation**

Houtman, E. (2022, October 12). *Aged human osteochondral explants as biomimetic osteoarthritis model: towards a druggable target in osteoarthritis*. Retrieved from <https://hdl.handle.net/1887/3480151>

Version: Publisher's Version

License: [Licence agreement concerning inclusion of doctoral thesis in the Institutional Repository of the University of Leiden](#)

Downloaded from: <https://hdl.handle.net/1887/3480151>

**Note:** To cite this publication please use the final published version (if applicable).

**Aged human osteochondral explants as  
biomimetic osteoarthritis model:**  
towards a druggable target in osteoarthritis

Evelyn Houtman

**Aged human osteochondral explants as biomimetic osteoarthritis model:  
towards a druggable target in osteoarthritis**

E. Houtman, MSc

PhD thesis with summary in Dutch

ISBN: 978-94-6458-543-8

© 2022 Evelyn Houtman

Copyright of each chapter is with the publisher of the journal in which the work was published. No parts of this thesis may be reproduced, stored in a retrieval system or transmitted in any form or by any means, without the permission of the author, or when appropriate, of the publisher of the represented published articles.

This research was financially supported by the Dutch Arthritis Society/ReumaNederland under grant agreement 15-4-401. In addition, this work was performed in the framework of the Medical Delta program Regenerative Medicine 4D:Generating complex tissues with stem cells and printing technology and Improving Mobility with Technology.

Medical Delta, the Nederlandse Vereniging voor Matrix Biologie (NVMB) and the LUMC are gratefully acknowledged for financial support for the printing costs of this thesis.

Cover design: Evelyn Houtman; cover designed using an image from Freepik.com (running person) and Protein network made with STRING ([string-db.org](http://string-db.org)).

Layout: Evelyn Houtman

Printing: Ridderprint | [www.ridderprint.nl](http://www.ridderprint.nl)

**Aged human osteochondral explants as  
biomimetic osteoarthritis model:  
towards a druggable target in osteoarthritis**

**Proefschrift**

ter verkrijging van  
de graad van doctor aan de Universiteit Leiden,  
op gezag van rector magnificus prof.dr.ir. H. Bijl,  
volgens besluit van het college voor promoties  
te verdedigen op woensdag 12 oktober 2022  
klokke 10.00 uur

door

**Evelyn Houtman**

geboren te New Plymouth, Nieuw-Zeeland  
in 1991

# Promotiecomissie

**Promotors** Prof. dr. I. Meulenbelt  
Prof. dr. R.G.H.H. Nelissen

**Co-promotor** Dr. Y.F.M. Ramos

## **Leden promotiecommissie**

Prof. dr. P.E. Slagboom

Prof. dr. R.J. Lories  
*Department of Development and Regeneration, KU Leuven*

Prof. dr. G. Kloppenburg

Prof. dr. J.B.J. van Meurs  
*Department of Internal Medicine and Orthopedics & Sports  
Medicine, Erasmus MC*

# Table of contents

<b>Chapter 1</b>	General introduction	<b>7</b>
<b>Chapter 2</b>	Human osteochondral explants: reliable biomimetic models to investigate disease mechanisms and develop personalized treatments for osteoarthritis	<b>35</b>
<b>Chapter 3</b>	Elucidating mechano-pathology of osteoarthritis: transcriptome-wide differences in mechanically stressed aged human cartilage explants	<b>63</b>
<b>Chapter 4</b>	Characterization of dynamic changes in matrix gla protein ( <i>MGP</i> ) gene expression as function of genetic risk alleles, osteoarthritis relevant stimuli, and the vitamin K inhibitor warfarin	<b>101</b>
<b>Chapter 5</b>	Inhibiting thyroid activation in aged human explants prevents mechanical induced detrimental signalling by mitigating metabolic processes	<b>127</b>
<b>Chapter 6</b>	General discussion and future perspectives	<b>155</b>
<b>Appendix</b>	Nederlandse samenvatting	<b>173</b>
	Curriculum Vitae	
	List of publications	
	Dankwoord	





# hapter 1

**General introduction**

## 1. Osteoarthritis

Osteoarthritis (OA) is a prevalent chronic age-related joint disease. Proper disease management is amongst others hampered by lack of insight into heterogeneity of disease pathophysiology [1]. As a result, OA is significantly decreasing quality of life while increasing healthcare costs and absenteeism from work [3]. It is estimated that 6.8% of Disability Adjusted Life Years (DALYs) worldwide can be accounted for by the burden of musculoskeletal disorders [4] and OA is ranked as the fifth disease contributing to DALYs in the Netherlands [5]. In 2019, the Netherlands counted almost 1.5 million OA cases (8.6% of population), responsible for 1.2 billion euro (1.4%) of total healthcare costs [2]. Prevalence of OA increases with age and affects more than 21% of men and 34% of women above 70 years (**Figure 1A**) and it is expected that cases of OA will keep rising in the coming years, due to the increasing ageing population (**Figure 1B**) [6].

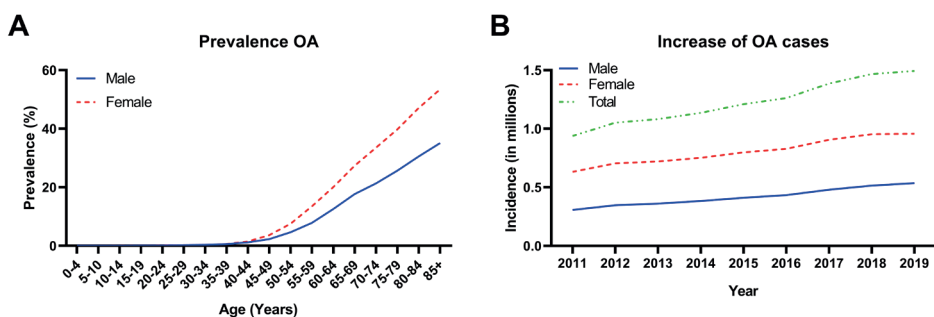


**Figure 1 | Prevalence and absolute cases of osteoarthritis reported by GPD in the Netherlands stratified by sex.** [A] Prevalence of OA per age groups in 2019. [B] Incidence of OA per year. Data from volkgezondheidszorg.info [2].

The OA disease process itself is characterized by gradual degradation of articular cartilage, thickening of the synovium, formation of bony spurs termed osteophytes and remodeling of the underlying subchondral bone (**Figure 2A**). Clinical symptoms of these processes include chronic pain, stiffness, joint instability, swelling and joint space narrowing [7]. In recent years it has become more apparent that OA is a disease of the whole joint, including the subchondral bone and synovium [8,9]. Pathologic changes in subchondral bone have even been found in some early-OA cases prior to cartilage degradation [9,10]. Currently, no treatment is available that stops disease progression and therefore patients are prescribed pain relief and physiotherapy to reduce symptoms until they are eligible to undergo a joint replacement surgery. While joint replacement are beneficial for patients, with revision rates of only 2-10% after 10 years [11,12], there is a considerable increase in revision rate in the 60 years and younger population [13]. Even more, results after revision surgery are worse than primary implant surgery in this younger population. Therefore a better understanding of OA pathophysiology is necessary to develop therapeutics that preferably target early disease triggers and/or processes and prevent this end-stage of OA necessitating arthroplasty surgery.

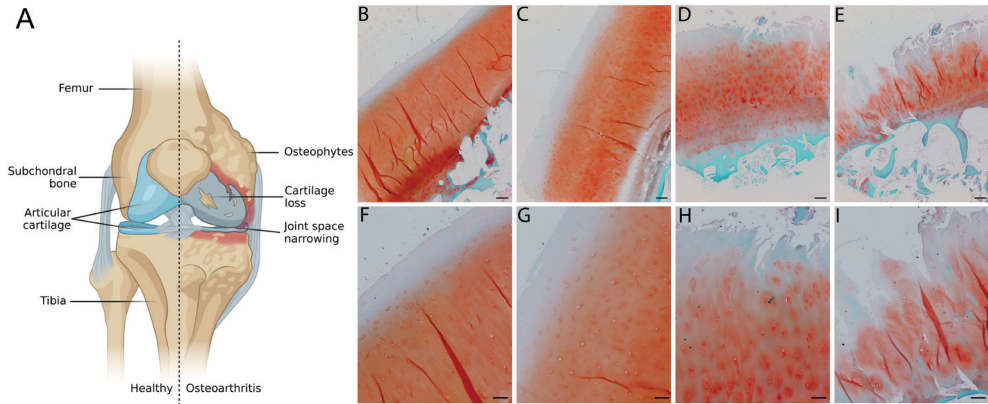


**Figure 2 | Schematic overview of OA symptoms and risk factors.** [A] Schematic drawing of a healthy knee (left) and a knee undergoing OA (right) created with BioRender.com. [B-I] Histological Safranin O staining for proteoglycans in articular cartilage taken from osteochondral explants from different areas of one knee joint shows the general cartilage degradation from mild OA (A) to severe OA (E) at 4x (B-E) and 10x (F-I) magnification. Black scale bar are 200 $\mu$ m (B-E) or 100  $\mu$ m (F-I).

## 2. Healthy joint tissues

Although OA is now commonly considered a whole-joint-disease, for long it primarily referred to the degeneration of articular cartilage. Articular cartilage is a highly specialized connective tissue that covers the contact surface of bones in joints and facilitates smooth movement. Cartilage is mainly composed of type 2 collagen, proteoglycans, chondrocytes and water, each with a specific function. The collagen fibres enable resistance to tensile stresses and transmission of mechanical loads, while proteoglycans and water enable osmotic pressure and elasticity to prevent friction. The sole cell type of cartilage, chondrocyte, makes up only 2-5% of cartilage volume and is retained in an extracellular matrix (ECM) environment lacking blood vessels, nerves and lymphatics [14]. Each chondrocyte creates and maintains its own pericellular matrix, preventing migration and limiting direct signal transduction via cell-to-cell interaction while enabling chondrocytes to respond to a variety of stimuli such as mechanical loads, hydrostatic pressures, inflammatory factors and growth factors. Low metabolic activity and limited potential to replicate and migrate contribute to limited intrinsic repair of articular cartilage in response to injury [15,16].

Directly underneath the articular cartilage is the subchondral bone, consisting of a thin cortical layer and a thicker trabecular bone layer. The subchondral bone exerts important shock-absorbing and nutritional functions for cartilage. As the subchondral bone is metabolically very active, structures are dynamically adapted to mechanical forces across the joint by bone remodelling [17,18]. Subchondral bone is formed via endochondral ossification at the secondary ossification centres of bone epiphyses during joint formation (**Figure 3A**). Articular cartilage is replaced by bone during endochondral ossification and starts with chondrocyte proliferation and multicellular cluster formation. Subsequently, these cells become hypertrophic, dramatically increasing their volume while simultaneously secreting ECM, which is eventually mineralized. Finally, hypertrophic chondrocytes undergo apoptosis and their ECM is partially broken down leaving space for entry of blood vessels, osteoclasts and osteoblasts to initiate ossification [19]. Some of the growth plate chondrocytes escape this process and populate the joint contact surface of bones to become and maintain articular

cartilage in a tightly controlled maturational arrested state. Important systemic factors regulating endochondral ossification are growth hormone (GH), Insulin-like growth factor (IGF) and thyroid hormone. GH and IGFs are potent stimulators of bone growth and both stimulate proliferation and initiate chondrocyte hypertrophy [20]. Locally produced IGF-I, induced by GH, is likely to play a more important role in chondrocytes than systemic IGF-I [21,22]. Active thyroid hormone, triiodothyronine (T<sub>3</sub>), induces expression of hypertrophic markers, such as alkaline phosphatase (ALPL), collagen X (COL10), as well as hypertrophic morphology and cartilage maturation [23-25].

### 3. OA pathophysiology

#### 3.1. Histopathology

During OA, cartilage undergoes drastic changes that can be observed by light microscopy. **Figure 2 B-I** gives a broad overview of these histological changes occurring from early OA to late OA. In early OA, some chondrocytes cluster and superficial surface fibrillations form (**Figure 2C** and **G**). This damage progresses to fissures and cracks that reach the middle zone, loss of proteoglycans and increased chondrocyte clustering (**Figure 2D** and **H**). In late OA, the fissures and cracks reach the deep zone, there is severe loss of cartilage, apoptosis of chondrocytes, duplication of the calcified layer of cartilage adjacent to the subchondral bone, termed the tidemark, and remodeling of subchondral bone (**Figure 2E** and **I**). This stage is followed by complete loss of cartilage and severe changes to the underlying bone. During OA histopathology chondrocytes start to proliferate, become enlarged and eventually go into apoptosis, resembling growth plate chondrocytes undergoing endochondral ossification (**Figure 3**) [26-28]. To better classify these histological changes several grading systems for OA were developed. For example, Mankin et al [29] developed a histological grading system that scores from 0-14, based on architectural cartilage surface, cellular, proteoglycan content and tidemark changes and is often referred to as Histological-Histochemical Grading System (HHGS). Over the years several other grading systems for *in vitro* or *in vivo* OA were generated, however a modified version of the Mankin score is still one of the most well-known and validated grading systems [30].

#### 3.2 Molecular pathology

Deregulated signalling pathways in OA have been characterized by comparing genome-wide differential expression differences between preserved versus end-stage lesioned OA cartilage [31] and subchondral bone [32]. These studies revealed that OA pathology is marked by recuperation of growth plate signalling, cell adhesion, extracellular matrix organisation and skeletal system development, characterized by deregulated expression of, among others, genes involved in endochondral ossification: *BMP3*, *MGP* and *FRZB*. Similar as during endochondral ossification, OA chondrocytes start proliferating and differentiate into hypertrophic chondrocytes, accompanied by expression of ossification related genes such as alkaline phosphatase (*ALPL*), collagen X (*COL10A1*), runt-related transcription factor 2 (*RUNX2*) and matrix metalloproteinase 13 (*MMP13*), resulting in calcium crystal deposition and apoptotic chondrocyte death in cartilage (**Figure 3B**) [27,28,33-35]. In addition, two genome-wide differential expression studies have highlighted inherent differences in preserved OA cartilage

gene expression patterns between individuals using unsupervised clustering, designating clear subtypes of OA [36,37]. Both studies identified two distinct groups of OA patients, independent of joint site, with a considerable overlap (45%) of significant differentially expressed genes between the two clusters [36]. Strikingly, one group was marked by increased expression of non-chondrogenic genes involved in mechanoreceptors, such as calcium signaling (KCNN3), ion channels (TRPV4) and cytoskeletal organizers (ACTA2). The study by Coutinho et al [36] combined their transcriptomic data with radiographic OA data and determined that the non-chondrogenic group had higher joint space narrowing (JSN) scores and lower osteophyte (OP) scores. These results suggest that with respect to treatment modalities these subgroups of OA patients should be taken into account in the study setup. For example, IL-11 is much more upregulated during OA pathophysiology in one subgroup (FC=60) than in the other OA group (FC=19) and might therefore be a more attractive therapeutic target for the latter group. Likewise, some targets such as CCL2 may be more appropriate for the first OA subgroup.

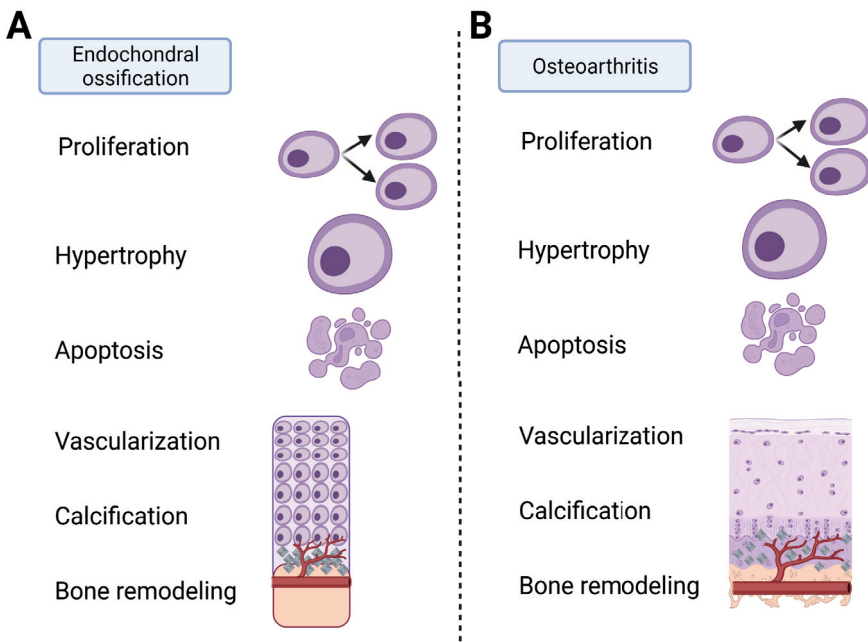


**Figure 3 | The overlap between processes occurring in endochondral ossification and osteoarthritis.** [A] During endochondral ossification stem cells differentiate into proliferating chondrocytes. This is followed by hypertrophy, terminal maturation, mineralization and eventually chondrocyte apoptosis to make space for bone. [B] A similar process is reiterated in osteoarthritis, where chondrocytes escape their resting state and start proliferating, become hypertrophic and eventually go into apoptosis. Created with BioRender.com.

As crosstalk between articular cartilage and subchondral bone is likely involved in OA pathophysiology, overlap of differentially expressed genes between cartilage and bone [32] was investigated and was enriched for processes related to the extracellular matrix, characterized by the expression of, among others, *FRZB*, *CCN4* (*WISP1*) and *GDF6*. Nonetheless, the preserved versus lesioned study design by definition captures end-stage pathophysiological OA disease processes and lacks information on early processes triggering cartilage to its diseased state. In contrast, disease-modifying OA drugs should preferably

target early OA disease triggers when irreversible damage of cartilage is not yet occurring. Therefore additional knowledge on the (early) effects of OA relevant stresses should be gathered from an appropriate model in response to OA-relevant triggers, such as mechanical stress, hypertrophy or inflammation.

#### 4. Risk factors for OA

Epidemiology studies have identified that OA has a multifactorial aetiology and results from an interplay between systemic and local risk factors. As shown in **Figure 4**, factors such as obesity, age, gender, repeated mechanical stress and joint injury play a role in OA onset [38]. Importance of these risk factors may vary per joint and stage of diseases. For example, obesity has been associated with both knee and hand OA, indicating that in addition to increased mechanical forces also aberrant metabolism in obesity play a role in OA risk [39,40].

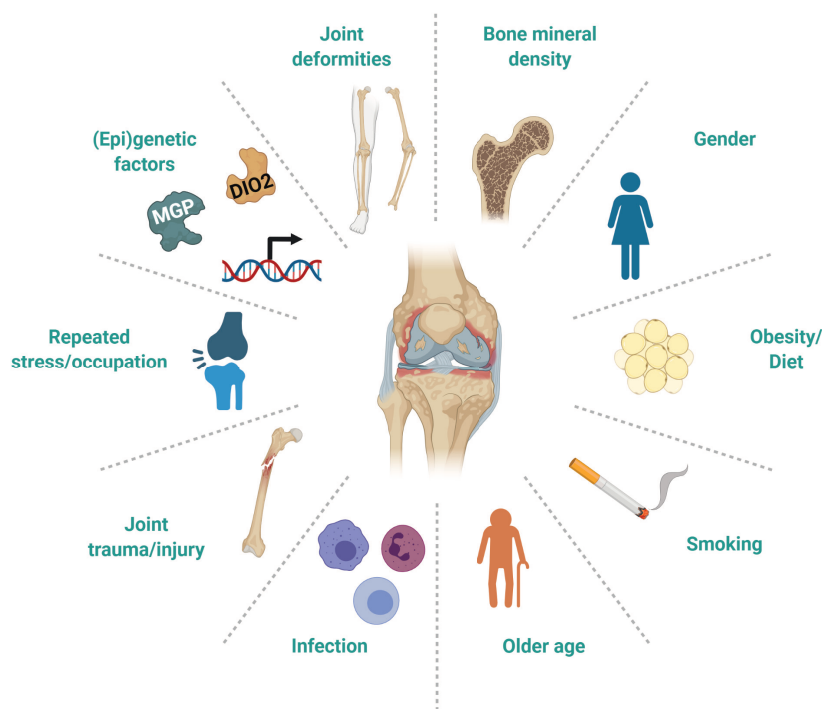


**Figure 4 | Risk factor for osteoarthritis.** The most common and well-studied risk factors for osteoarthritis. Figure created with BioRender.com.

##### 4.1 Age

The strongest risk factor for OA in all joints is age, likely due to a combination of cumulative exposure to risk factors and the natural changes of cartilage and chondrocytes that occur with ageing [41,42]. With ageing, the articular cartilage matrix changes in amount and composition, resulting in a stiffer environment correlating with biomechanical dysfunctions [43], prone to tensile fatigue [44]. One of the changes is the increased glycation of proteins

(AGEs) [45], likely due to slow turnover of ECM components, increasing cross-linking of collagen molecules resulting in a stiffer matrix susceptible to injury at lower impact loads [46]. Next to collagens, size of proteoglycan aggregates decreases likely due to proteolytic damage, greatly affects the permeability of cartilage [47]. Another highly prevalent change in aged cartilage is the deposition of calcium crystals, such as calcium pyrophosphate (CPP) and basic calcium phosphate (BCP) [48]. Consequently, these calcium crystals stimulate production of inflammatory proteins and matrix degrading enzymes, further contributing to onset and progression of cartilage degradation [49].

In addition to cartilage matrix changes, chondrocytes also undergo ageing-associated changes conferring OA risk. These include cell depletion [50,51] and impaired responses to extracellular stimuli [52,53], resulting in a changed gene expression, increased cell differentiation and cellular senescence [54]. This reduced responsiveness to stimuli such as growth factors contributes to an imbalance in cartilage homeostasis. For example, IGF-1, important for chondrocyte survival and matrix synthesis, induces a lower anabolic response [52,53]. This reduced response is likely partially due to increased production of insulin-like growth factor binding proteins (IGFBPs) [52]. Another explanation for the changed response to IGF-1 is the altered signaling observed in aged chondrocytes [55-57]. The increased cellular senescence found in aged cartilage might also contribute to its reduced anabolic response. Reactive oxygen species (ROS) production initiated by mechanical stress could be a large contributor of stress-induced chondrocyte senescence [58,59]. Since senescent cells typically produce pro-inflammatory cytokines and matrix degrading enzymes, they could greatly contribute to cartilage degradation [60]. Taken together, these age related changes in the cartilage matrix lead to a tissue with reduced ability to bear mechanical stress and make it more susceptible for degeneration.

#### **4.2 Mechanical stress**

Physiological mechanical loading is necessary to maintain a healthy state and function of articular cartilage and subchondral bone [61,62]. Both the proteoglycan content and collagen patterns are conditioned to local stresses to maintain functionality [63,64]. For example, the patellar surface of femoral condyles, an area regularly subject to high shear stress levels, has a thicker superficial zone and higher collagen content than the tibial plateaus, an area subjected to weightbearing loads and rich in proteoglycans [65,66]. Normal ranges of stresses in joints have been measured to be between 3 and 10 MPa, but maximum forces of up to 18 MPa are reached in the hip joint [67]. The frequency of these stresses during walking is in the magnitude of 1 Hz in humans [68] and cartilage height is displaced between 7% and 23% [69]. Higher peak forces are measured during sport activities, such as running, increasing strains up to 35% [70]. Physiologic levels of cyclical dynamic loading can stimulate anabolic and/or anti-inflammatory functions of chondrocytes [71-73], while hyper-physiologic levels of dynamic loading and injurious loading can induce damage via induction of catabolism in chondrocytes [74-76], and cellular damage, such as apoptosis and necrosis [77,78]. Local biomechanical factors (e.g. amount of joint loading, joint injury/trauma or joint deformity) influence risk of degenerative changes of articular cartilage due to wear and tear, especially when they are repetitive. Approximately 12% of the overall OA burden in hips, knees and ankles arises as a result of previous joint trauma [79]. Depending on the type of injury, OA development was estimated to be between 23% [80] and 44% [81] in people after an injury. In addition,

adequate response of chondrocytes to a load depends on parameters such as frequency, duration, history and age of cartilage. Interesting is also to mention the discrepancy between the degree of radiographic osteoarthritis and clinical symptoms experienced by patients, as was previously observed in a cohort of nearly 7000 Dutch patients [82] and later observed in several other populations [83].

Considering the previously discussed changes occurring during ageing, aged articular cartilage can likely withstand lesser and shorter mechanical compressions when compared to the more flexible younger tissues. However, inactivity of middle-aged joints has also been shown to be unbeneficial for joint health, suggesting that balanced active life style should be initiated from a certain age on [84]. Nonetheless, little knowledge exists on the inherent dysregulation of signaling pathways in human aged articular cartilage upon mechanical stress and there is a knowledge gap on which strains, speed and duration of mechanical stress on aged cartilage is considered beneficial or actually detrimental that needs to be addressed.

### **4.3 Genetic risk factors**

The genetic component of OA is estimated to be around 40%-60% [85,86], dependent on joint site. To gain more knowledge on inherent underlying processes in general OA pathophysiology, research groups have performed candidate and genome wide searches for genetic variants conferring risk of OA. OA has a complex genetic component in which many genetic variants with small effects sizes are expected to play a role in OA onset and progression [87-89]. Therefore, functional follow up is very important to confirm causality and has been performed for several genetic OA risk variants [90-92]. **Table 1** summarizes some of the most robust OA genetic risk variants to date, such as *DIO2*, *MGP* and *IL11*, for which successful and extensive functional follow up has been performed. These risk genes can be associated to one specific joint (*MGP*), or to multiple joints or patients with generalized OA (*DIO2*).

**Table 1 | Summary of some of the most interesting OA genetic risk variants for which functional follow up has been performed**

Gene	Risk SNP	Risk allele	AEI effect SNP	Expression in OA tissues <sup>*</sup>	In vitro FFU	In vivo FFU	Implication mutation
<i>ALDH1A2</i>	rs3204689 [93]	C	↓ ALDH1A2 [93,94]	↓ AC [94]	RNAi hACs [94]	<i>Aldh1a2</i> <sup>-/-</sup> mice [95]	Acts by decreasing <i>ALDH1A2</i>
<i>DIO2</i>	rs225014 [96]	C	↑ DIO2 [97]	↑ SB & AC ↑ AC compared to healthy [97]	Lentiviral overexpression in hBMSCs [90]	<i>Dio2</i> <sup>-/-</sup> mice [98], cartilage-specific <i>DIO2</i> overexpression in rats [99]	Acts by increasing <i>DIO2</i> , increasing active thyroid hormone levels
<i>DOT1L</i>	rs12982744 [100]	C	-	↑ in synovial tissue [101]	Inhibition of <i>DOT1L</i> [102]	Cartilage-specific <i>Dot1l</i> <sup>-/-</sup> in mice [102]	Abnormal histone modification
<i>GDF5</i>	rs143383 [103]	T	↓ GDF5 [104]	↑ AC [105]	EMSA, ChIP, RNAi, overexpression in different cell types [106]	Functional null mutation mice [107], heterozygous <i>Gdf5</i> <sup>h9/+</sup> mice [108]	Acts by decreasing <i>GDF5</i> expression
<i>IL11</i>	rs4252548 [109,110]	T	↓ IL11	↑ AC & SB	-	-	Acts by decreasing <i>IL11</i> expression
<i>MGP</i>	rs4764133/ rs1800801 [111]	T/T	↓ MGP [92,111]	↑ AC & SB	RNAi in hACs [92]	<i>Mgp</i> <sup>-/-</sup> mice [112]	Acts by decreasing <i>MGP</i> , likely necessary to inhibit mineralization
<i>SMAD3</i>	rs12901071 [113]/ rs12901372 [109,110]	A/C	No AEI	↓ AC	RNAi and overexpression in ATDC5 [114]	<i>Col2-Cre;Smad3</i> <sup>fl/fl</sup> mice [114], <i>Smad3</i> <sup>em8/em8</sup> [115]	Unknown mechanism of risk SNPs
<i>TNC</i>	rs2480930 [109]	A	↓ TNC	↑ AC	Addition of TNC in hACs [116] and explants [117]	TNC antibody and <i>Tnc</i> <sup>-/-</sup> [118], <i>Tnc</i> <sup>-/-</sup> [119]	Acts by decreasing <i>TNC</i> expression

<sup>\*</sup> Genome wide significant differential gene expression in lesioned compared to preserved articular cartilage (AC) [31] or subchondral bone (SB) [32], unless otherwise indicated. **Legend:** SNP= single nucleotide polymorphisms; AC=articular cartilage; SB=subchondral bone; AEI=Allelic expression imbalance; FFU=functional follow up; EMSA=electrophoretic mobility shift assays; ChIP=chromatin immunoprecipitation; RNAi=RNA interference; hACs=human articular chondrocytes; hBMSCs=human bone marrow stem cells.

## 5. Functional follow up

The investigation of an OA risk single nucleotide polymorphism (SNP) does not stop at its identification, but (functional) follow up is necessary to demonstrate causality. Freedman et al [120] have suggested a systematic strategy for the post-genome wide association studies (GWAS) functional follow-up to identify causality and the additional hurdles. For complex diseases such as OA, many SNPs from non-protein coding regions have been associated with disease risk. These trait-associated alleles likely exert their effects by changing transcription through different mechanisms. Often, multiple independently associated risk SNPs in a locus may be functionally linked to the disease and therefore it is important to first identify the causal allele. After the causal allele has been identified, knowledge on the regulatory landscape of the risk region can elude how risk alleles affect transcription. For example, if it is in a regulatory area such as a promotor, enhancer or silencer, altered transcription factor binding could change efficiency of transcriptional induction. As regulatory sequences are often very tissue-specific [121], this could explain why common susceptibility alleles often associate with a specific trait or disease. To identify which transcription factor binds to which DNA region, chromatin immunoprecipitation followed by sequencing (CHIP-Seq) can be performed. In addition, reporter gene assays, such as luciferase assays, can be used to provide evidence whether a SNP is localized in such a regulatory region. To connect SNPs to their target gene, the association between genotype and local and distant gene expression can be determined. After causality of an allele has been determined, a next step is to investigate if the SNP and/or gene affect tissues in appropriate *in vitro* or *in vivo* OA models. Examples of some well-studied OA risk SNPs for which functional follow up was performed are summarized in **Table 1**. Another approach for which these OA risks SNPs can be used for is to identify common pathways or mechanisms underlying OA pathophysiology. This knowledge can further increase our understanding of the onset and progression of OA.

### 5.1 Common underlying mechanisms in OA based on genomics

Large-scale GWASes have identified reproducible and highly significant OA risk SNPs in genes involved in OA aetiology. Functional follow-up studies have demonstrated that risk SNPs frequently modulate pathology by altering transcription of genes in *cis* in both bone and cartilage [91,94,97,122]. A striking overlap between many of these OA risk genes is their involvement in different processes vital in endochondral ossification (**Figure 5**). For example, *DOT1L*, *FRZB* and *TNC* are involved in the differentiation of stem cells to chondrocytes; *GDF5* and *BMP3* initiate hypertrophy in proliferating chondrocytes; *DIO2* and *MGP* are involved in terminal maturation and mineralization.

### 5.2 Follow up studies on SNPs function

With the increase of OA tissues being sequenced, generating large mRNA, miRNA and methylation datasets in combination with freely online expression databases, such as the Genotype-Tissue Expression (GTEx) Project [123], *in silico* functional follow up has become more readily available and allows for investigation of functional effects of intergenic and intronic variants. In addition, studies have already used such datasets to investigate the genome wide allelic expression imbalance of SNPs [124] and the epigenetic landscape [125] in

articular cartilage. Using these tools generates more insight into how OA risk SNPs could induce a life-long altered expression of a gene. To acquire knowledge on influences of the SNP on expression or stability of a transcript, researchers have measure expression and methylation fraction of genes in the vicinity of the SNP per genotype to determine expression quantitative trait loci (eQTL; **Figure 6A**), methylation quantitative trait loci (mQTL; **Figure 6B**) and allelic expression imbalance (AEI; **Figure 6C**). These SNPs can affect gene expression by, for example, influencing binding of transcription factors or influencing methylation fraction of a region.

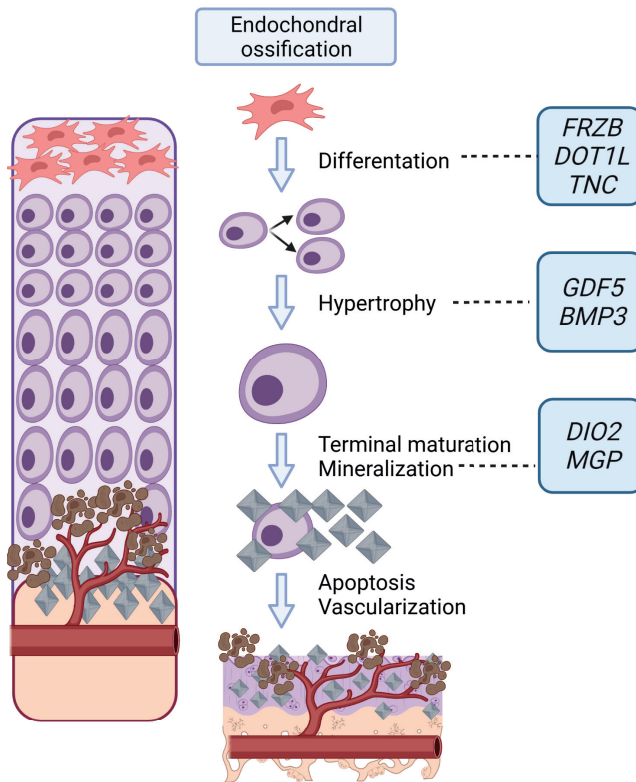


**Figure 5 | The overlap between processes occurring in osteoarthritis and endochondral ossification.** Many of the OA risk genes are involved in the different endochondral ossification steps. Some examples and the processes these genes are involved in are given. Figure created with BioRender.com.

A notable OA risk gene with strong evidence for allelic imbalance is Matrix Gla protein (MGP). A SNP in this gene was identified as a strong OA risk SNP for hand OA in a genome wide association study (GWAS) via rs4764133 [111] with proxy SNPs rs1800801 and rs4236 (**Table 1**) [126]. Identification was followed up by measuring AEI of rs1800801, showing its mechanism to be decreased expression of the OA conferring rs1800801-T allele relative to the rs1800801-C non-risk allele in a range of joint tissues [92,111]. The MGP protein regulates extracellular calcium levels via high affinity to its  $\gamma$ -carboxyglutamic acid (Gla) residues and inhibits calcification. Prior to identification of *MGP* as OA risk gene, *mgp* deficient mice were shown to have severe and lethal vascular calcifications in combination with abnormal calcification of growth place cartilage increasing premature bone mineralization resulting in

reduced bone mass [112,127]. As the OA risk allele leads to a reduced *MGP* gene expression [128] and increased vascular calcification [129], this would suggest simultaneous increased cartilage calcification and a reduced bone mineral density in carriers of the OA risk allele [112,128,130].

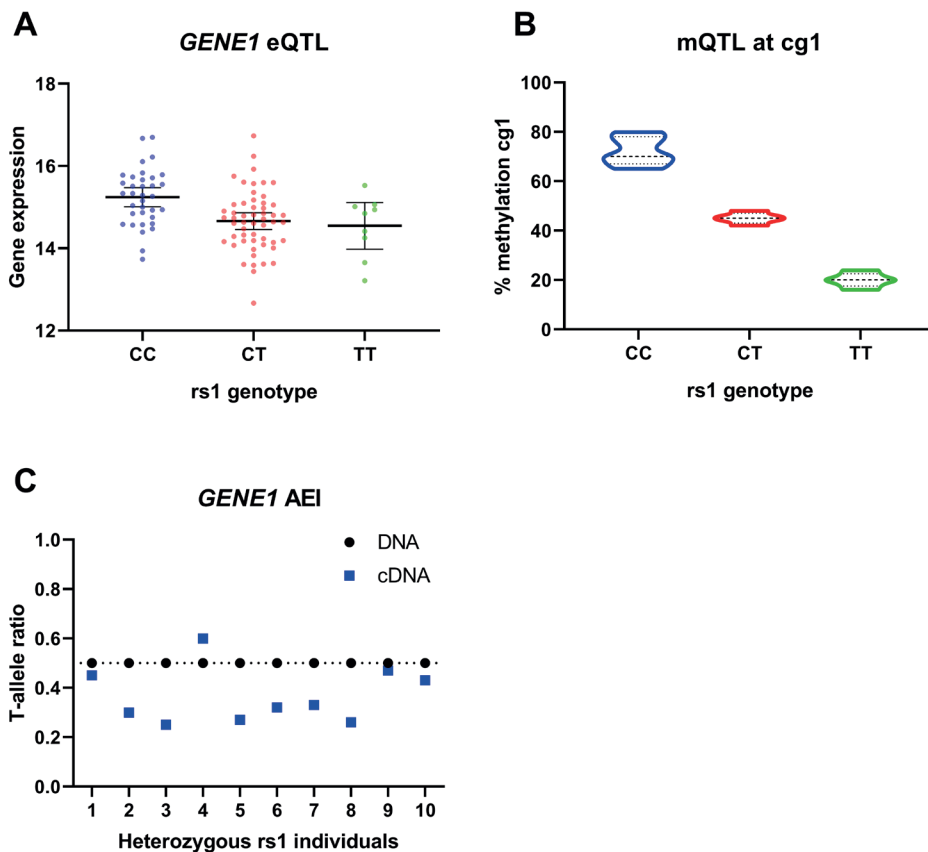


**Figure 6 | Functional follow up of the SNP Methods to investigate how risk SNP affects transcription.** [A] Comparing gene expression for the genotypes of a risk SNP. [B] Comparing methylation fraction of a cg site for the genotypes of a risk SNP. [C] T-allele ratio of cDNA for the risk SNP in comparison to the reference allele in heterozygous individuals. [D] Schematic representation of a cis allelic expression imbalance. Legend: eQTL=expression quantitative trait loci; mQTL=methylation quantitative trait loci, AEI=allelic expression imbalance; UTR=untranslated region.

### 5.3 Functional follow up in OA models

A major problem in the field of OA is the lack of appropriate *in vitro* and *in vivo* models for functional follow up of genetic risk variants and drug screening. In the current models used to investigate OA, the choice of cell type, species and culture method can greatly influence the results. Nevertheless, these models are crucial to advance research into the different aspects of OA pathophysiology and subsequent design and testing for safe drug development. **Table 2** summarizes the main advantages and disadvantages of the most commonly used OA models (**Figure 7**).

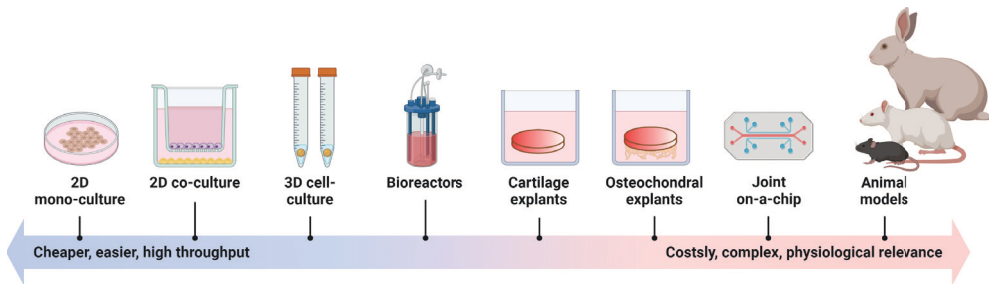


**Figure 7 | Most commonly used OA models.** Several models can be applied to investigate OA, ranging from more easy and cheap models such as 2D cell culture to more complex and expensive models such as animal models. Table 1 summarizes the advantages, disadvantages and applications of these models. Figure created with BioRender.com.

### 5.3.1 *In vitro* models

Established cell lines, easy and cheap to obtain and culture, have extensively been used to perform short term experiments. However, these cell lines are likely to have accumulated mutations and other stable modifications, increasing the possibility that they might not reflect a ‘normal’ chondrocyte environment. Therefore, the preferred cell source are primary chondrocytes that can be isolated from cartilage while maintaining their methylation profile [131] and can be used to investigate genetic alterations, such as overexpression or point mutations. To understand the consequences of an OA risk gene, overexpression or silencing of a gene can help determine if changes in its expression are vital for cartilage formation or maintenance. For example, AEI determined decreased *MGP* expression associated with the OA risk SNP rs1800801. To understand consequences of decreased *MGP* expression, small interfering RNA (siRNA) targeting *MGP* were transfected in monolayer primary human articular chondrocytes [92]. After 48 hours, *MGP* depletion resulted in altered expression of several cartilage markers, including the cartilage degrading enzymes *MMP13* and *ADAMTS4* and the ossification markers *COL1A1*, *ALPL*, *COL10A1* and *VEGFA*. However, a major downside of experiments with primary chondrocytes in monolayer is that they have limited proliferation capacity and are prone to change their phenotype into a fibroblastic-like cell type [132]. Therefore, such short-term experiments in an environment that does not completely encompass the cartilage environment and thus (expression) changes should be interpreted carefully.

Another component to consider in OA models is their highly specialized ECM. This ECM is likely very important in maintaining primary chondrocytes, as studies have observed a hypertrophic phenotype when cultured in monolayer that is resolved by 3D culture [132,133]. For 3D culture, cells can be pelleted by centrifugation or cultured in a biomimetic environment, such as a scaffold. Subsequently, stimulating chondrogenesis will enable cells to produce their own ECM. Some major advantages of these models are the cell-ECM interaction and the provided structural support. However, as the ECM needs to be produced, this model can be time consuming and only allows culture of one cell type. For example, the OA associated risk SNP rs225014 located near *DIO2*, for which increased expression was the likely culprit resulting from AEI and gene and protein levels investigation[97], was investigated in a 3D *in vitro* chondrogenesis model with human bone marrow derived mesenchymal stem cell (hBMSC). Lentiviral overexpression of *DIO2* in this model confirmed increased *DIO2* to

be unbeneficial for cartilage homeostasis, as observed by greatly reduced expression of articular cartilage genes (*COL2A1*, *ACAN* and *COL10A1*) and upregulation of hypertrophic and breakdown markers (*MMP13*, *ADAMTS5*, *RUNX2* and *EPAS1*) [90]. In addition, such (mature) 3D pellet cultures can be used to investigate the effects of stimulation or inhibition of a target. For example, 14 day old 3D pellets were treated with active thyroid hormone (T<sub>3</sub>) or iopanoic acid (IOP), to respectively simulate increased and decreased D2 enzyme functionality [90]. Another OA risk gene for which functional follow up was performed in 3D cultures is increased *WISP1* expression associated with decreased methylation via rs6982341 [134,135]. Addition of recombinant human *WISP1* to 3D *in vitro* pellet cultures from primary aged human chondrocytes resulted in reduced proteoglycan content, pellet size and matrix component production, suggesting that indeed increased *WISP1* levels are detrimental for cartilage [134].

### **5.3.2 *In vivo* models**

The most accurate reflection of the whole-joint are *in vivo* animal models. Animals, especially small animals such as mice and rats, have been extensively used for genetic manipulation and subsequently to investigate the effects of knockout or knock-in to model gene expression changes from conception to birth and during ageing. There are also techniques creating tissue-specific overexpression in animals, which can be very useful to investigate diseases. For example, in a forced running OA model, *Dio2*<sup>-/-</sup> mice did not show a different phenotype but these mice were protected from cartilage degradation when compared to their wild-type littermates [98]. In line with this, Nagase et al [99] observed that transgenic rats with cartilage-specific overexpression of human DIO2 (hD2Tg) had no articular cartilage defects, however, upon increasing the biomechanical burden by applying an injury-induced OA model, hD2Tg rats had increased cartilage damage when compared to their wild-type littermates.

It should be taken into account, however, that animal models can be difficult to manipulate and the shift towards the 3Rs on refining, reducing and replacing makes them less desirable. On another note, small animals such as mice are used because they are cheaper and easier to house, but due to their smaller size contain less material for biochemical assays. Another factor to consider is that animal joints are not fully translatable to the human situation given the different structure and biomechanical loading [136], and spontaneous OA is often absent. Currently, most experiments are performed in relative young animals subjected to a hyper-physiological trigger such as collagenase or DMM to initiate OA pathophysiology, likely not completely representing the slow progressive OA occurring in aged human tissues. Larger animals, such as bovine are likely more suited to study OA due to their larger joints and longer life-span, however they are also a lot more expensive and come with more ethical considerations. Therefore, careful conclusions should be taken from results obtained in OA animal studies and species, animal strains and OA triggers used should be critically reviewed prior to initiating investigation in human clinical studies.

### 5.3.3 *Ex vivo* models

As increasing evidence show crosstalk between multiple tissues to be involved in OA, systems such as co-cultures or osteochondral explants might be more suitable to study treatment modalities. The advantage that explants have over co-culture systems is that it retains chondrocytes in their natural 'aged' ECM, likely representing age-related joint tissues prone to enter the OA process upon disease-initiating cues. However, genetic manipulation studies cannot be performed in this model, limiting its purpose to investigation of OA relevant triggers and treatment modalities. The osteochondral explant model typically encompasses both the cartilage and bone compartments and therefore allows a readily investigation of the interplay between articular cartilage and the underlying subchondral bone. The finding that IL-1 $\beta$  treatment induced TNF- $\alpha$  production only in cartilage explants and not in osteochondral explants is an example highlighting that this interplay between tissues is important to take into account when investigating OA pathophysiology [137]. Most commonly used explant-based models thus far were often derived of bovine origin and applied a hyperphysiological perturbing factor of either a fierce inflammatory cytokines treatment [138-140] or mechanical loading [74,75,141] to induce detrimental signaling. Next to inflammation and mechanical loading, recapitulation of endochondral ossification and thereby hypertrophy is also thought to be one of the major mechanisms driving the processes in OA [142]. In cartilage explants, active thyroid hormone triiodothyronine (T<sub>3</sub>) induced expression of hypertrophic markers (ALPL, COL10), hypertrophic morphological changes and cartilage degradation and formation [143]. Even though the closest human OA-like model would be the use of human osteochondral explants obtained from macroscopically preserved areas of OA joints or cadavers, some limitations are that their number is limited, with high dependency on surgeries, ethical issues, heterogeneity between patients and difficulty to maintain tissues in long-term culture. Nevertheless, once the experimental set-up is achieved, these models can greatly benefit knowledge of OA pathophysiology and treatment modalities in the OA field. In addition, since ageing is the largest risk factor partially due to ECM and chondrocyte changes, using older tissues for research could be an important extra step to predict if a drug can be used to treat OA, thereby reducing the number of failing clinical studies. For example, treatment of IGF-1 greatly increased cartilage synthesis in calf explants [144]. Contrarily, in an aged human explant model, IGF-1 only slightly increased *COL2A1* and cell viability, and failed to abolish trauma-induced MMP13 secretion and type II collagen breakdown, likely due to desensitization to IGF-1 in aged tissue [145].

### 5.3.4 *DIO2*

An example of an OA susceptibility gene following many of these functional follow up steps is the previously mentioned deiodinase iodothyronine type II (D<sub>2</sub>) gene (*DIO2*). Genetic linkage studies identified an association of rs225014 (**Table 1**) located in the *DIO2* gene (*DIO2*), with generalized OA [96]. D<sub>2</sub> activates thyroid hormone intracellularly by converting the prohormone thyroxine (T<sub>4</sub>) into active triiodothyronine (T<sub>3</sub>). To determine the direction of effect, AEI was measured and a 30% increased expression of the OA risk associated rs225014-C allele, likely due to loss of epigenetic silencing, was identified as the underlying risk mechanism [90]. This was followed up by investigating the role of *DIO2* and D<sub>2</sub> in OA tissues. In human lesioned OA articular cartilage, a marked higher amount of *DIO2* expression and D<sub>2</sub> staining was observed relative to healthy cartilage [90,146]. However, it should be noted that the

still macroscopically healthy looking preserved OA cartilage also has these increased *DIO2* levels. Therefore it was hypothesised that high D2 was not enough for cartilage breakdown, but that an additional trigger, such as mechanical stress, is necessary to initiate OA [142]. *In vitro* functional follow up in a 3D *in vitro* chondrogenesis model of hBMCs confirmed that increased expression of *DIO2* was an OA risk by determining detrimental effects of lentiviral overexpression of D2 [90]. Furthermore, in the same 3D model after ECM was established, pellets were treated with T3 or IOP, to simulate increased and decreased D2 activity, respectively. The results found herein confirmed the hypothesis that increased D2 activity was detrimental for cartilage homeostasis, while reducing its activity was beneficial [90]. *In vivo* animal functional follow up experiments were performed in a forced running OA mouse model and an injury-induced OA rat model. *Dio2*<sup>-/-</sup> mice did not show a different phenotype but were protected from running induced cartilage damage when compared to their wild-type littermates [98]. In rats with cartilage-specific overexpression of human *DIO2* also no phenotypical differences were observed. However, upon increasing the biomechanical burden by applying an injury-induced OA model, hD2Tg rats had increased cartilage damage when compared to their wild-type littermates [99]. Before clinical studies should be initiated there is still a missing step in this line of work. Since species and age are such important factor in the mechanisms of cartilage response, a logical follow up step is to investigate if inhibition of D2 activity can prevent mechanical stress induced detrimental signaling in an aged human osteochondral explant model.

Table 2 | Advantages and disadvantages of the most commonly used models of osteoarthritis.

Type of model	Examples of applications	Advantages	Disadvantages	Examples of the application of the model
Monolayer culture	Cytokine/protein stimulation, osmotic pressure, genetic manipulation	Inexpensive, high throughput, equal exposure of cells, allows for preliminary investigation of mechanisms and compounds, easy to manipulate gene/protein expression	Not representative of normal chondrocyte environment, dedifferentiation, one cell type at a time, cell lines may have modifications	Mgp depletion [92], Aldh1a2 depletion [94], T3 or IGF-1 stimulation [147], osmotic pressure [148]
Co-culture	Cytokine/protein stimulation, osmotic pressure, genetic manipulation	Crosstalk between different cell types, easy to manipulate	Different conditions for each cell type, can result in altered phenotype when isolated, does not allow the natural 3D environment.	MSCs and ACs static [149,150] or with mechanical stress [151]
3D cell culture	Cytokine/protein stimulation, osmotic pressure, genetic manipulation, physical injury and loading regimens	Cell-ECM interaction, provides structural strength, easy to manipulate	One cell type at a time, slow proliferation rate, structural strength differs between material cultured in (Scaffold/hydrogel)	DIO2 overexpression, stimulation with T3 or IOP [90], WISP1 addition [134], osmotic pressure [152]
Explant based models	Cytokine/protein stimulation, osmotic pressure, physical injury and loading regimens	Cell-ECM interaction, natural ECM, simple, cheap and easy to produce	Difficult to culture long term, cell death at edge, limited number of cells, limited tissue available, inter-experimental variability	IGF-1 addition [144], TNC addition [117], mechanical injury [74,75,141,153], inflammatory [138-140], hypertrophy [143]
Animal models	Cytokine/protein stimulation, osmotic pressure, genetic manipulation, physical injury and loading regimens	Whole joint is investigated, possibility to investigate synovial	Costly, many animals necessary, ethical issues, huge variation between strains and species, anatomy, biomechanics and histology of joints differ from humans, natural occurrence of OA is uncommon in most species	Dio2-/- forced running [98], hD2 overexpression injury-induced OA model [99], destabilization of the medial meniscus (DMM), repeated tibial compression [154]

Different type of models used in OA are shown together with the variables that can be applied, their advantages, disadvantages and examples of some applications in the OA field. Legend: ECM = extracellular matrix; OA = osteoarthritis; Mgp = matrix gla protein; aldh1a2 = Aldehyde dehydrogenase 1 family member a2; T3 = triiodothyronine; DIO2 = Type II iodothyronine deiodinase; IOP = iopanoic acid; WISP1 = WNT1-Inducible-Signaling Pathway Protein 1; IGF-1 = insulin-like growth factor 1; TNC = tenascin; MSC = Mesenchymal stem cell; AC = articular chondrocyte

## 6. Current clinical trials

Another problem in the OA field is incorrect usage of OA models for drug testing prior to clinical trials. Next to the arising evidence of subtypes between OA patients that is often not taken into account when starting a clinical trial, drugs are often tested in non-human non-aged models subjected to a hyper-physiological trigger. Examples of trials that likely failed partially due to being based on unrepresentative models are given in **Table 3**. The most recent example is the failed phase II clinical trial of the ADAMTS<sub>5</sub>-inhibitor GLPG1972. Their evidence of functionality was mainly based on mouse cartilage explants subjected to high levels of IL-1 treatment [155], while IL-1 OA synovial fluid levels are variable between patients but much lower in comparison to the experimental condition [156,157]. As mentioned earlier, it is already known that aged chondrocytes respond differently to certain stimuli [52,53], showing the importance of including older tissues in the pre-clinical development. In addition, changing the focus of drug targets in OA towards those based on functional data of OA risk genes and their pathways could increase chances of developing effective disease modifying OA drugs, given that genetically supported drug targets have been shown to double clinical success rate [158,159]. Therefore we advocate that for clinical trials to have a higher chance of success, OA models that represent the human aged-chondrocyte environment should also be included and may even be prioritized in the pre-clinical screening and clinical trials should target drugs based on genetically supported data.

**Table 3 | Examples of clinical trials for OA therapies with discouraging findings that had promising results in pre-clinical *in vitro* and/or *in vivo* studies.**

Drug Name	Druggable target	Evidence underlying drug	Outcome clinical trial
GLPG1972/S201086	ADAMTS <sub>5</sub> -Inhibitor	Reduction of glycosaminoglycan release after interleukin-1 stimulation in mouse cartilage explants [155]. Reduced cartilage structural damage and bone sclerosis in mice and rat OA models [160]	Phase II clinical trial: No difference of cartilage thickness with placebo [NCT03595618]
PG-116800	MMP inhibitor	Reduced joint damage induced by iodoacetate injection into rat knees [161]	Terminated in phase II trial due to musculoskeletal toxicity [162]
Risedronate	Bisphosphonates	Reduced cartilage degeneration and no osteophyte formation in a rat anterior cruciate ligament transection (ACLT) model [163]; Inhibited bone resorption and some chondroprotective effects in a papain rabbit model [164]	phase III trial: No reduction of radiographic progression compared to placebo [164]
Anakinra	IL-1 receptor antagonist	Protected from surgery induced OA in rabbits [165] and dogs [166]	No clinical effect [167]
Adalimumab	Tumor necrosis factor-alpha	Inhibits progression in a number of arthritic diseases, including rheumatoid arthritis and psoriatic arthritis [168]	No effect in erosive hand OA patients on pain, synovitis or bone marrow lesions [169]
Tocilizumab	IL-6 receptor	Slowed the progression of experimental OA in mice [170,171]	No effect on pain relief in patients with hand OA and more adverse events than placebo [172]

Legend: ADAMTS<sub>5</sub>=A disintegrin and metalloproteinase with thrombospondin motifs 5; MMP=Matrix metalloproteinase; IL-1=Interleukin 1; IL-6=Interleukin 6; OA=osteoarthritis.

## 7. Outline of this thesis

This thesis aims to increase the understanding of human OA pathophysiology by developing reliable biomimetic *ex vivo* human osteochondral explant models and focussing on the role of injurious mechanical stress and interacting genetic factors for developing increasingly necessary treatment targets in these models. Human aged joint tissues used for the studies performed in this thesis were collected as part of the Research in Articular Osteoarthritis Cartilage (RAAK) biobank [173], containing patients that undergo a joint replacement surgery for symptomatic end-stage OA.

To add to existing knowledge of OA pathophysiological processes, in **chapter 2** aged human *ex vivo* osteochondral explants were subject to three OA relevant triggers, being inflammation, hypertrophy and injurious mechanical stress. Subsequently, a range of output measures were investigated to determine specific mechanisms of the different OA triggers.

In **chapter 3**, knowledge on early initiating processes occurring in mechano-pathology was generated by applied RNA-sequencing to cartilage of aged human osteochondral explants subjected to injurious mechanical stress.

To show that the human osteochondral explant model could also be used for genetic interaction studies, we investigated expression of the OA risk gene *MGP* in relation to rs1800801 genotypes in **chapter 4**. By combining information from RNA-sequencing datasets of cartilage and bone with OA-relevant triggers in cartilage and bone explants we investigated the role of *MGP* and vitamin K in OA.

Lastly, the *ex vivo* osteochondral explant model was exploited in **chapter 5** to determine the efficiency and effectivity of inhibition of the OA risk gene *DIO2* produced protein D2 by iopanoic acid (IOP) treatment either by burst or prolonged release by PLGA-PEG nanoparticles in preventing injurious mechanical induced stress.

## REFERENCES

1. Atkins GJ, Welldon KJ, Halbout P, et al. Strontium ranelate treatment of human primary osteoblasts promotes an osteocyte-like phenotype while eliciting an osteoprotegerin response. *Osteoporosis Int.* 2009;20(4):653-64.
2. Volksgezondheidszorg.info. <https://www.volksgezondheidszorg.info/onderwerp/artrose/cijfers-context/huidige-situatie>. *RIVM: Bilthoven, 09 June 2018.* 2021.
3. Woolf AD, Erwin J, March L. The need to address the burden of musculoskeletal conditions. *Best Pract Res Clin Rheumatol.* 2012;26(2):183-224.
4. Lozano R, Naghavi M, Foreman K, et al. Global and regional mortality from 235 causes of death for 20 age groups in 1990 and 2010: a systematic analysis for the Global Burden of Disease Study 2010. *Lancet.* 2012;380(9859):2095-128.
5. Volksgezondheidszorg.info. <https://www.volksgezondheidszorg.info/ranglijst/ranglijst-aandoeningen-op-basis-van-zieketelast-dalys>. *RIVM: Bilthoven, 09 June 2021.* 2021.
6. Christensen K, Doblhammer G, Rau R, et al. Ageing populations: the challenges ahead. *Lancet.* 2009;374(9696):1196-208.
7. Felson DT. Clinical practice. Osteoarthritis of the knee. *N Engl J Med.* 2006;354(8):841-8.
8. Loeuille D, Chary-Valckenaere I, Champigneulle J, et al. Macroscopic and microscopic features of synovial membrane inflammation in the osteoarthritic knee: correlating magnetic resonance imaging findings with disease severity. *Arthritis Rheum.* 2005;52(11):3492-501.
9. Thambyah A, Broom N. On new bone formation in the pre-osteoarthritic joint. *Osteoarthritis Cartilage.* 2009;17(4):456-63.
10. Zamli Z, Robson Brown K, Tarlton JF, et al. Subchondral bone plate thickening precedes chondrocyte apoptosis and cartilage degradation in spontaneous animal models of osteoarthritis. *Biomed Res Int.* 2014;2014:606870.
11. Gademan MGJ, Van Steenberghe LN, Cannegieter SC, et al. Population-based 10-year cumulative revision risks after hip and knee arthroplasty for osteoarthritis to inform patients in clinical practice: a competing risk analysis from the Dutch Arthroplasty Register. *Acta Orthop.* 2021;92(3):280-4.
12. Revision per component - LROI Report - Information on orthopaedic prosthesis procedures in the Netherlands. <https://www.lroi-report.nl/knee/survival/revision-per-component/>; <https://www.lroi-report.nl/hip/survival/revision-per-component/>. 2020; Accessed 2022.
13. Bayliss LE, Culliford D, Monk AP, et al. The effect of patient age at intervention on risk of implant revision after total replacement of the hip or knee: a population-based cohort study. *Lancet.* 2017;389(10077):1424-30.
14. Hunziker EB, Quinn TM, Hauselmann HJ. Quantitative structural organization of normal adult human articular cartilage. *Osteoarthritis Cartilage.* 2002;10(7):564-72.
15. Goldring MB. The role of the chondrocyte in osteoarthritis. *Arthritis Rheum.* 2000;43(9):1916-26.
16. Lapadula G, Iannone F. Metabolic activity of chondrocytes in human osteoarthritis as a result of cell-extracellular matrix interactions. *Semin Arthritis Rheum.* 2005;34(6 Suppl 2):9-12.
17. Walker WT, Kawcak CE, Hill AE. Medial femoral condyle morphometrics and subchondral bone density patterns in Thoroughbred racehorses. *Am J Vet Res.* 2013;74(5):691-9.
18. Goldring SR. Alterations in periarticular bone and cross talk between subchondral bone and articular cartilage in osteoarthritis. *Ther Adv Musculoskelet Dis.* 2012;4(4):249-58.
19. Mackie EJ, Ahmed YA, Tataarczuch L, et al. Endochondral ossification: how cartilage is converted into bone in the developing skeleton. *Int J Biochem Cell Biol.* 2008;40(1):46-62.
20. Hunziker EB, Wagner J, Zapf J. Differential effects of insulin-like growth factor I and growth hormone on developmental stages of rat growth plate chondrocytes in vivo. *J Clin Invest.* 1994;93(3):1078-86.
21. Nilsson A, Isgaard J, Lindahl A, et al. Regulation by growth hormone of number of chondrocytes containing IGF-I in rat growth plate. *Science.* 1986;233(4763):571-4.
22. Isaksson OG, Lindahl A, Nilsson A, et al. Mechanism of the stimulatory effect of growth hormone on longitudinal bone growth. *Endocr Rev.* 1987;8(4):426-38.
23. Ballock RT, Reddi AH. Thyroxine is the serum factor that regulates morphogenesis of columnar cartilage from isolated chondrocytes in chemically defined medium. *J Cell Biol.* 1994;126(5):1311-8.

24. Burch WM, Lebovitz HE. Triiodothyronine stimulates maturation of porcine growth-plate cartilage in vitro. *J Clin Invest.* 1982;70(3):496-504.
25. Fell HB, Mellanby E. The biological action of thyroxine on embryonic bones grown in tissue culture. *J Physiol.* 1955;127(2):427-47.
26. Dreier R. Hypertrophic differentiation of chondrocytes in osteoarthritis: the developmental aspect of degenerative joint disorders. *Arthritis Res Ther.* 2010;12(5):216.
27. Fuerst M, Bertrand J, Lammers L, et al. Calcification of articular cartilage in human osteoarthritis. *Arthritis Rheum.* 2009;60(9):2694-703.
28. Kuhn K, D'Lima DD, Hashimoto S, et al. Cell death in cartilage. *Osteoarthritis Cartilage.* 2004;12(1):1-16.
29. Mankin HJ, Dorfman H, Lippiello L, et al. Biochemical and metabolic abnormalities in articular cartilage from osteo-arthritic human hips. II. Correlation of morphology with biochemical and metabolic data. *J Bone Joint Surg Am.* 1971;53(3):523-37.
30. Rutgers M, van Pel MJ, Dhert WJ, et al. Evaluation of histological scoring systems for tissue-engineered, repaired and osteoarthritic cartilage. *Osteoarthritis Cartilage.* 2010;18(1):12-23.
31. Coutinho de Almeida R, Ramos YFM, Mahfouz A, et al. RNA sequencing data integration reveals an miRNA interactome of osteoarthritic cartilage. *Ann Rheum Dis.* 2019;78(2):270-7.
32. Tuerlings M, van Hoolwerff M, Houtman E, et al. RNA Sequencing Reveals Interacting Key Determinants of Osteoarthritis Acting in Subchondral Bone and Articular Cartilage: Identification of IL11 and CHADL as Attractive Treatment Targets. *Arthritis Rheumatol.* 2021;73(5):789-99.
33. Pfander D, Swoboda B, Kirsch T. Expression of early and late differentiation markers (proliferating cell nuclear antigen, syndecan-3, annexin VI, and alkaline phosphatase) by human osteoarthritic chondrocytes. *Am J Pathol.* 2001;159(5):1777-83.
34. von der Mark K, Kirsch T, Nerlich A, et al. Type X collagen synthesis in human osteoarthritic cartilage. Indication of chondrocyte hypertrophy. *Arthritis Rheum.* 1992;35(7):806-11.
35. Poole AR, Nelson F, Dahlberg L, et al. Proteolysis of the collagen fibril in osteoarthritis. *Biochem Soc Symp.* 2003(70):115-23.
36. Coutinho de Almeida R, Mahfouz A, Mei H, et al. Identification and characterization of two consistent osteoarthritis subtypes by transcriptome and clinical data integration. *Rheumatology (Oxford).* 2021;60(3):1166-75.
37. Soul J, Dunn SL, Anand S, et al. Stratification of knee osteoarthritis: two major patient subgroups identified by genome-wide expression analysis of articular cartilage. *Ann Rheum Dis.* 2018;77(3):423.
38. Haq I, Murphy E, Dacre J. Osteoarthritis. *Postgrad Med J.* 2003;79(933):377-83.
39. Carman WJ, Sowers M, Hawthorne VM, et al. Obesity as a risk factor for osteoarthritis of the hand and wrist: a prospective study. *Am J Epidemiol.* 1994;139(2):119-29.
40. Grotle M, Hagen KB, Natvig B, et al. Obesity and osteoarthritis in knee, hip and/or hand: an epidemiological study in the general population with 10 years follow-up. *BMC Musculoskelet Disord.* 2008;9:132.
41. Felson DT, Zhang Y. An update on the epidemiology of knee and hip osteoarthritis with a view to prevention. *Arthritis Rheum.* 1998;41(8):1343-55.
42. Felson DT, Lawrence RC, Dieppe PA, et al. Osteoarthritis: new insights. Part 1: the disease and its risk factors. *Ann Intern Med.* 2000;133(8):635-46.
43. Armstrong CG, Mow VC. Variations in the intrinsic mechanical properties of human articular cartilage with age, degeneration, and water content. *J Bone Joint Surg Am.* 1982;64(1):88-94.
44. Weightman B, Chappell DJ, Jenkins EA. A second study of tensile fatigue properties of human articular cartilage. *Ann Rheum Dis.* 1978;37(1):58-63.
45. Bank RA, Bayliss MT, Lafeber FP, et al. Ageing and zonal variation in post-translational modification of collagen in normal human articular cartilage. The age-related increase in non-enzymatic glycation affects biomechanical properties of cartilage. *Biochem J.* 1998;330 ( Pt 1):345-51.
46. Chen AC, Temple MM, Ng DM, et al. Induction of advanced glycation end products and alterations of the tensile properties of articular cartilage. *Arthritis Rheum.* 2002;46(12):3212-7.
47. Roughley PJ, Mort JS. The role of aggrecan in normal and osteoarthritic cartilage. *J Exp Orthop.* 2014;1(1):8.
48. Mitsuyama H, Healey RM, Terkeltaub RA, et al. Calcification of human articular knee cartilage is primarily an effect of aging rather than osteoarthritis. *Osteoarthritis Cartilage.* 2007;15(5):559-65.

49. Terkeltaub RA. What does cartilage calcification tell us about osteoarthritis? *J Rheumatol*. 2002;29(3):411-5.
50. Vignon E, Arlot M, Patricot LM, et al. The cell density of human femoral head cartilage. *Clin Orthop Relat Res*. 1976(121):303-8.
51. Mitrovic D, Quintero M, Stankovic A, et al. Cell density of adult human femoral condylar articular cartilage. Joints with normal and fibrillated surfaces. *Lab Invest*. 1983;49(3):309-16.
52. Martin JA, Ellerbroek SM, Buckwalter JA. Age-related decline in chondrocyte response to insulin-like growth factor-I: the role of growth factor binding proteins. *J Orthop Res*. 1997;15(4):491-8.
53. Loeser RF, Shanker G, Carlson CS, et al. Reduction in the chondrocyte response to insulin-like growth factor 1 in aging and osteoarthritis: studies in a non-human primate model of naturally occurring disease. *Arthritis Rheum*. 2000;43(9):2110-20.
54. Loeser RF. Aging and osteoarthritis: the role of chondrocyte senescence and aging changes in the cartilage matrix. *Osteoarthritis Cartilage*. 2009;17(8):971-9.
55. Boehm AK, Seth M, Mayr KG, et al. Hsp90 mediates insulin-like growth factor 1 and interleukin-1beta signaling in an age-dependent manner in equine articular chondrocytes. *Arthritis Rheum*. 2007;56(7):2335-43.
56. Fortier LA, Miller BJ. Signaling through the small G-protein Cdc42 is involved in insulin-like growth factor-I resistance in aging articular chondrocytes. *J Orthop Res*. 2006;24(8):1765-72.
57. Messai H, Duchossoy Y, Khatib AM, et al. Articular chondrocytes from aging rats respond poorly to insulin-like growth factor-1: an altered signaling pathway. *Mech Ageing Dev*. 2000;115(1-2):21-37.
58. Yamazaki K, Fukuda K, Matsukawa M, et al. Cyclic tensile stretch loaded on bovine chondrocytes causes depolymerization of hyaluronan: involvement of reactive oxygen species. *Arthritis Rheum*. 2003;48(11):3151-8.
59. Green DM, Noble PC, Ahuero JS, et al. Cellular events leading to chondrocyte death after cartilage impact injury. *Arthritis Rheum*. 2006;54(5):1509-17.
60. Freund A, Orjalo AV, Desprez PY, et al. Inflammatory networks during cellular senescence: causes and consequences. *Trends Mol Med*. 2010;16(5):238-46.
61. Oettmeier R, Arokoski J, Roth AJ, et al. Quantitative study of articular cartilage and subchondral bone remodeling in the knee joint of dogs after strenuous running training. *J Bone Miner Res*. 1992;7 Suppl 2:S419-24.
62. Arokoski J, Kiviranta I, Jurvelin J, et al. Long-distance running causes site-dependent decrease of cartilage glycosaminoglycan content in the knee joints of beagle dogs. *Arthritis Rheum*. 1993;36(10):1451-9.
63. Quinn TM, Hauselmann HJ, Shintani N, et al. Cell and matrix morphology in articular cartilage from adult human knee and ankle joints suggests depth-associated adaptations to biomechanical and anatomical roles. *Osteoarthritis Cartilage*. 2013;21(12):1904-12.
64. Seedholm BB, Takeda T, Tsubuku M, et al. Mechanical factors and patellofemoral osteoarthrosis. *Annals of the rheumatic diseases*. 1979;38(4):307-16.
65. Arokoski JP, Hyttinen MM, Helminen HJ, et al. Biomechanical and structural characteristics of canine femoral and tibial cartilage. *J Biomed Mater Res*. 1999;48(2):99-107.
66. Quinn TM, Hunziker EB, Hauselmann HJ. Variation of cell and matrix morphologies in articular cartilage among locations in the adult human knee. *Osteoarthritis Cartilage*. 2005;13(8):672-8.
67. Hodge WA, Fijan RS, Carlson KL, et al. Contact pressures in the human hip joint measured in vivo. *Proc Natl Acad Sci U S A*. 1986;83(9):2879-83.
68. Waters RL, Lunsford BR, Perry J, et al. Energy-speed relationship of walking: standard tables. *J Orthop Res*. 1988;6(2):215-22.
69. Liu F, Kozanek M, Hosseini A, et al. In vivo tibiofemoral cartilage deformation during the stance phase of gait. *J Biomech*. 2010;43(4):658-65.
70. Mosher TJ, Smith HE, Collins C, et al. Change in knee cartilage T2 at MR imaging after running: a feasibility study. *Radiology*. 2005;234(1):245-9.
71. Torzilli PA, Bhargava M, Chen CT. Mechanical Loading of Articular Cartilage Reduces IL-1-Induced Enzyme Expression. *Cartilage*. 2011;2(4):364-73.
72. Mauck RL, Nicoll SB, Seyhan SL, et al. Synergistic action of growth factors and dynamic loading for articular cartilage tissue engineering. *Tissue Eng*. 2003;9(4):597-611.
73. Bonassar LJ, Grodzinsky AJ, Frank EH, et al. The effect of dynamic compression on the response of articular cartilage to insulin-like growth factor-I. *J Orthop Res*. 2001;19(1):11-7.

74. Quinn TM, Grodzinsky AJ, Hunziker EB, et al. Effects of injurious compression on matrix turnover around individual cells in calf articular cartilage explants. *J Orthop Res.* 1998;16(4):490-9.
75. Chan PS, Schlueter AE, Coussens PM, et al. Gene expression profile of mechanically impacted bovine articular cartilage explants. *J Orthop Res.* 2005;23(5):1146-51.
76. Ashwell MS, O'Nan AT, Gonda MG, et al. Gene expression profiling of chondrocytes from a porcine impact injury model. *Osteoarthritis Cartilage.* 2008;16(8):936-46.
77. Natoli RM, Scott CC, Athanasiou KA. Temporal effects of impact on articular cartilage cell death, gene expression, matrix biochemistry, and biomechanics. *Ann Biomed Eng.* 2008;36(5):780-92.
78. Stolberg-Stolberg JA, Furman BD, Garrigues NW, et al. Effects of cartilage impact with and without fracture on chondrocyte viability and the release of inflammatory markers. *J Orthop Res.* 2013;31(8):1283-92.
79. Brown TD, Johnston RC, Saltzman CL, et al. Posttraumatic osteoarthritis: a first estimate of incidence, prevalence, and burden of disease. *J Orthop Trauma.* 2006;20(10):739-44.
80. Volpin G, Dowd GS, Stein H, et al. Degenerative arthritis after intra-articular fractures of the knee. Long-term results. *J Bone Joint Surg Br.* 1990;72(4):634-8.
81. Honkonen SE. Degenerative arthritis after tibial plateau fractures. *J Orthop Trauma.* 1995;9(4):273-7.
82. van Saase JL, van Romunde LK, Cats A, et al. Epidemiology of osteoarthritis: Zoetermeer survey. Comparison of radiological osteoarthritis in a Dutch population with that in 10 other populations. *Ann Rheum Dis.* 1989;48(4):271-80.
83. Bedson J, Croft PR. The discordance between clinical and radiographic knee osteoarthritis: a systematic search and summary of the literature. *BMC Musculoskelet Disord.* 2008;9:116.
84. Peeters G, Edwards KL, Brown WJ, et al. Potential Effect Modifiers of the Association Between Physical Activity Patterns and Joint Symptoms in Middle-Aged Women. *Arthritis Care Res (Hoboken).* 2018;70(7):1012-21.
85. Spector TD, Cicutini F, Baker J, et al. Genetic influences on osteoarthritis in women: a twin study. *BMJ.* 1996;312(7036):940-3.
86. Felson DT. Risk factors for osteoarthritis: understanding joint vulnerability. *Clin Orthop Relat Res.* 2004(427 Suppl):S16-21.
87. MacGregor AJ, Spector TD. Twins and the genetic architecture of osteoarthritis. *Rheumatology (Oxford).* 1999;38(7):583-8.
88. Panoutsopoulou K, Southam L, Elliott KS, et al. Insights into the genetic architecture of osteoarthritis from stage 1 of the arcOGEN study. *Annals of the rheumatic diseases.* 2011;70(5):864-7.
89. Boer CG, Hatzikotoulas K, Southam L, et al. Deciphering osteoarthritis genetics across 826,690 individuals from 9 populations. *Cell.* 2021;184(18):4784-818 e17.
90. Bomer N, den Hollander W, Ramos YF, et al. Underlying molecular mechanisms of DIO2 susceptibility in symptomatic osteoarthritis. *Ann Rheum Dis.* 2015;74(8):1571-9.
91. Reynard LN, Bui C, Canty-Laird EG, et al. Expression of the osteoarthritis-associated gene GDF5 is modulated epigenetically by DNA methylation. *Human Molecular Genetics.* 2011;20(17):3450-60.
92. Shepherd C, Reese AE, Reynard LN, et al. Expression analysis of the osteoarthritis genetic susceptibility mapping to the matrix Gla protein gene MGP. *Arthritis Res Ther.* 2019;21(1):149.
93. Styrkarsdottir U, Thorleifsson G, Helgadóttir HT, et al. Severe osteoarthritis of the hand associates with common variants within the ALDH1A2 gene and with rare variants at 1p31. *Nat Genet.* 2014;46(5):498-502.
94. Shepherd C, Zhu D, Skelton AJ, et al. Functional Characterization of the Osteoarthritis Genetic Risk Residing at ALDH1A2 Identifies rs12915901 as a Key Target Variant. *Arthritis & Rheumatology (Hoboken, NJ).* 2018;70(10):1577-87.
95. Niederreither K, Subbarayan V, Dolle P, et al. Embryonic retinoic acid synthesis is essential for early mouse post-implantation development. *Nat Genet.* 1999;21(4):444-8.
96. Meulenbelt I, Min JL, Bos S, et al. Identification of DIO2 as a new susceptibility locus for symptomatic osteoarthritis. *Hum Mol Genet.* 2008;17(12):1867-75.
97. Bos SD, Bovee JVMG, Duijnsveld BJ, et al. Increased type II deiodinase protein in OA-affected cartilage and allelic imbalance of OA risk polymorphism rs225014 at DIO2 in human OA joint tissues. *Annals of the rheumatic diseases.* 2012;71(7):1254-8.
98. Bomer N, Cornelis FM, Ramos YF, et al. The effect of forced exercise on knee joints in Dio2(-/-) mice: type II iodothyronine deiodinase-deficient mice are less prone to develop OA-like cartilage damage upon excessive mechanical stress. *Ann Rheum Dis.* 2016;75(3):571-7.

99. Nagase H, Nagasawa Y, Tachida Y, et al. Deiodinase 2 upregulation demonstrated in osteoarthritis patients cartilage causes cartilage destruction in tissue-specific transgenic rats. *Osteoarthritis and cartilage*. 2013;21(3):514-23.
100. Evangelou E, Valdes AM, Castano-Betancourt MC, et al. The DOT1L rs12982744 polymorphism is associated with osteoarthritis of the hip with genome-wide statistical significance in males. *Annals of the rheumatic diseases*. 2013;72(7):1264-5.
101. He D, Liu J, Hai Y, et al. Increased DOT1L in synovial biopsies of patients with OA and RA. *Clin Rheumatol*. 2018;37(5):1327-32.
102. Monteagudo S, Cornelis FMF, Aznar-Lopez C, et al. DOT1L safeguards cartilage homeostasis and protects against osteoarthritis. *Nat Commun*. 2017;8:15889.
103. Miyamoto Y, Mabuchi A, Shi D, et al. A functional polymorphism in the 5' UTR of GDF5 is associated with susceptibility to osteoarthritis. *Nat Genet*. 2007;39(4):529-33.
104. Egli RJ, Southam L, Wilkins JM, et al. Functional analysis of the osteoarthritis susceptibility-associated GDF5 regulatory polymorphism. *Arthritis Rheum*. 2009;60(7):2055-64.
105. Kania K, Colella F, Riemen AHK, et al. Regulation of Gdf5 expression in joint remodelling, repair and osteoarthritis. *Sci Rep*. 2020;10(1):157.
106. Syddall CM, Reynard LN, Young DA, et al. The identification of trans-acting factors that regulate the expression of GDF5 via the osteoarthritis susceptibility SNP rs143383. *PLoS Genet*. 2013;9(6):e1003557.
107. Harada M, Takahara M, Zhe P, et al. Developmental failure of the intra-articular ligaments in mice with absence of growth differentiation factor 5. *Osteoarthritis Cartilage*. 2007;15(4):468-74.
108. Daans M, Luyten FP, Lories RJ. GDF5 deficiency in mice is associated with instability-driven joint damage, gait and subchondral bone changes. *Annals of the rheumatic diseases*. 2011;70(1):208-13.
109. Styrkarsdottir U, Lund SH, Thorleifsson G, et al. Meta-analysis of Icelandic and UK data sets identifies missense variants in SMO, IL11, COL11A1 and 13 more new loci associated with osteoarthritis. *Nat Genet*. 2018;50(12):1681-7.
110. Tachmazidou I, Hatzikotoulas K, Southam L, et al. Identification of new therapeutic targets for osteoarthritis through genome-wide analyses of UK Biobank data. *Nat Genet*. 2019;51(2):230-6.
111. den Hollander W, Boer CG, Hart DJ, et al. Genome-wide association and functional studies identify a role for matrix Gla protein in osteoarthritis of the hand. *Ann Rheum Dis*. 2017;76(12):2046-53.
112. Luo G, Ducey P, McKee MD, et al. Spontaneous calcification of arteries and cartilage in mice lacking matrix GLA protein. *Nature*. 1997;386(6620):78-81.
113. Hackinger S, Trajanoska K, Styrkarsdottir U, et al. Evaluation of shared genetic aetiology between osteoarthritis and bone mineral density identifies SMAD3 as a novel osteoarthritis risk locus. *Hum Mol Genet*. 2017;26(19):3850-8.
114. Chen CG, Thuillier D, Chin EN, et al. Chondrocyte-intrinsic Smad3 represses Runx2-inducible matrix metalloproteinase 13 expression to maintain articular cartilage and prevent osteoarthritis. *Arthritis Rheum*. 2012;64(10):3278-89.
115. Yang X, Chen L, Xu X, et al. TGF-beta/Smad3 signals repress chondrocyte hypertrophic differentiation and are required for maintaining articular cartilage. *J Cell Biol*. 2001;153(1):35-46.
116. Nakoshi Y, Hasegawa M, Akeda K, et al. Distribution and role of tenascin-C in human osteoarthritic cartilage. *J Orthop Sci*. 2010;15(5):666-73.
117. Patel L, Sun W, Glasson SS, et al. Tenascin-C induces inflammatory mediators and matrix degradation in osteoarthritic cartilage. *BMC Musculoskelet Disord*. 2011;12:164.
118. Li Z, Chen S, Cui H, et al. Tenascin-C-mediated suppression of extracellular matrix adhesion force promotes enthesal new bone formation through activation of Hippo signalling in ankylosing spondylitis. *Annals of the rheumatic diseases*. 2021;80(7):891-902.
119. Gruber BL, Mienaltowski MJ, MacLeod JN, et al. Tenascin-C expression controls the maturation of articular cartilage in mice. *BMC Res Notes*. 2020;13(1):78.
120. Freedman ML, Monteiro AN, Gayther SA, et al. Principles for the post-GWAS functional characterization of cancer risk loci. *Nat Genet*. 2011;43(6):513-8.
121. Heintzman ND, Hon GC, Hawkins RD, et al. Histone modifications at human enhancers reflect global cell-type-specific gene expression. *Nature*. 2009;459(7243):108-12.
122. Loughlin J. Genetic contribution to osteoarthritis development: current state of evidence. *Current opinion in rheumatology*. 2015;27(3):284-8.

123. Consortium GT. The GTEx Consortium atlas of genetic regulatory effects across human tissues. *Science*. 2020;369(6509):1318-30.
124. den Hollander W, Pulyakhina I, Boer C, et al. Annotating Transcriptional Effects of Genetic Variants in Disease-Relevant Tissue: Transcriptome-Wide Allelic Imbalance in Osteoarthritic Cartilage. *Arthritis Rheumatol*. 2019;71(4):561-70.
125. den Hollander W, Ramos YF, Bomer N, et al. Transcriptional associations of osteoarthritis-mediated loss of epigenetic control in articular cartilage. *Arthritis & rheumatology (Hoboken, NJ)*. 2015;67(8):2108-16.
126. Misra D, Booth SL, Crosier MD, et al. Matrix Gla protein polymorphism, but not concentrations, is associated with radiographic hand osteoarthritis. *J Rheumatol*. 2011;38(9):1960-5.
127. Marulanda J, Gao C, Roman H, et al. Prevention of arterial calcification corrects the low bone mass phenotype in MGP-deficient mice. *Bone*. 2013;57(2):499-508.
128. Tunon-Le Poutel D, Cannata-Andia JB, Roman-Garcia P, et al. Association of matrix Gla protein gene functional polymorphisms with loss of bone mineral density and progression of aortic calcification. *Osteoporos Int*. 2014;25(4):1237-46.
129. Sheng K, Zhang P, Lin W, et al. Association of Matrix Gla protein gene (rs1800801, rs1800802, rs4236) polymorphism with vascular calcification and atherosclerotic disease: a meta-analysis. *Sci Rep*. 2017;7(1):8713.
130. Yagami K, Suh JY, Enomoto-Iwamoto M, et al. Matrix GLA protein is a developmental regulator of chondrocyte mineralization and, when constitutively expressed, blocks endochondral and intramembranous ossification in the limb. *J Cell Biol*. 1999;147(5):1097-108.
131. Bomer N, den Hollander W, Suchiman H, et al. Neo-cartilage engineered from primary chondrocytes is epigenetically similar to autologous cartilage, in contrast to using mesenchymal stem cells. *Osteoarthritis Cartilage*. 2016;24(8):1423-30.
132. Goldring MB. Human chondrocyte cultures as models of cartilage-specific gene regulation. *Methods Mol Med*. 2005;107:69-95.
133. Caron MM, Emans PJ, Coolsen MM, et al. Redifferentiation of dedifferentiated human articular chondrocytes: comparison of 2D and 3D cultures. *Osteoarthritis Cartilage*. 2012;20(10):1170-8.
134. van den Bosch MHJ, Ramos YFM, den Hollander W, et al. Increased WISP1 expression in human osteoarthritic articular cartilage is epigenetically regulated and decreases cartilage matrix production. *Rheumatology (Oxford)*. 2019;58(6):1065-74.
135. Urano T, Narusawa K, Shiraki M, et al. Association of a single nucleotide polymorphism in the WISP1 gene with spinal osteoarthritis in postmenopausal Japanese women. *J Bone Miner Metab*. 2007;25(4):253-8.
136. Proffen BL, McElfresh M, Fleming BC, et al. A comparative anatomical study of the human knee and six animal species. *Knee*. 2012;19(4):493-9.
137. Byron CR, Trahan RA. Comparison of the Effects of Interleukin-1 on Equine Articular Cartilage Explants and Cocultures of Osteochondral and Synovial Explants. *Front Vet Sci*. 2017;4:152.
138. Bird JL, Wells T, Platt D, et al. IL-1 beta induces the degradation of equine articular cartilage by a mechanism that is not mediated by nitric oxide. *Biochem Biophys Res Commun*. 1997;238(1):81-5.
139. Clutterbuck AL, Mobasheri A, Shakibaei M, et al. Interleukin-1beta-induced extracellular matrix degradation and glycosaminoglycan release is inhibited by curcumin in an explant model of cartilage inflammation. *Ann NY Acad Sci*. 2009;1171:428-35.
140. Geurts J, Juric D, Muller M, et al. Novel Ex Vivo Human Osteochondral Explant Model of Knee and Spine Osteoarthritis Enables Assessment of Inflammatory and Drug Treatment Responses. *Int J Mol Sci*. 2018;19(5):1314.
141. Kurz B, Jin M, Patwari P, et al. Biosynthetic response and mechanical properties of articular cartilage after injurious compression. *J Orthop Res*. 2001;19(6):1140-6.
142. Bomer N, den Hollander W, Ramos YF, et al. Translating genomics into mechanisms of disease: Osteoarthritis. *Best Pract Res Clin Rheumatol*. 2015;29(6):683-91.
143. Chen-An P, Andreassen KV, Henriksen K, et al. Investigation of chondrocyte hypertrophy and cartilage calcification in a full-depth articular cartilage explants model. *Rheumatol Int*. 2013;33(2):401-11.
144. Sah RL, Chen AC, Grodzinsky AJ, et al. Differential effects of bFGF and IGF-I on matrix metabolism in calf and adult bovine cartilage explants. *Arch Biochem Biophys*. 1994;308(1):137-47.
145. Riegger J, Joos H, Palm HG, et al. Striking a new path in reducing cartilage breakdown: combination of antioxidative therapy and chondroanabolic stimulation after blunt cartilage trauma. *J Cell Mol Med*. 2018;22(1):77-88.
146. Karlsson C, Dehne T, Lindahl A, et al. Genome-wide expression profiling reveals new candidate genes associated with osteoarthritis. *Osteoarthritis Cartilage*. 2010;18(4):581-92.

147. Ohlsson C, Nilsson A, Isaksson O, et al. Effects of tri-iodothyronine and insulin-like growth factor-I (IGF-I) on alkaline phosphatase activity, [3H]thymidine incorporation and IGF-I receptor mRNA in cultured rat epiphyseal chondrocytes. *J Endocrinol.* 1992;135(1):115-23.
148. Nguyen TD, Oloyede A, Singh S, et al. Investigation of the Effects of Extracellular Osmotic Pressure on Morphology and Mechanical Properties of Individual Chondrocyte. *Cell Biochem Biophys.* 2016;74(2):229-40.
149. Yang YH, Lee AJ, Barabino GA. Coculture-driven mesenchymal stem cell-differentiated articular chondrocyte-like cells support neo-cartilage development. *Stem Cells Transl Med.* 2012;1(11):843-54.
150. Lettry V, Hosoya K, Takagi S, et al. Coculture of equine mesenchymal stem cells and mature equine articular chondrocytes results in improved chondrogenic differentiation of the stem cells. *Jpn J Vet Res.* 2010;58(1):5-15.
151. Abusharkh HA, Mallah AH, Amr MM, et al. Enhanced matrix production by cocultivated human stem cells and chondrocytes under concurrent mechanical strain. *In Vitro Cell Dev Biol Anim.* 2021;57(6):631-40.
152. Negoro K, Kobayashi S, Takeno K, et al. Effect of osmolarity on glycosaminoglycan production and cell metabolism of articular chondrocyte under three-dimensional culture system. *Clin Exp Rheumatol.* 2008;26(4):534-41.
153. Lee JH, Fitzgerald JB, Dimicco MA, et al. Mechanical injury of cartilage explants causes specific time-dependent changes in chondrocyte gene expression. *Arthritis Rheum.* 2005;52(8):2386-95.
154. Christiansen BA, Guilak F, Lockwood KA, et al. Non-invasive mouse models of post-traumatic osteoarthritis. *Osteoarthritis Cartilage.* 2015;23(10):1627-38.
155. Brebion F, Gosmini R, Deprez P, et al. Discovery of GLPG1972/S201086, a Potent, Selective, and Orally Bioavailable ADAMTS-5 Inhibitor for the Treatment of Osteoarthritis. *J Med Chem.* 2021;64(6):2937-52.
156. Kahle P, Saal JG, Schaudt K, et al. Determination of cytokines in synovial fluids: correlation with diagnosis and histomorphological characteristics of synovial tissue. *Annals of the rheumatic diseases.* 1992;51(6):731-4.
157. Westacott CI, Whicher JT, Barnes IC, et al. Synovial fluid concentration of five different cytokines in rheumatic diseases. *Annals of the rheumatic diseases.* 1990;49(9):676-81.
158. Nelson MR, Tipney H, Painter JL, et al. The support of human genetic evidence for approved drug indications. *Nat Genet.* 2015;47(8):856-60.
159. King EA, Davis JW, Degner JF. Are drug targets with genetic support twice as likely to be approved? Revised estimates of the impact of genetic support for drug mechanisms on the probability of drug approval. *PLoS Genet.* 2019;15(12):e1008489.
160. Clement-Lacroix P, Little CB, Smith MM, et al. Pharmacological characterization of GLPG1972/S201086, a potent and selective small-molecule inhibitor of ADAMTS5. *Osteoarthritis Cartilage.* 2021.
161. Guingamp C, Gegout-Pottier P, Philippe L, et al. Mono-iodoacetate-induced experimental osteoarthritis: a dose-response study of loss of mobility, morphology, and biochemistry. *Arthritis Rheum.* 1997;40(9):1670-9.
162. Krzeski P, Buckland-Wright C, Balint G, et al. Development of musculoskeletal toxicity without clear benefit after administration of PG-116800, a matrix metalloproteinase inhibitor, to patients with knee osteoarthritis: a randomized, 12-month, double-blind, placebo-controlled study. *Arthritis Res Ther.* 2007;9(5):R109.
163. Hayami T, Pickarski M, Wesolowski GA, et al. The role of subchondral bone remodeling in osteoarthritis: reduction of cartilage degeneration and prevention of osteophyte formation by alendronate in the rat anterior cruciate ligament transection model. *Arthritis Rheum.* 2004;50(4):1193-206.
164. Bingham CO, 3rd, Buckland-Wright JC, Garnero P, et al. Risedronate decreases biochemical markers of cartilage degradation but does not decrease symptoms or slow radiographic progression in patients with medial compartment osteoarthritis of the knee: results of the two-year multinational knee osteoarthritis structural arthritis study. *Arthritis Rheum.* 2006;54(11):3494-507.
165. Fernandes J, Tardif G, Martel-Pelletier J, et al. In vivo transfer of interleukin-1 receptor antagonist gene in osteoarthritic rabbit knee joints: prevention of osteoarthritis progression. *Am J Pathol.* 1999;154(4):1159-69.
166. Caron JP, Fernandes JC, Martel-Pelletier J, et al. Chondroprotective effect of intraarticular injections of interleukin-1 receptor antagonist in experimental osteoarthritis. Suppression of collagenase-1 expression. *Arthritis Rheum.* 1996;39(9):1535-44.
167. Chevalier X, Goupille P, Beaulieu AD, et al. Intraarticular injection of anakinra in osteoarthritis of the knee: a multicenter, randomized, double-blind, placebo-controlled study. *Arthritis Rheum.* 2009;61(3):344-52.

168. Poddubnyy D, Rudwaleit M. Efficacy and safety of adalimumab treatment in patients with rheumatoid arthritis, ankylosing spondylitis and psoriatic arthritis. *Expert Opin Drug Saf.* 2011;10(4):655-73.
169. Aitken D, Laslett LL, Pan F, et al. A randomised double-blind placebo-controlled crossover trial of HUMira (adalimumab) for erosive hand Osteoarthritis - the HUMOR trial. *Osteoarthritis Cartilage.* 2018;26(7):880-7.
170. Latourte A, Cherifi C, Maillot J, et al. Systemic inhibition of IL-6/Stat3 signalling protects against experimental osteoarthritis. *Annals of the rheumatic diseases.* 2017;76(4):748-55.
171. Ansari MY, Khan NM, Ahmad N, et al. Genetic Inactivation of ZCCHC6 Suppresses Interleukin-6 Expression and Reduces the Severity of Experimental Osteoarthritis in Mice. *Arthritis & rheumatology (Hoboken, NJ).* 2019;71(4):583-93.
172. Richette P, Latourte A, Sellam J, et al. Efficacy of tocilizumab in patients with hand osteoarthritis: double blind, randomised, placebo-controlled, multicentre trial. *Annals of the rheumatic diseases.* 2020.
173. Ramos YF, den Hollander W, Bovee JV, et al. Genes involved in the osteoarthritis process identified through genome wide expression analysis in articular cartilage; the RAAK study. *PLoS One.* 2014;9(7):e103056.





# Chapter 2

## **Human osteochondral explants: reliable biomimetic models to investigate disease mechanisms and develop personalized treatments for Osteoarthritis**

Evelyn Houtman<sup>1</sup>, Marcella van Hoolwerff<sup>1</sup>, Nico Lakenberg<sup>1</sup>, Eka H.D. Suchiman<sup>1</sup>, Enrike van der Linden-van der Zwaag<sup>2</sup>, Rob G.H.H Nelissen<sup>2</sup>, Yolande F.M Ramos<sup>1</sup>, Ingrid Meulenbelt<sup>1</sup>

<sup>1</sup>*Molecular Epidemiology, Department of Biomedical Data Sciences, Leiden University Medical Center, Leiden, The Netherlands.*

<sup>2</sup>*Department of Orthopaedics, Leiden University Medical Center, Leiden, The Netherlands.*

**Published in:** *Rheumatology and Therapy*. 2021 Mar;8(1):499-515.  
doi: 10.1007/s40744-021-00287-y

## Abstract

### Introduction

Likely due to ignored heterogeneity in disease pathophysiology, osteoarthritis (OA) has become the most common disabling joint disease without effective disease modifying treatment causing a large social and economic burden. In this study we set out to explore responses of aged human osteochondral explants upon different OA-related perturbing triggers (inflammation, hypertrophy and mechanical stress) for future tailored biomimetic human models.

### Methods

Human osteochondral explants were treated with IL-1 $\beta$  (10 ng/ml) or triiodothyronine (T3; 10 nM) or received 65% strains of mechanical stress (65% MS). Changes in chondrocyte signalling were determined by expression levels of nine genes involved in catabolism, anabolism and hypertrophy. Breakdown of cartilage was measured by sulphated glycosaminoglycans (sGAGs) release, scoring histological changes (Mankin score) and mechanical properties of cartilage.

### Results

All three perturbations (IL-1 $\beta$ , T3 and 65% MS) resulted in upregulation of the catabolic genes *MMP13* and *EPAS1*. IL-1 $\beta$  abolished *COL2A1* and *ACAN* gene expression and increased cartilage degeneration, reflected by increased Mankin scores and sGAGs released. Treatment with T3 resulted in a high and significant upregulation of the hypertrophic markers *COL1A1*, *COL10A1*, and *ALPL*. However, 65% MS increased sGAG release and detrimentally altered mechanical properties of cartilage.

### Conclusion

We present consistent and specific output on three different triggers of OA. Perturbation with the pro-inflammatory IL-1 $\beta$  mainly induced catabolic chondrocyte signalling and cartilage breakdown, while T3 initiated expression of hypertrophic and mineralization markers. Mechanical stress at a strain of 65% induced catabolic chondrocyte signalling and changed cartilage matrix integrity. The major strength of our *ex vivo* models was that they considered aged, preserved, human cartilage of a heterogeneous OA patient population. As a result, the explants may reflect a reliable biomimetic model prone to OA onset allowing for development of different treatment modalities.

### Keywords

cartilage, osteochondral explants, osteoarthritis, human biomimetic model, mechanical stress, hypertrophy, inflammation.

## Introduction

Osteoarthritis (OA) is the most prevalent chronic age-related joint disease, causing pain and disability [1]. Likely due to ignored heterogeneity in disease pathophysiology, osteoarthritis has become the most common disabling joint disease without effective disease-modifying OA drugs (DMOADs) causing great social and economic burdens. As a result, OA significantly decreases quality of life while increasing absenteeism from work, and healthcare costs [2].

The OA disease process itself is characterized by unfavourable dynamic regulation of chondrocytes upon environmental perturbations such as age or mechanical stress, likely in interaction with genetic variants that cause subtle changes in expression of OA risk genes. The OA pathophysiological process itself has been linked to enhanced metabolic activity of articular chondrocytes, resembling growth plate chondrocytes undergoing endochondral ossification [3]. OA chondrocytes enter a cascade of proliferation and hypertrophic differentiation, accompanied by expression of genes such as alkaline phosphatase (*ALPL*), collagen X (*COL10A1*) and matrix metalloproteinase 13 (*MMP13*), resulting in apoptotic death and mineralization of cartilage [4-8]. Other hallmarks of the OA disease pathophysiology include new bone formation at the joint margins, limited inflammation and changes in subchondral bone structure. Together, these OA risk factors impose a persistent, yet variable, negative influence on joint tissue homeostasis throughout life, inevitably leading to progressive joint tissue destruction with age [9].

To address shortcomings of translational research and the challenges of translating data from *in vitro* models and a preclinical animal model to humans and increase efficiency of effective and safe drug development, while being compliant with the guiding principles of reduction, refinement and replacement of animal experiments, validated human models mimicking the different aspects of OA pathophysiology are required. Nonetheless, preclinical models thus far are limited to post-traumatic animal models or analyses of cell signalling in 2D and 3D *in vitro* cultures of neo-cartilage derived from human articular chondrocytes or stem cells. However, none of these models reliably recapitulate the osteochondral compartment, let alone faithfully representing age-related joint tissues prone to enter the OA process upon disease-initiating cues.

Osteochondral explant-based models allow investigation of both bone and cartilage compartments at the same time. The major advantage of such a model is that the cell response can be determined in their natural environment and they are relatively simple and easy to produce. Most commonly used explant-based models thus far were of bovine origin and applied a super-physiological perturbing factor of either a fierce inflammatory cytokines treatment [10-12] or cartilage loading [13-15]. Next to inflammation and mechanical loading, recapitulation of endochondral ossification and thereby hypertrophy is also thought to be one of the major mechanisms driving the processes in OA [16].

The aim of the current study is to explore and compare responses of aged human osteochondral explants triggered by three different physiological perturbing cues: inflammation (IL-1 $\beta$ ) [17,18], hypertrophy (triiodothyronine (T3)) [19,20] and mechanical stress (65% strain) [21].

We determined different output measures related to catabolic, anabolic and hypertrophic chondrocyte signalling, sGAGs released into the media, cartilage structure by histology and changes in mechanical properties. The presented models enable in-depth studies on how such cues interfering with homeostasis of aged cartilage contribute to human OA onset. They also allow for personalized testing of new treatment regimes in a validated human model including interaction of joint tissues and essential environmental cues.

## **Material and Methods**

### ***Osteochondral explant cultures***

Osteochondral explants were obtained from joints included in the Research in Articular Osteoarthritis Cartilage (RAAK) study. The RAAK study was approved by the medical ethics committee of the Leiden University Medical Center (Po8.239/P19.013) and informed consent was obtained from subjects. Osteochondral explants were harvested from the macroscopically preserved area of knee joints of human OA patients, within 2 hours of joint replacement surgery. Donor characteristics are summarized in **Table S1**. Osteochondral explants containing both cartilage and bone (8 mm diameter) were washed in sterile PBS and equilibrated in serum-free chondrogenic differentiation medium (DMEM (high glucose; Gibco, Bleiswijk), supplemented with ascorbic acid (50 µg/ml; Sigma-Aldrich; Zwijndrecht, The Netherlands), L-proline (40 µg/ml; Sigma-Aldrich), sodium pyruvate (100 µg/ml; Sigma-Aldrich), dexamethasone (0.1 µM; Sigma-Aldrich), ITS+ and antibiotics (100 U/ml penicillin; 100 µg/ml streptomycin; Gibco)) in a 5% (v/v) CO<sub>2</sub> incubator at 37°C.

### ***Application of physiological relevant cues***

Three days after extraction, explant tissue was treated with IL-1β (10 ng/ml) or triiodothyronine (T<sub>3</sub>, 10 nM). After 6 days, dynamic unconfined compression was applied to explant tissue using the Mach-1 mechanical testing system on 4 subsequent days (Biomomentum Inc., Laval, QC, Canada). Physiological loading at a strain of 30% or 65% was applied to explants at a frequency of 1 Hz. The thickness of the cartilage was measured prior to loading and used to determine the strain for each explant. Media of explants was refreshed every 3-4 days. To investigate lasting effects of treatment, explants were harvested 3 days after the last treatment. Cartilage and bone were separated using a scalpel, snap-frozen in liquid nitrogen and stored at -80 °C for RNA isolation.

### ***RNA isolation, Reverse Transcription and quantitative Real-Time PCR***

RNA was extracted by pulverizing the tissue using a Mixer mill 200 (Retch, Germany) and homogenizing in TRIzol reagent (Invitrogen, San Diego, CA). RNA was extracted with chloroform, precipitated with ethanol and purified using the RNeasy Mini Kit (Qiagen, GmbH, Hilden, Germany). Genomic DNA was removed by DNase (Qiagen, GmbH, Hilden, Germany) digestion and the quantity of RNA was assessed using a Nanodrop spectrophotometer (Thermo Fischer Scientific Inc., Wilmington, DE, USA). Synthesis of cDNA was performed using 200 ng of total mRNA with the First Strand cDNA Synthesis Kit (Roche Applied Science, Almere,

The Netherlands) according to the manufacturer's protocol. Gene expression was determined with the Roche Lightcycler 480 II (Roche Applied Science) using Fast Start Sybr Green Master mix (Roche Applied Science). Primer sequences are listed in **Table S2**.

### ***Sulphated glycosaminoglycan (sGAGs) measurement***

Sulphated glycosaminoglycans (sGAGs) concentration was measured with the photometric 1.9 dimethylene blue (DMMB; Sigma-Aldrich) dye method [22]. Shark chondroitin sulphate (Sigma-Aldrich) was used as reference standard. To measure concentrations, absorbance at 525 and 595 was measured in a microplate reader (Synergy HT; BioTek, Winooski, VT, USA).

### ***Histology***

Osteochondral explants were fixed in 4% formaldehyde and decalcified using EDTA (12.5%, pH=7.4), dehydrated with an automated tissue processing apparatus and embedded in paraffin. Tissue sections of 5  $\mu\text{m}$  were stained with haematoxylin and eosin (H&E) or toluidine blue (Sigma-Aldrich) and mounted with Pertex (Sigma-Aldrich). Quantification of OA related cartilage damage was scored according to Mankin *et al* [23].

### ***Mechanical properties***

The fibril-network-reinforced biphasic model of cartilage in unconfined compression was used to measure the mechanical properties of explants [24]. After a 10% precompression 5 subsequent ramps of 2% were performed and each ramp was allowed to continue until the relaxation rate was  $< 0.05$  N/min. The tensile stiffness of the fibril network ( $E_f$ ), equilibrium modulus ( $E_m$ ) and hydraulic permeability ( $k$ ) were determined using MACH-1 software (Biomomentum Inc., Laval, QC, Canada).

### ***Statistical analysis***

Statistics were performed for all data in IBM SPSS statistics 23. In the absence of perfect pairs, the significance of mean difference in gene expression between controls and treated explants was estimated by the generalized estimating equation (GEE) with robust variance estimators to account for donor effects. RT-PCR data were normalized using the housekeeping gene *SDHA*. We used *SDHA*, as this gene was previously identified as a stable housekeeping gene in cartilage and particularly not responsive to mechanical stress [25,26]. Fold changes were calculated according to the  $2^{-\Delta\Delta\text{CT}}$  method. Significance was declared at  $P < 0.05$ .

## Results

### Baseline characteristics of donors of the osteochondral explants

As shown in **Table S1**, age and BMI are comparable across donors in the three different perturbations applied; IL-1 $\beta$ , T3 and 65% mechanical stress (65% MS). Of note, IL-1 $\beta$  was applied by chance in explants from females only. Prior to applying our models we explored effects of 30% stress to osteochondral explants as compared to controls and IL-1 $\beta$  or T3 treatment. As shown in **Figure S1** and **Figure S2** and **Table S2** and **Table S3**, 30% mechanical stress as compared to controls had no significant effect on gene expression levels, Mankin score or sGAG concentrations (data not published). To enlarge our sample sizes for the remaining analysis, the 30% stressed control samples were pooled with controls of the IL-1 $\beta$  and T3 treated groups.

### Changes in chondrocyte signaling across the three models

As shown in **Table 1**, applying the three different perturbations (IL-1 $\beta$ , T3 and 65% MS) resulted in significant upregulation of the catabolic genes *MMP13* and *EPAS1* as compared to controls (**Figure 1**). Upregulation of *MMP13* (**Figure 1C**) was modest in response to T3 (FC=3.7;  $P=3.0 \times 10^{-3}$ ) relative to that with IL-1 $\beta$  (FC=12.7;  $P=3.6 \times 10^{-2}$ , **Figure 1A**) and 65% MS (FC=10.3;  $P=1.4 \times 10^{-2}$ , **Figure 1B**). Upregulation of *EPAS1* was highly significant in response to IL-1 $\beta$ , 65% MS and T3 treatment (FC=4.6;  $P=3.6 \times 10^{-2}$ , FC=1.8;  $P=1.8 \times 10^{-20}$  and FC=1.8,  $P=1.0 \times 10^{-3}$ , respectively **Figure 1**). Notable is the observed absence in expression changes of the aggrecanase *ADAMTS5* in all three perturbations (**Table 1** and **Figure 1**).

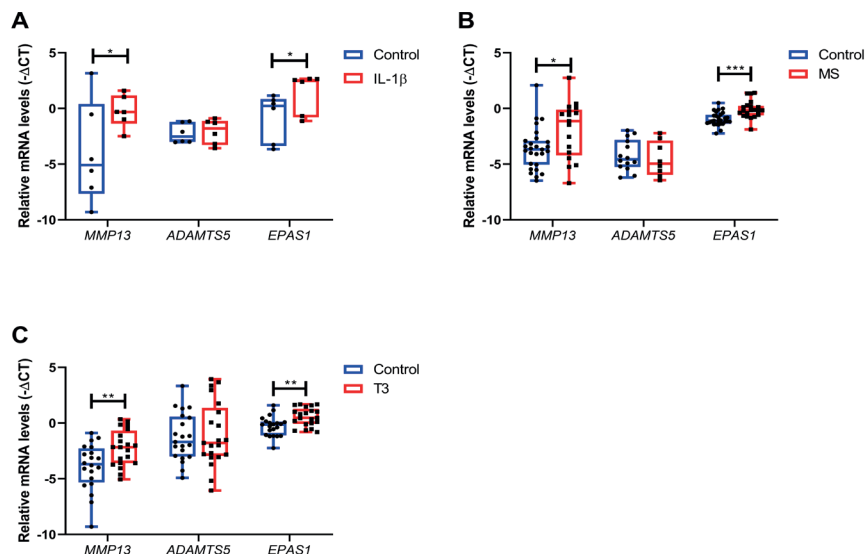


**Figure 1 | Gene expression of catabolic markers after treatment with IL-1 $\beta$ , mechanical stress (MS) or T3.** RT-PCR analysis of *MMP13*, *ADAMTS5* and *EPAS1* after [A] IL-1 $\beta$  (10ng/ml; n=6), [B] 65% MS (n=19-23) or [C] T3 (10nM; n=21) treatment. Data is presented in a boxplot depicting the median, lower and upper quartiles and each dot represents a single explant. P-values of mean differences in gene expression between controls and treated explants were estimated by generalized estimating equations (GEE) with robust variance estimators to account for donor effects. \* $P < 0.05$ , \*\* $P < 0.01$ , \*\*\* $P < 0.001$ .

Regarding the matrix genes known to be responsible for a substantial part of the matrix deposition, we showed that *COL2A1* and *ACAN* expression was almost absent in the IL-1 $\beta$  treated osteochondral explants with a FC=0.01;  $P=2.6\times 10^{-12}$  and FC=0.03;  $P=1.1\times 10^{-19}$ , respectively (**Figure 2A**). 65% MS resulted in a slight, non-significant, downregulation of *COL2A1* (FC=0.9;  $P=8.7\times 10^{-2}$ , **Figure 2B**) and no changes in *ACAN* expression. In contrast, treatment with T3 resulted in a highly significant upregulation of *COL2A1* (FC=3.5;  $P=2.4\times 10^{-10}$ , **Figure 2C**). As shown in **Table 1** and **Figure 3C**, treatment with T3 resulted in a high and significant upregulation of the hypertrophic markers *COL1A1* (FC=144.7;  $P=0.3\times 10^{-3}$ ), *COL10A1* (FC=5.0;  $P=6\times 10^{-3}$ ), and *ALPL* (FC=665.8  $P=7.4\times 10^{-9}$ ) compared to controls.

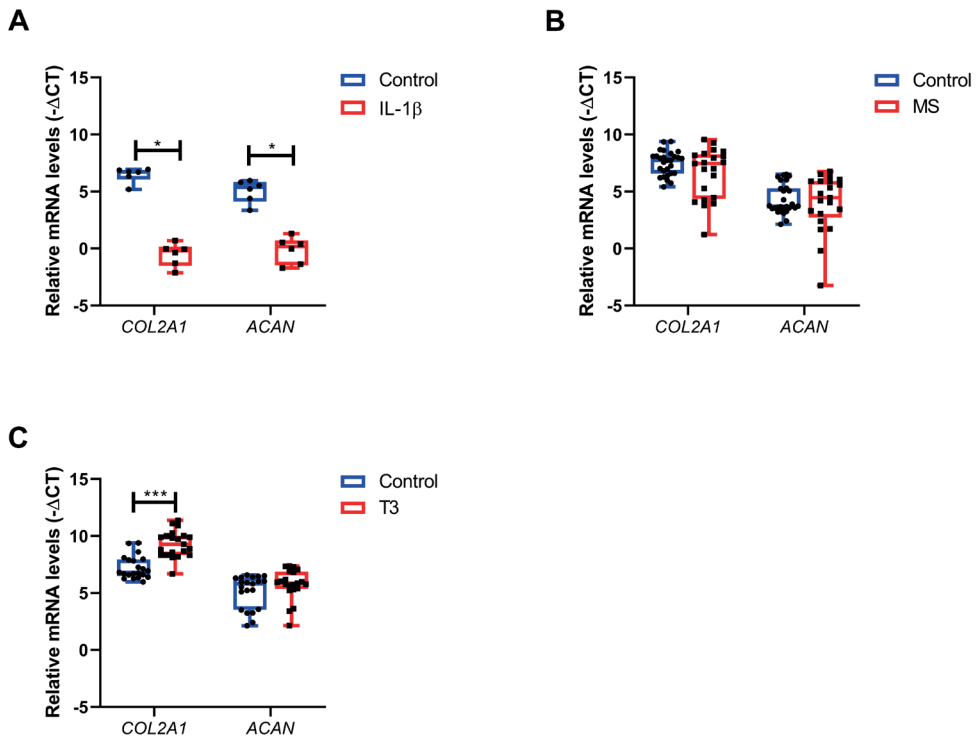


**Figure 2 | Gene expression of anabolic markers after treatment with IL-1 $\beta$ , mechanical stress (MS) or T3.** RT-PCR analysis of *COL2A1* and *ACAN* after **[A]** IL-1 $\beta$  (10ng/ml; n=6), **[B]** 65% MS (n=19-23) or **[C]** T3 (10nM; n=21) treatment. Data is presented in a boxplot depicting the median, lower and upper quartiles and each dot represents a single explant. P-values of mean differences in gene expression between controls and treated explants were estimated by generalized estimating equations (GEE) with robust variance estimators to account for donor effects. \* $P<0.05$ , \*\* $P<0.01$ , \*\*\* $P<0.001$ .

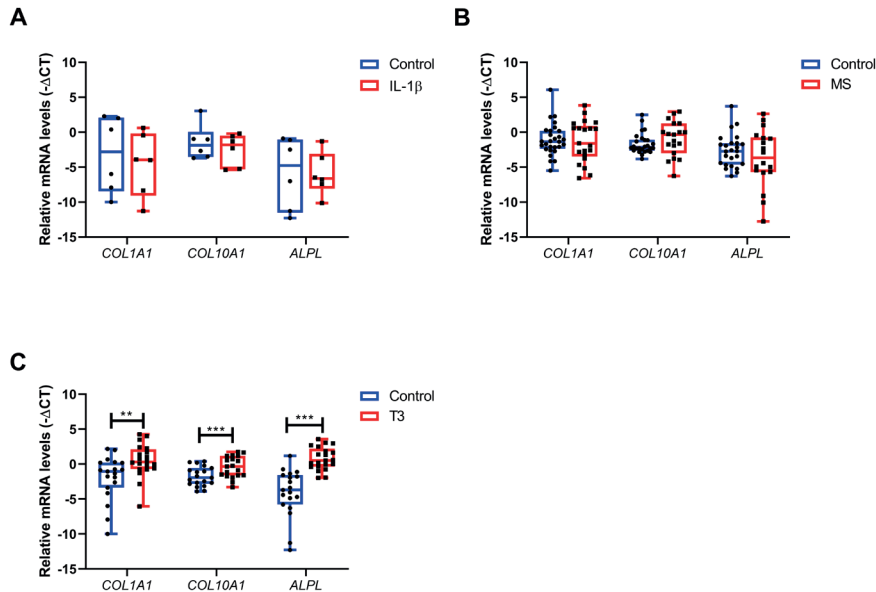


**Figure 3 | Gene expression of hypertrophic and mineralization markers after treatment with IL-1 $\beta$ , mechanical stress (MS) or T<sub>3</sub>.** RT-PCR analysis of COL1A1, COL10A1 and ALPL after [A] IL-1 $\beta$  (10ng/ml; n=6), [B] 65% MS (n=19-23) or [C] T<sub>3</sub> (10nM; n=21) treatment. Data is presented in a boxplot depicting the median, lower and upper quartiles and each dot represents a single explant. P-values of mean differences in gene expression between controls and treated explants were estimated by generalized estimating equations (GEE) with robust variance estimators to account for donor effects. \*P<0.05, \*\*P<0.01, \*\*\*P<0.001.

**Table 1 | Summary of the different outcome parameters in response to perturbation with IL-1 $\beta$ , T<sub>3</sub> or 65% mechanical stress (MS).**

Outcome measure	IL-1 $\beta$		T <sub>3</sub>		65% MS	
	FC*	P value <sup>§</sup>	FC*	P value <sup>§</sup>	FC*	P value <sup>§</sup>
Gene expression						
Catabolism						
<i>MMP13</i>	12.66	3.60x10 <sup>-2</sup>	3.74	3.00x10 <sup>-3</sup>	10.27	1.40x10 <sup>-2</sup>
<i>ADAMTS5</i>	1.26	NS	0.74	NS	1.04	NS
<i>EPAS1</i>	4.56	3.60x10 <sup>-2</sup>	1.83	1.00x10 <sup>-3</sup>	1.77	1.80x10 <sup>-20</sup>
Anabolism						
<i>ACAN</i>	0.03	1.08x10 <sup>-19</sup>	0.97	NS	1.18	NS
<i>COL2A1</i>	0.01	2.56x10 <sup>-12</sup>	3.45	2.40x10 <sup>-10</sup>	0.91	NS
Hypertrophy						
<i>COL1A1</i>	0.22	NS	144.68	3.00x10 <sup>-3</sup>	1.91	NS
<i>COL10A1</i>	0.23	NS	5.04	6.11x10 <sup>-3</sup>	3.82	NS
<i>ALP</i>	2.80	NS	665.82	7.42 x10 <sup>-9</sup>	2.73	NS
<i>RUNX2</i>	0.68	5.00x10 <sup>-2</sup>	1.18	NS	1.78	NS

Outcome Measure	IL-1 $\beta$		T3		65% MS	
	Beta**	P value <sup>\$</sup>	Beta**	P value <sup>\$</sup>	Beta**	P value <sup>\$</sup>
Histology						
Mankin score						
Cartilage structure	0.83	8.12 x10 <sup>-3</sup>	0.45	NS	0.20	NS
Cellularity	0.36	NS	0.09	NS	0.04	NS
Toluidine blue	0.79	3.15x10 <sup>-3</sup>	-0.07	NS	0.16	NS
Tidemark integrity	-0.02	NS	0.06	NS	0.10	NS
Mankin Score	1.95	5.47x10 <sup>-4</sup>	0.53	NS	0.50	NS
sGAG						
Medium						
Day 4	-0.10	NS	23.19	NS	10.21	NS
Day 6	60.51	7.87x10 <sup>-2</sup>	-1.95	NS	1.56	NS
Day 10	26.48	6.01x10 <sup>-3</sup>	2.59	NS	7.85	NS
Day 13	59.09	4.85x10 <sup>-8</sup>	1.27	NS	10.31	NS
Cartilage tissue						
Day 13	-1.95	NS	0.04	NS	2.72	NS
Mechanical properties						
Fibril network modulus						
Day 6	-0.11	NS	0.01	NS	-0.07	NS
Day 10	-0.04	NS	0.21	NS	-0.48	2.57x10 <sup>-2</sup>
Day 13	-0.03	NS	0.19	NS	-0.35	NS
Equilibrium Modulus						
Day 6	-0.02	NS	0.05	NS	-0.02	NS
Day 10	-0.02	NS	0.02	NS	-0.10	2.68x10 <sup>-2</sup>
Day 13	-0.01	NS	0.08	NS	-0.07	NS
Permeability						
Day 6	6.44	NS	0.93	NS	0.84	NS
Day 10	3.62	NS	4.17	NS	2.46	NS
Day 13	0.71	NS	-2.62	NS	1.45	NS

\*FC is determined by the  $2^{-\Delta\Delta CT}$  method and compared to its respective controls. \*\*Beta is determined by the GEE during the modelling and represents the difference between the perturbation and control groups. \$ significance of mean difference in gene expression between controls and treated explants were estimated by generalized estimating equation (GEE) with robust variance estimators to account for donor effects. Legend: MS= Mechanical stress; NS= not significant; sGAG=sulphated glycosaminoglycans

### ***sGAG release following cartilage perturbation***

To explore breakdown of cartilage, we measured sGAG released by the cartilage in the media on day 3, day 6, day 10 and day 13. In **Figure S3** we outlined the accumulation of sGAG release from explants to the medium between day 3 and 6, and in **Figure 4** between day 6 and 13, representing early and late release, respectively. IL-1 $\beta$  significantly increased release of sGAG into the medium at day 6 relative to day 3 (19% increase from 194.4  $\mu\text{g/ml}$  to 426.1  $\mu\text{g/ml}$  versus 194.5  $\mu\text{g/ml}$  to 366.0  $\mu\text{g/ml}$ ;  $P=0.03$ ; **Figure S3A**) compared to controls. This increased release was prolonged at a significant and higher rate at day 10 (52% increase of 51.4  $\mu\text{g/ml}$  versus 77.8  $\mu\text{g/ml}$ ;  $P=6.0 \times 10^{-3}$ ; **Figure 4A**) and day 13 (99% increase of 59.8  $\mu\text{g/ml}$  versus 118.9  $\mu\text{g/ml}$ ;  $P=4.9 \times 10^{-8}$ ; **Figure 4A**). Although some increased sGAG release after 65% MS and T3 treatment was observed at day 13, there was no significant difference as compared to controls (30% increase of 32.3  $\mu\text{g/ml}$  versus 42.6  $\mu\text{g/ml}$ ;  $P=0.09$  and 4% increase of 28.8  $\mu\text{g/ml}$  versus 30.0  $\mu\text{g/ml}$ ;  $P=0.8$ , respectively; **Figure 4B and 4C**).

### ***Changes of the cartilage integrity observed by histology***

To evaluate the microscopic changes in the cartilage tissue quality, we applied Mankin scoring to control and perturbed explants at day 13. As shown in **Figure 5A** and **Table 1**, IL-1 $\beta$  significantly increased the overall Mankin score (2.7 vs 4.1;  $P=6.3 \times 10^{-4}$ ) compared to controls. Upon investigating the different components of the Mankin score separately (cartilage structure, cellularity, loss of sGAG and integrity of tidemark), it appeared that the difference observed for IL-1 $\beta$  treatment was mainly driven by differences in cartilage structure such as fibrillations and fissures and loss of sGAGs by toluidine blue staining (1.2 vs 2.0,  $P=8.1 \times 10^{-3}$  and 0.4 vs 1.3,  $P=3.2 \times 10^{-3}$ , respectively **Table 1**, **Figure 5D** and **Figure S4**). Although we observed visible fissures and surface deformations only in explants upon 65% MS (**Figure S5**), suggesting cartilage breakdown, this was not reflected by a significant change in the Mankin scores (**Table 1** and **Figure 5C**).

### ***Changes in mechanical properties of the cartilage***

To explore the mechanical properties of cartilage in response to the treatments, we determined three different aspects of mechanical properties available at the MACH1 apparatus on day 6, day 10 and day 13. These aspects were the fibril network modulus ( $E_f$ ), the equilibrium modulus ( $E_m$ ) and hydraulic permeability ( $k$ ), reflecting the tensile stiffness, elastic coefficient (Young's modulus) and water retention respectively. As shown in **Figure 6**, 65% MS significantly negatively affected the fibril network modulus (0.9 vs 0.5 MPa;  $P=2.6 \times 10^{-2}$ ; **Figure 6A**) and equilibrium modulus (0.2 vs 0.1 MPa;  $P=2.7 \times 10^{-2}$ ; **Figure 6B**) at day 10 while simultaneously, though not significantly, increasing the hydraulic permeability of the cartilage by 300% (control vs 65% MS; 0.8 vs 3.2  $\text{mm}^2/\text{MPa}\cdot\text{s}$ ;  $P=0.2$ ; **Figure 6C**). No significant differences in mechanical properties were detected for IL-1 $\beta$  and T3 treated osteochondral explants.

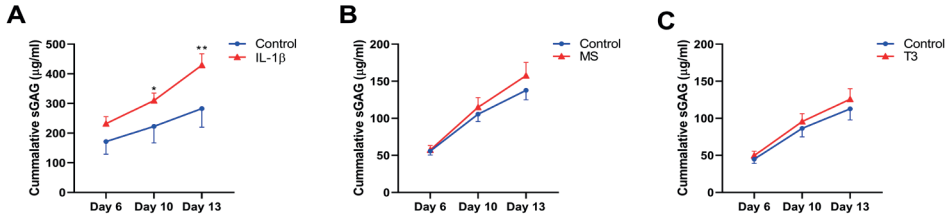


**Figure 4 | sGAG concentration in the media of osteochondral explants.** Cumulative sGAG release (µg/ml) in media of osteochondral explants in presence of [A] IL-1 $\beta$  (10ng/ml;n=2), [B] MS (n=19-23) or [C] T3 (10nM; n=17) as determine by the DMMB assay. Data is represented as mean  $\pm$  s.e.m. P-values of mean differences between controls and treated explants were estimated by generalized estimating equations (GEE) with robust variance estimators to account for donor effects. \*P<0.05, \*\*P<0.01. S.e.m.<0.05 are not distinguishable in the figure.

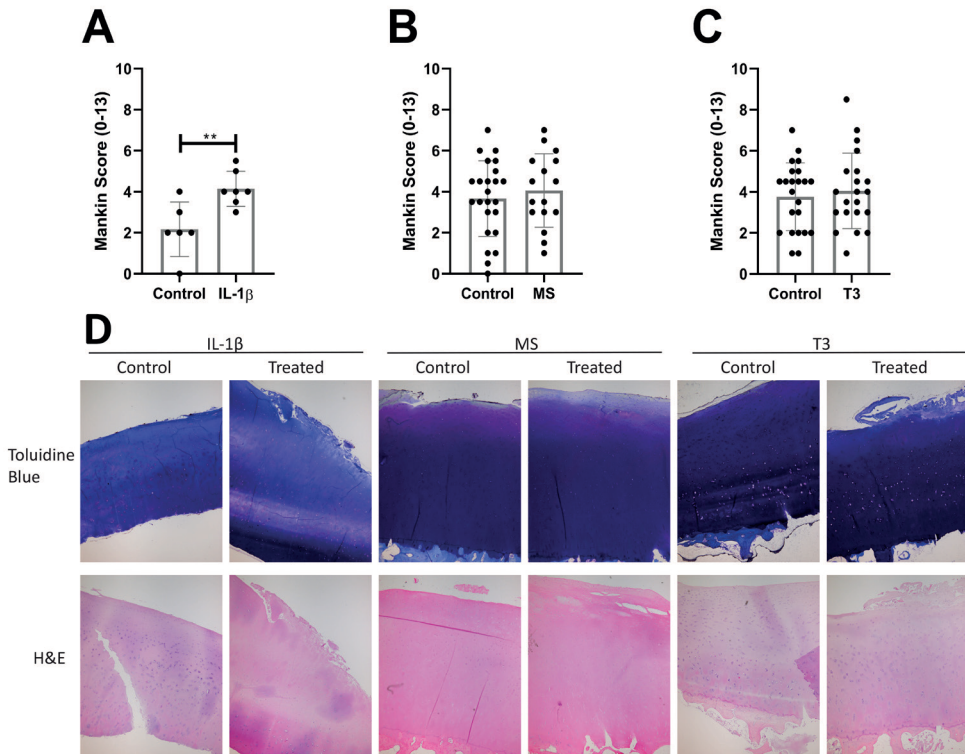


**Figure 5 | Mankin Score summary and representative histological pictures of cartilage after treatment with either IL-1 $\beta$ , T3 or 65% mechanical stress.** Cartilage damage was assessed on histology after perturbation with [A] IL-1 $\beta$  (n=6), [B] 65% MS (n=16/24) or [C] T3 (n=22/24). Data is represented as mean  $\pm$  s.e.m and each dot represents a single explant. [D] Representative histological pictures are given of Toluidine blue and H&E stainings performed on slides from the different conditions. P-values of mean differences between controls and treated explants were estimated by generalized estimating equations (GEE) with robust variance estimators to account for donor effects.\*P<0.05, \*\*P<0.01.

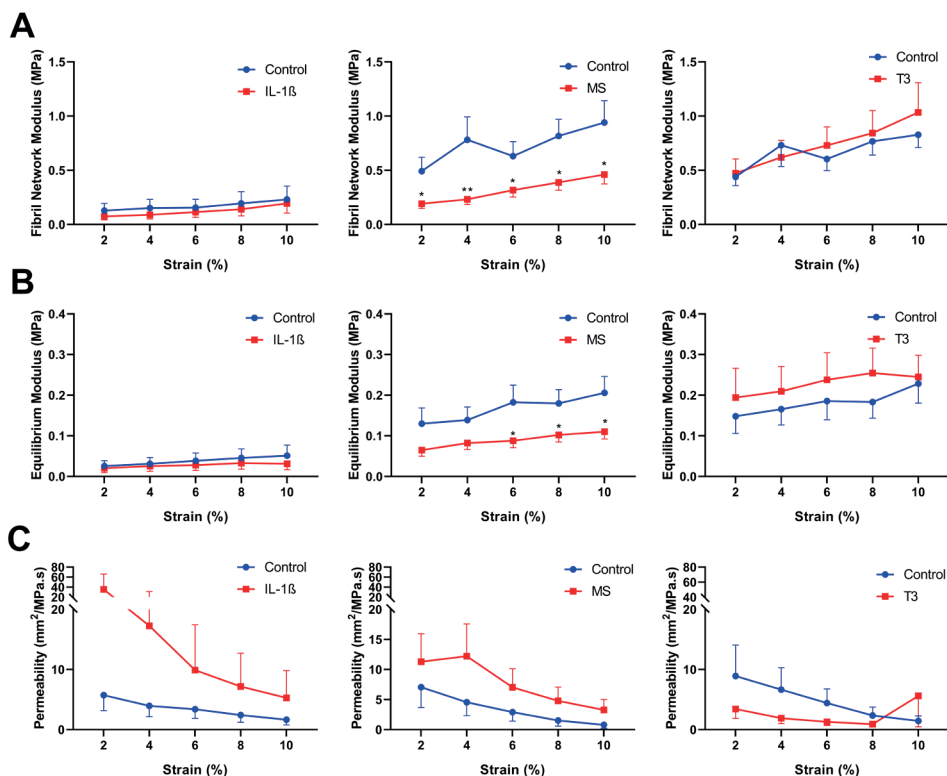


**Figure 6 | Mechanical properties of cartilage of osteochondral explants on day 10.** Mechanical properties of cartilage was determined after perturbation with IL-1 $\beta$  (n=3), 65% MS (n=19/21) or T<sub>3</sub> (n=19/23) using the fibril-network-reinforced biphasic model to calculate the **[A]** Fibril Network modulus, **[B]** Young's Modulus and **[C]** hydraulic permeability. Data is represented as mean  $\pm$  s.e.m. P-values of mean differences between controls and treated explants were estimated by generalized estimating equations (GEE) with robust variance estimators to account for donor effects. \*P<0.05, \*\*P<0.01.

## Discussion

We present human *ex vivo* osteochondral explants as a model system to study OA related changes after three known pathophysiological perturbations. We applied IL-1 $\beta$ , T<sub>3</sub>, and 65% MS as relevant perturbing factors and studied a variety of output measures including chondrocyte signalling, cartilage structure and breakdown, and mechanical properties. Our data provide a relevant personalized human model for research on OA, which can be used for target identification and/or drug efficacy testing. The biomimetic model also complies with the guiding principles of reduction, refinement and replacement of animal experiments.

An increased catabolic response was measured after perturbation in all three models. The highest increase in *MMP13* gene expression was measured in response to IL-1 $\beta$  (FC=12.7), followed by mechanical stress (FC=10.3), while the lowest increase was observed after T<sub>3</sub> treatment (FC=3.7). Strikingly, none of the treatments induced a significant increase in *ADAMTS5* gene expression. Moreover, we measured a greatly significant increase of *EPAS1* in all three OA models, indicating its sensitivity to a perturbed cartilage homeostasis.

The *EPAS1* gene encodes HIF-2 $\alpha$  and its role in the onset of OA in humans is unclear as both increased [27,28] and decreased [29] expression has been reported in human OA cartilage. Functionally, HIF-2 $\alpha$  has been shown to regulate endochondral ossification in mouse studies by inducing expression of genes mediating chondrocyte hypertrophy (*Col10a1*), matrix degradation (*Mmp13*) and vascular invasion (*Vegfa*) [27].

We observed that the three different perturbations were diverse in the other outcome measures. The most severe cartilage breakdown was observed after treatment with the pro-inflammatory IL-1 $\beta$  and this breakdown was also characterized by an increased chondrocyte cell signalling of catabolism (*MMP13* and *EPAS1*, **Figure 1A**) and abolishment of anabolic cell signalling (*ACAN* and *COL2A1*, **Figure 2A**). Gene expression of *COL2A1* and *ACAN* was downregulated by IL-1 $\beta$ , 100 and 33 times respectively, suggesting a very low expression of these normally highly expressed cartilage genes. This shift in chondrocyte signalling towards catabolism is confirmed by cartilage breakdown, as measured by a stark 99% increased release of sGAG from cartilage (**Figure 4A**) and by a 1.95 times increased Mankin score (**Figure 5A**). Upon investigation of the different subcategories of the Mankin scoring we observed that IL-1 $\beta$  greatly reduced cartilage quality as measured by a 3.2 times reduction of staining for sGAG (**Figure S4C**) and 1.7 times increased cartilage surface damage (**Figure S4A**). These results of high cartilage breakdown in response to IL-1 $\beta$  are in line with many previous studies, which often observed an increased release of matrix metalloproteinases (MMPs) and other degradative enzymes, production of nitric oxide and inhibition of the synthesis of matrix proteins [17,30]. This model might be most suitable to study interventions aimed at a subgroup of OA patients that have more inflammatory characteristics and might even suffer from rheumatic arthritis.

The perturbation with 65% MS can be considered a posttraumatic model, triggering modest OA related changes particularly via catabolism, as reflected by the consistent yet particular effect on *MMP13* and *EPAS1* (FC=1.8;  $P=1.8 \times 10^{-20}$  and FC=10.3;  $P=1.4 \times 10^{-2}$ , respectively). In addition, we showed a slight decrease in cartilage anabolism as measured by reduced *COL2A1* gene expression (FC=0.9;  $p=8.7 \times 10^{-3}$ ). At the protein level we measured a 30% increase of sGAG released from cartilage (**Figure 4C**) after 65% MS, corresponding with the measured slightly higher scoring for sGAG loss in toluidine blue staining (**Figure S4C**). Macroscopically we observed more macrocracks on the cartilage surface (**Figure S5**) of explants receiving 65% MS and this damage was reflected in a substantial unbeneficial change of mechanical properties of the cartilage (**Figure 6**). Compared to controls, explants receiving 65% MS had a 48% reduced tensile stiffness (**Figure 6A**), 55% reduced Young's modulus (**Figure 6B**) and a 300% increased hydraulic permeability (**Figure 6C**). These results suggest that the cartilage extracellular matrix is damaged after 65% MS has been applied as it no longer appears to have the normal elastic properties and water-retaining capabilities that allow cartilage to withstand high loads. We hypothesize that this mechanism of function could be similar to exceeding the injury threshold of mechanical loading during one's life [31]. Exceeding this threshold could occur when the mechanical load is suddenly increased or when the joint has lost its natural mechanoprotective properties.

It is generally accepted that biomechanical loading is necessary for the maintenance of cartilage homeostasis, as evidenced by the rapid loss of proteoglycans in joints that are immobilised or in disuse [32]. However, abnormal, altered or injurious loading is associated with inflammatory and metabolic imbalances that may eventually lead to OA-like damage

[13,15,33-35]. Moreover, *ex vivo* cartilage explants subjected to these magnitudes of stress exhibit a significant suppression of metabolic activity, and particularly biosynthesis of aggrecan and collagen is affected [13,15,33,34,36] similar to the *in vivo* situation [37]. Consistent upregulation of catabolic genes such as *RUNX2*, *MMP1*, *MMP3*, *MMP13* and *ADAMTS5* has been found in several mechanical injury models using either chondrocytes or cartilage explants [14,15,38-40]. The literature has shown that levels of measured genes can vary greatly, depending on the magnitude of force, speed, age of cartilage, and at which time point gene expression is measured [41-43]. In our model we measured targeted genes and in follow-up studies it would be interesting to measure the whole genomic transcript using RNA-sequencing to identify different pathways modulating the lasting response to mechanical stress. Our model applying 65% MS might be most suitable to study interventions aimed at post-traumatic OA patients who would benefit most from a reduction of the (early) response of cartilage to mechanical stress.

In our third model we showed that in response to T<sub>3</sub>, chondrocyte signalling increased expression of the early hypertrophic markers *COL10A1* and *MMP13* (FC=5.0;  $P=6.1 \times 10^{-3}$  and FC=3.7;  $P=3.0 \times 10^{-3}$ , respectively), while also greatly increasing the mineralization markers *COL1A1* and *ALPL* (FC=144.7;  $P=3.0 \times 10^{-3}$  and FC=665.8;  $P=7.4 \times 10^{-9}$ , respectively). Together, these results suggest that T<sub>3</sub> induces terminal differentiation towards bone in chondrocytes. Treatment with T<sub>3</sub> also induced a greatly consistent increased gene expression of *COL2A1* (FC=3.5;  $P=2.4 \times 10^{-10}$ ), but did not affect *ACAN* expression. Nonetheless, upregulation of *COL2A1* does not necessarily mean that T<sub>3</sub> induces a beneficial response of chondrocytes, as *COL2A1* is also upregulated in response to damage. In addition, a microarray study has shown that *COL2A1* gene expression is upregulated in preserved compared to healthy cartilage, suggesting that there might be an early role for *COL2A1* in the OA process when the cartilage is still trying to repair matrix damage [44]. To understand downstream transcriptional effects of T<sub>3</sub> we measured *RUNX2* and *EPAS1*, two critical transcription factors hallmarking OA and acting downstream of T<sub>3</sub>. We measured an upregulation of both *EPAS1* and *RUNX2* (FC=1.8;  $P=1.0 \times 10^{-3}$  and FC=1.2;  $P=7.1 \times 10^{-2}$ , respectively), suggesting a possible role for both transcription factors as downstream targets of T<sub>3</sub>. The changes in chondrocyte signalling after T<sub>3</sub> perturbation did not lead to significant changes of cartilage matrix integrity. Our results indicate that hypertrophy was induced by T<sub>3</sub> in our explant model and that this was not necessarily detrimental to the cartilage matrix. T<sub>3</sub> can induce changes in chondrocyte signalling directly, by binding to specific thyroid responsive elements (TREs) on the DNA whereby it regulates transcription, or more indirectly by activating the transcription of another transcriptional regulator such as *RUNX2*. However, which genes are transcriptionally regulated by T<sub>3</sub> needs to be elucidated and regulation has been shown to be very tissue-specific because of the different levels and isotypes of thyroid hormone receptors present in different cell types. It is possible that T<sub>3</sub> is able to induce multiple genes such as *MMP13* in cartilage via binding to TREs. For example, in *trβ* crisprant tadpoles, T<sub>3</sub> did not induce *MMP13* gene expression suggesting that T<sub>3</sub> acts via Trβ on inducing transcription [45].

Other researchers have seen similar effects using T<sub>3</sub> and T<sub>4</sub>, with T<sub>3</sub> being a more potent inducer of collagen production [46,47]. However, these two studies did not observe an increase in hypertrophic markers such as *COL10* and *COL1*, and this could be due to the cell type and concentration used in their experiments. On the contrary, in an *in vitro* chondrogenesis model using human bone marrow-derived stem cells (hBMSCs), perturbation with T<sub>3</sub> increased chondrocyte cell signalling of terminal maturation markers (*ALPL*, *COL1A1*) [37].

Overexpression of *DIO2*, encoding for the D2 enzyme which converts T4 into T3, in the same model had even more detrimental effects. This explant model perturbed by T3 might be most suitable to study interventions aimed at investigating mild types of OA that are more characterized by occurrence of hypertrophy and mineralization of cartilage.

The observation that we did not measure a response of *ADAMTS5* in our three models was unexpected. Possible explanations could be that in general expression levels of *ADAMTS5* were too low to be accurately assessed or that *ADAMTS5* expression was too heterogeneous between patients to lead to concluding results. A more biological explanation could be the temporal and tight regulation of *ADAMTS5* gene expression, peaking 10 hours after injury and declining thereafter [42].

A major strength of our models is that they consider aged, yet preserved, human osteochondral explants of a heterogeneous OA patient population. As a result cartilage explants may reflect a reliable biomimetic model, prone to OA onset. Moreover, despite the heterogeneous patient population we present consistent output specific for three different relevant triggers of OA, allowing for development of different treatment modalities. Some weaknesses of the models concern the scalability and dependency of patients undergoing joint replacement surgery. In addition, we only measured changes of the overall cartilage matrix and not changes of specific proteins that make up the articular cartilage, such as collagen type II. Nonetheless, we advocate that focusing clinical development on directly counteracting these specific unbeneficial responses of chondrocytes upon these OA triggers will facilitate further personalized development and testing of desperately needed disease modifying OA drugs. Our data provide a reference for development of advanced 3D *in vitro* model systems of cartilage, bone or osteochondral models aiming towards a joint on a chip using the sensitive changes in gene expression. Moreover, our model offers a next step opportunity for in depth molecular exploration with and without perturbations, e.g., by RNA sequencing in bulk or at the single-cell level.

## Conclusions

Our study demonstrates that it is possible to set up personalized human OA disease models reflecting different relevant aspects (inflammation, hypertrophy and mechanical stress) of OA pathophysiology. The different perturbing factors and their variety in downstream effects could facilitate the development of novel targeted treatment modalities reflecting different aspects of the OA pathophysiology. Applying the here presented aged human explant model could result in a paradigm shift for biomedical research and the pharmaceutical industry leading to new ways to identify desperately needed effective drugs for OA.

## Acknowledgements

### Funding

The research leading to these results has received funding from the Dutch Arthritis Society/ ReumaNederland (DAF-15-4-401) and the Dutch Scientific Research council NWO /ZonMW VICI scheme (91816631/528). The Leiden University Medical Centre have and are supporting the RAAK study. The Rapid Service Fee and the Open Access fee were funded by the Dutch

Scientific Research council NWO /ZonMW VICI scheme (91816631/528).

### ***Authors' contributions***

All named authors meet the International Committee of Medical Journal Editors (ICMJE) criteria for authorship for this article, take responsibility for the integrity of the work as a whole, and have given their approval for this version to be published. Study concept and design: EH, YFM, IM. Acquisition of material and data: EH, MvH, HED, NL, EL-Z, RGHHN. Data analysis: EH, YFM and IM. Preparation of the manuscript: EH, IM. Critical reviewing and approval of the manuscript: All authors.

### ***Disclosures***

Evelyn Houtman, Marcella van Hoolwerff, Nico Lakenberg, Eka Suchiman, Enrike van der Linden – van der Zwaag, Rob Nelissen, Yolande Ramos and Ingrid Meulenbelt declare that they have no conflict of interest.

### ***Compliance with ethics guidelines***

The RAAK study has been approved by the medical ethical committee of the Leiden University Medical Center (P08.239/P19.013). Patients provided written informed consent to participate in the study and had the right to withdraw at any time.

### ***Data availability***

The datasets during and/or analysed during the current study available from the corresponding author on reasonable request.

### ***Patients and other acknowledgments***

We would like to thank all study participants of the RAAK study. We thank all the members of our group; Alejandro Rodríguez Ruiz, Ritchie Timmermans, Margo Tuerlings, Rodrigo Coutinho de Almeida and Niek Bloks. We also thank Anika Rabelink-Hoogenstraaten, Demiën Broekhuis, Robert van der Wal, Peter van Schie, Shaho Hasan, Maartje Meijer, Daisy Latijnhouwers and Geertje Spierenburg for assistance in collecting RAAK samples.

## REFERENCES

1. Atkins GJ, Welldon KJ, Halbout P, et al. Strontium ranelate treatment of human primary osteoblasts promotes an osteocyte-like phenotype while eliciting an osteoprotegerin response. *Osteoporos Int.* 2009;20(4):653-64.
2. Woolf AD, Erwin J, March L. The need to address the burden of musculoskeletal conditions. *Best Pract Res Clin Rheumatol.* 2012;26(2):183-224.
3. Dreier R. Hypertrophic differentiation of chondrocytes in osteoarthritis: the developmental aspect of degenerative joint disorders. *Arthritis Res Ther.* 2010;12(5):216.
4. Pfander D, Swoboda B, Kirsch T. Expression of early and late differentiation markers (proliferating cell nuclear antigen, syndecan-3, annexin VI, and alkaline phosphatase) by human osteoarthritic chondrocytes. *Am J Pathol.* 2001;159(5):1777-83.
5. von der Mark K, Kirsch T, Nerlich A, et al. Type X collagen synthesis in human osteoarthritic cartilage. Indication of chondrocyte hypertrophy. *Arthritis Rheum.* 1992;35(7):806-11.
6. Poole AR, Nelson F, Dahlberg L, et al. Proteolysis of the collagen fibril in osteoarthritis. *Biochem Soc Symp.* 2003(70):115-23.
7. Fuerst M, Bertrand J, Lammers L, et al. Calcification of articular cartilage in human osteoarthritis. *Arthritis Rheum.* 2009;60(9):2694-703.
8. Kuhn K, D'Lima DD, Hashimoto S, et al. Cell death in cartilage. *Osteoarthritis Cartilage.* 2004;12(1):1-16.
9. Goldring MB, Goldring SR. Articular cartilage and subchondral bone in the pathogenesis of osteoarthritis. *Ann N Y Acad Sci.* 2010;1192:230-7.
10. Bird JL, Wells T, Platt D, et al. IL-1 beta induces the degradation of equine articular cartilage by a mechanism that is not mediated by nitric oxide. *Biochem Biophys Res Commun.* 1997;238(1):81-5.
11. Clutterbuck AL, Mobasheri A, Shakibaei M, et al. Interleukin-1beta-induced extracellular matrix degradation and glycosaminoglycan release is inhibited by curcumin in an explant model of cartilage inflammation. *Ann N Y Acad Sci.* 2009;1171:428-35.
12. Geurts J, Jurić D, Müller M, et al. Novel Ex Vivo Human Osteochondral Explant Model of Knee and Spine Osteoarthritis Enables Assessment of Inflammatory and Drug Treatment Responses. *International Journal of Molecular Sciences.* 2018;19(5):1314.
13. Kurz B, Jin M, Patwari P, et al. Biosynthetic response and mechanical properties of articular cartilage after injurious compression. *J Orthop Res.* 2001;19(6):1140-6.
14. Chan PS, Schlueter AE, Coussens PM, et al. Gene expression profile of mechanically impacted bovine articular cartilage explants. *J Orthop Res.* 2005;23(5):1146-51.
15. Quinn TM, Grodzinsky AJ, Hunziker EB, et al. Effects of injurious compression on matrix turnover around individual cells in calf articular cartilage explants. *J Orthop Res.* 1998;16(4):490-9.
16. Bomer N, den Hollander W, Ramos YF, et al. Translating genomics into mechanisms of disease: Osteoarthritis. *Best Pract Res Clin Rheumatol.* 2015;29(6):683-91.
17. Lv M, Zhou Y, Polson SW, et al. Identification of Chondrocyte Genes and Signaling Pathways in Response to Acute Joint Inflammation. *Sci Rep.* 2019;9(1):93.
18. Vincent TL. IL-1 in osteoarthritis: time for a critical review of the literature. *F1000Res.* 2019;8.
19. Mackay AM, Beck SC, Murphy JM, et al. Chondrogenic differentiation of cultured human mesenchymal stem cells from marrow. *Tissue Eng.* 1998;4(4):415-28.
20. Mueller MB, Tuan RS. Functional characterization of hypertrophy in chondrogenesis of human mesenchymal stem cells. *Arthritis Rheum.* 2008;58(5):1377-88.
21. Sanchez-Adams J, Leddy HA, McNulty AL, et al. The mechanobiology of articular cartilage: bearing the burden of osteoarthritis. *Curr Rheumatol Rep.* 2014;16(10):451.
22. Farndale RW, Buttle DJ, Barrett AJ. Improved quantitation and discrimination of sulphated glycosaminoglycans by use of dimethylmethylene blue. *Biochim Biophys Acta.* 1986;883(2):173-7.
23. Mankin HJ, Dorfman H, Lippiello L, et al. Biochemical and metabolic abnormalities in articular cartilage from osteo-arthritic human hips. II. Correlation of morphology with biochemical and metabolic data. *J Bone Joint Surg Am.* 1971;53(3):523-37.
24. Soulhat J, Buschmann MD, Shirazi-Adl A. A fibril-network-reinforced biphasic model of cartilage in unconfined compression. *J Biomech Eng.* 1999;121(3):340-7.

25. McCulloch RS, Ashwell MS, O'Nan AT, et al. Identification of stable normalization genes for quantitative real-time PCR in porcine articular cartilage. *J Anim Sci Biotechnol*. 2012;3(1):36.
26. Al-Sabah A, Stadnik P, Gilbert SJ, et al. Importance of reference gene selection for articular cartilage mechanobiology studies. *Osteoarthritis Cartilage*. 2016;24(4):719-30.
27. Saito T, Fukai A, Mabuchi A, et al. Transcriptional regulation of endochondral ossification by HIF-2 $\alpha$  during skeletal growth and osteoarthritis development. *Nat Med*. 2010;16(6):678-86.
28. Yang S, Kim J, Ryu JH, et al. Hypoxia-inducible factor-2 $\alpha$  is a catabolic regulator of osteoarthritic cartilage destruction. *Nat Med*. 2010;16(6):687-93.
29. Bohensky J, Terkhorst SP, Freeman TA, et al. Regulation of autophagy in human and murine cartilage: hypoxia-inducible factor 2 suppresses chondrocyte autophagy. *Arthritis Rheum*. 2009;60(5):1406-15.
30. Pelletier JP, Mineau F, Ranger P, et al. The increased synthesis of inducible nitric oxide inhibits IL-1 $\alpha$  synthesis by human articular chondrocytes: possible role in osteoarthritic cartilage degradation. *Osteoarthritis and cartilage*. 1996;4(1):77-84.
31. Vincent TL, Wann AKT. Mechanoadaptation: articular cartilage through thick and thin. *J Physiol*. 2019;597(5):1271-81.
32. Sun HB. Mechanical loading, cartilage degradation, and arthritis. *Ann NY Acad Sci*. 2010;1211:37-50.
33. Patwari P, Cook MN, DiMicco MA, et al. Proteoglycan degradation after injurious compression of bovine and human articular cartilage in vitro: interaction with exogenous cytokines. *Arthritis Rheum*. 2003;48(5):1292-301.
34. Patwari P, Cheng DM, Cole AA, et al. Analysis of the relationship between peak stress and proteoglycan loss following injurious compression of human post-mortem knee and ankle cartilage. *Biomech Model Mechanobiol*. 2007;6(1-2):83-9.
35. Guilak F. Biomechanical factors in osteoarthritis. *Best Pract Res Clin Rh*. 2011;25(6):815-23.
36. Guilak F, Meyer BC, Ratcliffe A, et al. The effects of matrix compression on proteoglycan metabolism in articular cartilage explants. *Osteoarthritis and cartilage*. 1994;2(2):91-101.
37. Bomer N, den Hollander W, Ramos YF, et al. Underlying molecular mechanisms of DIO2 susceptibility in symptomatic osteoarthritis. *Annals of the rheumatic diseases*. 2015;74(8):1571-9.
38. Riegger J, Joos H, Palm HG, et al. Antioxidative therapy in an ex vivo human cartilage trauma-model: attenuation of trauma-induced cell loss and ECM-destructive enzymes by N-acetyl cysteine. *Osteoarthritis and cartilage*. 2016;24(12):2171-80.
39. Tetsunaga T, Nishida K, Furumatsu T, et al. Regulation of mechanical stress-induced MMP-13 and ADAMTS-5 expression by RUNX-2 transcriptional factor in SW1353 chondrocyte-like cells. *Osteoarthritis and cartilage*. 2011;19(2):222-32.
40. Ashwell MS, Gonda MG, Gray K, et al. Changes in chondrocyte gene expression following in vitro impaction of porcine articular cartilage in an impact injury model. *J Orthop Res*. 2013;31(3):385-91.
41. Madej W, van Caam A, Blaney Davidson EN, et al. Physiological and excessive mechanical compression of articular cartilage activates Smad2/3P signaling. *Osteoarthritis and cartilage*. 2014;22(7):1018-25.
42. Lee JH, Fitzgerald JB, Dimicco MA, et al. Mechanical injury of cartilage explants causes specific time-dependent changes in chondrocyte gene expression. *Arthritis Rheum*. 2005;52(8):2386-95.
43. Fitzgerald JB, Jin M, Dean D, et al. Mechanical compression of cartilage explants induces multiple time-dependent gene expression patterns and involves intracellular calcium and cyclic AMP. *J Biol Chem*. 2004;279(19):19502-11.
44. Ramos YF, den Hollander W, Bovee JV, et al. Genes involved in the osteoarthritis process identified through genome wide expression analysis in articular cartilage; the RAAK study. *PLoS One*. 2014;9(7):e103056.
45. Sakane Y, Iida M, Hasebe T, et al. Functional analysis of thyroid hormone receptor beta in *Xenopus tropicalis* founders using CRISPR-Cas. *Biol Open*. 2018;7(1).
46. Whitney GA, Kean TJ, Fernandes RJ, et al. Thyroxine Increases Collagen Type II Expression and Accumulation in Scaffold-Free Tissue-Engineered Articular Cartilage. *Tissue Eng Part A*. 2018;24(5-6):369-81.
47. Glade MJ, Kanwar YS, Stern PH. Insulin and thyroid hormones stimulate matrix metabolism in primary cultures of articular chondrocytes from young rabbits independently and in combination. *Connect Tissue Res*. 1994;31(1):37-44.

## Supplementary Files

### *List of contents:*

### *Supplementary Tables*

**Table S1.** Baseline information of the donors included in the three perturbations.

**Table S2.** Primer sequence used to determine gene expression levels in real-time PCR.

**Table S3.** Gene expression after treatment with IL-1 $\beta$  in combination with 30% loading

**Table S4.** Gene expression after treatment with T3 in combination with 30% mechanical loading.

### *Supplementary Figures*

**Figure S1.** Gene expression after treatment with IL-1 $\beta$  in combination with 30% mechanical loading.

**Figure S2.** Gene expression after treatment with T3 in combination with 30% mechanical loading.

**Figure S3.** sGAG concentration in the media of osteochondral explants on day 3 and 6.

**Figure S4.** Sub categories of the Mankin Score of cartilage after treatment with either IL-1 $\beta$ , T3 or 65% mechanical stress.

**Figure S5.** Macroscopical pictures of osteochondral explants after 65% mechanical stress (65% MS) is applied and controls.

## Supplementary Tables

**Table S1 | Baseline information of the donors included in the three perturbations.** Characteristics of donors included in the three different perturbation models. The table represents the age, sex, and BMI per treatment group on the day of joint replacement surgery. Age and BMI are represented as average with standard deviations.

	<b>IL-1<math>\beta</math></b>	<b>T3</b>	<b>65% mechanical stress (MS)</b>
N (donors)	3	8	9
F/M	3/0	4/4	3/6
(% F)	100%	50%	33%
Mean age	62.3 $\pm$ 9.0	66.6 $\pm$ 9.5	65.1 $\pm$ 8.8
(range)	55-75	53-81	53-81
Mean BMI	28.9 $\pm$ 7.9	25.9 $\pm$ 2.4	27.9 $\pm$ 3.4
(range)	22.5-40.1	22.5-31.2	24.8-35.1

**Legend:** F=Females, M=Males; age given in years

**Table S2 | Primer sequence used to determine gene expression levels in real-time PCR.**

<b>Gene</b>	<b>Forward (F) and reverse (R) primers (5' to 3')</b>
<i>SDHA</i>	F: TGGAGCTGCAGAACCTGATG
	R: TGTAGTCTTCCCTGGCATGC
<i>MMP13</i>	F: TTGAGCTGGACTCATTGTGCG
	R: GGAGCCTCTCAGTCATGGAG
<i>ADAMTS5</i>	F: TGGCTCACGAAATCGGACAT
	R: GCGCTTATCTTCTGTGGAACC
<i>EPAS1</i>	F: ACAGGTGGAGCTAACAGGAC
	R: CCGTGCACTTCATCCTCATG
<i>COL2A1</i>	F: CTACCCCAATCCAGCAAACGT
	R: AGGTGATGTTCTGGGAGCCTT
<i>ACAN</i>	F: AGAGACTCACACAGTCGAAACAGC
	R: CTATGTTACAGTGCTCGCCAGTG
<i>COL1A1</i>	F: GTGCTAAAGGTGCCAATGGT
	R: ACCAGGTTACCCGCTGTTAC
<i>COL10A1</i>	F: GGCAACAGCATTATGACCCA
	R: TGAGATCGATGATGGCACTCC
<i>ALPL</i>	F: CAAAGGCTTCTTCTGTGCTGGTG
	R: CCTGCTGGCTTTTCCITCA
<i>RUNX2</i>	F: CTGTGGTTACTGTCATGGCG
	R: AGGTAGTACTTGGGGAGGA

Table S3 | Gene expression after treatment with IL-1 $\beta$  in combination with 30% loading.

Gene	Control vs IL1 $\beta$			Control vs 30% MS			Control vs IL1 $\beta$ + 30% MS			Merged groups		
	Beta	SE	P-value	Beta	SE	P-value	Beta	SE	P-value	Beta	SE	P-value
MMP13	4.2	1.7	1.3x10 <sup>-2</sup>	0.2	3.4	NS	0.4	1.8	NS	3.7	1.8	3.6x10 <sup>-2</sup>
ADAMTSS	0.6	0.8	NS	0.3	0.7	NS	0	0.8	NS	0.2	0.5	NS
EPAS1	1.9	1.4	NS	-0.6	1.6	NS	1.8	1.5	NS	2.2	1	3.6x10 <sup>-2</sup>
ACAN	-5.8	0.7	2.6x10 <sup>-17</sup>	-0.7	0.7	NS	-5.3	0.8	3.6x10 <sup>-12</sup>	-5.2	0.6	1.1x10 <sup>-19</sup>
COL2A1	-7.3	0.7	2.9x10 <sup>-13</sup>	-0.7	0.4	NS	-7.4	0.3	1.4x10 <sup>-13</sup>	-7	0.5	2.6x10 <sup>-12</sup>
COL10A1	-0.4	1.5	NS	0.9	1.8	NS	-0.9	1.4	NS	-1	1.3	NS
COL1A1	-2	3.3	NS	-2.7	3.9	4.8x10 <sup>-2</sup>	-3.4	3.6	NS	-1.4	2.6	NS
ALP	0.8	3	NS	-1.8	3.7	NS	-2.8	2.8	NS	-0.1	2.2	NS

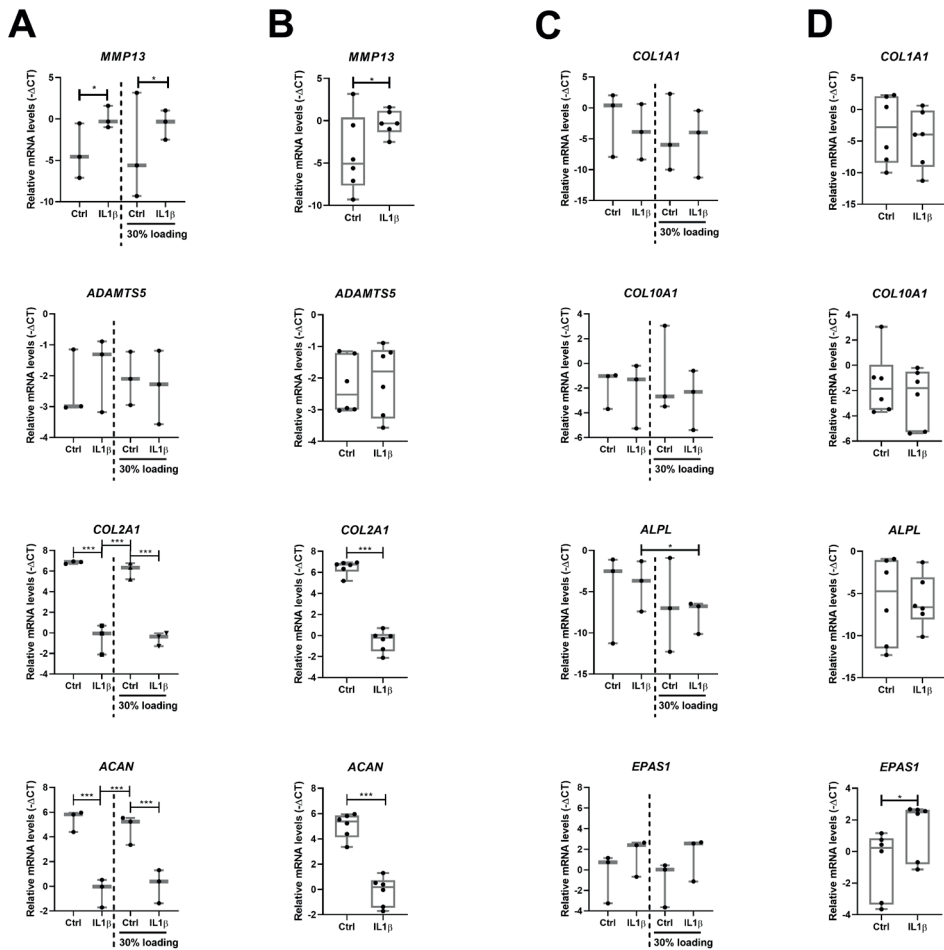
Table S3: Gene expression after treatment with IL-1 $\beta$  in combination with 30% loading. RT-PCR analysis of MMP13, ADAMTSS, COL2A1, ACAN, COL1A1, COL10A1, ALPL gene expression comparing [first column] IL-1 $\beta$  (n=3) versus controls (n=3), [second column] 30% MS (n=3) to controls (n=3), [third column] IL-1 $\beta$ +30% MS (n=3) versus controls (n=3) and [fourth column] Control and 30% MS merged (n=6) versus IL-1 $\beta$  and IL-1 $\beta$ +30% MS merged (n=6). Beta is determined by the GEE during the modelling and represents the difference between the perturbation and control groups.

Table S4 | Gene expression after treatment with T3 in combination with 30% mechanical loading.

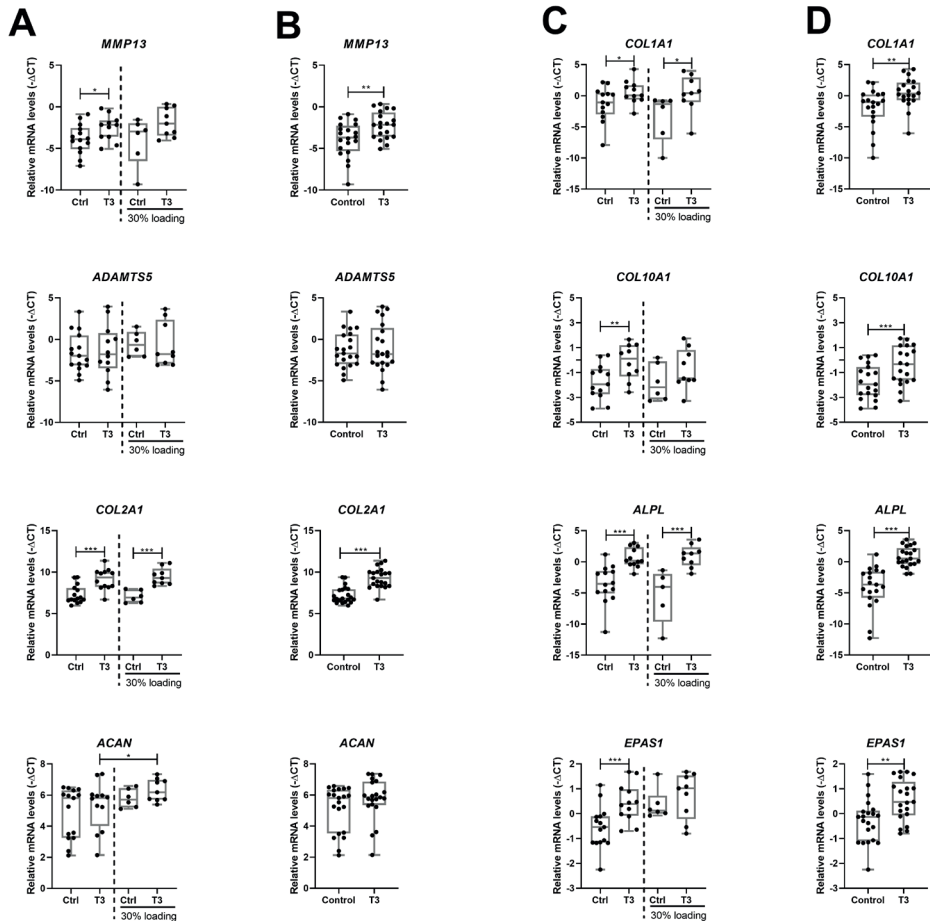
Gene	Control vs T3			Control vs 30% MS			Control vs T3 + 30% MS			Merged groups		
	Beta	SE	P-value	Beta	SE	P-value	Beta	SE	P-value	Beta	SE	P-value
MMP13	1.3	0.6	3.9x10 <sup>-2</sup>	-0.2	1.2	NS	2	0.7	5.0x10 <sup>-3</sup>	1.7	0.6	3.0x10 <sup>-3</sup>
ADAMTS5	0.2	1	NS	1	0.8	NS	0.9	1	NS	0.2	0.8	NS
EPAS1	1	0.3	1.0x10 <sup>-3</sup>	0.9	0.3	4.0x10 <sup>-3</sup>	1.3	0.4	4.1x10 <sup>-4</sup>	0.8	0.3	1.0x10 <sup>-3</sup>
ACAN	0.5	0.6	NS	0.9	0.5	4.3x10 <sup>-2</sup>	1.5	0.5	2.0x10 <sup>-3</sup>	0.6	0.4	NS
COL2A1	1.9	0.5	3.5x10 <sup>-5</sup>	-0.2	0.4	NS	2.2	0.4	2.2x10 <sup>-7</sup>	2.1	0.3	2.4x10 <sup>-10</sup>
COL10A1	1.6	0.6	5.0x10 <sup>-3</sup>	-0.1	0.7	NS	1	0.6	NS	1.3	0.5	3.0x10 <sup>-3</sup>
COL1A1	1.9	0.9	4.2x10 <sup>-2</sup>	-2.1	1.6	NS	1.6	1.2	NS	2.4	0.9	6.1x10 <sup>-3</sup>
ALP	4.2	0.9	3.0x10 <sup>-6</sup>	-1.9	1.9	NS	4.5	1	3.0x10 <sup>-6</sup>	4.9	0.8	7.4x10 <sup>-9</sup>

Table S4. Gene expression after treatment with T3 in combination with 30% mechanical loading. RT-PCR analysis of MMP13, ADAMTS, COL1A1, ACAN, COL1A1, COL10A1, ALPL gene expression comparing [first column] T3 (n=12) versus controls (n=15), [second column] 30% MS (n=6) to controls (n=15), [third column] T3+30% MS (n=9) versus controls (n=15) and [fourth column] Control and 30% MS merged (n=21) versus T3 and T3+30% MS merged (n=21). Beta is determined by the GEE during the modelling and represents the

## Supplementary Figures



**Figure S1 | Gene expression after treatment with IL-1 $\beta$  in combination with 30% mechanical loading.** RT-PCR analysis of MMP13, ADAMTS, COL2A1 and ACAN after **[A]** IL-1 $\beta$  (10 ng/ml; n=3), 30% loading (n=3) and IL-1 $\beta$ +30% loading (10 ng/ml; n=3), **[B]** Control and 30% loading merged (n=6) versus IL-1 $\beta$  and IL-1 $\beta$ +30% loading merged (10 ng/ml; n=6). RT-PCR analysis of COL1A1, COL10A1, ALPL and EPAS1 after **[C]** IL-1 $\beta$  (10 ng/ml; n=3), 30% loading (n=3) and IL-1 $\beta$ +30% loading (10 ng/ml; n=3) **[D]** Control and 30% loading merged (n=6) versus IL-1 $\beta$  and IL-1 $\beta$ +30% loading merged (10 ng/ml; n=6). Data is presented in a boxplot depicting the median, lower and upper quartiles and each black dot represents a single explant. \*P<0.05, \*\*P<0.01, \*\*\*P<0.001.



**Figure S2 | Gene expression after treatment with T3 in combination with 30% mechanical loading.** RT-PCR analysis of MMP13, ADAMTS, COL2A1 and ACAN after **[A]** T3 (10 nM; n=12), 30% loading (n=6) and T3+30% loading (10 nM; n=9), **[B]** Control and 30% loading merged (n=21) versus T3 and T3+30% loading merged (10 nM; n=21). RT-PCR analysis of COL1A1, COL10A1, ALPL and EPAS1 after **[C]** T3 (10 nM; n=12), 30% loading (n=6) and T3+30% loading (10 nM; n=9) **[D]** Control and 30% loading merged (n=21) versus T3 and T3+30% loading merged (10 nM; n=21). Data is presented in a boxplot depicting the median, lower and upper quartiles and each black dot represents a single explant. \* $P < 0.05$ , \*\* $P < 0.01$ , \*\*\* $P < 0.001$ .

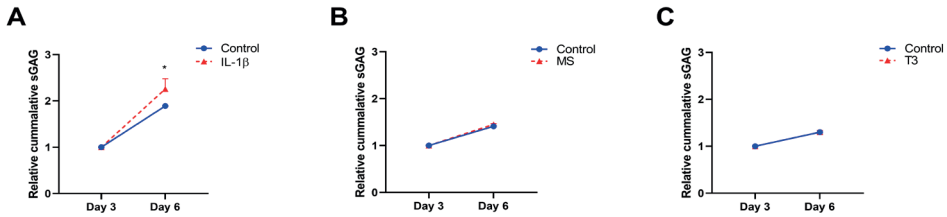


**Figure S3 | sGAG concentration in the media of osteochondral explants on day 3 and 6.** Cumulative sGAG released relative to day 3 levels from cartilage into conditioned media of osteochondral explants in presence of **[A]** IL-1 $\beta$  (10ng/ml; n=2), **[B]** MS (n=13-17) or **[C]** T3 (10nM; n=7-9) as determine by the DMMB assay. Data is represented as mean  $\pm$  s.e.m. \*P<0.05, \*\*P<0.01. S.e.m.<0.05 are not distinguishable in the figure.

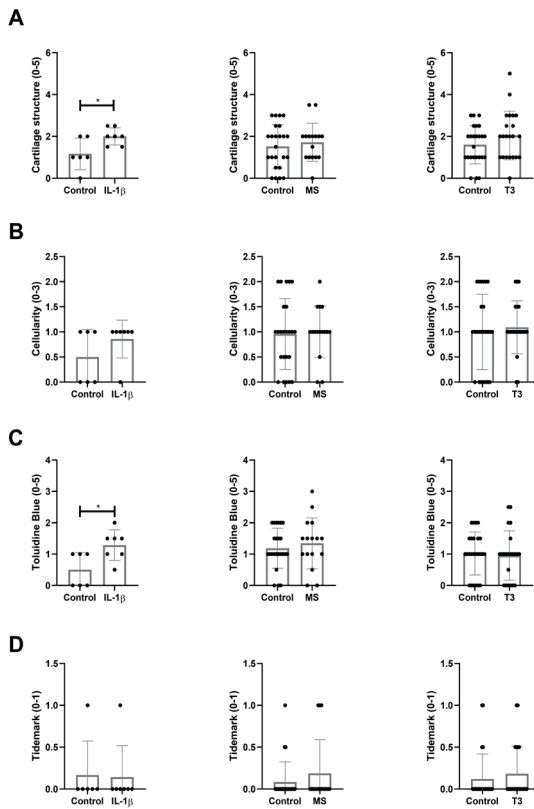


**Figure S4 | Sub categories of the Mankin Score of cartilage after treatment with either IL-1 $\beta$ , T3 or 65% mechanical stress.** Cartilage damage was assessed after perturbation with IL-1 $\beta$  (n=6), 65% MS (n=16/24) or T3 (n=22/24) with a modified Mankin Score. In this scoring system cartilage was scored based on **[A]** cartilage structure, **[B]** cellularity, **[C]** loss of sGAG in toluidine blue stainings and **[D]** tidemark integrity. Data is represented as mean  $\pm$  s.e.m and each black dot represents a single explant. \*P<0.05, \*\*P<0.01, \*\*\*P<0.001.

2

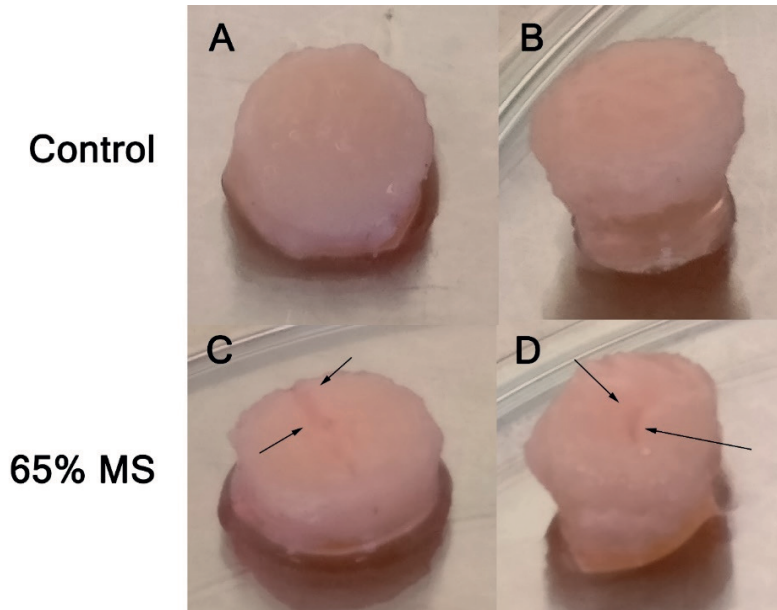


**Figure S5. Macroscopical pictures of osteochondral explants after 65% mechanical stress (65% MS) is applied and controls.** Prior to harvest on day 13, pictures were taken of the cartilage surface of all osteochondral explants. **[A and B]** Photograph of control osteochondral explants show no major abnormalities on the cartilage surface. **[C and D]** Photograph of 65% mechanical stressed osteochondral explants. Arrows indicate visible cartilage fissures and cracks.







# Chapter 3

## Elucidating mechano-pathology of osteoarthritis: transcriptome-wide differences in mechanically stressed aged human cartilage explants

Evelyn Houtman<sup>1</sup>, Margo Tuerlings<sup>1</sup>, Janne Riechelman<sup>1</sup>, Eka (H.E.D.) Suchiman<sup>1</sup>, Robert van der Wal<sup>2</sup>, Rob G.H.H. Nelissen<sup>2</sup>, Hailing Mei<sup>3</sup>, Yolande F.M. Ramos<sup>1</sup>, Rodrigo Coutinho de Almeida<sup>1</sup>, Ingrid Meulenbelt<sup>1</sup>

<sup>1</sup>*Molecular Epidemiology, Department of Biomedical Data Sciences, Leiden University Medical Center, Leiden, The Netherlands.*

<sup>2</sup>*Department of Orthopaedics, Leiden University Medical Center, Leiden, The Netherlands.*

<sup>3</sup>*Sequencing Analysis Support Core, Leiden University Medical Centre, Leiden, The Netherlands.*

**Published in:** *Arthritis Research & Therapy*. 2021;Vol 23: 215  
doi: 10.1186/s13075-021-02595-8

## Abstract

### Background

Failing of intrinsic chondrocyte repair after mechanical stress is known as one of the most important initiators of osteoarthritis. Nonetheless, insight into these early mechano-pathophysiological processes in age related human articular cartilage is still lacking. Such insights are needed to advance clinical development. To highlight important molecular processes of osteoarthritis mechano-pathology, the transcriptome-wide changes following injurious mechanical stress on human aged osteochondral explants were characterized.

### Methods

Following mechanical stress at a strain of 65% (65%MS) on human osteochondral explants ( $n_{65\%MS}=14$  versus  $n_{control}=14$ ), RNA sequencing was performed. Differential expression analysis between control and 65%MS was performed to determine mechanical stress-specific changes. Enrichment for pathways and protein-protein interactions was analyzed with Enrichr and STRING.

### Results

We identified 156 genes significantly differentially expressed between control and 65%MS human osteochondral explants. Of note, *IGFBP5* (FC=6.01; FDR=7.81x10<sup>-3</sup>) and *MMP13* (FC=5.19; FDR=4.84x10<sup>-2</sup>) were the highest upregulated genes, while *IGFBP6* (FC=0.19; FDR=3.07x10<sup>-4</sup>) was the most downregulated gene. Protein-protein interactions were significantly higher than expected by chance ( $P=1.44x10^{-15}$  with connections between 116 out of 156 genes). Pathway analysis showed, among others, enrichment for cellular senescence, insulin-like growth factor (IGF) I & II binding, and focal adhesion.

### Conclusions

Our results faithfully represent transcriptomic wide consequences of mechanical stress in human aged articular cartilage with *MMP13*, IGF binding proteins, and cellular senescence as the most notable results. Acquired knowledge on the as such identified initial, osteoarthritis related, detrimental responses of chondrocytes may eventually contribute to the development of effective disease-modifying osteoarthritis treatments.

### Keywords

Osteoarthritis, cartilage, chondrocytes, mechanical stress, mechanopathology, RNA-sequencing, cellular senescence, IGF-1 signalling, MMP13

## Introduction

Osteoarthritis (OA) is an age-related joint disease, affecting diarthrodial joints [1,2]. Despite the fact that OA is the most prevalent and disabling disease among elderly, resulting in high social and economic burden, no effective treatment exists except for lifestyle changes, pain medication and eventually a joint replacement surgery at end stage-disease [3,4].

To characterize deregulated signalling pathways in OA cartilage, comprehensive differential expression analyses have been performed comparing preserved versus end-stage lesioned OA cartilage [5]. These studies revealed that OA pathology is marked by recuperation of growth plate signaling, wound healing, and skeletal system development, while also highlighting inherent differences in OA pathophysiology between patient subtypes based on gene expression changes [5-7]. Nonetheless, the preserved versus lesioned study design by definition captures end-stage pathophysiological OA disease processes and gives no information on early initial processes triggering cartilage to become diseased. In contrast, disease-modifying OA drugs should preferably target early OA disease triggers when irreversible damage of cartilage has not yet taken place. Therefore more knowledge on the initial response of chondrocytes to OA relevant stresses, such as mechanical trauma, should be investigated in an appropriate model.

In this regard, failing of intrinsic chondrocyte repair after mechanical stress is known to impact the integrity of articular cartilage via cell apoptosis [8], increased catabolic gene expression [9], and reduced matrix production [10] and is, as such, an important trigger to OA onset. Nonetheless, little knowledge exists on the inherent dysregulation of signaling pathways initiating repair responses in human aged articular cartilage upon mechanical stress. To gain some insight, several *in vivo* animal studies have investigated the effect of joint overuse or trauma on gene expression in cartilage [11-16]. Some examples of non-invasive *in vivo* mechanical loading studies are Bomer et al. [11], reporting on involvement of metabolic processes and skeletal system development pathways upon physiological forced running in 6-month-old mice, Chang et al. [12], reporting on involvement of cell proliferation and chondroitin sulfate proteoglycan metabolic process upon injurious tibial compression in 16-week-old mice and Sebastian et al. [13], reporting on single-Cell RNA-seq upon tibial compression in 10-week-old mice. Thus far, one study has investigated genome-wide expression consequences of an impact injury in porcine explants and identified involvement of genes associated with matrix molecules, protein biosynthesis, skeletal development, and cell proliferation [17]. Nevertheless, most studies were performed using relatively young animal tissues and likely do not cover the biological response to a trauma in adult (human) tissue [18]. More recently, global gene expression profiling in 14-month-old mice subjected to non-invasive injurious tibial compression identified genes involved in inflammation and matrix regeneration to be involved in the response of aged tissue [14].

A more appropriate model to identify which molecular processes are initiated in response to mechanical stress in humans would comprise of aged human *ex vivo* osteochondral explants. Injurious compression reaching strains above 50% induced catabolic processes in cartilage and eventually led to cell death [19]. In aged human osteochondral explants, injurious cyclic mechanical stress at a strain of 65% (65%MS), mimicking trauma, was previously shown to induce OA like damage [20]. In the current study we therefore exploited our previously established *ex vivo* osteochondral explant model by performing RNA sequencing on explants subjected to injurious mechanical stress in comparison to controls. The hypothesis free,

transcriptome wide approach presented here contributes to further understanding the debilitating response of aged chondrocytes to mechanical injury and how this affects their propensity to enter an OA disease state.

## **Material and Methods**

### ***Sample description***

To generate osteochondral explants, biopsies (diameter of 8 mm) were punched from the macroscopically preserved load-bearing area of femoral condyles of human knee joints obtained within the Research in Articular Osteoarthritis Cartilage (RAAK) biobank containing patients that undergo a joint replacement surgery as a consequence of OA [21]. For this study, a total of 60 osteochondral explants were investigated originating from nineteen independent donors in which multiple explants were taken from each donor. This difference between the amount of samples taken per donor was dependent on several factors. Among them were size of the knee condyle, size of the preserved area, surgical damage area, and other simultaneous experiments this donor was used for. RNA-sequencing was performed on samples from nine donors, while the remaining ten donors were used for replication purposes. All donor characteristics are given in **Table S1** and were equal between mechanical stressed and control explant donors.

### ***Application of mechanical stress***

Explants of nineteen donors were equilibrated in serum-free chondrogenic differentiation medium (DMEM, supplemented with Ascorbic acid (50 µg/ml; Sigma-Aldrich; Zwijndrecht, The Netherlands), L-proline (40 µg/ml; Sigma-Aldrich), sodium pyruvate (100 µg/ml; Sigma-Aldrich), dexamethasone (0.1 µM; Sigma-Aldrich), ITS+ and antibiotics (100 U/ml penicillin; 100 µg/ml streptomycin) in a 5% (v/v) CO<sub>2</sub> incubator at 37°C. As depicted in **Figure 1a**, after a six day period, dynamic unconfined compression was applied to explants (diameter of 8 mm) using the Mach-1 mechanical testing system on four subsequent days (Biomomentum Inc., Laval, QC, Canada). In short, osteochondral explants were placed under an indenter (diameter of 10 mm) attached to a 250N MACH-1 load cell (Figure 1a) and unconfined cyclic compression was applied at a strain of 65% of cartilage height at a frequency of 1 Hz (1 compression cycle per second), mimicking walking speed, during 10 minutes, long enough to be injurious and short enough for chondrocytes to survive, at strains suggested to be detrimental [22]. Dynamic (cyclic) compression means that a force was applied that varied over time to simulate a more cyclic compression such as walking. To investigate lasting effects of mechanical stress, four days after mechanical stress, the cartilage and bone were separated, snap-frozen in liquid nitrogen and stored at -80 °C.

### **Determining cartilage integrity**

#### ***Histology***

A sagittal section of the osteochondral explant was fixed in 4% formaldehyde for one week and

decalcified using EDTA (12.5%, pH=7.4) during two weeks, dehydrated with an automated tissue processing apparatus and embedded in paraffin. Tissue sections were cut at a thickness of 5  $\mu\text{m}$ , deparaffinized, rehydrated, subsequently stained for 1 minute in a toluidine blue solution with a pH of 2.5 (Sigma-Aldrich) and mounted with Pertex (Sigma-Aldrich) to investigate cartilage integrity as quantified by applying Mankin Score [23].

### ***Sulfated glycosaminoglycan (sGAG) measurement***

Sulfated glycosaminoglycan (sGAG) concentrations in conditioned media collected from osteochondral explants were measured with the photometric 1.9 dimethylene blue (DMMB; Sigma-Aldrich) dye method [24]. Shark chondroitin sulfate (Sigma-Aldrich) was used as the reference standard. The concentration of sGAG was determined in conditioned media collected on day 13, by measuring absorbance at 525nm and 595nm in a microplate reader (Synergy HT; BioTek, Winooski, USA).

### ***RNA sequencing***

RNA from cartilage was extracted by pulverizing the tissue and subsequently homogenizing the powder in TRIzol reagent (Invitrogen, San Diego, CA) using a Mixer mill 200 (Retsch, Germany). RNA was extracted using chloroform, followed by precipitation using ethanol, and purified with the RNeasy Mini Kit (Qiagen, Chatsworth, CA). Genomic DNA was removed by DNase digestion. Paired-end 2x150 base pair RNA sequencing (Illumina TruSeq mRNA Library Prep Kit, Illumina HiSeq X ten) was performed. Strand specific RNA-sequencing libraries were generated which yielded on average 14 million reads per sample. Data from the Illumina platform was analysed with an in-house pipeline as previously described [5]. The adapters were clipped using Cutadapt v1.1. RNA-seq reads were then aligned using GSNAP against GRCh38 [25]. Read abundances per sample were estimated using HTSeq count v0.11.1 [26] with Ensembl gene annotation version 94. Only uniquely mapping reads were used for estimating expression. The quality of the raw reads and initial processing for RNA-sequencing was checked using MulitQC v1.7 [27]. Samples containing >50% genes with zero values and average read count <10 were removed from further analysis. To identify outliers, principal component analysis (PCA) was applied. For further analysis, samples not in the main cluster were removed, resulting in n=28 samples from 9 unique donors. In total, 58735 unique genes were detected by RNA sequencing of which 6509 were protein-coding genes that were included in further analyses.

### ***Differential expression analysis, protein-protein interactions and pathway enrichment***

Differential expression analysis was performed in 65%MS cartilage compared to control cartilage obtained from osteochondral explants using DESeq2 R package version 1.24 [28] on 6509 protein-coding genes. A general linear model assuming a negative binominal distribution was applied and followed by a Wald-test between control and 65%MS samples in which donor number was added as a random effect to correct for inter-individual differences. In all analyses,

control samples were set as reference. To correct for multiple testing the Benjamini-Hochberg method was used, as indicated by the false discovery rate (FDR) in which a significant cutoff value of 0.05 was used. Furthermore, the comprehensive gene set enrichment analysis web tool Enrichr [29] was used to identify enrichment for gene ontologies (Cellular Component, Biological Process, Molecular Function) and pathways (KEGG and Reactome). For protein-protein interactions, analysis was performed using the online tool STRING version 11.0 [30].

### ***Real-time quantitative PCR (RT-qPCR) validation***

250 ng of RNA was processed into cDNA using the First Strand cDNA Synthesis Kit (Roche Applied Science, Almere, The Netherlands). RT-qPCR was performed on 10 paired 65%MS samples with matched controls included in the RNA-sequencing (Technical validation) and 10 novel paired 65%MS samples with matched controls (Biological validation) to determine the expression of six downregulated (*IGFBP6*, *CNTFR*, *WISP2*, *FRZB*, *COL9A3*, and *GADD45A*) and four upregulated genes (*IGFBP5*, *PTGES*, *TNC*, and *IGFBP4*). Primer sequences are listed in **Table S2**. The relative gene expression was normalized for two endogenous reference genes, *SDHA* and *YWHAZ*, to determine  $-\Delta\Delta CT$  values. To determine effect sizes, fold changes (FC) were calculated according to the  $2^{-\Delta\Delta CT}$  method, in which expression of 65%MS was extracted from controls ( $-\Delta\Delta CT$ ). These two endogenous reference genes were chosen based on literature stating the stability of these genes in response to mechanical stress, which was confirmed by our RNA-sequencing [31,32].

### ***Statistical analysis***

Analysis on RNA-sequencing data was performed in R as described above. Statistical analysis for RT-qPCR and sGAG concentrations were performed using IBM SPSS statistics 25. The P-values were determined by applying a linear generalized estimating equation (GEE) to effectively adjust for dependencies among donors of the explants by adding a random effect for the sample donor as we did not have perfect pairs for each analysis [33]. The following GEE was fitted in which gene expression was the dependent variable and treatment the covariate: *Gene expression*  $\sim$  *Treatment* + (1|*donor*). To determine differences in sGAG concentration on day 13, another linear GEE model was fitted with sGAG concentration as dependent variable and treatment as covariate: *sGAG concentration*  $\sim$  *Treatment* + (1|*donor*).

## Results

Prior to RNA-sequencing, cartilage tissue integrity of human osteochondral explants was characterized by performing histology and measuring sGAG concentrations in conditioned media. Mechanical strains at 65% cause detrimental changes to cartilage integrity as previously shown [20] (**Figure 1B**) and these effects were further explored in a larger samples size ( $n_{\text{control}}=31$ ;  $n_{65\%MS}=28$ ), where an increased sGAG release was measured in 65%MS cartilage when compared to controls (**Figure 1C**).

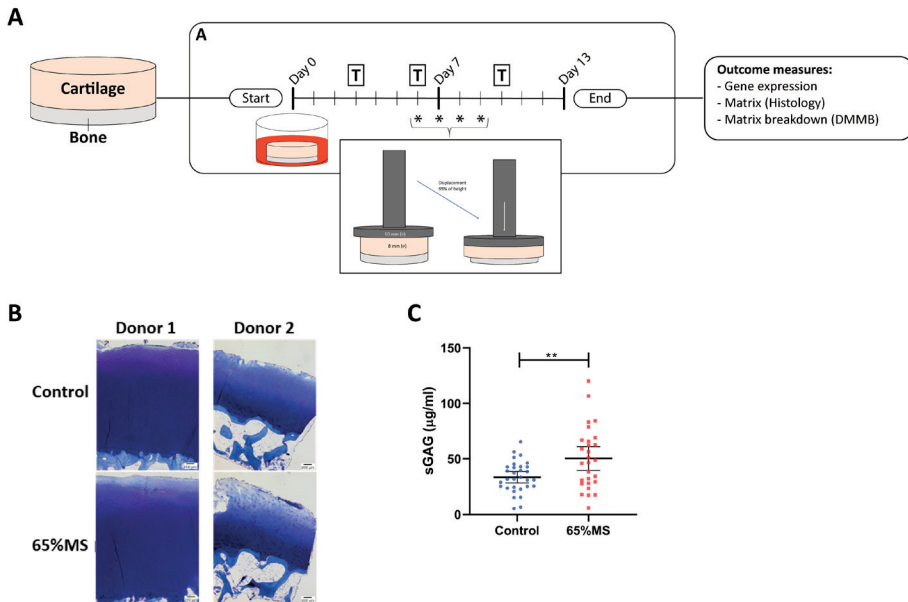


**Figure 1 | Study setup of human osteochondral explants receiving 65% MS.** [A] osteochondral explants were punched from preserved areas of knee joints and medium is refreshed on indicated days (T). [B] Damage in our mechanical stress model was confirmed by degradation of sGAG in cartilage by toluidine blue staining (histology of two independent donors) and measuring [C] sGAG release in conditioned media on day 13 ( $n_{\text{control}}=31$  versus  $n_{65\%MS}=28$ ). Figure 1C shows the average  $\pm$  95%CI and each dot represents a sample. To adjust for donor variation, P-values were estimated by performing logistic generalized estimation equations, with sGAG concentration as dependent variable and treatment as covariate:  $\text{sGAG concentration} \sim \text{Treatment} + (1|\text{Donor})$ .  $***P \leq 0.01$ . Legend: 65%MS= 65% mechanical stress, DMMB= dimethylmethylene blue, sGAG= sulphated glycosaminoglycans.

### Differential expression of genes responsive to injurious mechanical stress

To characterize the response of cartilage to mechanical stress at a strain of 65% indentation in aged articular cartilage, we performed RNA-sequencing on control ( $n=14$  samples) and 65% mechanically stressed ( $n=14$  samples) articular cartilage samples obtained from macroscopically preserved osteochondral explants of human patients that underwent a knee replacement surgery due to OA. Baseline characteristics of donors of the RNA-sequencing dataset are depicted in **Table S1a**. We found 156 genes to be significantly differentially expressed (DE) ( $\text{FDR} < 0.05$ ) with absolute fold changes (FC) ranging between 1.1 and 6.0 (**Figure 2, Table S3**). Among these 156 DE genes, 46 (29%) were upregulated and 110 (71%) were downregulated. The 20 genes with the highest absolute FC, and their respective direction of effect previously identified in OA cartilage [5], are shown in **Table 1**. Notable among the upregulated genes were *IGFBP5* ( $\text{FC}=6.01$ ;  $\text{FDR}=7.81 \times 10^{-3}$ ), *MMP13* ( $\text{FC}=5.19$ ;

FDR=4.84x10<sup>-2</sup>), *TNC* (FC=2.80; FDR=8.51x10<sup>-3</sup>), and *PTGES* (FC=2.92; FDR=8.29x10<sup>-3</sup>). Notable genes among the downregulated genes were *IGFBP6* (FC=0.19; FDR=3.07x10<sup>-4</sup>), *CNTFR* (FC=0.27; FDR=1.44x10<sup>-2</sup>), *WISP2* (FC=0.31; FDR=1.08x10<sup>-3</sup>), and *FRZB* (FC=0.32; FDR=8.51x10<sup>-3</sup>).

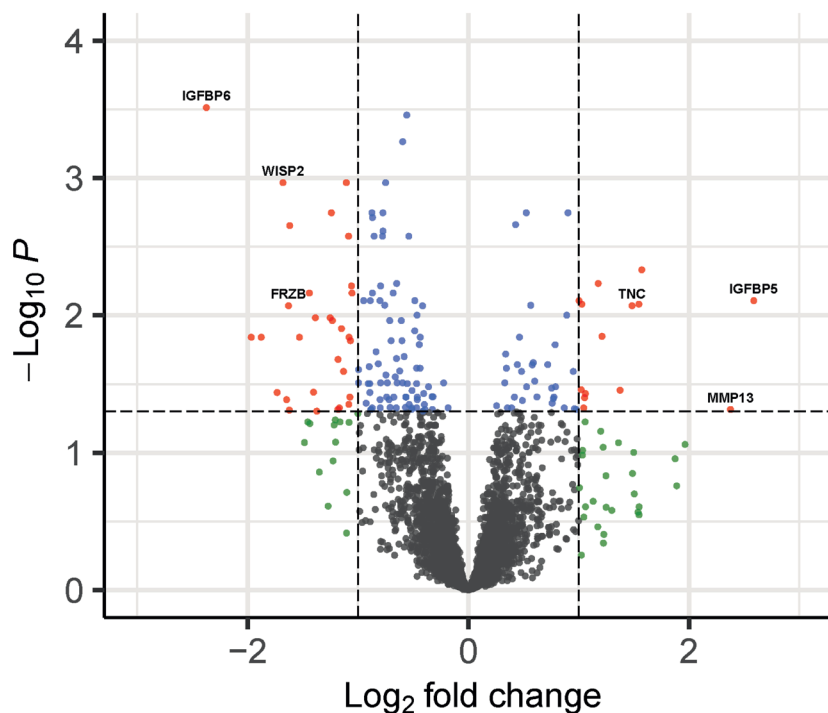


**Figure 2 | Volcano plot of differentially expressed genes.** Dots represent genes expressed in mechanically stressed cartilage in comparison to control osteochondral explant cartilage. Red dots represent significantly differentially expressed (DE) genes that have an absolute fold change (FC) of  $\geq 2$ , blue dots represent significantly DE genes, green dots represent genes that have an absolute FC of  $\geq 2$  but are not significantly DE and grey dots represent genes not DE expressed between controls and 65% mechanically stressed cartilage. The FC presented here is the gene expression of 65% mechanically stressed relative to control cartilage.

### Validation of differentially expressed genes with mechanical stress

For validation and replication of the differentially expressed genes identified, a set of samples for technical (n=10 pairs) and biological (n=10 pairs) replication was selected for RT-qPCR. Baseline characteristics of donors in the replication dataset are depicted in **Table S1b**. Replication was performed for ten genes (**Figure 3**), of which six were upregulated (*IGFBP6*, *CNTFR*, *WISP2*, *FRZB*, *COL9A3*, and *GADD45A*) and four were downregulated (*IGFBP5*, *PTGES*, *TNC*, and *IGFBP4*). Technical replication showed a significant difference for all ten genes between controls and 65%MS cartilage, with similar direction and size of effects. Biological replication also showed the same direction of effects and similar effect sizes as identified in the RNA-sequencing data. For *GADD45A*, however, the difference was not significant (P-value=0.12). Taken together, technical and biological replication confirmed the robustness of our RNA-sequencing results.

**Table 1 | Top 20 genes with the highest absolute FC in 65% mechanically stressed cartilage compared to controls.**

Ensemble ID	Gene name	FC	FDR <sup>a</sup>	Differential expression in OA cartilage[5] <sup>b</sup>
ENSG00000115461	<i>IGFBP5</i>	6.01	7.81x10 <sup>-3</sup>	
ENSG00000137745	<i>MMP13</i>	5.19	4.84x10 <sup>-2</sup>	
ENSG00000204103	<i>MAFB</i>	2.97	4.66x10 <sup>-3</sup>	↓
ENSG00000148344	<i>PTGES</i>	2.92	8.29x10 <sup>-3</sup>	↑
ENSG00000041982	<i>TNC</i>	2.80	8.51x10 <sup>-3</sup>	↑
ENSG00000141753	<i>IGFBP4</i>	2.59	3.50x10 <sup>-2</sup>	↑
ENSG00000160111	<i>CPAMD8</i>	0.39	4.98x10 <sup>-2</sup>	↓
ENSG00000166165	<i>CKB</i>	0.38	1.04x10 <sup>-2</sup>	↑
ENSG00000106258	<i>CYP3A5</i>	0.38	3.62x10 <sup>-2</sup>	
ENSG00000107736	<i>CDH23</i>	0.37	6.88x10 <sup>-3</sup>	
ENSG00000187720	<i>THSD4</i>	0.35	1.44x10 <sup>-2</sup>	
ENSG00000144908	<i>ALDH1L1</i>	0.33	2.22x10 <sup>-3</sup>	↓
ENSG00000092758	<i>COL9A3</i>	0.32	4.89x10 <sup>-2</sup>	
ENSG00000162998	<i>FRZB</i>	0.32	8.51x10 <sup>-3</sup>	↓
ENSG00000170891	<i>CYTL1</i>	0.32	4.11x10 <sup>-2</sup>	
ENSG00000064205	<i>WISP2</i>	0.31	1.08x10 <sup>-3</sup>	↓
ENSG00000082196	<i>C1QTNF3</i>	0.30	3.64x10 <sup>-2</sup>	↑
ENSG00000122756	<i>CNTFR</i>	0.27	1.44x10 <sup>-2</sup>	↓
ENSG00000165966	<i>PDZRN4</i>	0.26	1.44x10 <sup>-2</sup>	↓
ENSG00000167779	<i>IGFBP6</i>	0.19	3.07x10 <sup>-4</sup>	

<sup>a</sup> To correct for multiple testing, the Benjamini-Hochberg method was applied to p-values and reported as the false discovery rate (FDR). <sup>b</sup> Gene expression changes measured in RNA-sequencing data between preserved and lesioned OA articular cartilage, with preserved as reference [5]. Legend: FC=fold change; FDR= false discovery rate.

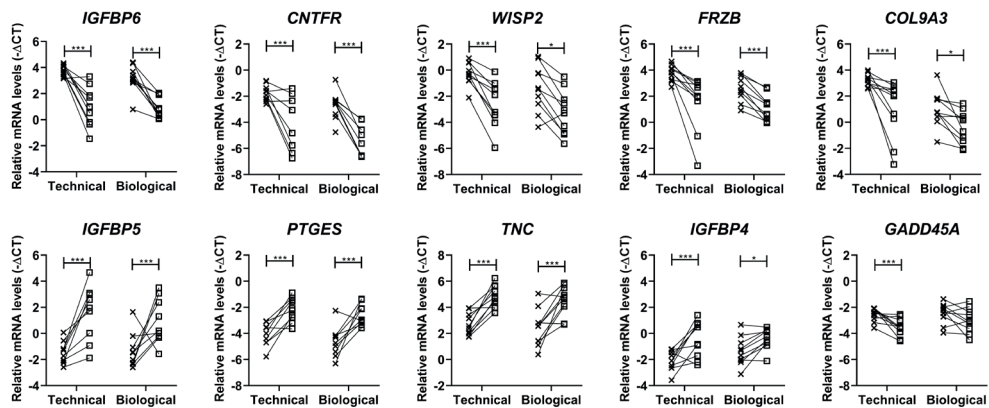


**Figure 3 | Technical and biological validation of the highest up- and downregulated genes was performed using RT-qPCR.** Expression of six downregulated (*IGFBP6*, *CNTFR*, *WISP2*, *FRZB* and *GADD45A*) and four upregulated (*IGFBP5*, *PTGES*, *TNC* and *IGFBP4*) genes was measured in n=10 paired technical and n=10 paired biological osteochondral explants. Figures show connected paired samples and  $-\Delta CT$  of each independent sample is depicted by crosses (control) or open squares (65%MS) in the graphs. Statistical differences between gene expression in control and 65% mechanically stressed was determined with a linear generalized estimation equation (GEE) with mRNA level as dependent variable. \*P $\leq$ 0.05; \*\*\*P $\leq$ 0.001. Legend: 65%MS: 65% mechanical stress, RT-qPCR: reverse transcriptase-quantitative PCR.

3

### *In silico exploration of differentially expressed genes*

To explore whether significant DE genes (N=156 genes) were involved in particular pathways, they were further analyzed using Enrichr. Gene enrichment was observed, among others, for insulin-like growth factor I & II binding (GO:0031995; GO:0031994, Padj=1.83x10<sup>-2</sup>; Padj=2.89x10<sup>-2</sup>, involving *IGFBP4*, *IGFBP5*, and *IGFBP6*), cellular senescence (hsa04218, Padj=1.15x10<sup>-2</sup>, involving 8 genes, e.g. *GADD45A*, *MYC*, *SERPINE1*, and *FOXO1*) and focal adhesion (GO:0005925; hsa04510, Padj=2.54x10<sup>-2</sup>; Padj=1.33x10<sup>-2</sup>, involving 11 and 6 genes, respectively, e.g. *TNC*, *CAV1*, and *TLN2*) (**Table 2**; **Table S4a**).

**Table 2 | Gene ontology and pathway enrichment analysis of differentially expressed genes in mechanically stressed cartilage.**

Term	Entry	Overlap	Adj P-value <sup>a</sup>	Odds Ratio	Genes
Cellular senescence	hsa04218	8/160	1.15x10 <sup>-2</sup>	6.41	GADD45A, MYC, SERPINE1, AKT3, EIF4EBP1, SLC25A5, ETS1, FOXO1
Focal adhesion	hsa04510	8/199	1.33x10 <sup>-2</sup>	5.15	SHC4, CAV1, ITGA10, AKT3, LAMA3, TNC, COL9A3, TLN2
Insulin-like growth factor II binding	GO:0031995	3/7	1.83x10 <sup>-2</sup>	54.95	IGFBP5, IGFBP4, IGFBP6
Focal adhesion	GO:0005925	11/356	2.54x10 <sup>-2</sup>	3.96	ENAH, EHD3, GSN, CAV1, TNC, CD9, TLN2, RPL10A, DCAF6, RHOB, ENG
Insulin-like growth factor I binding	GO:0031994	3/13	2.89x10 <sup>-2</sup>	29.59	IGFBP5, IGFBP4, IGFBP6

<sup>a</sup> Enrichr uses a modified Fishers exact test to compute enrichment and this is reported as the adjusted p-value [29]. Legend: Adj P-value= adjusted P-value.

To visualize interacting proteins, the online tool STRING was used. Among the 156 genes, 116 of the encoded proteins showed significant protein-protein interactions (PPI) ( $P=1.44 \times 10^{-15}$ ; **Figure 4**). Among these proteins we found several that have many connections with other proteins in the DE gene network, such as *GAPDH* with 35 connections, *IGFBP5* with 12 connections and the in cellular senescence involved genes *MYC* and *FOXO1* with respectively 26 and 13 connections to other DE genes. Moreover, two clusters of genes are observed that correspond with two of the pathways identified. One cluster corresponds with genes found mainly in the cellular senescence pathway (**Figure 4**, dotted circle), while the other cluster consists of proteins that are involved in IGF-1 signaling (**Figure 4**, black circle).

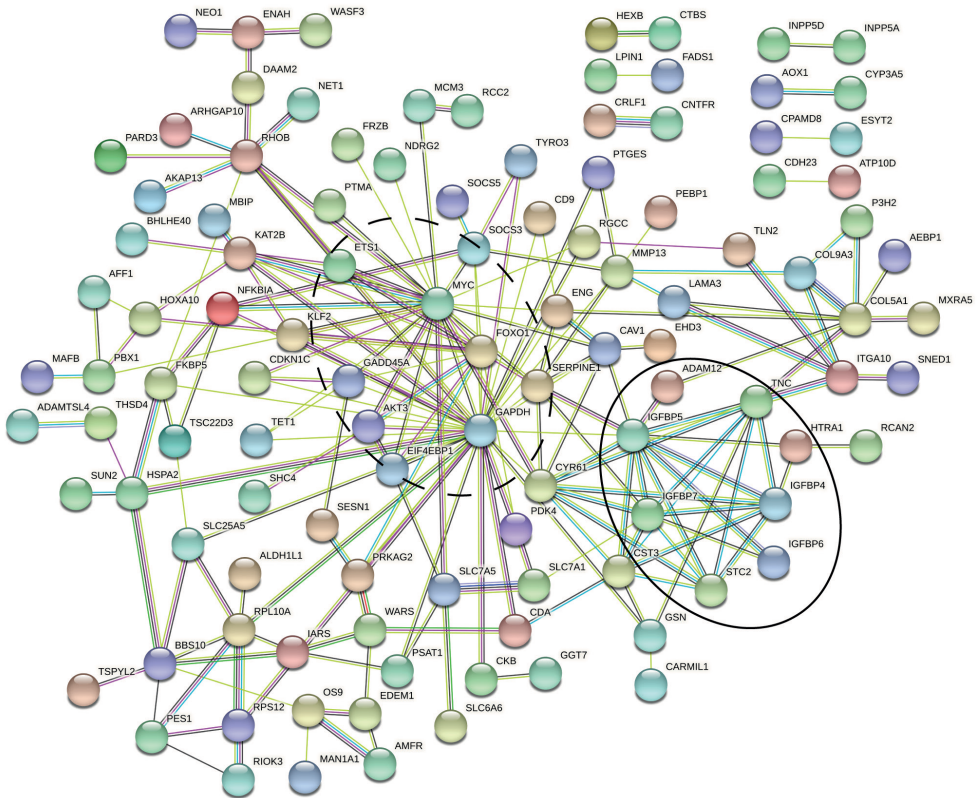


**Figure 4 | Protein-protein interaction network in STRING of proteins encoded by differentially expressed genes.** Only connected (N=116 genes) genes that were identified to be differentially expressed between mechanically stressed and control cartilage of osteochondral explants are shown. Two clusters with high interactions were identified upon studying connections within String. One cluster corresponds with genes found in the cellular senescence pathway (dotted circle), while the other cluster consists of proteins that are involved in IGF-1 signaling (black circle).

### **Comparison between mechanical stress genes and OA responsive genes.**

To investigate to what extent the genes DE with mechanical stress ( $DE_{MS}$ ) coincide with OA pathophysiology, we next compared the  $DE_{MS}$  genes (**Table S3**) to previously identified genes DE between preserved and lesioned OA cartilage ( $DE_{OA}$ ) [5]. Of the 156  $DE_{MS}$  genes, 64 were previously identified with OA pathophysiology and their majority (48 genes, 75%) had the same direction of effect (**Table 1** and **Table S5a**, **Figure S1**). Notable genes coinciding with OA pathophysiology and showing the same direction of effect are the highly downregulated *FRZB*, *WISP2*, and *CNTFR* and the upregulated *PTGES* and *CRLF1*.

Next, we selected for exclusive mechanical stress responsive genes i.e.  $DE_{MS}$  genes, not overlapping with previously identified  $DE_{OA}$  genes [5]. This resulted in 92 genes that were differentially expressed exclusively in response to mechanical stress ( $DE_{ExclusiveMS}$ ; **Table S6**; **Figure S1**). Notable  $DE_{ExclusiveMS}$  genes are the downregulated *IGFBP6*, *ITGA10*, and *COL9A3* and the upregulated *IGFBP5*, *MMP13*, and *GAPDH*. Subsequent pathway analyses showed gene enrichment among genes involved in focal adhesion (GO:0005925,  $P_{adj}=0.02$ , 9 genes, e.g. *CD9*, *RPL10A*, and *ENAH*) and kinase inhibitor activity (GO:0019210,  $P_{adj}=0.01$ , 5 genes,

e.g. *CDKN1C*, *SOCS3*, and *SOCS5*) (**Table S4b**). Upon exploring protein-protein interactions between the 92 DE<sub>ExclusiveMS</sub> genes using STRING, a highly significant enrichment for PPI was identified ( $P=1.07 \times 10^{-4}$ ; **Figure S2**), indicating that these genes act together or respond in concert to detrimental mechanical stress.

### **OA risk genes responding to mechanical stress**

Finally, to investigate which OA risk genes are represented among the mechanically stress responsive genes in cartilage, we checked  $N=90$  genes previously recognized as strong OA risk genes [34] identified in recent genome-wide association studies (GWAS) [35,36]. As shown in **Table S7**, two of our identified DE<sub>MS</sub> genes were also shown to be an OA risk gene in previous studies. These genes were *TNC*, encoding for tenascin C, which was highly increased ( $FC=2.80$ ;  $FDR=8.5 \times 10^{-3}$ ) upon 65%MS and *SCUBE1*, encoding for signal peptide, CUB domain and EGF like domain containing 1, which was decreased ( $FC=0.53$ ;  $FDR=0.04$ ) upon 65%MS.

## **Discussion**

To our knowledge we are the first to report genome-wide differentially expressed mRNAs in articular cartilage following repeated exposure to 65% mechanical stress using a human *ex vivo* osteochondral explant model. Since injurious loading is considered a major trigger in the initiation of OA onset, the results presented in our manuscript contribute important insight into how injurious stress affects the propensity of aged human articular chondrocytes to lose their steady state towards a debilitating OA disease state. Notable genes identified were different members of the insulin-like growth factor I & II binding family (*IGFBP6*, *IGFBP5*, and *IGFBP4*) and the catabolic gene *MMP13*. Gene enrichment analyses showed that cellular senescence (*GADD45A*, *MYC*, *SERPINE1*, and *FOXO1*) and focal adhesion (*ITGA10*, *TLN2*, and *CAV1*) processes are significantly changing in articular cartilage with injurious loading. Together, identified genes and pathways facilitate clinical development by exploring ways to counteract these initial unbeneficial responses to injurious loading by supplementing or inhibiting of key genes. Moreover, we advocate that here identified specific responsive genes to injurious loading can function as sensitive markers facilitating the development of scientifically founded strategies with respect to preventive or curative exercise OA therapy among elderly.

Among the highest FDR significantly upregulated genes with 65% mechanical stress we identified *MMP13*, encoding matrix metalloproteinase 13 ( $FC=5.19$ ;  $FDR=4.84 \times 10^{-2}$ ) [20]. *MMP13* is involved in the detrimental breakdown of extracellular matrix in articular cartilage by cleaving, among others, collagen type II. Despite the well-known role of *MMP13* in collagen type II breakdown, it should be noted that the *MMP13* gene is not found to be responsive with end-stage OA pathophysiology, i.e., not consistent and not among the genes highest differentially expressed between preserved and lesioned OA cartilage (**Table 1**) [5,21,37]. We therefore advocate that *MMP13* expression could specifically mark initial responses to cartilage damage and not that of a chronic degenerative OA disease state. Henceforth, abrogating the *MMP13* signaling shortly after an injurious cartilage event could prevent the detrimental downstream enzymatic breakdown of extracellular matrix proteins. Moreover, and as indicated above, *MMP13* may be a suitable candidate sensitively marking injurious

loading of aged human articular cartilage independent of other physiological factors such as OA disease state.

Four out of seven members of the insulin growth factor binding proteins (*IGFBP4*, *IGFBP5*, *IGFBP6*, and *IGFBP7*; **Table S8**), were found to be FDR DE. *IGFBP1-6* have an equal or greater affinity for binding IGF-1 when compared to IGF-1R; hence most of IGF-1 in the body is bound to IGFBPs, antagonizing IGF-1 signaling [38-41]. On the other hand, *IGFBP7* has a low affinity for IGF and therefore more likely affects cell metabolism via binding to activin A, influencing the growth-suppressing effects of TGF- $\beta$ , and antagonizing bone morphogenetic protein (BMP) signaling [42,43]. *IGFBP4* and *IGFBP5* can also function as transporter and bring IGF-1 close to its receptor, where IGF-1 is released via cleavage by proteins such as pregnancy-associated plasma protein-A (PAPPA), HtrA Serine Peptidase 1 (*HTRA1*) and disintegrin and metalloproteinase domain-containing protein 12 (*ADAM12*) [44-46]. Additionally notable in this respect is that three genes, *HTRA1*, *ADAM12* and *STC2* [47], involved in IGF-1 cleavage were found among the FDR significant upregulated genes in our dataset (**Table S3**). IGFBPs can also affect cells via IGF-independent mechanisms. The most noteworthy IGF-independent mechanism is observed for the highly upregulated *IGFBP5*, being induction of cell proliferation and apoptosis [48,49]. In summary our data showed that, despite the fact that the mechanical stress applied affected cartilage integrity (**Figure 1**), the upregulation of *IGFBP4* and *IGFBP5* in combination with the upregulation of its cleaving proteins might reflect an anabolic response of chondrocytes to initiate repair by increasing bio-availability of IGF-1. Two studies support our suggestion that IGF-1 signaling might be a beneficial anabolic response to mechanical stress. In an OA dog model, increasing intact *IGFBP5* proteins resulted in increased IGF-1 levels and reduced destruction of cartilage [50]. While in a human explant model, addition of IGF-1 after mechanical stress increased *COL2A1* gene expression and slightly increased cell viability [51]. Our results in combination with those previously found, suggest that addition of *IGFBP4* and/or *IGFBP5* would be an interesting therapy to further explore in combatting the catabolic response.

To identify upstream processes and to put our results in a broader perspective, we investigated connections between genes on the protein level in STRING (**Figure 4**) and determined pathway enrichment (**Table 2**) of the differentially expressed genes. Based on this pathway analysis, we identified enrichment for proteins involved in cellular senescence. DE genes with mechanical stress in this pathway have already been linked to aging and OA, such as *GADD45A*, *SERPINE1*, *MYC*, and *FOXO1*. Notable are the two transcription factors, *MYC* and *FOXO1*, showing many connections to other proteins (**Figure 4**) and previously shown to be dysregulated in OA chondrocytes [52,53]. *FOXO1* is an essential mediator of cartilage growth and homeostasis and its expression is decreased in aged and OA cartilage [52]. In addition, *FOXO1* was shown to be an antagonist of *MYC* and prevents, among others, ROS production [54,55]. Our results suggest that reduced expression of *FOXO1* could be one of the reasons for increased expression of *MYC*. As one of the known responses of chondrocytes to mechanical stress is ROS production, this would be a promising target to follow up on in future research. Next to genes in this pathway, lookup of our DE<sub>MS</sub> genes in a proteomic atlas of senescence-associated secretory phenotype (SASP) identified 35 of our DE<sub>MS</sub> genes to have previously been found in different senescent cells (**Figure S3**)[56]. Taken together, the upregulation of *MYC* in combination with upregulation of several important SASP protein markers suggests increased cellular damage is occurring upon mechanical stress likely driving cells to go into senescence. As cellular senescence is a factor that is thought to play a significant role in the OA

pathophysiology, our model could provide more knowledge on how this pathway is involved in the onset of OA and how therapeutics could be used to minimize this response [57].

To investigate whether OA risk loci could confer risk via modifying response to mechanical stress, we compared  $DE_{MS}$  genes to strong OA risk genes identified in the most recent GWAS [35,36]. This resulted in the identification of two OA risk genes, *TNC* and *SCUBE1* present in our dataset (**Table S7**). Based on allelic imbalanced expression and linkage disequilibrium, the *TNC* OA risk allele rs1330349-C, in high linkage disequilibrium with the transcript SNP rs2274836-T, appeared to act via decreasing expression of *TNC* [58]. For that matter, the observed high upregulation of *TNC* expression with mechanical stress ( $FC=2.80$ ;  $FDR=8.51 \times 10^{-3}$ ) as well as, the previously observed upregulation with OA pathophysiology ( $FC=1.41$ ;  $FDR=1.09 \times 10^{-2}$ ) [5] is likely a beneficial response to rescue or maintain articular cartilage integrity. This is further confirmed by animal studies showing that addition of exogenous TNC reduced cartilage degeneration and repaired cartilage [59,60]. In contrast, for the intronic OA risk SNP located in the vicinity of *SCUBE1* (rs528981060) we were not able to determine a transcript proxy SNP, hence potential AEI of *SCUBE1* could not be explored.

With regard to overlap with *in vivo* animal models, we compare our DE genes to those found in physiological [11], surgical destabilization of the medial meniscus (DMM) [18] and non-invasive tibial compression (TC) models [12,14]. The most striking overlap in DE genes (46 genes) was found between our model and the non-invasive TC model using gene expression data of 14 month old mice 1 week after injury. Among the overlapping genes we confirmed involvement of all *IGFBPs*, *HTRA1*, *ADAM12* and of OA associated genes such as, *FRZB*, *TNC* and *SCUBE1* in both models [14]. As also shown by other studies [14,18], age of animals used in these models can greatly influence results. This could also, next to a difference in species, partially explain why there is little overlap with other injurious mechanical stress studies.

A strength of our aged human *ex vivo* osteochondral model is that it allowed us to investigate the chondrocyte response to an OA-relevant trigger in its natural environment. In addition, our model comprises aged cartilage, which is likely more vulnerable to OA onset, and hence, results are relevant to the population at risk. Another strong point in our model is that we measure the changes in gene expression that are measured 4 days post-injury as such reflecting representative lasting changes in chondrocyte signaling rather than acute stress responses only. On the other hand, our data could facilitate treatment strategies, prior to irreversible damage of OA affected cartilage. Some limitations of our study are the relatively low sample size of 14 explants per condition, hence limiting our power. As a result we may have missed subtle gene expression changes in response to detrimental mechanical stress. Another point of our study to address is the heterogeneity of preserved cartilage collected from OA patients with Mankin scores ranging from 0 to 7. Although such heterogeneity may also have affected the power of our study, hence the total number of differentially expressed genes with injurious loading, we want to highlight that despite the differences in Mankin scores we were able to consistently detect (at the genome-wide significant level) 156 differentially expressed genes reflecting strong and/or very consistent mechano-pathological processes triggered after mechanical stress. Moreover, due to the heterogeneity in eligible waste articular cartilage after joint replacement surgery (i.e., osteochondral explants) we were not able to generate a RNA-sequencing dataset of perfect control – mechanically stressed sample pairs. Henceforth, to adjust for dependencies among control and/or mechanically stressed samples we added donor as random effect during differential expression analyses. Adding to the validity of this

approach was the fact that we successfully replicated expression changes for ten genes in ten novel independent perfectly paired samples. A final limitation of our study is that we have focused on exploring gene expression changes following mechanical stress and have not studied changes at the protein level. However, we advocate that chondrocyte signaling at the gene expression level is a more sensitive measure of underlying ongoing processes.

### **Conclusions**

To conclude, our results faithfully represent transcriptomic wide consequences of injurious loading in human aged articular cartilage with *MMP13*, IGF binding proteins, and cellular senescence as the most notable results. Since injurious loading is considered a major trigger of OA onset, these findings provide important insight into how injurious stress affects the propensity of aged human articular chondrocytes to lose their steady state towards a debilitating OA disease state. Exploring ways to counteract the initial unbeneficial responses to injurious loading may facilitate clinical development prior to the onset of irreversible damage. Moreover, we advocate that the here identified unique responsive genes to injurious loading, such as *MMP13*, can function as a sensitive marker to strategically develop preventive and/or curative exercise therapy for OA independent of other physiological factors. Preferably such an endeavor would exploit our established *ex vivo* osteochondral model while applying variable mechanical loading regimes.

### **Declarations**

#### ***Ethics approval and consent to participate***

Informed consent was obtained from participants of the RAAK biobank and ethical approval was given by the medical ethics committee of the Leiden University Medical Center (P08.239/P19.013).

#### ***Consent for publication***

Not applicable

#### ***Availability of data and materials***

The list of all significantly affected genes is included in the Supplementary data (Table S3).

#### ***Competing interests***

The authors declare that they have no competing interests

### ***Funding***

This work was supported by the Dutch Scientific Research council NWO/ZonMW VICI scheme [91816631/528] and Dutch Arthritis Society/ReumaNederland [DAF-15-4-401]. The funding body played no role in the design of the study, the collection, analysis, and interpretation of data and in writing the manuscript.

### ***Authors' contributions***

All authors have made contributions to the completion of this study. Study concept and design: EH, YFM, RCA, IM. Acquisition of material and data: EH, MT, JR, HED, RJPvdW, RGHHN, HM. Data analysis: EH, MT, RCA, IM. Preparation of the manuscript: EH, IM. Critical reviewing and approval of the manuscript: All authors.

### ***Acknowledgements***

We thank all the participants of the RAAK study. The LUMC has and is supporting the RAAK study. We also thank Enrike van der Linden, Demiën Broekhuis, Peter van Schie, Anika Rabelink-Hoogenstraaten, Shaho Hasan, Maartje Meijer, Daisy Latijnhouwers and Geert Spierenburg for collecting surgical waste material and all members of our research group. Data is generated within the scope of the Medical Delta Programs Regenerative Medicine 4D: Generating complex tissues with stem cells and printing technology and Improving Mobility with Technology. We thank the Sequence Analysis Support Core (SASC) of the Leiden University Medical Center for their support.

## REFERENCES

1. Englund M, Guermazi A, Gale D, et al. Incidental meniscal findings on knee MRI in middle-aged and elderly persons. *N Engl J Med*. 2008;359(11):1108-15.
2. Jordan JM, Helmick CG, Renner JB, et al. Prevalence of knee symptoms and radiographic and symptomatic knee osteoarthritis in African Americans and Caucasians: the Johnston County Osteoarthritis Project. *J Rheumatol*. 2007;34(1):172-80.
3. Woolf AD, Erwin J, March L. The need to address the burden of musculoskeletal conditions. *Best Pract Res Clin Rheumatol*. 2012;26(2):183-224.
4. Tonge DP, Pearson MJ, Jones SW. The hallmarks of osteoarthritis and the potential to develop personalised disease-modifying pharmacological therapeutics. *Osteoarthritis Cartilage*. 2014;22(5):609-21.
5. Coutinho de Almeida R, Ramos YFM, Mahfouz A, et al. RNA sequencing data integration reveals an miRNA interactome of osteoarthritis cartilage. *Ann Rheum Dis*. 2019;78(2):270-7.
6. Soul J, Dunn SL, Anand S, et al. Stratification of knee osteoarthritis: two major patient subgroups identified by genome-wide expression analysis of articular cartilage. *Ann Rheum Dis*. 2018;77(3):423.
7. Coutinho de Almeida R, Mahfouz A, Mei H, et al. Identification and characterization of two consistent osteoarthritis subtypes by transcriptome and clinical data integration. *Rheumatology (Oxford)*. 2021;60(3):1166-75.
8. Chen CT, Burton-Wurster N, Borden C, Hueffer K, Bloom SE, Lust G. Chondrocyte necrosis and apoptosis in impact damaged articular cartilage. *J Orthop Res*. 2001;19(4):703-11.
9. Lee JH, Fitzgerald JB, Dimicco MA, Grodzinsky AJ. Mechanical injury of cartilage explants causes specific time-dependent changes in chondrocyte gene expression. *Arthritis Rheum*. 2005;52(8):2386-95.
10. Kurz B, Jin M, Patwari P, Cheng DM, Lark MW, Grodzinsky AJ. Biosynthetic response and mechanical properties of articular cartilage after injurious compression. *J Orthop Res*. 2001;19(6):1140-6.
11. Bomer N, Cornelis FM, Ramos YF, et al. The effect of forced exercise on knee joints in *Dio2(-/-)* mice: type II iodothyronine deiodinase-deficient mice are less prone to develop OA-like cartilage damage upon excessive mechanical stress. *Ann Rheum Dis*. 2016;75(3):571-7.
12. Chang JC, Sebastian A, Muruges DK, et al. Global molecular changes in a tibial compression induced ACL rupture model of post-traumatic osteoarthritis. *J Orthop Res*. 2017;35(3):474-85.
13. Sebastian A, McCol JL, Hum NR, et al. Single-Cell RNA-Seq Reveals Transcriptomic Heterogeneity and Post-Traumatic Osteoarthritis-Associated Early Molecular Changes in Mouse Articular Chondrocytes. *Cells*. 2021;10(6).
14. Sebastian A, Muruges DK, Mendez ME, et al. Global Gene Expression Analysis Identifies Age-Related Differences in Knee Joint Transcriptome during the Development of Post-Traumatic Osteoarthritis in Mice. *Int J Mol Sci*. 2020;21(1).
15. Gardiner MD, Vincent TL, Driscoll C, et al. Transcriptional analysis of micro-dissected articular cartilage in post-traumatic murine osteoarthritis. *Osteoarthritis Cartilage*. 2015;23(4):616-28.
16. Appleton CT, Pitelka V, Henry J, Beier F. Global analyses of gene expression in early experimental osteoarthritis. *Arthritis Rheum*. 2007;56(6):1854-68.
17. Ashwell MS, O'Nat AT, Gonda MG, Mente PL. Gene expression profiling of chondrocytes from a porcine impact injury model. *Osteoarthritis Cartilage*. 2008;16(8):936-46.
18. Loeser RF, Olex AL, McNulty MA, et al. Microarray analysis reveals age-related differences in gene expression during the development of osteoarthritis in mice. *Arthritis Rheum*. 2012;64(3):705-17.
19. Loening AM, James IE, Levenston ME, et al. Injurious mechanical compression of bovine articular cartilage induces chondrocyte apoptosis. *Arch Biochem Biophys*. 2000;381(2):205-12.
20. Houtman E, van Hoolwerff M, Lakenberg N, et al. Human Osteochondral Explants: Reliable Biomimetic Models to Investigate Disease Mechanisms and Develop Personalized Treatments for Osteoarthritis. *Rheumatol Ther*. 2021.
21. Ramos YF, den Hollander W, Bovee JV, et al. Genes involved in the osteoarthritis process identified through genome wide expression analysis in articular cartilage; the RAAK study. *PLoS One*. 2014;9(7):e103056.
22. Sanchez-Adams J, Leddy HA, McNulty AL, O'Connor CJ, Guilak F. The mechanobiology of articular cartilage: bearing the burden of osteoarthritis. *Curr Rheumatol Rep*. 2014;16(10):451.

23. Mankin HJ, Dorfman H, Lippiello L, Zarins A. Biochemical and metabolic abnormalities in articular cartilage from osteo-arthritic human hips. II. Correlation of morphology with biochemical and metabolic data. *J Bone Joint Surg Am.* 1971;53(3):523-37.
24. Farndale RW, Buttle DJ, Barrett AJ. Improved quantitation and discrimination of sulphated glycosaminoglycans by use of dimethyl-methylene blue. *Biochim Biophys Acta.* 1986;883(2):173-7.
25. Wu TD, Watanabe CK. GMAP: a genomic mapping and alignment program for mRNA and EST sequences. *Bioinformatics.* 2005;21(9):1859-75.
26. Anders S, Pyl PT, Huber W. HTSeq--a Python framework to work with high-throughput sequencing data. *Bioinformatics.* 2015;31(2):166-9.
27. Ewels P, Magnusson M, Lundin S, Kaller M. MultiQC: summarize analysis results for multiple tools and samples in a single report. *Bioinformatics.* 2016;32(19):3047-8.
28. Love MI, Huber W, Anders S. Moderated estimation of fold change and dispersion for RNA-seq data with DESeq2. *Genome Biol.* 2014;15(12):550.
29. Kuleshov MV, Jones MR, Rouillard AD, et al. Enrichr: a comprehensive gene set enrichment analysis web server 2016 update. *Nucleic Acids Res.* 2016;44(W1):W90-7.
30. Szklarczyk D, Gable AL, Lyon D, et al. STRING v11: protein-protein association networks with increased coverage, supporting functional discovery in genome-wide experimental datasets. *Nucleic Acids Res.* 2019;47(D1):D607-D13.
31. Al-Sabah A, Stadnik P, Gilbert SJ, Duance VC, Blain EJ. Importance of reference gene selection for articular cartilage mechanobiology studies. *Osteoarthritis Cartilage.* 2016;24(4):719-30.
32. McCulloch RS, Ashwell MS, O'Nan AT, Mente PL. Identification of stable normalization genes for quantitative real-time PCR in porcine articular cartilage. *J Anim Sci Biotechnol.* 2012;3(1):36.
33. Diggle P, Liang K-Y, Zeger SL. Analysis of longitudinal data. Oxford New York: Clarendon Press ; Oxford University Press; 1994. xi, 253 p. p.
34. Reynard LN, Barter MJ. Osteoarthritis year in review 2019: genetics, genomics and epigenetics. *Osteoarthritis Cartilage.* 2020;28(3):275-84.
35. Styrkarsdottir U, Lund SH, Thorleifsson G, et al. Meta-analysis of Icelandic and UK data sets identifies missense variants in SMO, IL11, COL11A1 and 13 more new loci associated with osteoarthritis. *Nat Genet.* 2018;50(12):1681-7.
36. Tachmazidou I, Hatzikotoulas K, Southam L, et al. Identification of new therapeutic targets for osteoarthritis through genome-wide analyses of UK Biobank data. *Nat Genet.* 2019;51(2):230-6.
37. Dunn SL, Soul J, Anand S, Schwartz JM, Boot-Handford RP, Hardingham TE. Gene expression changes in damaged osteoarthritic cartilage identify a signature of non-chondrogenic and mechanical responses. *Osteoarthritis Cartilage.* 2016;24(8):1431-40.
38. Firth SM, Baxter RC. Cellular actions of the insulin-like growth factor binding proteins. *Endocr Rev.* 2002;23(6):824-54.
39. Duan C, Xu Q. Roles of insulin-like growth factor (IGF) binding proteins in regulating IGF actions. *Gen Comp Endocrinol.* 2005;142(1-2):44-52.
40. Baxter RC. IGF binding proteins in cancer: mechanistic and clinical insights. *Nat Rev Cancer.* 2014;14(5):329-41.
41. Clemmons DR. Role of IGF Binding Proteins in Regulating Metabolism. *Trends Endocrinol Metab.* 2016;27(6):375-91.
42. Kato MV. A secreted tumor-suppressor, mac25, with activin-binding activity. *Mol Med.* 2000;6(2):126-35.
43. Esterberg R, Delalande JM, Fritz A. Tailbud-derived Bmp4 drives proliferation and inhibits maturation of zebrafish chordamesoderm. *Development.* 2008;135(23):3891-901.
44. Laursen LS, Overgaard MT, Soe R, et al. Pregnancy-associated plasma protein-A (PAPP-A) cleaves insulin-like growth factor binding protein (IGFBP)-5 independent of IGF: implications for the mechanism of IGFBP-4 proteolysis by PAPP-A. *FEBS Lett.* 2001;504(1-2):36-40.
45. Hou J, Clemmons DR, Smeekens S. Expression and characterization of a serine protease that preferentially cleaves insulin-like growth factor binding protein-5. *J Cell Biochem.* 2005;94(3):470-84.
46. Loechel F, Fox JW, Murphy G, Albrechtsen R, Wewer UM. ADAM 12-S cleaves IGFBP-3 and IGFBP-5 and is inhibited by TIMP-3. *Biochem Biophys Res Commun.* 2000;278(3):511-5.
47. Jepsen MR, Kloverpris S, Mikkelsen JH, et al. Stanniocalcin-2 inhibits mammalian growth by proteolytic inhibition of the insulin-like growth factor axis. *J Biol Chem.* 2015;290(6):3430-9.

48. Cobb LJ, Salih DA, Gonzalez I, et al. Partitioning of IGFBP-5 actions in myogenesis: IGF-independent anti-apoptotic function. *J Cell Sci.* 2004;117(Pt 9):1737-46.
49. Tripathi G, Salih DA, Drozd AC, Cosgrove RA, Cobb LJ, Pell JM. IGF-independent effects of insulin-like growth factor binding protein-5 (Igfbp5) in vivo. *FASEB J.* 2009;23(8):2616-26.
50. Clemmons DR, Busby WH, Jr., Garmonj A, et al. Inhibition of insulin-like growth factor binding protein 5 proteolysis in articular cartilage and joint fluid results in enhanced concentrations of insulin-like growth factor 1 and is associated with improved osteoarthritis. *Arthritis Rheum.* 2002;46(3):694-703.
51. Riegger J, Joos H, Palm HG, et al. Striking a new path in reducing cartilage breakdown: combination of antioxidative therapy and chondroanabolic stimulation after blunt cartilage trauma. *J Cell Mol Med.* 2018;22(1):77-88.
52. Matsuzaki T, Alvarez-Garcia O, Mokuda S, et al. FoxO transcription factors modulate autophagy and proteoglycan 4 in cartilage homeostasis and osteoarthritis. *Sci Transl Med.* 2018;10(428).
53. Wu YH, Liu W, Zhang L, et al. Effects of microRNA-24 targeting C-myc on apoptosis, proliferation, and cytokine expressions in chondrocytes of rats with osteoarthritis via MAPK signaling pathway. *J Cell Biochem.* 2018;119(10):7944-58.
54. Tan P, Guan H, Xie L, et al. FOXO1 inhibits osteoclastogenesis partially by antagonizing MYC. *Sci Rep.* 2015;5:16835.
55. Peck B, Ferber EC, Schulze A. Antagonism between FOXO and MYC Regulates Cellular Powerhouse. *Front Oncol.* 2013;3:96.
56. Basisty N, Kale A, Jeon OH, et al. A proteomic atlas of senescence-associated secretomes for aging biomarker development. *PLoS Biol.* 2020;18(1):e3000599.
57. McCulloch K, Litherland GJ, Rai TS. Cellular senescence in osteoarthritis pathology. *Aging Cell.* 2017;16(2):210-8.
58. den Hollander W, Pulyakhina I, Boer C, et al. Annotating Transcriptional Effects of Genetic Variants in Disease-Relevant Tissue: Transcriptome-Wide Allelic Imbalance in Osteoarthritic Cartilage. *Arthritis Rheumatol.* 2019;71(4):561-70.
59. Matsui Y, Hasegawa M, Iino T, Imanaka-Yoshida K, Yoshida T, Sudo A. Tenascin-C Prevents Articular Cartilage Degeneration in Murine Osteoarthritis Models. *Cartilage.* 2018;9(1):80-8.
60. Unno H, Hasegawa M, Suzuki Y, et al. Tenascin-C promotes the repair of cartilage defects in mice. *J Orthop Sci.* 2020;25(2):324-30.

## Supplementary Files

### *List of contents:*

#### *Supplementary Tables*

**Supplementary Table S1.** [a] Donor characteristics of samples for which RNA was sequenced. [b] Donor characteristics of independent samples used for replication of RNA-sequencing findings.

**Supplementary Table S2.** Primer sequences used for replication and validation by RT-qPCR.

**Supplementary Table S3.** Genes differentially expressed in 65%MS (DE<sub>MS</sub>) cartilage compared to control cartilage of human osteochondral explants.

**Supplementary Table S4.** Gene enrichment found in Enrichr.

**Supplementary Table S5.** DE<sub>MS</sub> genes coinciding with previously reported DE genes in OA pathophysiology (DE<sub>OA</sub>).

**Supplementary Table S6.** Exclusive mechanical response genes (DE<sub>ExclusiveMS</sub>).

**Supplementary Table S7.** Previously reported OA risk loci present in our DE gene dataset.

**Supplementary Table S8.** All insulin growth factor binding proteins (IGFBPs) and related DE genes identified in our analysis.

#### *Supplementary Figures*

**Supplementary Figure S1.** Venn diagram of coinciding genes between differentially expressed genes in mechanically stressed versus control cartilage from osteochondral explants (DE<sub>MS</sub>) and previously identified differentially expressed genes in preserved versus lesioned OA cartilage (DE<sub>OA</sub>).

**Supplementary Figure S2.** Protein-protein interaction network in STRING of proteins encoded by differentially expressed genes (N=92 genes) not coinciding with OA pathophysiology (DE<sub>ExclusiveMS</sub>).

**Supplementary Figure S3.** Heat-map of proteins present in SASP.

## Supplementary Tables

**Supplementary Table S1** | [A] Donor characteristics of samples for which RNA was sequenced. [B] Donor characteristics of independent samples used for replication of RNA-sequencing findings.

**A**

	<b>Control (N=8 donors)</b>	<b>65%MS (N=7 donors)</b>	<b>All samples (N=9 donors)</b>
<b>Age (Average ± stdev)</b>	61.88 ± 6.06	64.29 ± 9.05	63.78 ± 8.04
<b>Age (Range)</b>	53-70	53-79	53-79
<b>Sex (M/F)</b>	3/5	3/4	3/6
<b>% Female</b>	63%	57%	67%
<b>BMI (Average ± stdev)</b>	30.36 ± 4.90	28.42 ± 3.68	29.88 ± 4.80
<b>BMI (range)</b>	24.9-39.2	24.9-35.11	24.9-39.2

**B**

	<b>All samples (N=10 donors)</b>
<b>Age (Average ± stdev)</b>	66.90 ± 12.11
<b>Age (Range)</b>	52-85
<b>Sex (M/F)</b>	4/6
<b>% Female</b>	60%
<b>BMI (Average ± stdev)</b>	29.09 ± 4.47
<b>BMI (range)</b>	24.78-38.06

**Supplementary Table S2 | Primer sequences used for replication and validation by RT-qPCR.**

<b>Gene name</b>	<b>Forward (5'-3')</b>	<b>Reverse (5'-3')</b>
<i>SDHA</i>	TGGAGCTGCAGAACCTGATG	TGTAGTCTTCCCTGGCATGC
<i>YWHAZ</i>	CTGAGGTTGCAGCTGGTGATGACA	AGCAGGCTTTCTCAGGGGAGTTCA
<i>TNC</i>	TGTCATCTCCTACACAGGCG	TCGAGGTCGGTCAGAGCATA
<i>IGFBP4</i>	ATCGAGGCCATCCAGGAAAG	CTGAAGCTGTTGTTGGGGTG
<i>IGFBP5</i>	GTGCTGTGTACCTGCCAAT	CGTCAACGTACTIONCATGCCT
<i>IGFBP6</i>	GTCTACCGAGGGCTCAAAC	GACTTGCCCATCCGATCCAC
<i>CNTFR</i>	AAGGGCTTCTACTGCAGCTG	CATGTAGCGAATGTGGCAGC
<i>WISP2</i>	ATGAGAGGCACACCGAAGAC	TGGGTACGCACCTTTGAGAG
<i>FRZB</i>	ATTGACTTCCAGCACGAGCC	CGAGTGGCGTACTTGTATGAG
<i>COL9A3</i>	AAGTATCTGCCCGCCAGGTC	TCCCTTGAACCTTGGCATTTC
<i>GADD45A</i>	GCGAGAACGACATCAACATCC	AATGTGGATTTCGTCACCAGCA
<i>PTGES</i>	GGAAGAAGGCCTTTGCCAAC	AGACGAAGCCAGGAAAAGG

**Supplementary Table S3 | Genes differentially expressed in 65%MS (DE<sub>MS</sub>) cartilage compared to control cartilage of human osteochondral explants.**

Ensembl ID	Gene Name	log2FC	FC	pvalue	FDR
ENSG00000167779	IGFBP6	-2.37	0.19	4.72E-08	3.07E-04
ENSG00000114126	TFDP2	-0.56	0.68	1.07E-07	3.48E-04
ENSG00000100906	NFKBIA	-0.59	0.66	2.51E-07	5.44E-04
ENSG00000064205	WISP2	-1.68	0.31	9.97E-07	1.08E-03
ENSG00000116717	GADD45A	-0.75	0.59	6.73E-07	1.08E-03
ENSG00000171914	TLN2	-1.11	0.46	8.39E-07	1.08E-03
ENSG00000134324	LPIN1	-0.87	0.55	2.79E-06	1.79E-03
ENSG00000140105	WARS	0.53	1.44	2.23E-06	1.79E-03
ENSG00000157514	TSC22D3	-0.77	0.58	2.66E-06	1.79E-03
ENSG00000163453	IGFBP7	-1.24	0.42	2.05E-06	1.79E-03
ENSG00000179051	RCC2	0.90	1.87	3.03E-06	1.79E-03
ENSG00000102760	RGCC	-0.87	0.55	3.57E-06	1.94E-03
ENSG00000196305	IARS	0.43	1.35	4.36E-06	2.18E-03
ENSG00000144908	ALDH1L1	-1.62	0.33	4.78E-06	2.22E-03
ENSG00000068383	INPP5A	-0.77	0.58	5.60E-06	2.43E-03
ENSG00000126803	HSPA2	-0.85	0.55	7.74E-06	2.65E-03
ENSG00000143416	SELENBP1	-1.09	0.47	7.67E-06	2.65E-03
ENSG00000148498	PARD3	-0.78	0.58	6.56E-06	2.65E-03
ENSG00000159461	AMFR	-0.54	0.69	6.98E-06	2.65E-03
ENSG00000204103	MAFB	1.57	2.97	1.43E-05	4.66E-03
ENSG00000119408	NEK6	1.18	2.26	1.91E-05	5.86E-03
ENSG00000142871	CYR61	-0.65	0.64	1.98E-05	5.86E-03
ENSG00000138356	AOX1	-1.06	0.48	2.18E-05	6.10E-03
ENSG00000155324	GRAMD2B	-0.80	0.58	2.25E-05	6.10E-03
ENSG00000107736	CDH23	-1.44	0.37	2.72E-05	6.88E-03
ENSG00000150907	FOXO1	-0.68	0.62	2.86E-05	6.88E-03
ENSG00000163686	ABHD6	-1.05	0.48	2.96E-05	6.88E-03
ENSG00000167191	GPRC5B	-0.87	0.55	2.94E-05	6.88E-03
ENSG00000100612	DHRS7	-0.48	0.71	3.97E-05	7.81E-03
ENSG00000115461	IGFBP5	2.59	6.01	3.54E-05	7.81E-03
ENSG00000115468	EFHD1	-0.80	0.57	3.73E-05	7.81E-03
ENSG00000134107	BHLHE40	1.00	2.00	4.08E-05	7.81E-03
ENSG00000146122	DAAM2	-0.95	0.52	4.08E-05	7.81E-03
ENSG00000173641	HSPB7	-0.89	0.54	3.81E-05	7.81E-03
ENSG00000135069	PSAT1	1.03	2.04	4.52E-05	8.29E-03
ENSG00000148344	PTGES	1.55	2.92	4.58E-05	8.29E-03
ENSG00000166348	USP54	-0.76	0.59	4.79E-05	8.43E-03

ENSG00000139514	SLC7A1	0.57	1.48	4.93E-05	8.44E-03
ENSG00000041982	TNC	1.48	2.80	5.15E-05	8.51E-03
ENSG00000162998	FRZB	-1.63	0.32	5.23E-05	8.51E-03
ENSG00000132970	WASF3	-0.41	0.75	5.36E-05	8.51E-03
ENSG00000103257	SLC7A5	0.89	1.86	6.44E-05	9.96E-03
ENSG00000104324	CPQ	-0.46	0.72	6.58E-05	9.96E-03
ENSG00000166165	CKB	-1.39	0.38	7.19E-05	1.04E-02
ENSG00000168918	INPP5D	-1.25	0.42	7.13E-05	1.04E-02
ENSG00000129757	CDKN1C	-1.23	0.43	7.90E-05	1.09E-02
ENSG00000143878	RHOB	-0.61	0.66	8.05E-05	1.09E-02
ENSG00000183864	TOB2	-0.71	0.61	7.96E-05	1.09E-02
ENSG00000053747	LAMA3	-1.15	0.45	9.40E-05	1.25E-02
ENSG00000145246	ATP10D	-0.49	0.71	9.96E-05	1.30E-02
ENSG00000101825	MXRA5	1.21	2.32	1.11E-04	1.42E-02
ENSG00000122756	CNTFR	-1.88	0.27	1.15E-04	1.44E-02
ENSG00000117020	AKT3	-0.44	0.74	1.26E-04	1.44E-02
ENSG00000134954	ETS1	0.46	1.38	1.26E-04	1.44E-02
ENSG00000165966	PDZRN4	-1.97	0.26	1.26E-04	1.44E-02
ENSG00000169116	PARM1	-1.08	0.47	1.26E-04	1.44E-02
ENSG00000187720	THSD4	-1.53	0.35	1.18E-04	1.44E-02
ENSG00000113739	STC2	-1.07	0.48	1.39E-04	1.53E-02
ENSG00000180354	MTURN	-0.60	0.66	1.37E-04	1.53E-02
ENSG00000185630	PBX1	-0.70	0.62	1.41E-04	1.53E-02
ENSG00000117151	CTBS	-0.44	0.73	1.53E-04	1.63E-02
ENSG00000136997	MYC	0.79	1.73	1.56E-04	1.64E-02
ENSG00000080546	SESN1	-0.84	0.56	1.78E-04	1.84E-02
ENSG00000198755	RPL10A	0.34	1.26	1.88E-04	1.91E-02
ENSG00000080298	RFX3	-0.58	0.67	1.99E-04	1.99E-02
ENSG00000114166	KAT2B	-0.65	0.64	2.09E-04	2.06E-02
ENSG00000127528	KLF2	-1.18	0.44	2.15E-04	2.09E-02
ENSG00000106991	ENG	0.59	1.50	2.31E-04	2.21E-02
ENSG00000100242	SUN2	-0.82	0.57	2.39E-04	2.25E-02
ENSG00000100029	PES1	0.44	1.36	2.49E-04	2.28E-02
ENSG00000185201	IFITM2	0.72	1.65	2.46E-04	2.28E-02
ENSG00000111640	GAPDH	0.58	1.49	2.53E-04	2.29E-02
ENSG00000173848	NET1	-0.90	0.54	2.65E-04	2.36E-02
ENSG00000138336	TET1	-0.47	0.72	2.75E-04	2.42E-02
ENSG00000101782	RIOK3	-0.44	0.74	2.81E-04	2.43E-02
ENSG00000159322	ADPGK	0.35	1.27	2.83E-04	2.43E-02
ENSG00000111885	MAN1A1	-0.99	0.50	2.94E-04	2.48E-02

ENSG00000089220	PEBP1	-0.62	0.65	3.04E-04	2.54E-02
ENSG00000005022	SLC25A5	0.48	1.40	3.16E-04	2.56E-02
ENSG00000137699	TRIM29	-1.13	0.46	3.18E-04	2.56E-02
ENSG00000166033	HTRA1	0.95	1.93	3.17E-04	2.56E-02
ENSG00000184205	TSPYL2	-0.75	0.60	3.42E-04	2.71E-02
ENSG00000143382	ADAMTSL4	-0.66	0.63	3.58E-04	2.81E-02
ENSG00000062716	VMP1	0.60	1.52	3.89E-04	3.01E-02
ENSG00000067141	NEO1	-0.80	0.58	4.24E-04	3.10E-02
ENSG00000078596	ITM2A	-1.00	0.50	4.18E-04	3.10E-02
ENSG00000096060	FKBP5	-0.64	0.64	4.07E-04	3.10E-02
ENSG00000134109	EDEM1	0.33	1.26	4.20E-04	3.10E-02
ENSG00000148180	GSN	-0.60	0.66	4.16E-04	3.10E-02
ENSG00000157600	TMEM164	-0.73	0.60	4.28E-04	3.10E-02
ENSG00000143164	DCAF6	-0.22	0.86	4.34E-04	3.10E-02
ENSG00000071205	ARHGAP10	-0.47	0.72	4.57E-04	3.14E-02
ENSG00000079691	CARMIL1	-0.55	0.68	4.51E-04	3.14E-02
ENSG00000131844	MCCC2	-0.89	0.54	4.58E-04	3.14E-02
ENSG00000168874	ATOH8	-0.91	0.53	4.53E-04	3.14E-02
ENSG00000106624	AEBP1	0.79	1.73	4.98E-04	3.31E-02
ENSG00000154380	ENAH	0.53	1.44	4.97E-04	3.31E-02
ENSG00000253293	HOXA10	-0.36	0.78	4.97E-04	3.31E-02
ENSG00000006016	CRLF1	0.76	1.69	5.15E-04	3.38E-02
ENSG00000106366	SERPINE1	1.02	2.03	5.33E-04	3.47E-02
ENSG00000141753	IGFBP4	1.38	2.59	5.44E-04	3.50E-02
ENSG00000179532	DNHD1	-0.51	0.70	5.53E-04	3.53E-02
ENSG00000106258	CYP3A5	-1.40	0.38	5.74E-04	3.62E-02
ENSG00000082196	C1QTNF3	-1.73	0.30	5.86E-04	3.64E-02
ENSG00000164106	SCRG1	-0.89	0.54	5.87E-04	3.64E-02
ENSG00000151332	MBIP	-0.40	0.76	6.10E-04	3.71E-02
ENSG00000187840	EIF4EBP1	1.06	2.09	6.04E-04	3.71E-02
ENSG00000132824	SERINC3	-0.32	0.80	6.54E-04	3.91E-02
ENSG00000135506	OS9	-0.33	0.80	6.48E-04	3.91E-02
ENSG00000148848	ADAM12	0.62	1.54	6.63E-04	3.92E-02
ENSG00000013016	EHD3	0.42	1.34	6.75E-04	3.93E-02
ENSG00000101439	CST3	-0.74	0.60	6.77E-04	3.93E-02
ENSG00000179941	BBS10	-0.57	0.67	6.83E-04	3.93E-02
ENSG00000104714	ERICH1	-0.46	0.73	7.07E-04	3.93E-02
ENSG00000106351	AGFG2	-0.68	0.63	6.97E-04	3.93E-02
ENSG00000158825	CDA	-1.07	0.48	7.07E-04	3.93E-02
ENSG00000184557	SOCS3	0.78	1.71	7.07E-04	3.93E-02

---

ENSG00000162627	SNX7	-0.56	0.68	7.13E-04	3.93E-02
ENSG00000136295	TTYH3	1.05	2.08	7.27E-04	3.97E-02
ENSG00000092445	TYRO3	0.77	1.71	7.45E-04	4.04E-02
ENSG0000010278	CD9	-0.80	0.57	7.82E-04	4.11E-02
ENSG00000049860	HEXB	-0.46	0.73	7.79E-04	4.11E-02
ENSG00000165795	NDRG2	-0.72	0.61	7.65E-04	4.11E-02
ENSG00000170891	CYTL1	-1.65	0.32	7.72E-04	4.11E-02
ENSG00000187514	PTMA	0.49	1.40	8.00E-04	4.17E-02
ENSG00000112559	MDFI	0.76	1.69	8.45E-04	4.36E-02
ENSG00000159307	SCUBE1	-0.93	0.53	8.50E-04	4.36E-02
ENSG00000144857	BOC	-1.08	0.47	8.75E-04	4.45E-02
ENSG00000131067	GGT7	-0.54	0.69	8.90E-04	4.45E-02
ENSG00000171150	SOCS5	-0.40	0.76	8.85E-04	4.45E-02
ENSG00000112306	RPS12	0.26	1.19	9.15E-04	4.54E-02
ENSG00000119938	PPP1R3C	-0.71	0.61	9.54E-04	4.68E-02
ENSG00000164237	CMBL	-0.57	0.67	9.56E-04	4.68E-02
ENSG00000090530	P3H2	-1.17	0.44	1.02E-03	4.71E-02
ENSG00000106617	PRKAG2	-0.51	0.70	1.01E-03	4.71E-02
ENSG00000112118	MCM3	0.39	1.31	1.01E-03	4.71E-02
ENSG00000117868	ESYT2	-0.18	0.88	9.79E-04	4.71E-02
ENSG00000141258	SGSM2	-0.87	0.55	1.01E-03	4.71E-02
ENSG00000143127	ITGA10	-0.47	0.72	9.98E-04	4.71E-02
ENSG00000149485	FADS1	-0.65	0.64	1.04E-03	4.71E-02
ENSG00000162804	SNED1	0.87	1.83	1.04E-03	4.71E-02
ENSG00000169184	MN1	-0.80	0.58	1.04E-03	4.71E-02
ENSG00000169902	TPST1	0.36	1.28	1.04E-03	4.71E-02
ENSG00000185634	SHC4	1.05	2.07	9.91E-04	4.71E-02
ENSG00000130635	COL5A1	0.96	1.95	1.06E-03	4.78E-02
ENSG00000004799	PDK4	-0.88	0.54	1.13E-03	4.84E-02
ENSG00000105974	CAV1	-0.51	0.70	1.12E-03	4.84E-02
ENSG00000131389	SLC6A6	0.98	1.97	1.12E-03	4.84E-02
ENSG00000137745	MMP13	2.38	5.19	1.13E-03	4.84E-02
ENSG00000172348	RCAN2	-0.88	0.54	1.10E-03	4.84E-02
ENSG00000172493	AFF1	-0.39	0.76	1.09E-03	4.84E-02
ENSG00000187151	ANGPTL5	-1.18	0.44	1.11E-03	4.84E-02
ENSG00000100814	CCNB1IP1	-0.33	0.80	1.14E-03	4.84E-02
ENSG00000092758	COL9A3	-1.62	0.32	1.16E-03	4.89E-02
ENSG00000160111	CPAMD8	-1.37	0.39	1.19E-03	4.98E-02
ENSG00000170776	AKAP13	-0.41	0.75	1.19E-03	4.98E-02

---

Legend: Log2FC, log2 fold change; FC, fold change; FDR, False discovery rate

**Supplementary Table S4 | Gene enrichment found in Enrichr.** Enrichment for [A] 156 DE<sub>MS</sub> genes in and [B] 92 DE<sub>ExclusiveMS</sub> for the gene ontology terms: biological process, molecular function and cellular component 2018, and pathways: KEGG 2019 human and reactome.

**A**

Term	Overlap	P-value	Adj P-value	Odds Ratio	Combined Score	Genes
endoplasmic reticulum lumen (GO:0005788)	12/270	1.44E-06	6.42E-04	5.70	76.64	CST3;IGFBP5;COL5A1;OS9;IGFBP4;ADAMTSL4;STC2;TNC;P3H2;IGFBP7;COL9A3;CYR61
negative regulation of cellular process (GO:0048523)	17/534	9.82E-07	5.01E-03	4.08	56.46	TSPYL2;CDA;WARS;-CAV1;P3H2;ETS1;-CYR61;WISP2;RHOB;KAT2B;RGCC;FRZB;MYC;BHLHE40;CD9;IGFBP7;IGFBP6
Cellular senescence	8/160	3.75E-05	1.15E-02	6.41	65.33	GADD45A;MYC;SERPINE1;AKT3;EIF4EBP1;SLC25A5;ETS1;-FOXO1
protein kinase regulator activity (GO:0019887)	7/107	2.08E-05	1.20E-02	8.39	90.40	CDKN1C;SOCS3;GPRC5B;RGCC;M-BIP;PRKAG2;SOCS5
Insulin resistance	6/108	2.03E-04	1.25E-02	7.12	60.55	NFKBIA;SOCS3;PPP1R3C;AKT3;PRKAG2;FOXO1
Focal adhesion	8/199	1.72E-04	1.33E-02	5.15	44.67	SHC4;CAV1;ITGA10;AKT3;LAMA3;TNC;COL9A3;TLN2
Longevity regulating pathway	6/102	1.49E-04	1.53E-02	7.54	66.47	SESN1;AKT3;EIF4EBP1;PRKAG2;HSPA2;FOXO1
Insulin signaling pathway	7/137	1.01E-04	1.56E-02	6.55	60.26	SHC4;SOCS3;PPP1R3C;AKT3;EIF4EBP1;PRKAG2;FOXO1
Chronic myeloid leukemia	5/76	3.20E-04	1.64E-02	8.43	67.87	SHC4;NFKBIA;GADD45A;MYC;AKT3
insulin-like growth factor II binding (GO:0031995)	3/7	1.59E-05	1.83E-02	54.95	607.02	IGFBP5;IGFBP4;IGFBP6
focal adhesion (GO:0005925)	11/356	1.14E-04	2.54E-02	3.96	35.97	ENAH;EHD3;GSN;CAV1;TNC;CD9;TLN2;RPL10A;DCAF6;RHOB;ENG
insulin-like growth factor I binding (GO:0031994)	3/13	1.26E-04	2.89E-02	29.59	265.73	IGFBP5;IGFBP4;IGFBP6
insulin-like growth factor binding (GO:0005520)	3/14	1.59E-04	3.05E-02	27.47	240.28	IGFBP5;IGFBP4;IGFBP6
kinase binding (GO:0019900)	12/418	1.11E-04	3.20E-02	3.68	33.51	SHC4;KAT2B;GPRC5B;RGCC;WARS;GADD45A;CAV1;RC-C2;NEK6;PEBP1;PRKAG2;RHOB
extracellular matrix organization (GO:0030198)	10/229	1.30E-05	3.31E-02	5.60	62.99	SCUBE1;MMP13;COL5A1;ITGA10;-SERPINE1;ADAM12;LAMA3;TNC;HTRA1;COL9A3
Vitamin B6 metabolism	2/6	8.88E-04	3.42E-02	42.74	300.26	PSAT1;AOX1

Small cell lung cancer	5/93	8.10E-04	3.56E-02	6.89	49.06	NFKBIA;GADD45A;MYC;AKT3;LAMA3
kinase inhibitor activity (GO:0019210)	5/59	9.65E-05	3.70E-02	10.86	100.45	CDKN1C;SOCS3;WARS;MBIP;SOCS5
protein alpha-1,2-de-mannosylation (GO:0036508)	4/24	3.35E-05	4.27E-02	21.37	220.16	OS9;EDEM1;AMFR;MAN1A1
negative regulation of cell proliferation (GO:0008285)	12/363	2.88E-05	4.90E-02	4.24	44.31	CDKN1C;KAT2B;RGCC;WARS;IGFBP5;FRZB;MYC;BHLHE40;P3H2;IGFBP7;IGFBP6;ETS1

**B**

<b>Term</b>	<b>Overlap</b>	<b>P-value</b>	<b>Adj P-value</b>	<b>Odds Ratio</b>	<b>Combined Score</b>	<b>Genes</b>
kinase inhibitor activity (GO:0019210)	5/59	7.59E-06	8.74E-03	18.42	217.17	CDKN1C; SOCS3;WARS;MBIP ;SOCS5
focal adhesion (GO:0005925)	9/356	3.84E-05	1.71E-02	5.50	55.88	ENAH;EHD3;GSN;C-D9;TLN2;RPL10A;DCAF6;RHOB;ENG

**Supplementary Table S5 | DE<sub>MS</sub> genes coinciding with previously reported DE genes in OA pathophysiology (DE<sub>OA</sub>). [A] DE<sub>MS</sub> genes with same direction of effect as DE<sub>OA</sub> genes. [B] DE<sub>MS</sub> genes with opposite direction of effect as DE<sub>OA</sub> genes.**

A	65%MS versus control cartilage (n=14/ group)				Lesioned versus Preserved OA cartilage (n=35/ group)			
	Gene Name	log- 2FC	FC	pvalue	FDR	log- 2FC	FC	pvalue
<i>TFDP2</i>	-0.56	0.68	1.07E-07	3.48E-04	-0.23	0.85	2.02E-03	2.27E-02
<i>WISP2</i>	-1.68	0.31	9.97E-07	1.08E-03	-1.20	0.44	1.48E-04	3.06E-03
<i>ALDH1L1</i>	-1.62	0.33	4.78E-06	2.22E-03	-1.02	0.49	5.56E-09	7.24E-07
<i>INPP5A</i>	-0.77	0.58	5.60E-06	2.43E-03	-0.31	0.81	1.69E-03	1.99E-02
<i>GRAMD2B</i>	-0.80	0.58	2.25E-05	6.10E-03	-0.30	0.81	1.18E-04	2.54E-03
<i>GPRC5B</i>	-0.87	0.55	2.94E-05	6.88E-03	-1.02	0.49	2.10E-09	3.32E-07
<i>DAAM2</i>	-0.95	0.52	4.08E-05	7.81E-03	-0.50	0.71	2.40E-04	4.48E-03
<i>EFHD1</i>	-0.80	0.57	3.73E-05	7.81E-03	-0.40	0.76	2.37E-03	2.54E-02
<i>FRZB</i>	-1.63	0.32	5.23E-05	8.51E-03	-1.88	0.27	4.07E-12	1.87E-09
<i>TOB2</i>	-0.71	0.61	7.96E-05	1.09E-02	-0.26	0.84	4.72E-05	1.22E-03
<i>CNTFR</i>	-1.88	0.27	1.15E-04	1.44E-02	-1.69	0.31	3.32E-12	1.56E-09
<i>PDZRN4</i>	-1.97	0.26	1.26E-04	1.44E-02	-1.37	0.39	2.70E-05	7.76E-04
<i>PARM1</i>	-1.08	0.47	1.26E-04	1.44E-02	-0.65	0.64	2.63E-05	7.61E-04
<i>STC2</i>	-1.07	0.48	1.39E-04	1.53E-02	-1.03	0.49	1.05E-08	1.24E-06
<i>MTURN</i>	-0.60	0.66	1.37E-04	1.53E-02	-0.42	0.75	3.76E-06	1.58E-04
<i>KAT2B</i>	-0.65	0.64	2.09E-04	2.06E-02	-0.33	0.80	1.33E-03	1.66E-02
<i>ADAMTSL4</i>	-0.66	0.63	3.58E-04	2.81E-02	-0.42	0.75	1.26E-03	1.61E-02
<i>ITM2A</i>	-1.00	0.50	4.18E-04	3.10E-02	-0.60	0.66	8.86E-05	2.02E-03
<i>NEO1</i>	-0.80	0.58	4.24E-04	3.10E-02	-0.32	0.80	1.38E-03	1.71E-02
<i>FKBP5</i>	-0.64	0.64	4.07E-04	3.10E-02	-0.20	0.87	5.39E-03	4.59E-02
<i>ATOX1</i>	-0.91	0.53	4.53E-04	3.14E-02	-0.48	0.72	1.67E-03	1.97E-02
<i>HOXA10</i>	-0.36	0.78	4.97E-04	3.31E-02	-0.36	0.78	2.32E-04	4.37E-03
<i>AGFG2</i>	-0.68	0.63	6.97E-04	3.93E-02	-0.30	0.81	5.47E-03	4.64E-02
<i>NDRG2</i>	-0.72	0.61	7.65E-04	4.11E-02	-0.70	0.62	1.67E-08	1.83E-06
<i>CYTL1</i>	-1.65	0.32	7.72E-04	4.11E-02	-0.46	0.73	4.94E-03	4.31E-02
<i>SCUBE1</i>	-0.93	0.53	8.50E-04	4.36E-02	-1.26	0.42	2.03E-08	2.15E-06
<i>BOC</i>	-1.08	0.47	8.75E-04	4.45E-02	-0.70	0.62	3.96E-07	2.54E-05
<i>CMBL</i>	-0.57	0.67	9.56E-04	4.68E-02	-0.41	0.75	1.34E-07	1.02E-05
<i>RCAN2</i>	-0.88	0.54	1.10E-03	4.84E-02	-2.03	0.25	8.20E-15	9.19E-12
<i>CPAMD8</i>	-1.37	0.39	1.19E-03	4.98E-02	-1.19	0.44	2.90E-09	4.23E-07
<i>IARS</i>	0.43	1.35	4.36E-06	2.18E-03	0.40	1.32	1.35E-04	2.85E-03
<i>BHLHE40</i>	1.00	2.00	4.08E-05	7.81E-03	0.30	1.23	4.89E-04	7.78E-03
<i>PSAT1</i>	1.03	2.04	4.52E-05	8.29E-03	0.77	1.70	1.14E-03	1.49E-02

<i>PTGES</i>	1.55	2.92	4.58E-05	8.29E-03	1.61	3.06	2.33E-15	3.61E-12
<i>SLC7A1</i>	0.57	1.48	4.93E-05	8.44E-03	0.53	1.44	1.43E-06	7.10E-05
<i>TNC</i>	1.48	2.80	5.15E-05	8.51E-03	0.50	1.41	7.53E-04	1.09E-02
<i>SLC7A5</i>	0.89	1.86	6.44E-05	9.96E-03	0.99	1.99	2.91E-10	6.25E-08
<i>MXRA5</i>	1.21	2.32	1.11E-04	1.42E-02	0.53	1.44	3.42E-04	5.94E-03
<i>HTRA1</i>	0.95	1.93	3.17E-04	2.56E-02	1.26	2.39	1.80E-14	1.65E-11
<i>EDEM1</i>	0.33	1.26	4.20E-04	3.10E-02	0.23	1.17	2.38E-03	2.55E-02
<i>CRLF1</i>	0.76	1.69	5.15E-04	3.38E-02	1.60	3.04	4.59E-13	2.96E-10
<i>SERPINE1</i>	1.02	2.03	5.33E-04	3.47E-02	1.57	2.97	3.22E-13	2.24E-10
<i>IGFBP4</i>	1.38	2.59	5.44E-04	3.50E-02	0.67	1.60	2.27E-03	2.47E-02
<i>ADAM12</i>	0.62	1.54	6.63E-04	3.92E-02	0.99	1.98	4.58E-06	1.85E-04
<i>TYRO3</i>	0.77	1.71	7.45E-04	4.04E-02	0.94	1.92	1.19E-11	5.00E-09
<i>SHC4</i>	1.05	2.07	9.91E-04	4.71E-02	1.07	2.10	1.43E-11	5.87E-09
<i>COL5A1</i>	0.96	1.95	1.06E-03	4.78E-02	0.46	1.38	4.94E-03	4.31E-02
<i>SLC6A6</i>	0.98	1.97	1.12E-03	4.84E-02	0.60	1.51	1.13E-04	2.45E-03

Legend: Log2FC, log2 fold change; FC, fold change; FDR, False discovery rate

<b>B</b>	<b>Control versus 65% MS cartilage (n=14/group)</b>				<b>Lesioned versus Preserved OA cartilage (n=35/ group)</b>			
	<b>Gene Name</b>	<b>log2FC</b>	<b>FC</b>	<b>pvalue</b>	<b>FDR</b>	<b>log2FC</b>	<b>FC</b>	<b>pvalue</b>
<i>TMEM164</i>	-0.73	0.60	4.28E-04	3.10E-02	0.24	1.18	5.09E-03	4.41E-02
<i>FOXO1</i>	-0.68	0.62	2.86E-05	6.88E-03	0.29	1.22	6.52E-04	9.72E-03
<i>CAV1</i>	-0.51	0.70	1.12E-03	4.84E-02	0.33	1.25	4.58E-03	4.07E-02
<i>AKAP13</i>	-0.41	0.75	1.19E-03	4.98E-02	0.33	1.26	1.11E-04	2.42E-03
<i>CDA</i>	-1.07	0.48	7.07E-04	3.93E-02	0.39	1.31	2.31E-03	2.50E-02
<i>IGFBP7</i>	-1.24	0.42	2.05E-06	1.79E-03	0.47	1.38	3.42E-03	3.30E-02
<i>RGCC</i>	-0.87	0.55	3.57E-06	1.94E-03	0.47	1.39	1.59E-05	5.13E-04
<i>AKT3</i>	-0.44	0.74	1.26E-04	1.44E-02	0.52	1.43	1.01E-04	2.25E-03
<i>SNX7</i>	-0.56	0.68	7.13E-04	3.93E-02	0.53	1.45	3.24E-04	5.67E-03
<i>C1QTNF3</i>	-1.73	0.30	5.86E-04	3.64E-02	0.60	1.52	9.93E-04	1.35E-02
<i>CKB</i>	-1.39	0.38	7.19E-05	1.04E-02	0.63	1.55	1.37E-03	1.70E-02
<i>TSC22D3</i>	-0.77	0.58	2.66E-06	1.79E-03	0.67	1.59	2.81E-09	4.16E-07
<i>TRIM29</i>	-1.13	0.46	3.18E-04	2.56E-02	0.78	1.72	1.48E-05	4.85E-04
<i>P3H2</i>	-1.17	0.44	1.02E-03	4.71E-02	1.69	3.23	0.00E+00	0.00E+00
<i>MAFB</i>	1.57	2.97	1.43E-05	4.66E-03	-0.69	0.62	1.32E-03	1.66E-02
<i>MDFI</i>	0.76	1.69	8.45E-04	4.36E-02	-0.42	0.75	5.76E-03	4.82E-02

Legend: Log2FC, log2 fold change; FC, fold change; FDR, False discovery rate

**Supplementary Table S6 | Exclusive mechanical response genes (DE<sub>ExclusiveMS</sub>).**

Gene name	log2FC	FC	pvalue	FDR
IGFBP6	-2.37	0.19	4.72E-08	3.07E-04
NFKBIA	-0.59	0.66	2.51E-07	5.44E-04
TLN2	-1.11	0.46	8.39E-07	1.08E-03
GADD45A	-0.75	0.59	6.73E-07	1.08E-03
RCC2	0.90	1.87	3.03E-06	1.79E-03
WARS	0.53	1.44	2.23E-06	1.79E-03
LPIN1	-0.87	0.55	2.79E-06	1.79E-03
AMFR	-0.54	0.69	6.98E-06	2.65E-03
PARD3	-0.78	0.58	6.56E-06	2.65E-03
SELENBP1	-1.09	0.47	7.67E-06	2.65E-03
HSPA2	-0.85	0.55	7.74E-06	2.65E-03
CYR61	-0.65	0.64	1.98E-05	5.86E-03
NEK6	1.18	2.26	1.91E-05	5.86E-03
AOX1	-1.06	0.48	2.18E-05	6.10E-03
ABHD6	-1.05	0.48	2.96E-05	6.88E-03
CDH23	-1.44	0.37	2.72E-05	6.88E-03
HSPB7	-0.89	0.54	3.81E-05	7.81E-03
IGFBP5	2.59	6.01	3.54E-05	7.81E-03
DHRS7	-0.48	0.71	3.97E-05	7.81E-03
USP54	-0.76	0.59	4.79E-05	8.43E-03
WASF3	-0.41	0.75	5.36E-05	8.51E-03
CPQ	-0.46	0.72	6.58E-05	9.96E-03
INPP5D	-1.25	0.42	7.13E-05	1.04E-02
RHOB	-0.61	0.66	8.05E-05	1.09E-02
CDKN1C	-1.23	0.43	7.90E-05	1.09E-02
LAMA3	-1.15	0.45	9.40E-05	1.25E-02
ATP10D	-0.49	0.71	9.96E-05	1.30E-02
THSD4	-1.53	0.35	1.18E-04	1.44E-02
ETS1	0.46	1.38	1.26E-04	1.44E-02
PBX1	-0.70	0.62	1.41E-04	1.53E-02
CTBS	-0.44	0.73	1.53E-04	1.63E-02
MYC	0.79	1.73	1.56E-04	1.64E-02
SESN1	-0.84	0.56	1.78E-04	1.84E-02
RPL10A	0.34	1.26	1.88E-04	1.91E-02
RFX3	-0.58	0.67	1.99E-04	1.99E-02
KLF2	-1.18	0.44	2.15E-04	2.09E-02
ENG	0.59	1.50	2.31E-04	2.21E-02

SUN2	-0.82	0.57	2.39E-04	2.25E-02
IFITM2	0.72	1.65	2.46E-04	2.28E-02
PES1	0.44	1.36	2.49E-04	2.28E-02
GAPDH	0.58	1.49	2.53E-04	2.29E-02
NET1	-0.90	0.54	2.65E-04	2.36E-02
TET1	-0.47	0.72	2.75E-04	2.42E-02
ADPGK	0.35	1.27	2.83E-04	2.43E-02
RIOK3	-0.44	0.74	2.81E-04	2.43E-02
MAN1A1	-0.99	0.50	2.94E-04	2.48E-02
PEBP1	-0.62	0.65	3.04E-04	2.54E-02
SLC25A5	0.48	1.40	3.16E-04	2.56E-02
TSPYL2	-0.75	0.60	3.42E-04	2.71E-02
VMP1	0.60	1.52	3.89E-04	3.01E-02
GSN	-0.60	0.66	4.16E-04	3.10E-02
DCAF6	-0.22	0.86	4.34E-04	3.10E-02
MCCC2	-0.89	0.54	4.58E-04	3.14E-02
CARMIL1	-0.55	0.68	4.51E-04	3.14E-02
ARHGAP10	-0.47	0.72	4.57E-04	3.14E-02
ENAH	0.53	1.44	4.97E-04	3.31E-02
AEBP1	0.79	1.73	4.98E-04	3.31E-02
DNHD1	-0.51	0.70	5.53E-04	3.53E-02
CYP3A5	-1.40	0.38	5.74E-04	3.62E-02
SCRG1	-0.89	0.54	5.87E-04	3.64E-02
EIF4EBP1	1.06	2.09	6.04E-04	3.71E-02
MBIP	-0.40	0.76	6.10E-04	3.71E-02
OS9	-0.33	0.80	6.48E-04	3.91E-02
SERINC3	-0.32	0.80	6.54E-04	3.91E-02
BBS10	-0.57	0.67	6.83E-04	3.93E-02
CST3	-0.74	0.60	6.77E-04	3.93E-02
EHD3	0.42	1.34	6.75E-04	3.93E-02
SOCS3	0.78	1.71	7.07E-04	3.93E-02
ERICH1	-0.46	0.73	7.07E-04	3.93E-02
TTYH3	1.05	2.08	7.27E-04	3.97E-02
HEXB	-0.46	0.73	7.79E-04	4.11E-02
CD9	-0.80	0.57	7.82E-04	4.11E-02
PTMA	0.49	1.40	8.00E-04	4.17E-02
SOCS5	-0.40	0.76	8.85E-04	4.45E-02
GGT7	-0.54	0.69	8.90E-04	4.45E-02
RPS12	0.26	1.19	9.15E-04	4.54E-02

PPP1R3C	-0.71	0.61	9.54E-04	4.68E-02
TPST1	0.36	1.28	1.04E-03	4.71E-02
MN1	-0.80	0.58	1.04E-03	4.71E-02
SNED1	0.87	1.83	1.04E-03	4.71E-02
FADS1	-0.65	0.64	1.04E-03	4.71E-02
ITGA10	-0.47	0.72	9.98E-04	4.71E-02
SGSM2	-0.87	0.55	1.01E-03	4.71E-02
ESYT2	-0.18	0.88	9.79E-04	4.71E-02
MCM3	0.39	1.31	1.01E-03	4.71E-02
PRKAG2	-0.51	0.70	1.01E-03	4.71E-02
ANGPTL5	-1.18	0.44	1.11E-03	4.84E-02
AFF1	-0.39	0.76	1.09E-03	4.84E-02
MMP13	2.38	5.19	1.13E-03	4.84E-02
PDK4	-0.88	0.54	1.13E-03	4.84E-02
CCNB1IP1	-0.33	0.80	1.14E-03	4.84E-02
COL9A3	-1.62	0.32	1.16E-03	4.89E-02

Legend: Log2FC, log2 fold change; FC, fold change; FDR, False discovery rate

**Supplementary Table S7 | Previously reported OA risk loci present in our DE gene dataset.**

Gene name	Control versus 65%MS cartilage (n=14/group)		Lesioned versus Pre-served OA cartilage (N=35/group)		Risk Loci (GWAS)		
	FC	FDR	FC	FDR	Risk SNPs	OR	Suggested mechanism
<i>TNC</i>	2.80	8.51E-03	1.41	1.09E-02	rs13321, rs2480930 and rs1330349	1.09	Allelic expression imbalance (AEI)
<i>SCUBE1</i>	0.53	4.36E-02	0.42	2.15E-06	rs528981060	1.68	

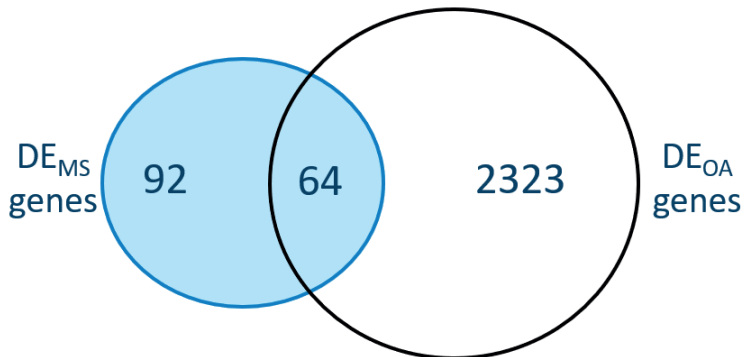
Legend: Log2FC, log2 fold change; FC, fold change; FDR, False discovery rate

**Supplementary Table S8 | All insulin growth factor binding proteins (IGFBPs) and related DE genes identified in our analysis.**

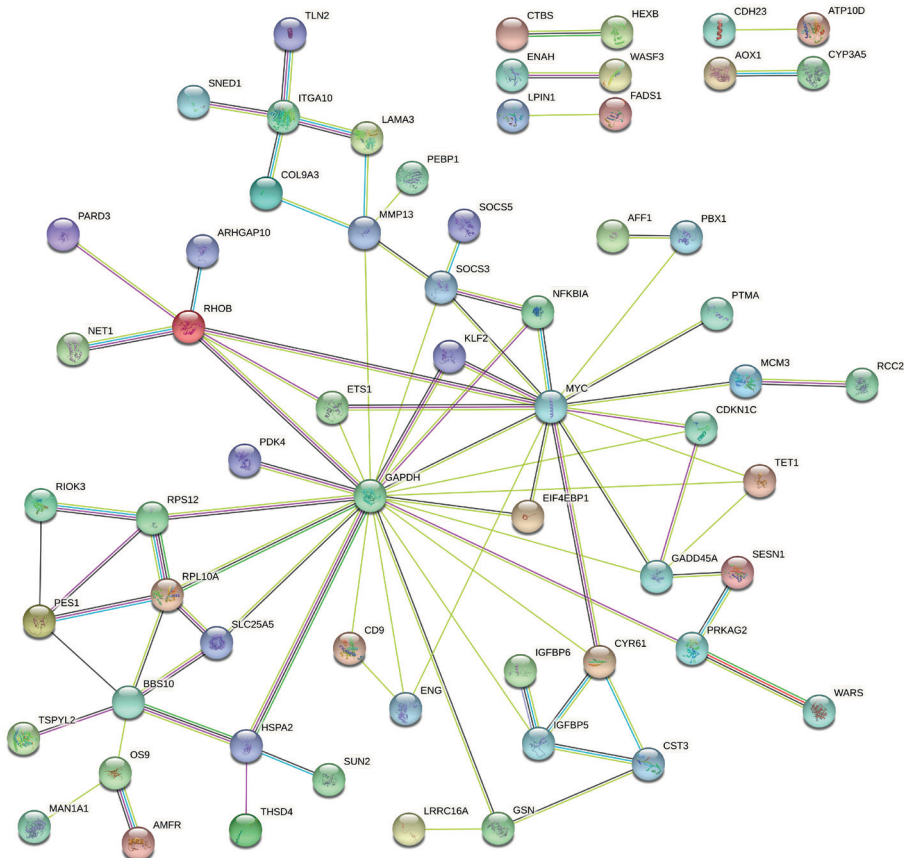
Gene name	log2FC	FC	pvalue	FDR
IGFBP4	1.38	2.59	5.44E-04	3.50E-02
IGFBP5	2.59	6.01	3.54E-05	7.81E-03
IGFBP6	-2.37	0.19	4.72E-08	3.07E-04
IGFBP7	-1.24	0.42	2.05E-06	1.79E-03
HTRA1	0.95	1.93	3.17E-04	2.56E-02
STC2	-1.07	0.48	1.39E-04	1.53E-02
ADAM12	0.62	1.54	6.63E-04	3.92E-02

Legend: Log2FC, log2 fold change; FC, fold change; FDR, False discovery rate

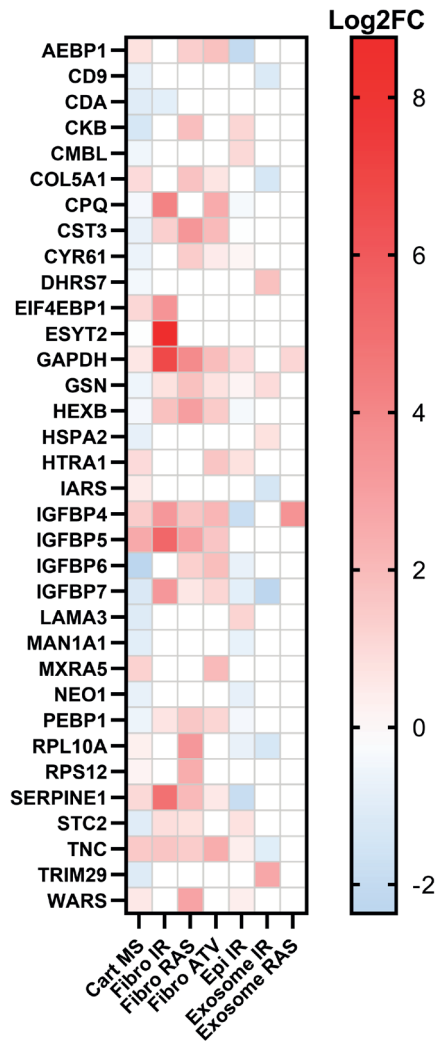
## Supplementary Figures



**Supplementary Figure S1** | Venn diagram of coinciding genes between differentially expressed genes in mechanically stressed versus control cartilage from osteochondral explants (DE<sub>MS</sub>) and previously identified differentially expressed genes in preserved versus lesioned OA cartilage (DE<sub>OA</sub>) [1].



**Supplementary Figure S2** | Protein-protein interaction network in STRING of proteins encoded by differentially expressed genes (N=92 genes) not coinciding with OA pathophysiology (DE<sub>ExclusiveMS</sub>).



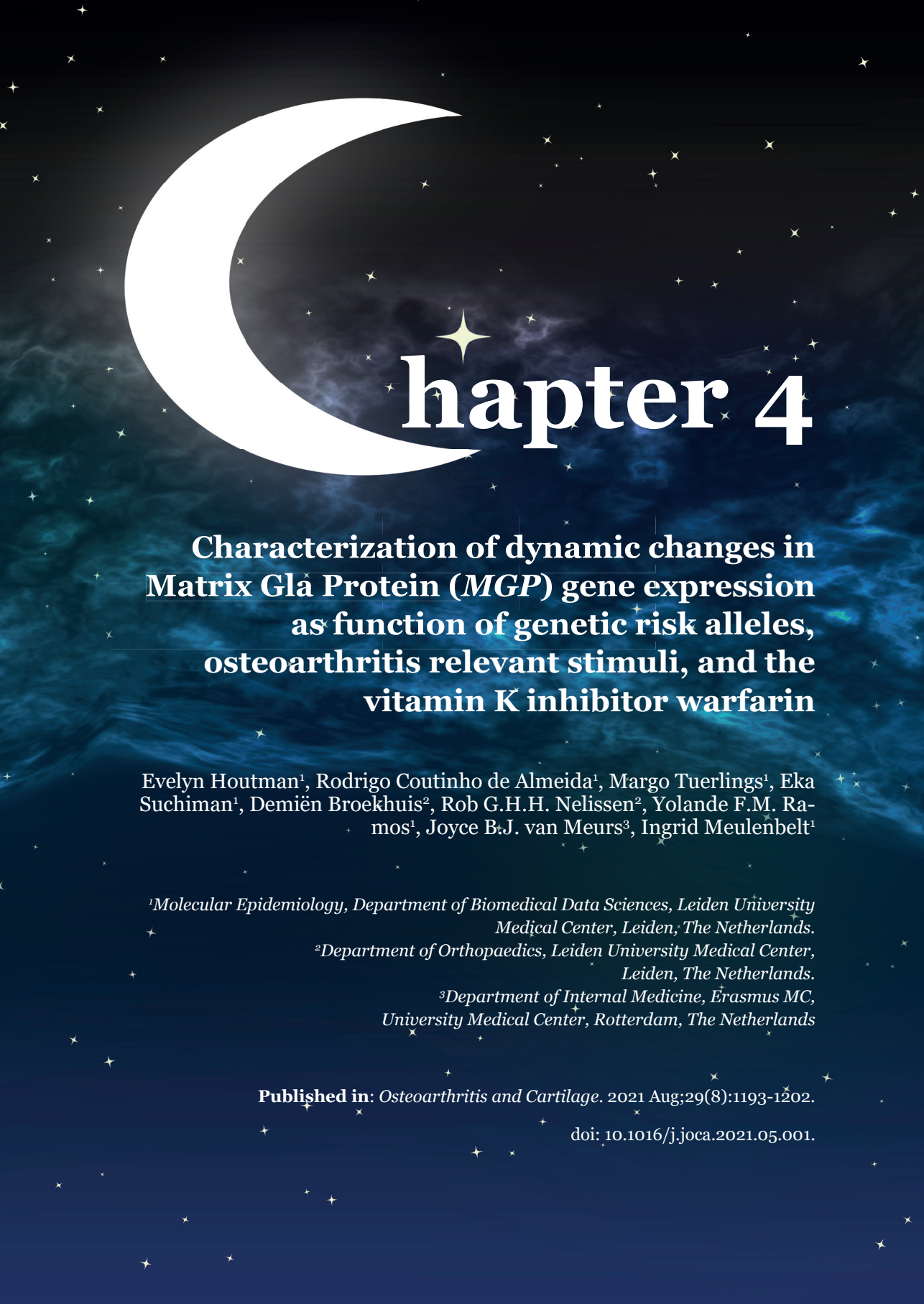
**Supplementary Figure S3 | Heat-map of proteins present in SASP.** The heat-map depicts the log<sub>2</sub> fold change (Log<sub>2</sub>FC) of gene expression changes in response to mechanical stress (Cart MS; first column) and proteins changes to several senescence inducing treatments found in the SASPatlas [2]. Abbreviations: cart, cartilage; MS, Mechanical stress; Fibro, fibroblasts; IR, X-irradiation; RAS, oncogenic RAS overexpression; ATV, atazanavir treatment; Epi, epithelial.

## REFERENCES

1. Coutinho de Almeida R, Ramos YFM, Mahfouz A, et al. RNA sequencing data integration reveals an miRNA interactome of osteoarthritis cartilage. *Annals of the rheumatic diseases*. 2019;78(2):270-7.
2. Basisty N, Kale A, Jeon OH, et al. A proteomic atlas of senescence-associated secretomes for aging biomarker development. *PLoS Biol*. 2020;18(1):e3000599.







# Chapter 4

## **Characterization of dynamic changes in Matrix Gla Protein (MGP) gene expression as function of genetic risk alleles, osteoarthritis relevant stimuli, and the vitamin K inhibitor warfarin**

Evelyn Houtman<sup>1</sup>, Rodrigo Coutinho de Almeida<sup>1</sup>, Margo Tuerlings<sup>1</sup>, Eka Suchiman<sup>1</sup>, Demiën Broekhuis<sup>2</sup>, Rob G.H.H. Nelissen<sup>2</sup>, Yolande F.M. Ramos<sup>1</sup>, Joyce B.J. van Meurs<sup>3</sup>, Ingrid Meulenbelt<sup>1</sup>

<sup>1</sup>*Molecular Epidemiology, Department of Biomedical Data Sciences, Leiden University Medical Center, Leiden, The Netherlands.*

<sup>2</sup>*Department of Orthopaedics, Leiden University Medical Center, Leiden, The Netherlands.*

<sup>3</sup>*Department of Internal Medicine, Erasmus MC, University Medical Center, Rotterdam, The Netherlands*

**Published in:** *Osteoarthritis and Cartilage*. 2021 Aug;29(8):1193-1202.

doi: 10.1016/j.joca.2021.05.001.

## Abstract

### Objective

We here aimed to characterize changes of Matrix Gla Protein (*MGP*) expression in relation to its recently identified OA risk allele rs1800801-T in OA cartilage, subchondral bone and human *ex vivo* osteochondral explants subjected to OA related stimuli. Given that *MGP* function depends on vitamin K bioavailability, we studied the effect of frequently prescribed vitamin K antagonist warfarin.

### Methods

Differential (allelic) mRNA expression of *MGP* was analyzed using RNA-sequencing data of human OA cartilage and subchondral bone. Human osteochondral explants were used to study exposures to interleukin 1 beta (IL-1 $\beta$ ; inflammation), triiodothyronine (T<sub>3</sub>; Hypertrophy), warfarin, or 65% mechanical stress (65%MS) as function of rs1800801 genotypes.

### Results

We confirmed that the *MGP* risk allele rs1800801-T was associated with lower expression and that *MGP* was significantly upregulated in lesioned as compared to preserved OA tissues, mainly in risk allele carriers, in both cartilage and subchondral bone. Moreover, *MGP* expression was downregulated in response to OA like triggers in cartilage and subchondral bone and this effect might be reduced in carriers of the rs1800801-T risk allele. Finally, warfarin treatment in cartilage increased *COL10A1* and reduced *SOX9* and *MMP3* expression and in subchondral bone reduced *COL1A1* and *POSTN* expression.

### Discussion & conclusions

Our data highlights that the genetic risk allele lowers *MGP* expression and upon OA relevant triggers may hamper adequate dynamic changes in *MGP* expression, mainly in cartilage. The determined direct negative effect of warfarin on human explant cultures functionally underscores the previously found association between vitamin K deficiency and OA.

### Keywords

Osteoarthritis, Articular cartilage, Subchondral bone, Matrix Gla Protein, Warfarin, Vitamin K, Genetic risk

## Introduction

Osteoarthritis (OA) is the most common degenerative disease of joints and its incidence is rising with increasing obesity and age, resulting in a high social and economic burden on society. Interacting risk factors for OA include obesity, age, sex, abnormal loading and genetic factors. The genetic component of OA is estimated to be in the range of 40%-60% [1,2]. For that matter, large-scale genome wide association studies (GWAS) have identified strong, in other words highly significant and reproducible, OA risk genes involved in the aetiology of OA, whereas follow-up studies have shown that risk single nucleotide polymorphisms (SNPs) frequently modulate pathology due to altering transcription of the genes in *cis* both in bone and cartilage [3-6].

In this regard Matrix Gla protein (*MGP*) via rs4764133 [7] with proxy SNPs rs1800801 and rs4236 [8], was previously identified as strong OA risk gene for hand OA with the OA conferring allele associated with lower expression of *MGP* relative to the non-risk allele [7] in a range of joint tissues but its effect was most profound in cartilage and subchondral bone [7,9]. On the other hand, these studies could not identify significant differential expression of *MGP* in OA pathophysiology in macroscopically lesioned OA compared to preserved cartilage [7] nor in macroscopically preserved cartilage compared to healthy cartilage [9]. These differential expression analyses were, however, determined in a relatively small sample size.

*MGP* regulates extracellular calcium levels via high affinity to its  $\gamma$ -carboxyglutamic acid (Gla) residues. Low *MGP* levels results in higher calcification of cartilage tissue and a reduced bone mineral density [10-12]. As the OA risk allele (rs1800801) has been associated with a reduced *MGP* gene expression [12] and with increased vascular calcification [13], this would suggest increased cartilage calcification in carriers of the OA risk allele. The latter was further justified by recapitulating downregulation of *MGP* in cartilage chondrocytes resulting in pro-catabolic (*ADAMTS4*, *MMP13*), as well as pro-hypertrophic (*COL10A1*, *VEGFA*) mRNA signalling [9]. The *MGP* protein is produced by the cell in inactive form and is dependent on vitamin K for activation, via carboxylation (c-*MGP*). As such, low vitamin K levels have been hypothesized to play a role in OA pathogenesis [14,15]. Similarly, vitamin K antagonists such as warfarin, that are frequently prescribed for the prevention of thromboembolic events in patients with atrial fibrillation [16], have been suggested to predispose to OA [17]. Nonetheless, the direct effect of warfarin on human articular cartilage tissue homeostasis has not been assessed.

Here we set out to explore *MGP* gene expression in relation to the OA risk allele rs1800801-T, in a large RNA-sequencing dataset containing both macroscopically preserved and lesioned cartilage [18] and subchondral bone [19] as well as in our recently established full thickness human *ex vivo* osteochondral explant model [20]. The latter allowing us to study the effect of the OA risk allele on the dynamic *MGP* response to different OA related stimuli, such as inflammation (Interleukin 1 beta (IL-1 $\beta$ )), hypertrophy (Triiodothyronine (T3)) and 65% mechanical stress (65%MS). Moreover, we used the human *ex vivo* explant model to study the direct effect of vitamin K antagonist, warfarin, on articular cartilage and subchondral bone homeostasis.

## Material and Methods

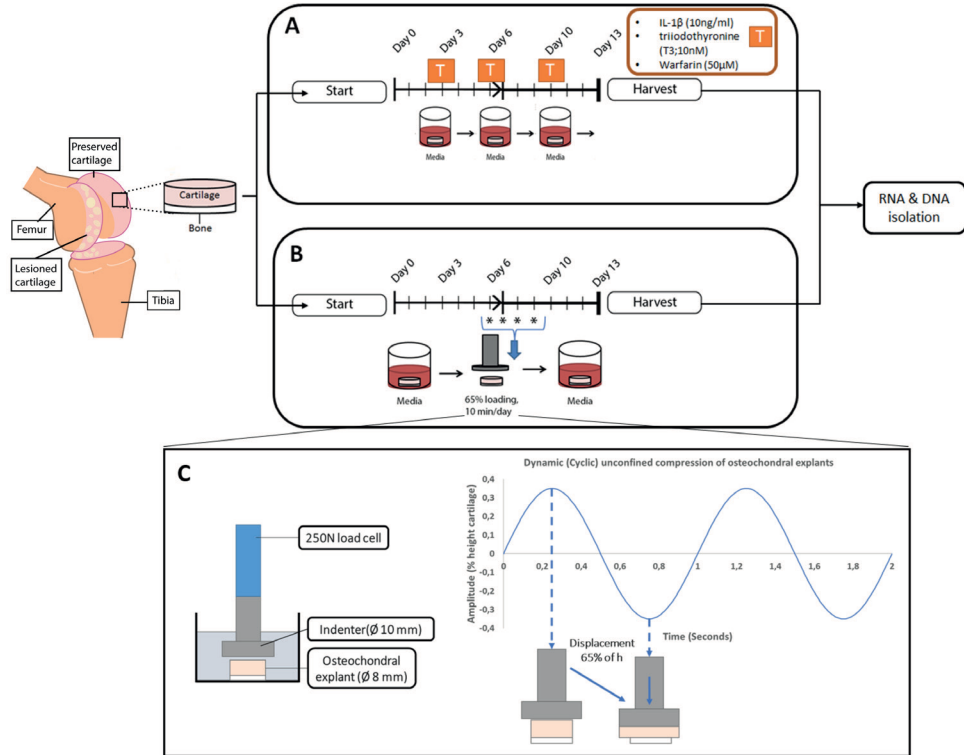


**Figure 1 | Schematic representation of different perturbations applied to osteochondral explants.** Osteochondral explants were punched from the still macroscopically preserved looking knee condyle area and taken into culture. **[A]** Explants were subjected to treatment with IL-1 $\beta$  (10 ng/ml), triiodothyronine (T<sub>3</sub>; 10 nM) or warfarin (50  $\mu$ M). **[B]** Explants received mechanical stresses at a strain of 65% for 10 minutes per day on four subsequent days. On day 13, cartilage and bone was separated, snap frozen and stored at -80C. **[C]** Schematic representation of the dynamic (cyclic) compression applied to osteochondral explants. Legend: N=Newton; h=height.

### Sample description

Human material was obtained from the Research in Articular Osteoarthritis Cartilage (RAAK) biobank as previously described in detail [21]. The RAAK study is approved by the medical ethics committee of the Leiden University Medical Center (P08.239/P19.013). In this study, RNA-sequencing data was included of paired macroscopically preserved and lesioned OA cartilage of N=35 participants [18] and subchondral bone of N=24 participants [19] for which sample characteristics have previously been described. In total 136 osteochondral explants were harvested from the macroscopically preserved condyle knee joints of N=18 participants and divided over the different experiment (**Supplementary Figure 1**). Multiple osteochondral explants containing both cartilage and bone (diameter of 8 mm) were extracted per participant and washed in sterile PBS before taking into culture. Donor characteristics of osteochondral explants are described in **Supplementary Table 1** and study design is described in **Supplementary Figure 1**. For additional details on neo-cartilage deposition, RNA and

DNA isolations, TaqMan genotyping, RNA sequencing data of cartilage and subchondral bone, unconfined dynamic (cyclic) compression, expression quantitative trait loci (eQTL), Allelic Expression Imbalance (AEI) and data analysis, see the **Supplementary Methods**.

### **Treatment of osteochondral explants**

Explants were cultured in 24 wells plates (Greiner CELLSTAR; Sigma) supplemented with 1.5 ml CDM in a 5% (v/v) CO<sub>2</sub> incubator at 37°C. Three days after extraction, explants were treated with either IL-1 $\beta$  (10 ng/ml), triiodothyronine (T<sub>3</sub>, 10 nM; Sigma) or warfarin (50  $\mu$ M; Sigma), depicted in **Figure 1A**. Six days after extraction, dynamic unconfined compression was applied to explant tissues using the Mach-1 mechanical testing system (Biomomentum Inc., Laval, QC, Canada) on four subsequent days (**Figure 1B**). Mechanical stress was applied at a strain of 65% of cartilage height and at a frequency of 1 Hz, mimicking walking speed (**Figure 1C**). Cartilage and bone were separated using a scalpel, snap-frozen in liquid nitrogen, and stored at -80°C for RNA isolation.

### **Reverse transcription and Real-Time PCR**

Real-Time PCR for gene expression was performed with QuantStudio 6 Real-Time PCR system (Applied Biosystems) using Fast Start Sybr Green Master mix (Roche Applied Science). Primer sequences (**Table 1**) used were tested for linear amplification and missing datapoints for genes are summarized in **Supplementary Table 2** and **3**. Details on normalization can be found in the **Supplementary Methods**.

**Table 1. Primer sequence used to determine gene expression levels in real-time PCR.**

<b>Gene name</b>	<b>Forward 5'-3'</b>	<b>Reverse 5'-3'</b>
<i>SDHA</i>	TGGAGCTGCAGAACCTGATG	TGTAGTCTTCCCTGGCATGC
<i>MGP</i>	CGCCCCAGATTGATAAGTA	TCTCCTTGACCCTCACTGC
<i>SOX9</i>	CCCCAACAGATCGCCTACAG	CTGGAGTTCTGGTGGTCGGT
<i>ACAN</i>	AGAGACTCACACAGTCGAAACAGC	CTATGTTACAGTCTCGCCAGTG
<i>COL2A1</i>	CTACCCCAATCCAGCAAACGT	AGGTGATGTTCTGGGAGCCTT
<i>RUNX2</i>	CTGTGGTTACTGTCATGGCG	AGGTAGCTACTTGGGGAGGA
<i>ALPL</i>	CAAAGGCTTCTTCTGTGCTGGTG	CCTGCTTGGCTTTTCCTTCA
<i>COL1A1</i>	GTGCTAAAGGTGCCAATGGT	ACCAGGTTCACCGCTGTTAC
<i>COL10A1</i>	GGCAACAGCATTATGACCCA	TGAGATCGATGATGGCACTCC
<i>MMP3</i>	GAGGCATCCACACCCTAGGTT	TCAGAAATGGCTGCATCGATT
<i>MMP13</i>	TTGAGCTGGACTCATTGTCTG	GGAGCCTCTCAGTCATGGAG
<i>ADAMTS5</i>	TGGCTCACGAAATCGGACAT	GCGCTTATCTTCTGTGGAACC
<i>COMP</i>	ACAATGACGGAGTCCCTGAC	TCTGCATCAAAGTCGTCTG
<i>OMD</i>	GGACACAACAAATTGAAGCAAGC	TGGTGGTAATGTAGTGGGTCA
<i>BGLAP</i>	CCCTCTGCTGYYGACACAAA	CACACTCTCGCCCTATTGG
<i>OGN</i>	TGATGAAATGCCACGTGTC	TTTGGTAAGGTTGGTACAGCA
<i>SPP1</i>	GCCAGTTGCAGCCTTCTCA	AAAAGCAAATCACTGAATTCTCA
<i>TNFRSF11B</i>	TTGATGAAAGCTTACCGGGA	TCTGGTCACTGGGTTTGCATG
<i>BMP2</i>	TCCATGTGGACGCTCTTCA	AGCAGCAACGCTAGAAGACA
<i>POSTN</i>	TACACTTTGCTGGCACCTGT	TTTAAGGAGGCGCTGATCCA

## Statistical analyses

Differential *MGP* expression analyses between preserved and lesioned OA cartilage and bone including false discovery rates (FDR) as multiple testing correction for the genome wide analyses were reproduced from Coutinho [18] and Tuerlings [19], respectively. Description on their study design and sample numbers are in **Supplementary Methods**. To assess allelic expression imbalance (AEI) we applied our previously published methodology in R [22] to RNA sequence data of *MGP* in the larger dataset of cartilage [18] and a dataset of bone [19] which is further outlined in **Supplementary Methods**. To test expression quantitative trait analyses (eQTL) and differential expression of *MGP* in genotype strata in the current manuscript, we used the variance stabilizing transformation (VST) normalized *MGP* expression levels of these RNA sequencing datasets and used generalized estimating equations (GEE) [23] to effectively adjust for dependencies of genotypes among donors by adding a random effect for sample donor. Details of the models applied are outlined in **Supplementary Methods**. *MGP* expression by RT-qPCR in the *in vitro* 3D-neo cartilage formation was estimated using a generalized linear mixed model (GLMM) using *MGP* levels ( $-\Delta\text{CT}$ ) as dependent variable and time as repeated measure:  $MGP\ level \sim Time + (1|Donor)$ . In the osteochondral explant models fold changes (FC) of RT-qPCR expression were determined by calculating the log<sub>2</sub> of the  $-\Delta\Delta\text{Ct}$  for each sample ( $2^{-\Delta\Delta\text{CT}}$ ) where  $\text{FC} > 1$  is upregulation and  $\text{FC} < 1$  is downregulation of treated samples compared to control samples. The reported P-values were determined by applying GEE to  $-\Delta\text{CT}$  values to effectively adjust for dependencies among donors of the explants by adding a random effect for sample donor as we did not have perfect pairs for each analysis. We followed a linear GEE model, with *MGP* level as dependent variable, treatment as factor and exchangeable working matrix:  $MGP\ level \sim Treatment + (1|Donor)$  [24]. Differences in effect sizes between strata was determined by performing unpaired student's t-test on the fold changes corrected for control samples. Warfarin treated osteochondral explants samples were paired hence a paired sample t-test was performed to determine between-group differences and p-values. Except for AEI, Statistical analyses were performed in SPSS statistics 23 (IBM). Outliers were investigated using Grubbs's test and normal distribution was determined using Shapiro-Wilk test and visually inspecting Q-Q plots. The boxplots represent 25th, 50th and 75th percentiles, and whiskers extend to the 95%CI.

## Results

### ***Expression patterns of MGP in previous established RNA sequencing datasets of preserved and lesioned OA cartilage and subchondral bone***

We used our previously established RNA sequencing dataset of macroscopically preserved and lesioned OA cartilage samples (N=35 pairs [18]) and subchondral bone (N=24 pairs [19]), to examine differential *MGP* expression with OA tissue status and with the OA risk SNPs (see **Supplementary Methods and Figures**). An increased expression of *MGP* in lesioned compared to preserved OA cartilage was observed ( $\text{FC}=1.45$ ,  $95\% \text{CI}[1.24;1.61]$ ,  $\text{P-value}=1.78 \times 10^{-3}$ ) and this increase of *MGP* was genome wide significant ( $\text{FDR}=0.021$ ). Similarly, *MGP* was upregulated in lesioned compared to preserved OA subchondral bone ( $\text{FC}=1.53$ ,  $95\% \text{CI}[1.22;1.64]$ ,  $\text{P-value}=0.023$ ), but this was not genome wide significant ( $\text{FDR}=0.12$ ). Together, these results show a robust upregulation of *MGP* expression with ongoing OA pathophysiology.

Here we studied whether the *MGP* differential expression between preserved and lesioned OA tissues was affected by *MGP* OA risk allele carriership. As shown in **Figure 2A**, the *MGP* upregulation occurs particularly among risk allele carriers rs1800801-T in lesioned compared to preserved OA cartilage independent of age and sex of donors (OR=2.70, 95%CI[1.16;6.29], P-value=0.021). Notably however, the overall *MGP* expression remains lower among risk allele carriers rs1800801-T as compared to carriers of the reference allele rs1800801-C. The same effect was observed in subchondral bone, where *MGP* was found to be upregulated in lesioned compared to preserved tissue only in risk allele carriers rs1800801-T (OR=3.04, 95%CI[1.24;7.45], P-value=0.015) independent of age and sex of donors (**Figure 2B**).

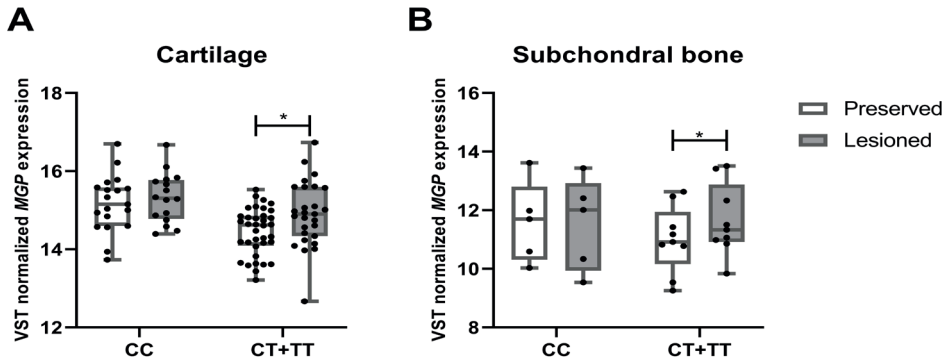


**Figure 2 | MGP expression as function of the transcript and OA risk SNP rs1800801.** [A] Variance stabilizing transformation (VST) normalized MGP expression levels extracted from the RNA sequencing dataset in preserved and lesioned OA cartilage stratified for rs1800801 genotype CC ( $n_{\text{Preserved}}=19$  versus  $n_{\text{Lesioned}}=16$ ) and CT+TT ( $n_{\text{Preserved}}=36$  versus  $n_{\text{Lesioned}}=27$ ). [B] Variance stabilizing transformation (VST) normalized MGP expression levels extracted from the RNA sequencing dataset in preserved and lesioned OA subchondral bone stratified for rs1800801 genotype CC ( $n_{\text{Preserved}}=5$  versus  $n_{\text{Lesioned}}=5$ ) and CT+TT ( $n_{\text{Preserved}}=9$  versus  $n_{\text{Lesioned}}=9$ ). The boxplots represent 25th, 50th and 75th percentiles, and whiskers extend to the 95%CI. Independent samples are depicted by black dots in each graph. To adjust for donor variation, P-values were estimated by performing logistic generalized estimation equations, with tissue status as dependent variable and MGP level, age and sex as covariate:  $Tissue\ status \sim MGP\ level + age + sex + (1|Donor)$ . \*  $P \leq 0.05$ .

Next, we attempted to replicate the previously shown AEI of *MGP* in association with the OA risk SNP rs1800801 [7] in heterozygous individuals in this larger RNA sequencing dataset of preserved and lesioned OA cartilage [18] and a novel dataset of OA subchondral bone [19]. Additionally, we explored whether the effect size in AEI differed in these tissues between preserved and lesioned areas. As shown in **Supplementary Figure 2A** we confirmed AEI expression of *MGP* in preserved OA cartilage with the risk-conferring allele rs1800801-T associated to a reduced *MGP* expression of 10% (95%CI[2.24;18.64]) relative to the reference allele rs1800801-C. In lesioned OA cartilage the AEI was very comparable with rs1800801-T associated to a reduced *MGP* expression of 11% (95%CI[2.25;19.49]) relative to the reference allele rs1800801-C. In subchondral bone, genotype of rs1800801 could not be called thus we used its proxy SNP rs4236 ( $r^2=0.93$  with rs1800801), which was also investigated previously [7]. As shown in **Supplementary Figure 2B**, we confirmed AEI of *MGP* in preserved OA subchondral bone with the risk-conferring allele rs4236-C associated to a reduced *MGP* expression of 10% (95%CI[5.70;14.52]) relative to the reference allele rs4236-T. In lesioned OA subchondral bone AEI was very comparable, with rs4236-C associated to a reduced *MGP* expression of 12% (95%CI[8.80;14.55]) relative to the reference allele rs4236-T.

Finally, we analysed *MGP* expression levels among genotype carriers of one or two of the OA risk alleles rs1800801-T (eQTL) and confirmed that also overall *MGP* expression in cartilage is reduced in a dose responsive manner with *MGP* risk alleles, independent of donor, age, sex, and OA status, i.e. preserved or lesioned (OR=0.73, 95%CI[0.64;0.84], P-value=4.00x10<sup>-6</sup>; **Supplementary Figure 3A**). In subchondral bone we observed a similar pattern, however this was not significant (**Supplementary Figure 3B**). Together these data confirm that innate lower *MGP* expression levels confer risk to OA, though its effect seems more pronounced in articular cartilage.

### ***MGP* expression patterns in human in vitro and ex vivo models and as function of OA related cues**

First, we investigated expression of *MGP* during neo-cartilage formation using a human *in vitro* 3D pellet culture with primary chondrocytes. As shown in **Figure 3**, *MGP* is expressed in primary chondrocytes (day-0) and increases during cartilage extracellular matrix (ECM) deposition until day-14, suggesting that *MGP* expression can be considered a marker of neo-cartilage formation.

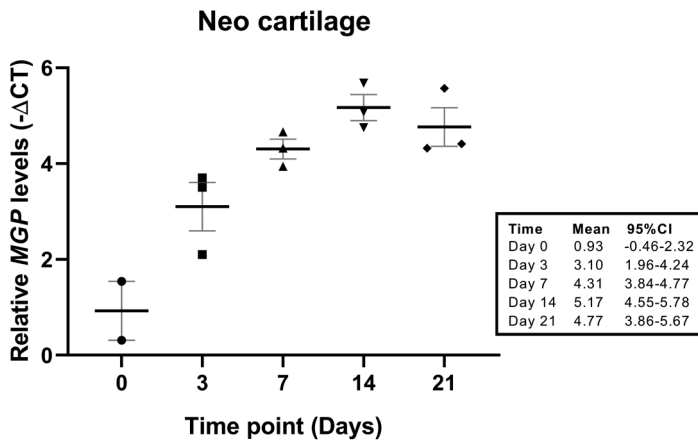


**Figure 3 | Gene expression of *MGP* in an in vitro 3D model of neo-cartilage.** Gene expression of *MGP* in an in vitro 3D chondrocyte pellet model of neo-cartilage formation (N=3 donors; day 0: n=2, all other time points: n=3). Data is depicted as mean expression (- $\Delta$ CT)  $\pm$  standard error of the mean (SEM) and each dot represent an sample of two combined biological duplicates. Statistical analysis was performed by generalized linear mixed model (GLMM) using *MGP* levels as dependent variable and time as repeated measure:  $MGP\ level \sim Time + (1|Donor)$ .

Next, we explored dynamic changes in *MGP* expression in cartilage and subchondral bone in an established human *ex vivo* osteochondral explant model [20] as function of OA related stimuli being inflammation (IL-1 $\beta$ ), hypertrophy (T3), and 65% mechanical stress (65%MS). As shown in **Figure 4**, we observed in cartilage a consistent and significant downregulation of *MGP* expression after treatment with IL-1 $\beta$  (FC=0.03, 95%CI[0.02;0.06], P-value=4.40x10<sup>-7</sup>), T3 (FC=0.80, 95%CI[0.56;0.97], P-value=0.046), as well as with mechanical stress (FC=0.65, 95%CI[0.45;0.85], P=0.002). Notable, in **Figure 4**, is an outlier

in the mechanical stress group, however removing this datapoint did not influence our result (FC=0.67, 95%CI[0.47;0.87], P-value=0.046). In subchondral bone we were not able to isolate RNA for IL-1 $\beta$  treated samples and only observed a significant downregulation of *MGP* expression after treatment with T3 (FC=0.81, 95%CI[0.52;1.10], P-value=0.015; **Figure 4 D-E**).

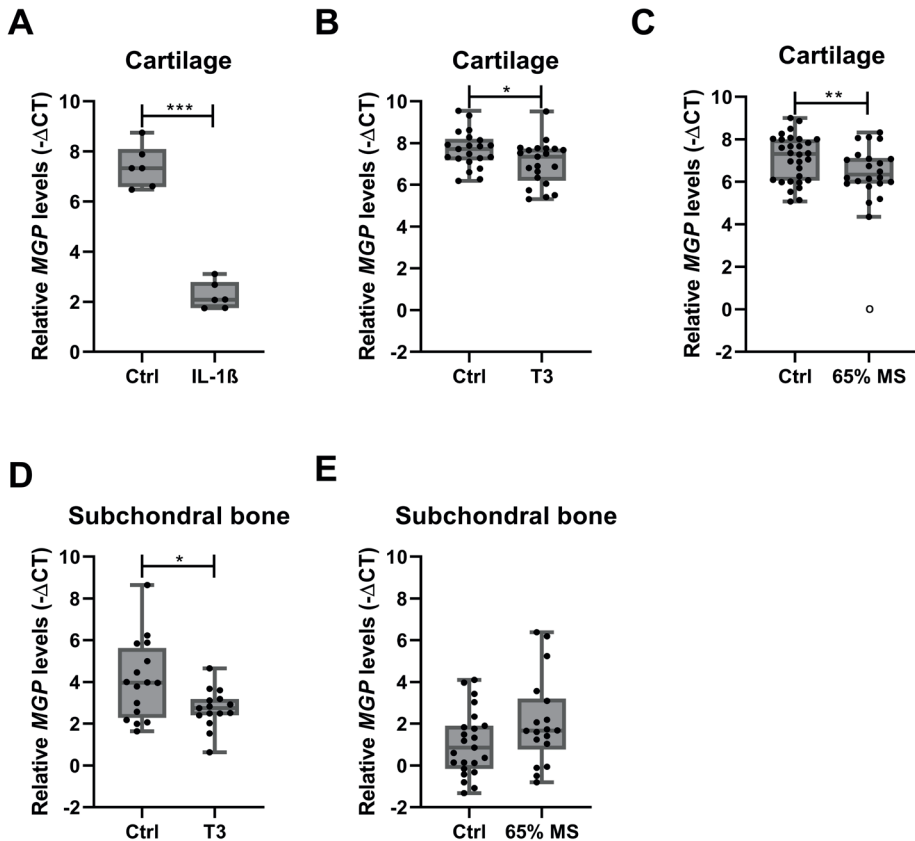


**Figure 4 | Gene expression of MGP in response to three different OA relevant cues in cartilage of osteochondral explants.** Gene expression of *MGP* ( $-\Delta\text{CT}$ ) in an *ex vivo* osteochondral explant model in articular cartilage (**A**, **B**, **C**) and subchondral bone (**D**, **E**). *MGP* expression, represented by the housekeeping gene corrected value ( $-\Delta\text{CT}$ ), in articular cartilage upon perturbation with **[A]** IL-1 $\beta$  ( $n_{\text{Control}}=6$  versus  $n_{\text{Treated}}=6$ ), **[B]** T3 ( $n_{\text{Control}}=21$  versus  $n_{\text{Treated}}=21$ ) and **[C]** posttraumatic OA after 65% MS ( $n_{\text{Control}}=30$  versus  $n_{\text{Treated}}=23$ ). *MGP* expression in subchondral bone upon perturbation with **[D]** T3 ( $n_{\text{Control}}=16$  versus  $n_{\text{Treated}}=16$ ) and **[E]** posttraumatic OA after 65% MS ( $n_{\text{Control}}=23$  versus  $n_{\text{Treated}}=19$ ). The boxplots represent 25th, 50th and 75th percentiles, and whiskers extend to the 95%CI.  $-\Delta\text{CT}$  of each independent sample is depicted by black dots in the graphs. To adjust for donor variation P-values were determined by performing linear generalized estimation equations, with *MGP* levels as dependent variable and treatment as factor:  $MGP\ level \sim Treatment + (1|Donor)$ . Far out values are represented by the white filled circle (o) which did not affect the result (see main body text) and therefore analysis including this sample is presented in **C**. \*  $P \leq 0.05$ , \*\*  $P \leq 0.01$ , \*\*\*  $P \leq 0.001$ . Legend: Ctrl=Control; 65% MS=65% mechanical stress.

### Changes in *MGP* expression in the *ex vivo* OA models as function of the transcript and OA risk SNP *rs1800801*

Since general *MGP* expression was identified to change between preserved and lesioned OA cartilage and subchondral bone, and in an osteochondral explant model to several OA related stimuli (**Figure 4**), we next explored whether the OA risk allele *rs1800801*-T modified these effects. Hereto we investigated the observed dynamic downregulation of *MGP*, upon inducing hypertrophy (T3 exposure; **Figure 5A** and **C**) and mechanical stress (65%MS; **Figure 5B** and **D**) in our *ex vivo* cartilage explant model stratified by *rs1800801* genotypes. For IL-1 $\beta$  treatment, donor numbers were too low to explore the effect of genotype.

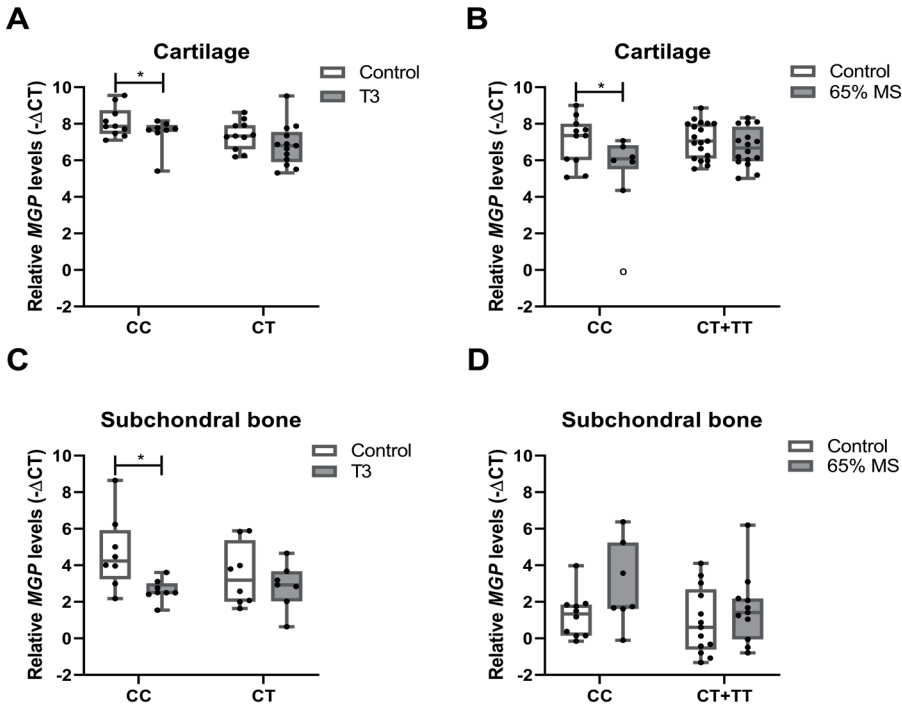


**Figure 5 | *MGP* expression as function of the transcript and OA risk SNP *rs1800801*.** *MGP* expression (- $\Delta$ CT) in an *ex vivo* osteochondral explant model stratified by *rs1800801* genotype in articular cartilage (**A**, **B**) and subchondral bone (**C**, **D**). *MGP* gene expression in articular cartilage upon perturbation with [**A**] T3 (CC:  $n_{\text{Control}}=10$  versus  $n_{\text{Treated}}=8$ ; CT:  $n_{\text{Control}}=11$  versus  $n_{\text{Treated}}=13$ ) and [**B**] posttraumatic OA upon 65% mechanical stress (CC:  $n_{\text{Control}}=11$  versus  $n_{\text{Treated}}=7$ ; CT+TT:  $n_{\text{Control}}=19$  versus  $n_{\text{Treated}}=16$ ). *MGP* gene expression in subchondral bone upon perturbation with [**C**] T3 (CC:  $n_{\text{Control}}=8$  versus  $n_{\text{Treated}}=9$ ; CT:  $n_{\text{Control}}=8$  versus  $n_{\text{Treated}}=7$ ) and [**D**] posttraumatic OA upon 65% mechanical stress (CC:  $n_{\text{Control}}=10$  versus  $n_{\text{Treated}}=7$ ; CT+TT:  $n_{\text{Control}}=13$  versus  $n_{\text{Treated}}=12$ ). The boxplots represent 25th, 50th and 75th percentiles, and whiskers extend to the 95%CI. Independent samples are depicted by black dots in each graph. Numeric values associated to this Figure are shown in **Supplementary Table 4**. To adjust for donor variation P-values were determined by performing linear generalized estimation equations, with *MGP* levels as dependent variable and treatment as factor:  $MGP\ level \sim Treatment + (1|Donor)$ . Far out values are represent by the white filled circle (o) which did not affect the result (see main body text) and therefore analysis including this sample is presented in **B**. \*  $P \leq 0.05$ . Legend: 65% MS=Mechanical stress.

In cartilage (**Figure 5A** and **Figure 5B**), we observed that downregulation of *MGP* occurred particularly among carriers of the reference allele rs1800801-C for hypertrophy (T<sub>3</sub>) (FC=0.69, 95%CI[0.49;0.89]) and for mechanical stress (FC=0.26, 95%CI[0.14;0.38]) as compared to carriers of the risk allele rs1800801-T for hypertrophy (FC=0.92, 95%CI[0.57;1.27]) and for mechanical stress (FC=0.85, 95%CI[0.61;1.09]). Also in the data shown in **Figure 5B** the previously identified outlier in the mechanical stress group did not influence our result upon removal (FC=0.29, 95%CI[0.17-0.41], P-value=0.045). As shown in **Supplementary Table 4**, the difference in response (FC) among carriers of the reference allele rs1800801-C relative to carriers of the OA risk allele rs1800801-T is significant for mechanical stress (FC=0.34, 95% CI[0.28-0.38], P-value=2.8x10<sup>-3</sup>). Similarly in bone (**Figure 5C** and **5D**), we observed that downregulation of *MGP* expression in subchondral bone upon hypertrophy induction (T<sub>3</sub>) was more pronounced among carriers of the reference allele rs1800801-C (FC=0.50, 95%CI[0.09;0.91]) as compared to the carriers of the risk allele rs1800801-T (FC=0.82, 95%CI[0.37;1.27]). This difference, however, did not reach statistical significance (**Supplementary Table 4**). For mechanical stress no effects were observed in subchondral bone. Together these data suggest that particularly in cartilage the OA risk allele rs1800801-T may have a different response in *MGP* expression upon OA relevant cues.

### ***Treatment of osteochondral explants with warfarin***

Since the activation of *MGP* is dependent on vitamin K and innate lower *MGP* expression confers risk to OA, we next investigated the direct effect of the vitamin K antagonist warfarin on articular chondrocyte and subchondral bone signalling. Hereto, *ex vivo* osteochondral explants (n=15 pairs for cartilage and n=13 pairs for subchondral bone) were treated with warfarin. The effect of this reduced vitamin K bioavailability on the cartilage homeostasis was determined by measuring chondroprotective genes (*SOX9*, *COL2A1* and *ACAN*), genes involved in early/late cartilage hypertrophy (*RUNX2*, *ALPL*, *COL1A1*, *COL10A1* and *MGP*) and catabolic genes (*MMP3*, *MMP13* and *ADAMTS5*). As shown in **Figure 6A**, warfarin exposure to cartilage reduced expression of *SOX9* (FC=0.87, 95%CI[0.77;0.97], P-value=0.023) and *MMP3* (FC=0.56, 95%CI[0.43;0.69], P-value=1.02x10<sup>-5</sup>), while increasing *COL10A1* (FC=2.26, 95%CI[1.14;3.38], P-value=0.045). In addition, *RUNX2* (FC=1.43, 95%CI[0.96;1.90], P-value=0.094), a master transcriptional regulator of chondrocyte maturation, and *ALPL* (FC=6.21, 95%CI[1.36;11.06], P-value=0.059) show a trend towards upregulation in response to warfarin treatment. In subchondral bone, genes involved in matrix formation (*COL10A1*, *RUNX2*, *ALPL*, *COL1A1*, *OMD*, *BGLAP* and *OGN*) and remodelling (*MGP*, *SPP1*, *TNFRSF11B*, *BMP2* and *POSTN*) were measured. As shown in **Figure 6B**, warfarin exposure to subchondral bone significantly reduced expression of the bone formation marker *COL1A1* (FC=0.81, 95%CI[0.59;1.03], P-value=0.046) and the remodelling marker *POSTN* (FC=0.67, 95%CI[0.42;0.92], P-value=0.011). Together these results show that addition of warfarin to aged osteochondral explants resulted in a significant upregulation of hypertrophic signalling among articular chondrocytes and reduced bone formation and altered remodelling signalling.

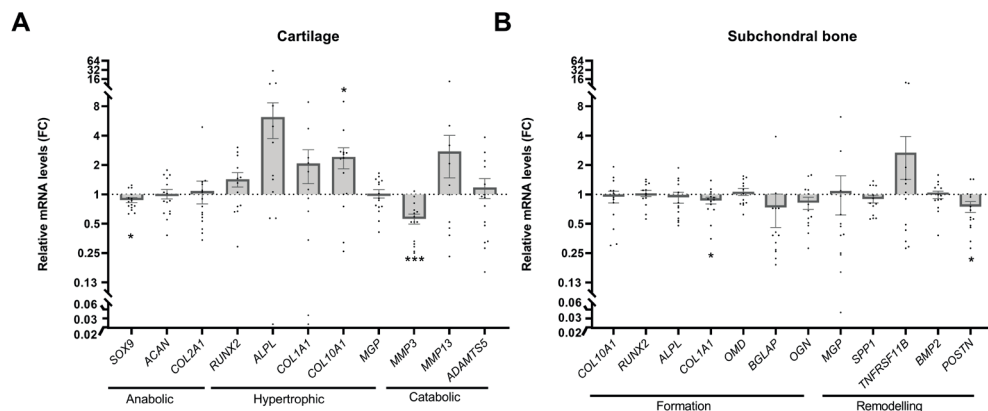


**Figure 6 | Gene expression after 10 days of warfarin treatment.** mRNA expression of genes depicted as a fold change (FC) following 50 $\mu$ M warfarin treatment relative to controls in **[A]** cartilage ( $n_{\text{Control}}=15$  versus  $n_{\text{Treated}}=15$ ) and **[B]** subchondral bone ( $n_{\text{Control}}=13$  versus  $n_{\text{Treated}}=13$ ). Controls are depicted by the dotted line, while each gray dot represents a warfarin treated sample. The number and percentage of missing data points per gene are summarized in **Supplementary Table 2** and **3**. The light gray bars represent the mean  $\pm$  standard error of the mean (SEM) of the Fold change (FC) in which FC>1 represent upregulation and FC<1 represents downregulation of warfarin treated samples relative to its paired control. The x-axis is given in a log<sub>2</sub> scale to depict the up and down regulation in the same scale. Differences in gene levels between warfarin exposure and controls were calculated by means of a paired t-test. \*P  $\leq$  0.05; \*\*\*\*P  $\leq$  0.001

## Discussion

In the current paper we explored (dynamic) changes of *MGP* expression in relation to the OA risk allele rs1800801-T, in preserved and lesioned OA cartilage, as well as, in a human *ex vivo* explant model subjected to OA related stimuli, such as inflammation, hypertrophy and mechanical stress. Furthermore, we studied the direct effect of the frequently used vitamin K antagonist, warfarin, on articular chondrocyte and subchondral bone signaling. In doing so, we confirm that *MGP* expression, as inhibitor of calcification via high affinity of calcium to its Gla-residues, should be considered a beneficial marker of articular cartilage. Consequently, the significantly upregulated *MGP* expression with ongoing OA pathophysiology is likely an attempt of chondrocytes to halt the OA associated osteo-induction. Noteworthy is our observation that the OA risk allele may also hamper adequate dynamic change in expression of *MGP* in response to OA and relevant cues like mechanical stress (65%MS) and this effect was most pronounced in cartilage. Finally, warfarin treatment to the aged human cartilage explants resulted in a significant upregulation of hypertrophic signalling among articular chondrocytes and reduced bone formation while altering remodelling.

Similar to previous reports [7,9], we here confirmed in a large RNA-sequencing dataset, that the OA risk allele rs1800801-T is associated with lower (overall) expression of *MGP* in articular cartilage (**Supplementary Figure 3A**). In addition, we confirmed that *MGP* gene expression is significantly upregulated in both articular cartilage and subchondral bone in OA pathophysiology. Although, our results showed that this effect was mainly driven by carriers of the rs1800801-T OA risk allele in both tissues the expression of *MGP* does not reach the level of that in carriers of the reference allele rs1800801-C (**Figure 2A** and **2B**).

We advocate that *MGP* upregulation with OA pathophysiology in cartilage is an attempt of chondrocytes to compensate for the osteo-inductive effect of low *MGP* levels and that this is not sufficient among the *MGP* OA risk allele carriers. On the other hand, the upregulation of *MGP* in bone may be a marker of active bone resorption as it was previously found that *MGP* inhibits mineralization by osteoblasts while increased *MGP* expression in osteoclasts mark increased osteoclastic commitment [25]. Together our data highlights that, similar to vascular calcification and bone loss [26], also articular cartilage calcification and bone loss in OA could share a common pathogenetic mechanism involving *MGP*.

We also explored the dynamic response of *MGP* in a human *ex vivo* explant model while applying OA relevant perturbing cues such as inflammation, hypertrophy, and mechanical stress. The strength of our explant model is that it represents physiological relevant aged human articular cartilage prone to OA pathophysiology, hence suitable to study the initial process of OA related cartilage destruction. Moreover, and despite the inherent heterogeneity between donors, we found in cartilage a consistent downregulation of *MGP*, associated with matrix mineralization, as general response to OA related perturbations (**Figure 4**). Additionally, we showed that the rs1800801-T OA risk allele may hamper such innate dynamic change in *MGP* expression upon stress. A possible mechanism by which the genetic risk variant modifies response to stress lies in the fact that rs1800801 is localized in the transcription factor binding site (POLR2A, CTCF, p300) of the *MGP* promoter (**Supplementary Figure 4**). In addition, the OA risk allele rs1800801-T was shown to reduce expression between 34-47% in a luciferase reporter assay and *in silico* prediction suggested this to be due to a loss of binding site for the transcription factor c-Ets [12]. In the subchondral bone compartment of the human *ex vivo* explants, the *MGP* response to the OA like perturbing cues were smaller and less consistent although a similar *MGP* response appeared for T3 exposure. This is likely the result of (slightly) lower sample sizes but, more importantly, a more complex innate regulation and signalling of *MGP* in bone as multicellular tissue type. As such, the observed variation in the *MGP* response in bone remains inconclusive and needs to be repeated in larger sample sizes.

Upon identifying *MGP*, encoding an inhibitor of ectopic calcifications, as strong OA risk gene, it was hypothesized that the OA risk was conferred via calcification of cartilage tissue [10, 11]. Moreover, as *MGP* protein is activated by vitamin k dependent carboxylation (c-*MGP*) this finding underscored the relevance of previous found associations between OA and low vitamin K status [14,15]. Here, we showed that exposure of the vitamin k inhibitor warfarin to intact human articular cartilage explants provoked unbeneficial functional chondrocyte signaling towards hypertrophy, as reflected by upregulation of *COL10A1* and almost significant upregulation of *RUNX2* and *ALPL*. Moreover, we showed a modest but significant downregulation of *SOX9*, a transcription factor marking healthy articular cartilage. These observed effects of warfarin on chondrocyte signaling were similar to those previously found during *in vitro* knockdown of *MGP* in chondrocyte monolayer cultures [9]. With regard to the seemingly increased *MMP13* and reduced *MMP3* gene expression, it has been suggested that *MMP3* plays a role mainly in healthy cartilage remodeling, while *MMP13* more so in pathophysiological processes. This was confirmed by performing a look-up in our RNA-sequencing data set [18] where *MMP3* showed a marked downregulation in lesioned compared to preserved OA cartilage. Exposure of warfarin to subchondral bone of osteochondral explants

also provoked unbeneficial functional signaling towards reduced bone formation, as reflected by downregulation of *COL1A1* and the suggestive downregulation of *BGLAP*, whereas the upregulation of the osteoclastogenesis inhibitor *TNFRSF11B* (although not significant) and downregulation of the vitamin K dependent protein *POSTN* suggests altered bone remodeling likely resulting in bone loss [25,27]. Due to the low numbers and heterogeneity of patients, future studies are necessary to investigate if rs1800801 genotype influences response of cells to warfarin. In light of our result we advocate that the frequent prescription of warfarin as vitamin K dependent blood anticoagulant [16] may have clinical consequences in evoking OA comorbidity. As such, the risk of OA comorbidity may be considerably reduced by preferred prescription of non-vitamin K antagonist as anticoagulants [28]. In addition, vitamin K supplementation should be considered a potential novel OA-modifying treatment option. In this respect, there has been one underpowered clinical trial studying the effect of vitamin K supplementation on OA progression. This ancillary study, originally designed to study vascular calcification, reported no overall beneficial effects of vitamin K supplementation. However, in individuals with insufficient vitamin K levels at baseline a beneficial effect was observed [29].

Although the human aged macroscopically normal osteochondral explants used in our study may represent physiological relevant human articular cartilage and subchondral bone model, prone to OA pathophysiology, hence suitable to study the initial process of OA related destruction, the model is inherently subject to heterogeneity. Moreover, it does not provide insight into the *MGP* effect of such environmental perturbations to healthy cartilage and bone. Another limiting factor was the low sample size of T3, IL-1 $\beta$  and warfarin treated explants upon stratifying for rs1800801 genotype, resulting in no or less robust results than upon investigating the response in the larger mechanically stressed group. It should also be noted that the modifying effect of the *MGP* OA risk allele rs1800801-T as function of the OA status in articular cartilage and subchondral bone was only measured as a static effect i.e. differential expression of *MGP* between paired preserved and lesioned OA cartilage samples. Finally, the focus of our paper was on exploring gene expression changes of *MGP* only. Although studying protein levels of *MGP* as function of the OA risk SNP and the OA relevant cues in joint tissue would be an interesting addition and a preferred next step, such analyses should involve the detection of activated (hence carboxylated) *MGP* protein.

Together our data highlight that, similar to the bi-directional interplay of vascular calcification and bone loss in osteoporosis and atherosclerosis [26], also articular cartilage calcification and bone loss in OA might share a common pathogenetic mechanism likely involving *MGP*. Moreover, warfarin on human osteochondral explant cultures functionally underscores the previously found association between vitamin K deficiency and OA.

### **Acknowledgments**

We thank all the participants of the RAAK study. The LUMC has and is supporting the RAAK study. We also thank Enrike van der Linden, Robert van der Wal, Peter van Schie, Anika Rabelink-Hoogenstraaten, Shaho Hasan, Maartje Meijer, Daisy Latijnhouwers and Geert Spierenburg for collecting surgical waste material. Data is generated within the scope of

the Medical Delta Programs Regenerative Medicine 4D: Generating complex tissues with stem cells and printing technology and Improving Mobility with Technology. We thank the Sequence Analysis Support Core (SASC) of the Leiden University Medical Center for their support.

### **Contributors**

All authors have made contributions to the completion of this study. Study concept and design: EH, RCA, JM, YFM, IM. Acquisition of material and data: EH, MT, HED, DB, RGHHN. Data analysis: EH, RCA, MT, IM. Preparation of the manuscript: EH, IM. Critical reviewing and approval of the manuscript: All authors.

### **Funding**

The study was funded by the Dutch Scientific Research council NWO/ZonMW VICI scheme (nr 91816631/528), Dutch Arthritis Society/ReumaNederland (DAF-15-4-401 and DAA\_10\_1-402) and European Commission Seventh Framework program (TreatOA, 200800).

### **Competing interests**

None declared.

### **Patient consent for publication**

Not required.

### **Data availability statement**

Data are available on reasonable request.

## **REFERENCES**

1. Spector TD, Cicuttini F, Baker J, et al. Genetic influences on osteoarthritis in women: a twin study. *BMJ*. 1996;312(7036):940-3.
2. Felson DT. Risk factors for osteoarthritis: understanding joint vulnerability. *Clin Orthop Relat Res*. 2004(427 Suppl):S16-21.
3. Bos SD, Bovee JV, Duijnisveld BJ, et al. Increased type II deiodinase protein in OA-affected cartilage and allelic imbalance of OA risk polymorphism rs225014 at DIO2 in human OA joint tissues. *Ann Rheum Dis*. 2012;71(7):1254-8.
4. Reynard LN, Bui C, Canty-Laird EG, et al. Expression of the osteoarthritis-associated gene GDF5 is modulated epigenetically by DNA methylation. *Hum Mol Genet*. 2011;20(17):3450-60.
5. Loughlin J. Genetic contribution to osteoarthritis development: current state of evidence. *Current opinion in rheumatology*. 2015;27(3):284-8.

6. Shepherd C, Zhu D, Skelton AJ, et al. Functional characterisation of the osteoarthritis genetic risk residing at ALDH1A2 identifies rs12915901 as a key target variant. *Arthritis & rheumatology (Hoboken, NJ)*. 2018.
7. den Hollander W, Boer CG, Hart DJ, et al. Genome-wide association and functional studies identify a role for matrix Gla protein in osteoarthritis of the hand. *Annals of the rheumatic diseases*. 2017;76(12):2046-53.
8. Misra D, Booth SL, Crosier MD, et al. Matrix Gla protein polymorphism, but not concentrations, is associated with radiographic hand osteoarthritis. *J Rheumatol*. 2011;38(9):1960-5.
9. Shepherd C, Reese AE, Reynard LN, et al. Expression analysis of the osteoarthritis genetic susceptibility mapping to the matrix Gla protein gene MGP. *Arthritis Res Ther*. 2019;21(1):149.
10. Luo G, Ducy P, McKee MD, et al. Spontaneous calcification of arteries and cartilage in mice lacking matrix GLA protein. *Nature*. 1997;386(6620):78-81.
11. Yagami K, Suh JY, Enomoto-Iwamoto M, et al. Matrix GLA protein is a developmental regulator of chondrocyte mineralization and, when constitutively expressed, blocks endochondral and intramembranous ossification in the limb. *J Cell Biol*. 1999;147(5):1097-108.
12. Tunon-Le Poutel D, Cannata-Andia JB, Roman-Garcia P, et al. Association of matrix Gla protein gene functional polymorphisms with loss of bone mineral density and progression of aortic calcification. *Osteoporos Int*. 2014;25(4):1237-46.
13. Sheng K, Zhang P, Lin W, et al. Association of Matrix Gla protein gene (rs1800801, rs1800802, rs4236) polymorphism with vascular calcification and atherosclerotic disease: a meta-analysis. *Sci Rep*. 2017;7(1):8713.
14. Neogi T, Booth SL, Zhang YQ, et al. Low vitamin K status is associated with osteoarthritis in the hand and knee. *Arthritis Rheum*. 2006;54(4):1255-61.
15. Shea MK, Kritchevsky SB, Hsu FC, et al. The association between vitamin K status and knee osteoarthritis features in older adults: the Health, Aging and Body Composition Study. *Osteoarthritis Cartilage*. 2015;23(3):370-8.
16. Holbrook A, Schulman S, Witt DM, et al. Evidence-based management of anticoagulant therapy: Antithrombotic Therapy and Prevention of Thrombosis, 9th ed: American College of Chest Physicians Evidence-Based Clinical Practice Guidelines. *Chest*. 2012;141(2 Suppl):e152S-e84S.
17. Chin KY. The Relationship between Vitamin K and Osteoarthritis: A Review of Current Evidence. *Nutrients*. 2020;12(5).
18. Coutinho de Almeida R, Ramos YFM, Mahfouz A, et al. RNA sequencing data integration reveals an miRNA interactome of osteoarthritis cartilage. *Annals of the rheumatic diseases*. 2019;78(2):270-7.
19. Tuerlings M, van Hoolwerff M, Houtman E, et al. RNA sequencing reveals interacting key determinants of osteoarthritis acting in subchondral bone and articular cartilage. *Arthritis & rheumatology (Hoboken, NJ)*. 2020.
20. Houtman E, van Hoolwerff M, Lakenberg N, et al. Human Osteochondral Explants: Reliable Biomimetic Models to Investigate Disease Mechanisms and Develop Personalized Treatments for Osteoarthritis. *Rheumatol Ther*. 2021.
21. Ramos YF, den Hollander W, Bovee JV, et al. Genes involved in the osteoarthritis process identified through genome wide expression analysis in articular cartilage; the RAAK study. *PLoS One*. 2014;9(7):e103056.
22. den Hollander W, Pulyakhina I, Boer C, et al. Annotating Transcriptional Effects of Genetic Variants in Disease-Relevant Tissue: Transcriptome-Wide Allelic Imbalance in Osteoarthritic Cartilage. *Arthritis & rheumatology (Hoboken, NJ)*. 2019;71(4):561-70.
23. Zeger SL, Liang KY. Longitudinal data analysis for discrete and continuous outcomes. *Biometrics*. 1986;42(1):121-30.
24. Diggle P, Liang K-Y, Zeger SL. Analysis of longitudinal data. Oxford New York: Clarendon Press; Oxford University Press; 1994. xi, 253 p. p.
25. Zhang Y, Zhao L, Wang N, et al. Unexpected Role of Matrix Gla Protein in Osteoclasts: Inhibiting Osteoclast Differentiation and Bone Resorption. *Mol Cell Biol*. 2019;39(12):e00012-19.
26. Vassalle C, Mazzone A. Bone loss and vascular calcification: A bi-directional interplay? *Vascul Pharmacol*. 2016;86:77-86.
27. Bonnet N, Gineyts E, Ammann P, et al. Periostin deficiency increases bone damage and impairs injury response to fatigue loading in adult mice. *PLoS One*. 2013;8(10):e78347.
28. Zhu J, Alexander GC, Nazarian S, et al. Trends and Variation in Oral Anticoagulant Choice in Patients with Atrial Fibrillation, 2010-2017. *Pharmacotherapy*. 2018;38(9):907-20.
29. Neogi T, Felson DT, Sarno R, et al. Vitamin K in hand osteoarthritis: results from a randomised clinical trial. *Annals of the rheumatic diseases*. 2008;67(11):1570-3.

## Supplementary Files

### *List of contents:*

### *Supplementary Materials and Methods*

### *Supplementary Figures*

**Supplementary Figure 1.** Schematic representation of the sample numbers used in the different osteochondral explant models.

**Supplementary Figure 2.** Allelic expression imbalance of the OA risk allele rs1800801-T in articular cartilage and rs4236-C in subchondral bone.

**Supplementary Figure 3.** Expression quantitative trait loci (eQTL) of MGP in articular cartilage and subchondral bone.

**Supplementary Figure 4.** Lookup of the rs1800801 SNP in USCS genome browser.

## Supplementary methods

### *Neo-cartilage deposition*

Primary chondrocytes were isolated from macroscopically preserved human articular cartilage and expanded as previously described [1] and a definition on what was determined as preserved and lesioned can be found in the first paper describing the Research in Articular Osteoarthritis Cartilage (RAAK) biobank [2]. *In vitro* 3D pellets were formed by centrifugation (1200 rpm, 5 minutes) using  $2.5 \times 10^5$  chondrocytes in 15 ml polypropylene conical tubes. Following maintenance in chondrogenic differentiation medium (CDM: DMEM (high glucose; Gibco, Bleiswijk), supplemented with Ascorbic acid (50  $\mu\text{g}/\text{ml}$ ; Sigma-Aldrich; Zwijndrecht, The Netherlands), L-Proline (40  $\mu\text{g}/\text{ml}$ ; Sigma-Aldrich), Sodium Pyruvate (100  $\mu\text{g}/\text{ml}$ ; Sigma-Aldrich), Dexamethasone (0.1  $\mu\text{M}$ ; Sigma-Aldrich), ITS+ and antibiotics (100 U/ml penicillin; 100  $\mu\text{g}/\text{ml}$  streptomycin; Gibco)), while refreshing every 3-4 days, two pellets of each donor were pooled and harvested on day 0, 3, 7, 14 and 21 for RNA isolation. Experiments were repeated in two (day 0) to three (other time points) biological donors (N=3 donors).

### *DNA isolation and TaqMan genotyping*

DNA was extracted from cartilage by pulverizing the tissue and homogenizing in Nuclei Lysis solution (Promega). DNA was extracted using the Wizard Genomic DNA purification kit (Promega) after overnight digestion using proteinase K (Qiagen) at 55°C. Conventional TaqMan genotyping was performed on genomic DNA using an allele-specific custom TaqMan assay for rs1800801 (Thermo Fisher Scientific) on a QuantStudio 6 Real-Time PCR system (Applied Biosystems).

### *RNA isolation*

RNA was extracted from the cartilage and subchondral bone by pulverizing the tissue and homogenizing in TRIzol reagent (Invitrogen, San Diego, CA). RNA was extracted with chloroform, precipitated with ethanol and purified using the RNeasy Mini Kit (Qiagen, Chatsworth, CA). Genomic DNA was removed by DNase digestion and quantity of the RNA was assessed using a nanodrop spectrophotometer (Thermo Fischer Scientific Inc., Wilmington, USA). 200 ng of RNA was processed with the First Strand cDNA Synthesis Kit (Roche Applied Science, Almere, The Netherlands) according to the manufacturer's protocol. For several subchondral bone samples RNA isolation was not successful, reducing final sample size in the warfarin treated subchondral bone to 13 paired samples and for the other treatments as summarized in **Supplementary Figure 1B**. To exclude cross contamination of bone and cartilage samples, we measured gene expression differences of two cartilage specific genes (*COL2A1* and *COMP*) and two bone specific genes (*COL1A1* and *SPP1*) in 10 paired samples. As shown in **Supplementary Table 5**, we observe a relative high expression of cartilage markers and a low expression of bone markers in cartilage when compared to subchondral bone isolated from the same osteochondral explant. In subchondral bone we observed a relative low expression of cartilage markers and a high expression of bone markers, suggesting no to minimal cross contamination between cartilage and subchondral bone.

### **Reverse Transcription and Real-Time PCR**

Real-Time PCR for gene expression was performed with QuantStudio 6 Real-Time PCR system (Applied Biosystems) using Fast Start Sybr Green Master mix (Roche Applied Science). Primer sequences used were tested for linear amplification and are listed in **Table 1**. Raw cycle threshold (CT) values for each sample were corrected for the average of one reference gene (*SDHA*) depicted as  $-\Delta Ct$ , and subsequently made relative to gene expression in controls ( $-\Delta\Delta Ct$ ). Fold change (FC) was determined by calculating the log base 2 of the  $-\Delta\Delta Ct$  for each sample ( $2^{-\Delta\Delta Ct}$ ) where  $FC > 1$  is upregulation and a  $FC < 1$  is downregulation of a treated sample compared to the control sample of a donor. We used *SDHA* as reference gene since this gene was previously identified as a stable housekeeping gene and not responsive to mechanical stress in cartilage [3, 4]. In **Supplementary Table 2** and **3**, missing datapoints for genes measured by Real-Time PCR in cartilage and subchondral bone are summarized.

### **Unconfined dynamic (cyclic) compression of osteochondral explants**

Explants were cultured in 24 wells plates (Greiner CELLSTAR; Sigma) supplemented with 1.5 ml CDM in a 5% (v/v) CO<sub>2</sub> incubator at 37°C. Six days after extraction, dynamic (cyclic) unconfined compression was applied to explant tissues using the Mach-1 mechanical testing system (Biomomentum Inc., Laval, QC, Canada) on four subsequent days (**Figure 1B**). In short, osteochondral explant (diameter of 8mm) were placed under an indenter (diameter of 10mm) attached to a 250N MACH-1 load cell (**Figure 1C**) and unconfined cyclic compression was applied at a strain of 65% of cartilage height at a frequency of 1 Hz (1 compression cycle per second), mimicking walking speed, to give mechanical stress at strains suggested to be detrimental [5]. Due to the compression being unconfined, cartilage was allowed to displace sideways during compression. As shown in **Figure 1C**, dynamic (cyclic) compression means that a force was applied that varied over time to simulate a more cyclic compression such as walking. Media of explants was refreshed every three to four days. To investigate lasting effects of treatment, explants were harvested three days after the last treatment. Cartilage and bone were separated using a scalpel, snap-frozen in liquid nitrogen, and stored at -80°C for RNA isolation.

### **RNA sequencing data of cartilage and subchondral bone**

In the current manuscript differential expression of *MGP* including false discovery rates (FDR) as multiple testing correction was taken from previously published transcriptome wide RNA-sequencing data of  $n=35$  paired preserved and lesioned OA cartilage samples [6] and  $n=24$  paired preserved and lesioned OA subchondral bone samples [7]. For  $n_{\text{cartilage}}=98$  and  $n_{\text{subchondral bone}}=28$  samples genotype of rs1800801 could be determined.

To test expression quantitative trait analyses (eQTL) and differential expression of *MGP* in genotype strata in the current manuscript, we used the variance stabilizing transformation (VST) normalized *MGP* expression levels of RNA sequencing datasets and used generalized estimating equations (GEE) [8] to effectively adjust for dependencies of genotypes among donors by adding a random effect for sample donor. For differential *MGP* expression analyses (**Figure 2**) a logistic model was applied with tissue status (preserved or lesioned) as

dependent variable and *MGP*, age and sex as covariates:  $Tissue\ status \sim MGP\ level + age + sex + (1|Donor)$  [9]. For genotype effects we show odds ratio's calculated from the exponent of the respective beta's. *MGP* expression quantitative trait loci (eQTL) analysis (**Supplementary Figure 3**) was performed by applying a linear GEE model with *MGP* level as dependent variable and dose response genotype, tissue status, age, and sex as covariate:  $MGP\ level \sim rs1800801\ genotype + tissue\ status + age + sex + (1|Donor)$ .

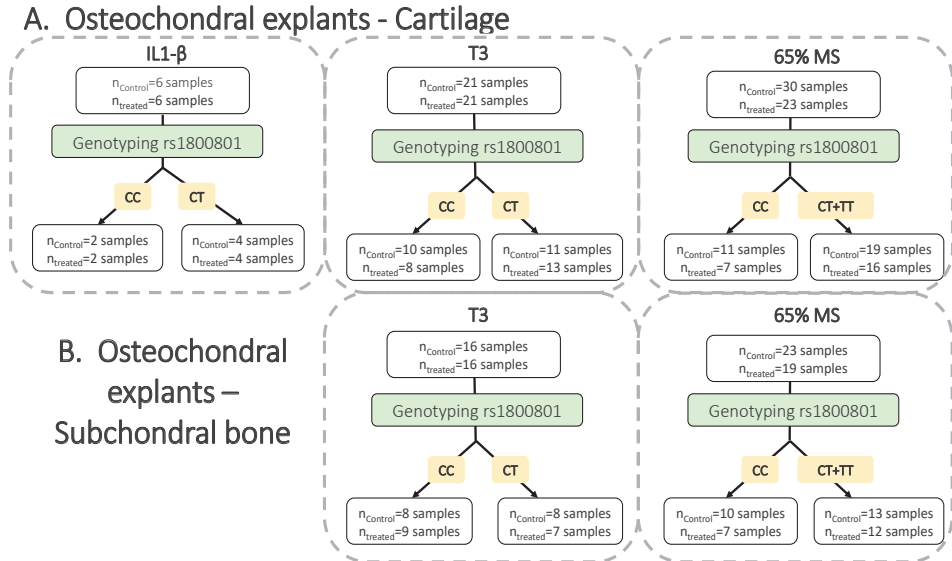
### **Allelic Expression Imbalance (AEI)**

Allelic expression imbalance (AEI) was measured from the cartilage [6] and subchondral bone [7] RNA sequencing datasets for heterozygous individuals of rs1800801 in cartilage ( $N_{preserved}=37$  and  $N_{lesioned}=28$  samples) and rs4236 ( $N_{preserved}=12$  and  $N_{lesioned}=12$  samples) in subchondral bone as previously described in detail [10]. In short, reads of RNA-sequencing data were aligned using GSNAP against the hg19 reference genome, while potential reference alignment bias was masked using known Dutch SNPs (GoNL). Genotype of rs1800801 and other SNPs was called using SNVMix2 with default settings[11], with minimum coverage of 25 and at least 10 reads ( $\mathbf{R}$ ) per allele. Allelic imbalance is reported as the average fraction ( $\varphi$ ) of the alternative allele reads ( $\mathbf{R}_{alternative}$ ) among the total number of reads ( $\mathbf{R}_{total}=\mathbf{R}_{alternative}+\mathbf{R}_{reference}$ ) at the position of the respective genetic variation per sample ( $\mathbf{i}$ ):

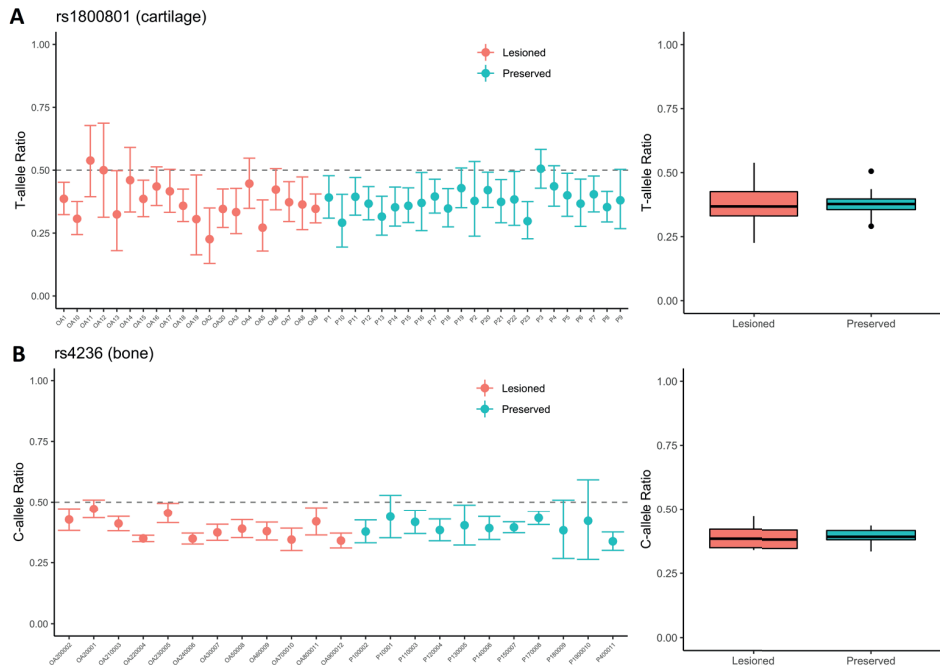
$$\varphi = \frac{1}{n} \sum_{i=1}^n \frac{R_{i, alternative}}{R_{i, reference}}$$

To detect SNPs that robustly mark imbalance two binomial tests were performed per heterozygote and per SNP under the null hypothesis that the amount of imbalance is either greater or smaller than 0.49. Subsequently, P-values per SNP were corrected for multiple testing (FDR) by the number of heterozygotes of the respective SNP and considered significant if all FDR corrected P-values were  $<0.05$  and in the same direction among all heterozygotes. Using the DESeq2 package, fragments per gene were used to assess the dispersion by quantile-adjusted conditional maximum likelihood (qCML)[12].

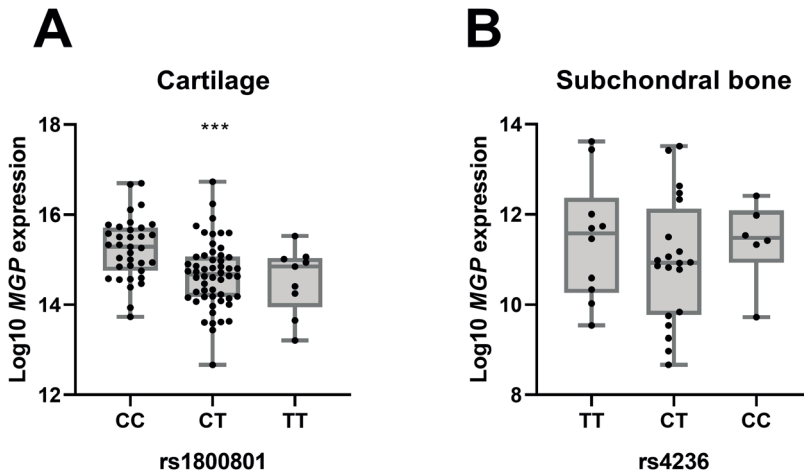
## Supplementary Figures



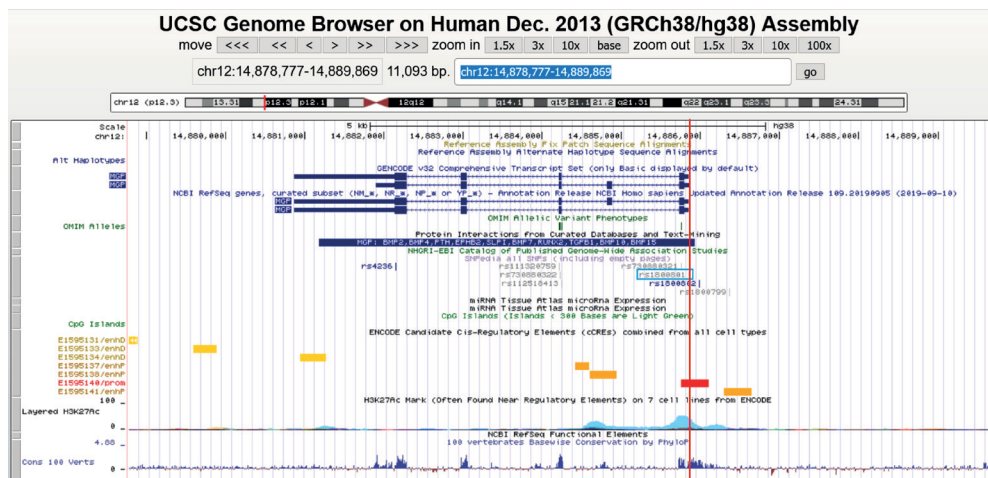
**Supplementary Figure 1 | Schematic representation of the sample numbers used in the different osteochondral explant models. [A]** Number of cartilage samples extracted from osteochondral explants for each condition (control and treated) and after splitting for rs1800801 genotype that were included for the different analysis on *MGP* expression. **[B]** Number of subchondral bone samples extracted from osteochondral explants for each condition (control and treated) and after splitting for rs1800801 genotype that were included for the different analysis on *MGP* expression. As we were not able to isolate RNA of all bone samples, numbers are lower when compared to cartilage.



**Supplementary Figure 2 | Allelic expression imbalance of the OA risk allele rs1800801-T in articular cartilage and rs4236-C in subchondral bone.** [A] The left part of the figure depicts the mean OA risk T-allele ratio with their 95%CI for the rs1800801 SNP in preserved and lesioned OA cartilage for each donor separate. The right part summarizes the T-allele ratio for independent lesioned (Red; N=28) and preserved (Blue; N=37) samples. A portion of this data was previously published by den Hollander W., et al [13]. [B] The left part of the figure depicts the mean OA risk C-allele ratio with their 95%CI for the proxy SNP rs4236 in preserved and lesioned OA subchondral bone for each donor separate. The right part summarizes the C-allele ratio for independent lesioned (Red; N=12) and preserved (Blue; N=12) samples. The dashed line at 0.50 represent the natural allele frequency when there is no allelic imbalance. The boxplots represent 25th, 50th and 75th percentiles, and whiskers extend to 1.5 times the interquartile range. Individual cartilage and bone samples are shown by random anonymised numbers.



**Supplementary Figure 3 | Expression quantitative trait loci (eQTL) of MGP in articular cartilage and subchondral bone.** [A] Variance Stabilizing Transformation (VST) normalized MGP expression levels extracted from the RNA sequencing dataset stratified for the OA risk SNP rs1800801 (CC: N=35; CT:N=54; TT: N=9) in preserved and lesioned OA cartilage. [B] Variance Stabilizing Transformation (VST) normalized MGP expression levels extracted from the RNA sequencing dataset stratified for a proxy ( $r^2=0.93$  with rs1800801) of the OA risk SNP rs4236 (CC: N=10; CT:N=20; TT: N=6) in preserved and lesioned OA subchondral bone. The boxplots represent 25th, 50th and 75th percentiles, and whiskers extend to 1.5 times the interquartile range. Each samples is depicted by a black dot. Differences between groups was determined by measuring a dose response effect of the risk allele by performing generalized estimation equation (GEE) to correct for independency of genotype among the donors. The following linear GEE model was applied with MGP level as dependent variable and dose response genotype, tissue status, age, and sex as covariate:  $MGP \text{ level} \sim rs1800801 \text{ genotype} + \text{tissue status} + \text{age} + \text{sex} + (1|Donor)$ . \*\*\*  $P \leq 0.001$



**Supplementary Figure 4 | Lookup of the rs1800801 SNP in UCSC genome browser.** The rs1800801 SNP (blue box) is found on chromosome 12 at nucleotide 14885854 (GRCh38/hg38) in the 5 Prime UTR of the *MGP* gene. The location of the SNP is depicted by the red line and is within the promoter region of the *MGP* gene. In addition, several transcription factor binding factors, such as *PORL2A* and *CTCF* are predicted to bind in this region (layer not shown).

## REFERENCES

1. Bomer N, den Hollander W, Suchiman H, et al. Neo-cartilage engineered from primary chondrocytes is epigenetically similar to autologous cartilage, in contrast to using mesenchymal stem cells. *Osteoarthritis Cartilage*. 2016;24(8):1423-30.
2. Ramos YF, den Hollander W, Bovee JV, et al. Genes involved in the osteoarthritis process identified through genome wide expression analysis in articular cartilage; the RAAK study. *PLoS One*. 2014;9(7):e103056.
3. McCulloch RS, Ashwell MS, O'Nan AT, Mentle PL. Identification of stable normalization genes for quantitative real-time PCR in porcine articular cartilage. *J Anim Sci Biotechnol*. 2012;3(1):36.
4. Al-Sabah A, Stadnik P, Gilbert SJ, et al. Importance of reference gene selection for articular cartilage mechanobiology studies. *Osteoarthritis Cartilage*. 2016;24(4):719-30.
5. Sanchez-Adams J, Leddy HA, McNulty AL, et al. The mechanobiology of articular cartilage: bearing the burden of osteoarthritis. *Curr Rheumatol Rep*. 2014;16(10):451.
6. Coutinho de Almeida R, Ramos YFM, Mahfouz A, et al. RNA sequencing data integration reveals an miRNA interactome of osteoarthritis cartilage. *Ann Rheum Dis*. 2019;78(2):270-7.
7. Tuerlings M, van Hoofterff M, Houtman E, et al. RNA sequencing reveals interacting key determinants of osteoarthritis acting in subchondral bone and articular cartilage. *Arthritis & rheumatology (Hoboken, NJ)*. 2020.
8. Zeger SL, Liang KY. Longitudinal data analysis for discrete and continuous outcomes. *Biometrics*. 1986;42(1):121-30.
9. Diggle P, Liang K-Y, Zeger SL. Analysis of longitudinal data. Oxford New York: Clarendon Press; Oxford University Press; 1994. xi, 253 p. p.
10. den Hollander W, Pulyakhina I, Boer C, et al. Annotating Transcriptional Effects of Genetic Variants in Disease-Relevant Tissue: Transcriptome-Wide Allelic Imbalance in Osteoarthritic Cartilage. *Arthritis Rheumatol*. 2019;71(4):561-70.
11. Goya R, Sun MG, Morin RD, et al. SNVMix: predicting single nucleotide variants from next-generation sequencing of tumors. *Bioinformatics*. 2010;26(6):730-6.
12. Robinson MD, McCarthy DJ, Smyth GK. edgeR: a Bioconductor package for differential expression analysis of digital gene expression data. *Bioinformatics*. 2010;26(1):139-40.
13. den Hollander W, Boer CG, Hart DJ, et al. Genome-wide association and functional studies identify a role for matrix Gla protein in osteoarthritis of the hand. *Annals of the rheumatic diseases*. 2017;76(12):2046-53







# Chapter 5

## Inhibiting thyroid activation in aged human explants prevents mechanical induced detrimental signalling by mitigating metabolic processes

Evelyn Houtman<sup>1</sup>, Margo Tuerlings<sup>1</sup>, H. Eka D. Suchiman<sup>1</sup>, Nico Lakenberg<sup>1</sup>, Frederique M.F. Cornelis<sup>2</sup>, Hailiang Mei<sup>3</sup>, Demiën Broekhuis<sup>4</sup>, Rob G.H.H. Nelissen<sup>4</sup>, Rodrigo Coutinho de Almeida<sup>1</sup>, Yolande F.M. Ramos<sup>1</sup>, Rik J. Lories<sup>2,5</sup>, Luis J. Cruz<sup>6</sup>, Ingrid Meulenbelt<sup>1</sup>

<sup>1</sup> Molecular Epidemiology, Department of Biomedical Data Sciences, Leiden University Medical Center, Leiden, The Netherlands, <sup>2</sup> Department of Development and Regeneration, Skeletal Biology and Engineering Research Centre, Laboratory of Tissue Homeostasis and Disease, KU Leuven, Leuven, Belgium,

<sup>3</sup> Sequencing Analysis Support Core, Leiden University Medical Centre, Leiden, The Netherlands, <sup>4</sup> Department of Orthopaedics, Leiden University Medical Center, Leiden, The Netherlands, <sup>5</sup> Division of Rheumatology, University Hospitals Leuven, Leuven, Belgium,

<sup>6</sup> Translational Nanobiomaterials and Imaging (TNI) Group, Department of Radiology, Leiden University Medical Centrum, Leiden, the Netherlands

Published in: *Rheumatology* (Oxford). 2022 Apr 5;keac202.  
doi: 10.1093/rheumatology/keac202.

## Abstract

### Objectives

To investigate whether the deiodinase inhibitor iopanoic acid (IOP) has chondroprotective properties, a mechanical stress induced model of human aged explants was used to test both repeated dosing and slow-release of IOP.

### Methods

Human osteochondral explants subjected to injurious mechanical stress (65%MS) were treated with IOP or IOP encapsulated in poly lactic-co-glycolic acid (PLGA)-polyethylene glycol (PEG) nanoparticles (NP) (PLGA-PEG NPs (NP(IOP))). Changes to cartilage integrity and signalling were determined by Mankin scoring of histology, sulphated glycosaminoglycan (sGAG) release and expression levels of catabolic, anabolic and hypertrophic markers. Subsequently, on a subgroup of samples, RNA-sequencing was performed on 65%MS (n=14) and 65%MS+IOP (n=7) treated cartilage to identify IOP's mode of action.

### Results

Damage from injurious mechanical stress was confirmed by increased cartilage surface damage in the Mankin score, increased sGAG release, and consistent upregulation of catabolic markers and downregulation of anabolic markers. IOP and, though less effective, PLGA NP(IOP) treatment, reduced *MMP13* and increased *COL2A1* expression. In line with this, IOP and PLGA NP(IOP) reduced cartilage surface damage induced by 65%MS, while only IOP reduced sGAG release from explants subjected to 65%MS. Lastly, differential expression analysis identified 12 genes in IOP's mode of action to be mainly involved in reducing metabolic processes (*INSIG1*, *DHCR7*, *FADS1* and *ACAT2*), and proliferation and differentiation (*CTGF*, *BMP5* and *FOXM1*).

### Conclusion

Treatment with the deiodinase inhibitor IOP reduced detrimental changes of injurious mechanical stress. In addition, we identified that its mode of action was likely on metabolic processes, cell proliferation and differentiation.

### Keywords

Osteoarthritis, DIO2, chondrocytes, cartilage, thyroid signalling, iopanoic acid, mechanical stress

## Introduction

Osteoarthritis (OA) is a prevalent and debilitating age-related disease. It is a progressive disease characterized by cartilage degeneration and osteophyte formation [1]. Given the ageing society with increasing obesity rates, OA is projected to be the most frequent disease in the Dutch population in 2040, affecting 2.3 million people. Due to the fact that there is no effective treatment, except for joint replacement surgery, OA has a considerable social and economic burden on the ageing population.

Chondrocytes reside in healthy articular cartilage in a maturation-arrested state without detectable proliferation and with low metabolic activity [2]. Yet, with an inherently low tissue repair capacity of chondrocytes, the integrity of cartilage tissue is irreversibly affected upon environmental challenges such as injurious mechanical stress [3]. By applying molecular profiling of human OA articular cartilage, it has been consistently shown that activated articular chondrocytes with OA pathophysiology lose their healthy maturation-arrested state and recapitulate an activated growth plate morphology with associated debilitating gene expression [4]. To delineate underlying OA disease aetiology, large-scale genetic studies have been performed and provided further evidence that indeed genes orchestrating the endochondral ossification processes of growth plate chondrocytes could be, among others, a common underlying OA pathway [5]. Basing clinical development on functional data of OA risk genes could have measurable impact on development of effective disease modifying OA drugs given that the presence of genetically supported targets doubles the success rate of a drug in clinical development [6].

An example of such an OA risk gene is *DIO2*, encoding the deiodinase iodothyronine type-2 (D2) [7]. D2 is an enzyme that converts intracellular thyroxine (T4) into triiodothyronine (T3) in specific tissues such as growth plate cartilage. Here, T3 initiates terminal maturation of hypertrophic chondrocytes leading to breakdown and mineralization of cartilage to allow transition to bone [8]. Functional genomic studies have demonstrated that the *DIO2* risk allele rs225014-C has an increased expression relative to the reference allele rs225014-T [9]. Moreover, in human preserved and lesioned OA articular cartilage, upregulated *DIO2* expression has been shown to be a common and consistent phenomenon, particularly relative to healthy cartilage [10]. *In vitro* 3D chondrogenesis with human bone marrow mesenchymal stem cells (hBMSC) indicated that overexpression of *DIO2* had a detrimental effect on matrix deposition while iopanoic acid (IOP), a potent inhibitor of deiodinases like D2, had beneficial effects on matrix deposition [11,12]. In line with this, *Dio2* knockout mice were protected from running induced joint damage [11]. Transgenic rats with cartilage-specific overexpression of human *DIO2* (hD2Tg), did not show any articular cartilage defects [13]. However, upon increasing the biomechanical burden by applying an injury-induced OA model, hD2Tg rats showed significantly higher levels of cartilage damage compared with their wild-type littermates. Taken together, it was hypothesized that *DIO2* might confer risk to OA by affecting the propensity of maturation-arrested articular chondrocytes to recuperate growth plate morphology upon environmental challenges such as injurious mechanical stress. Additionally, IOP, a previously approved pharmaceutical agent, was delineated as mitigating this process [14].

The current study aimed to confirm chondroprotective effects of the D2 inhibitor IOP in a previously established *ex vivo* aged human osteochondral explant model in which injurious

mechanical stress is applied to inflict OA-like damage [15]. To improve treatment efficacy of the small IOP molecule, we investigated efficiency of IOP encapsulated in poly lactic-co-glycolic acid (PLGA)-polyethylene glycol (PEG) nanoparticles (NP) to establish slow prolonged release. Finally, RNA-sequencing was performed to explore the mode of IOP treatment action by addressing transcriptome-wide gene expression changes.

## Material and Methods

### *Study design and culture condition*

Osteochondral explants were obtained from knee joints included in the Research in Articular Osteoarthritis Cartilage (RAAK) study [16]. The RAAK study has been approved by the medical ethical committee of the Leiden University Medical Center (Po8.239/P19.013) and informed consent was obtained from subjects. Osteochondral explants were punched from human OA knee joints and maintained in standard chondrogenic medium as described in Supplementary Materials and Methods, available at *Rheumatology* online. Medium was refreshed every 3–4 days. During mechanical stress, explants resided in phosphate buffered saline (PBS). In total 83 osteochondral explants were obtained from 16 donors for this study and divided over the following treatment groups: control (n = 30 explants; N = 16 donors), injurious mechanical stress (65%MS; n = 25 explants; N = 16 donors), injurious mechanical stress treated with IOP (65%MS+IOP; n = 11 explants; N = 6 donors) and injurious mechanical stress treated with NP-IOP (65%MS+NP-IOP; n = 17 explants; N = 10 donors). Donor characteristics are summarized in **Supplementary Table S1**, available at *Rheumatology* online.

### *Ethics*

Our study complies with the Declaration of Helsinki. Furthermore, the RAAK study has been approved by the medical ethical committee of the Leiden University Medical Center (Po8.239/P19.013) and written informed consent was obtained from subjects.

### *Injurious mechanical stress model*

Six days after extraction, dynamic unconfined compression was applied at a strain of 65% of explant height at a frequency of 1 Hz using the Mach-1 mechanical testing system (Biomomentum Inc., Laval, QC, Canada) on four subsequent days as described previously (**Supplementary Figure S1**, available at *Rheumatology* online) [15].

### *IOP Treatment*

Explants were treated with IOP (100 $\mu$ M; Sigma) or 24 $\mu$ l of IOP encapsulated in PLGA-PEG nanoparticles (70 $\mu$ g IOP/mg NP; 5 mg NP/mL PBS) from day 3 onwards (**Supplementary Figure S1**). On day 13, cartilage and bone were separated using a scalpel, snap-frozen in liquid nitrogen and stored at -80 °C for RNA isolation. For histology, a part was fixed in 4% formaldehyde. Medium was collected on day 13 and stored at -80 °C. Details on sGAG

measurement, histology and PLGA NP characterization can be found in **Supplementary Materials and Methods**.

### ***RNA isolation, Reverse Transcription and quantitative Real-Time PCR***

Cartilage RNA was extracted by pulverizing the tissue using a Mixer mill 200 (Retch, Germany) and homogenizing in TRIzol reagent (Invitrogen, San Diego, CA). RNA was extracted with chloroform, precipitated with ethanol, and purified using the RNeasy Mini Kit (Qiagen, GmbH, Hilden, Germany). Genomic DNA was removed by DNase (Qiagen, GmbH, Hilden, Germany) digestion and quantity of the RNA was assessed using a Nanodrop spectrophotometer (Thermo Fischer Scientific Inc., Wilmington, USA). Synthesis of cDNA was performed using 200 ng of total mRNA with the First Strand cDNA Synthesis Kit (Roche Applied Science, Almere, The Netherlands) according to the manufacturer's protocol. Subsequently, pre-amplification was performed and gene expression was determined with the Roche Lightcycler 480 II (Roche Applied Science) using Fast Start Sybr Green Master mix (Roche Applied Science). To measure changes in chondrocyte signalling upon perturbations, we measured gene expression levels by RT-qPCR. Primer sequences used are listed in **Supplementary Table S2**. Fold changes (FC) were determined using the  $2^{-\Delta\Delta CT}$  method, in which cyclic threshold (CT) levels were adjusted for the housekeeping gene *SDHA* ( $-\Delta CT$ ) and subsequently for control samples ( $-\Delta\Delta CT$ ). A  $FC > 1$  represents an upregulation, while  $FC < 1$  depicts a downregulation.

### ***RNA-sequencing***

Paired-end 2x150 base pair RNA sequencing (Illumina TruSeq mRNA Library Prep Kit, Illumina HiSeq X ten) was performed. Strand specific RNA-sequencing libraries were generated which yielded on average 14 million reads per sample. Data from the Illumina platform was analysed with an in-house pipeline as previously described [4]. See **Supplementary Materials** for detailed description of alignment, mapping, normalization and quality control. In total, 14,668 protein-coding genes were included in further analyses.

### ***Differential expression analysis and protein-protein interactions***

Differential expression analysis was performed for 65%MS+IOP cartilage compared with 65%MS cartilage obtained from osteochondral explants using DESeq2 R package version 1.24 [17] on 14,668 protein-coding genes. A general linear model assuming a negative binomial distribution was applied and followed by a Wald-test between 65%MS+IOP and 65%MS samples with correction for principal component 1. In all analyses, 65%MS samples were set as reference. To correct for multiple testing the Benjamini-Hochberg method was used, as indicated by the false discovery rate (FDR) in which a significant cut-off value of 0.05 was used. For protein-protein interactions, analysis was performed using the online tool STRING version 11.0 [18].

### **RNA-sequencing validation by Real-time quantitative PCR (RT-qPCR)**

For validation and replication a total of 8 paired samples were selected. 200 ng of RNA was processed into cDNA using the First Strand cDNA Synthesis Kit (Roche Applied Science, Almere, The Netherlands). Real-Time qPCR was performed and normalized as described above to determine gene expression of *INSIG1*, *DHCR7*, *FADS1*, *CTGF*, *BMP5* and *FOXM1*.

### **Statistical analysis**

RNA-sequencing data analysis was performed in R as described in **Supplementary Materials and Methods**. All other statistical analysis was performed using IBM SPSS statistics 25. *P*-values were determined by applying linear generalized estimating equation (GEE) to effectively adjust for dependencies among donors of the explants by adding a random effect for sample donor as we did not have perfect pairs for each analysis [19]. The following GEE was fitted in which gene expression was the dependent variable and treatment the covariate: *gene expression* ~ *treatment* + (1|*donor*). To determine differences in sGAG concentrations on day 13, another linear GEE model was fitted with sGAG concentration as dependent variable and treatment as covariate: *sGAG concentration* ~ *treatment* + (1|*donor*). Differences in Mankin score between groups was determined by applying the following linear GEE model with Mankin score as dependent variable and treatment as covariate: *Mankin score* ~ *treatment* + (1|*donor*). Results are described by showing their fold change (FC) or average ± standard error (s.e.).

## **Results**

### **IOP reduces detrimental chondrocyte signalling induced by 65%MS**

First we confirmed that injurious mechanical stress (65%MS) induced detrimental changes to cartilage integrity of control and 65%MS aged human osteochondral explants [15]. Changes in chondrocyte signalling in response to 65%MS were determined by measuring gene expression levels of catabolic (*MMP13*, *ADAMTS5* and *EPAS1*), anabolic (*COL2A1* and *ACAN*) and hypertrophic markers (*COL1A1*, *COL10A1* and *ALPL*). As shown in **Figure 1**, non-beneficial chondrocyte responses to 65%MS were particularly marked by increased expression of *MMP13* (FC=6.61; *P*-value=5.17x10<sup>-5</sup>, **Figure 1E**) and *EPAS1* (FC=1.79; *P*-value=5.49x10<sup>-6</sup>), and reduced expression of *COL2A1* (FC=0.49; *P*-value=3.43x10<sup>-3</sup>, **Figure 1F**) and *ACAN* (FC=0.75; *P*-value=1.79x10<sup>-2</sup>; **Table 1**).

Next, to investigate if attenuation of thyroid signalling is a promising treatment for OA, osteochondral explants subjected to 65%MS were simultaneously treated with the anti-deiodinase IOP. As shown in **Table 1**, upon administration of IOP to samples subjected to 65%MS, catabolic markers *MMP13* (FC=0.10; *P*-value=1.73x10<sup>-4</sup>) and *ADAMTS5* (FC=0.43; *P*-value=2.16x10<sup>-2</sup>) were downregulated compared to 65%MS. In addition, expression of the anabolic marker *COL2A1* (FC=3.58; *P*-value=3.71x10<sup>-5</sup>; **Figure 1F**) was no longer downregulated by 65%MS after IOP treatment. For hypertrophic markers, *COL10A1* (FC=0.23; *P*-value=1.05x10<sup>-3</sup>) was significantly downregulated after IOP treatment, while downregulation of *COL1A1* (FC=0.11; *P*-value=5.29x10<sup>-2</sup>) and *ALPL* (FC=0.03; *P*-value=5.71x10<sup>-2</sup>) did not reach statistical significance. With respect to catabolic marker *EPAS1*, no restoration or beneficial effects of IOP treatment with 65%MS was observed.

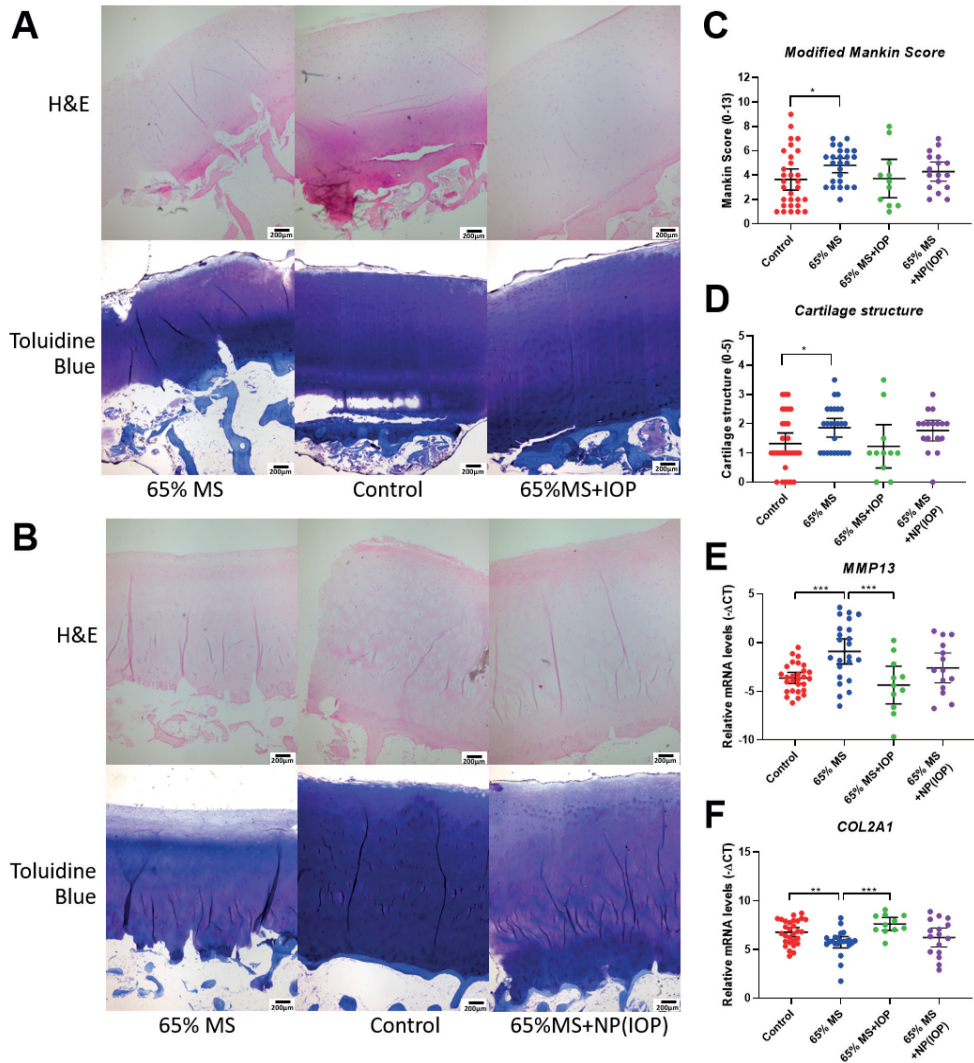


**Figure 1 | Mankin score and gene expression of human aged osteochondral explants after treatment with IOP.** [A, B] Representative histological pictures of Toluidine blue and H&E stainings. [C] Cartilage damage was assessed by determining the Mankin score with [D] scoring of cartilage structure. RT-PCR analysis of [E] *MMP13* and [F] *COL2A1*. Data is presented as scatter dot plots, with mean and 95%CI, and each dot represents a sample. P-values of mean differences between controls and treated explants were estimated by generalized estimating equations (GEE) with expression or Mankin score as dependent variable, treatment as factor and robust variance estimators to account for donor effects. Legend: H&E=haematoxylin and eosin; 65%MS=65% mechanical stress; IOP=iopanoic acid; NP=nanoparticle. \* $P < 0.05$ , \*\* $P < 0.01$ , \*\*\* $P < 0.001$ .

As a proof of concept and to determine whether IOP delivery from PLGA-PEG NP(IOP) is effective, chondrocyte signalling was measured in response to 65%MS now with PLGA NP(IOP) treatment. Upon administration of PLGA NP(IOP), decreased expression of *MMP13* in comparison with 65%MS as control was observed ( $FC=0.38$ ;  $P\text{-value}=9.53 \times 10^{-2}$ ; **Figure 1** and **Table 1**), albeit less pronounced and not significant. On the other hand, upon comparing

the 65%MS with NP(IOP) group to unperturbed controls, changes in *MMP13* and *COL2A1* expression were no longer significant (**Figure 1E-F** and **Supplementary Table S3**). For the hypertrophic markers, no changes were measured in cartilage treated with PLGA NP(IOP) receiving 65%MS. To conclude, IOP encapsulated in PLGA NPs appear to prevent unbeneficial gene expression changes induced by 65%MS, although effectiveness when compared with repeated treatment with free IOP is less pronounced.

**Table 1 | Summary of outcome parameters in response to the different perturbations.**

Outcome measure	control vs 65%MS		65%MS vs 65%MS+IOP		65%MS vs 65%MS+NP(IOP)	
	FC <sup>k</sup>	P-value <sup>s</sup>	FC <sup>k</sup>	P-value <sup>s</sup>	FC <sup>k</sup>	P-value <sup>s</sup>
Gene expression						
Catabolism						
<i>MMP13</i>	6.44	5.17x10 <sup>-5</sup>	0.10	1.73x10 <sup>-4</sup>	0.38	9.53x10 <sup>-2</sup>
<i>ADAMTS5</i>	0.90	NS	0.43	2.16x10 <sup>-2</sup>	0.85	NS
<i>EPAS1</i>	1.79	5.49x10 <sup>-6</sup>	1.32	NS	1.21	9.29x10 <sup>-2</sup>
Anabolism						
<i>ACAN</i>	0.66	1.79x10 <sup>-2</sup>	1.29	NS	1.18	NS
<i>COL2A1</i>	0.40	3.43x10 <sup>-3</sup>	3.58	3.71x10 <sup>-5</sup>	1.68	NS
Hypertrophy						
<i>COL1A1</i>	1.03	NS	0.11	5.29x10 <sup>-2</sup>	0.56	NS
<i>COL10A1</i>	1.81	NS	0.23	1.05x10 <sup>-3</sup>	0.93	NS
<i>ALPL</i>	1.27	NS	0.03	5.71x10 <sup>-2</sup>	0.54	NS
Outcome Measure	control vs 65%MS		65%MS vs 65%MS+IOP		65%MS vs 65%MS+NP(IOP)	
	Beta <sup>a</sup>	P-value <sup>s</sup>	Beta <sup>a</sup>	P-value <sup>s</sup>	Beta <sup>a</sup>	P-value <sup>s</sup>
Histology						
Mankin score	1.15	2.30x10 <sup>-2</sup>	-0.83	NS	-0.61	NS
Cartilage structure	0.54	1.90x10 <sup>-2</sup>	-0.48	NS	-0.16	NS
Cellularity	0.25	NS	0.12	NS	-0.21	NS
Toluidine blue	0.34	NS	-0.42	NS	-0.21	NS
Tidemark integrity	0.14	NS	-0.14	NS	-0.17	NS
sGAG						
Medium	33.68	1.58x10 <sup>-2</sup>	-19.81	NS	-3.94	NS

The comparisons outlined in the table are mechanical stress (65%MS) compared to unperturbed controls, injurious mechanical stress treated with IOP (65%MS+IOP) compared to 65%MS and injurious mechanical stress treated with PLGA nanoparticles filled with IOP (65%MS+NP(IOP)) compared to 65%MS. <sup>k</sup>FC is determined by the 2<sup>-ΔΔCT</sup> method and compared to its respective control. <sup>a</sup>Beta is determined by the GEE during modelling. <sup>s</sup>Significance of mean difference in parameters between explant treatment groups were estimated by generalized estimating equation (GEE) with robust variance estimators to account for donor effects. Legend: FC=fold change; MS=Mechanical stress; IOP=iopanoic acid; NP=nanoparticle; NS=not significant; sGAG=sulphated glycosaminoglycans.

### ***IOP reduces cartilage integrity changes in aged human osteochondral explants***

Next, we explored whether the gene expression changes translate to changes in the histological Mankin scores. As shown in **Figure 1A** and **Figure 1B**, an increased Mankin score among 65%MS explants as compared with controls (4.80±0.29 versus 3.65±0.43; *P*-value=2.34x10<sup>-2</sup>; **Figure 1C**) confirmed damage. More specifically, increased Mankin score was particularly due to increased cartilage structure damage score (1.86±0.15 versus 1.32±0.18; *P*-value=1.94x10<sup>-2</sup>;

**Figure 1D**). Upon investigating explants subjected to 65%MS with IOP or PLGA NP(IOP) we observed Mankin scores comparable to controls ( $3.72 \pm 0.71$  and  $4.29 \pm 0.37$ ; **Figure 1D**, **Supplementary Table S3**). In line with this, sGAG released from 65%MS osteochondral explants was increased by 49% compared with controls ( $91.85 \pm 13.00$   $\mu\text{g/ml}$  versus  $61.45 \pm 5.11$   $\mu\text{g/ml}$ ;  $P\text{-value} = 1.58 \times 10^{-2}$ ; **Table 1**). Whereas after free IOP treatment, 65%MS induced no change in sGAG release in comparison to controls ( $61.68 \pm 9.13$   $\mu\text{g/ml}$  versus  $61.45 \pm 5.11$   $\mu\text{g/ml}$ ; **Supplementary Table S3**). PLGA NP(IOP) treatment did not reduce sGAG release to the media with 65%MS ( $95.91 \pm 14.32$   $\mu\text{g/ml}$  versus  $61.45 \pm 5.11$   $\mu\text{g/ml}$ ;  $P\text{-value} = 4.07 \times 10^{-2}$ ; **Supplementary Table S3**).

### RNA-sequencing of IOP treated explants upon applying 65%MS

To investigate the mode of action of IOP on injurious mechanical stress induced changes, genome-wide gene expression was measured by sequencing RNA of explant cartilage treated with free IOP and 65%MS ( $n_{65\%MS+IOP} = 7$ ) and compared them with the 65%MS group as control ( $n_{65\%MS} = 14$ ), as such identifying genes that sequester the damaging response upon injurious loading.

Prior to genome wide analysis, we confirmed expression changes of genes previously measure by RT-qPCR in our osteochondral explant model (**Table 1**). As shown in **Supplementary Table S4**, RNA-sequencing replicated downregulated expression of *MMP13* ( $FC = 0.06$ ;  $P\text{-value} = 9.00 \times 10^{-3}$ ) and of hypertrophic markers *COL1A1* ( $FC = 0.02$ ;  $P\text{-value} = 4.72 \times 10^{-4}$ ) and *ALPL* ( $FC = 0.01$ ;  $P\text{-value} = 3.65 \times 10^{-3}$ ) in 65%MS+IOP cartilage when compared to 65%MS cartilage. For *COL10A1* ( $FC = 0.18$ ;  $P\text{-value} = 6.36 \times 10^{-2}$ ) reduced expression was observed in the RNA-sequencing, but did not reach statistical significance. Moreover, despite the similar effect sizes of *COL2A1* in RT-qPCR and RNA-sequencing, these effects were not significant in the latter.

**Table 2 | The 12 FDR significantly differentially expressed genes between IOP and 65% MS cartilage.**

Gene	FC	P-value	FDR <sup>a</sup>
<i>INSIG1</i>	3.25	$6.12 \times 10^{-6}$	$2.24 \times 10^{-2}$
<i>DHCR7</i>	2.92	$1.47 \times 10^{-5}$	$3.28 \times 10^{-2}$
<i>FADS1</i>	2.91	$1.88 \times 10^{-5}$	$3.28 \times 10^{-2}$
<i>LRP8</i>	2.87	$3.75 \times 10^{-5}$	$4.58 \times 10^{-2}$
<i>ACAT2</i>	2.25	$1.55 \times 10^{-5}$	$3.28 \times 10^{-2}$
<i>LTBP2</i>	0.43	$2.01 \times 10^{-5}$	$3.28 \times 10^{-2}$
<i>CTGF</i>	0.35	$3.78 \times 10^{-6}$	$2.24 \times 10^{-2}$
<i>BMP5</i>	0.29	$2.47 \times 10^{-5}$	$3.29 \times 10^{-2}$
<i>LOX</i>	0.23	$4.14 \times 10^{-6}$	$2.24 \times 10^{-2}$
<i>ADGRV1</i>	0.21	$4.66 \times 10^{-6}$	$2.24 \times 10^{-2}$
<i>FOXM1</i>	0.16	$1.74 \times 10^{-5}$	$3.28 \times 10^{-2}$
<i>MASP1</i>	0.13	$2.27 \times 10^{-5}$	$3.29 \times 10^{-2}$

<sup>a</sup>To correct for multiple testing, the Benjamini-Hochberg method was applied to P-values and reported as the false discovery rate (FDR). Legend: FC=fold change; FDR=False discovery rate

Next, genome wide differential expression analysis with 65%MS as control versus 65%MS+IOP was performed, indicating 12 FDR significant differentially expressed (DEGs; **Table 2**). Of these 12 DEGs, five were upregulated while seven were downregulated with absolute fold changes ranging from 2.25 to 7.69. The highest upregulated gene was *INSIG1* (FC=3.25; FDR=2.24x10<sup>-2</sup>), encoding for insulin induced gene 1, a protein inhibiting lipogenesis and cell proliferation [20]. The most downregulated gene was *MASP1* (FC=0.13; FDR=3.29x10<sup>-2</sup>), encoding for mannan binding lectin serine peptidase 1, a serine protease involved in complement activation [21]. Of interest is also the identification of downregulated genes promoting chondrocyte proliferation and differentiation such as *BMP5* (FC=0.29; FDR=3.29x10<sup>-2</sup>), encoding for bone morphogenetic protein 5, and *CTGF* (FC=0.35; FDR=2.24x10<sup>-2</sup>), encoding connective tissue growth factor [22,23].

Protein-protein interactions of the DEGs were investigated in STRING and showed significantly more interactions than expected by chance ( $P$ -value=2.61x10<sup>-7</sup>), with 7 out of 12 proteins having connections (**Figure 2**). Of note is that connected proteins (*INSIG1*, *DHCR7*, *FADS1* and *ACAT2*) consists of those involved in cholesterol biosynthetic processes (GO:0006695). To conclude, treatment with IOP shows changes in gene expression patterns that suggest a response in metabolic processes (*INSIG1*, *DHCR7*, *FADS1* and *ACAT2*) and reduction of proliferation and differentiation (*CTGF*, *BMP5* and *FOXM1*) in chondrocytes.

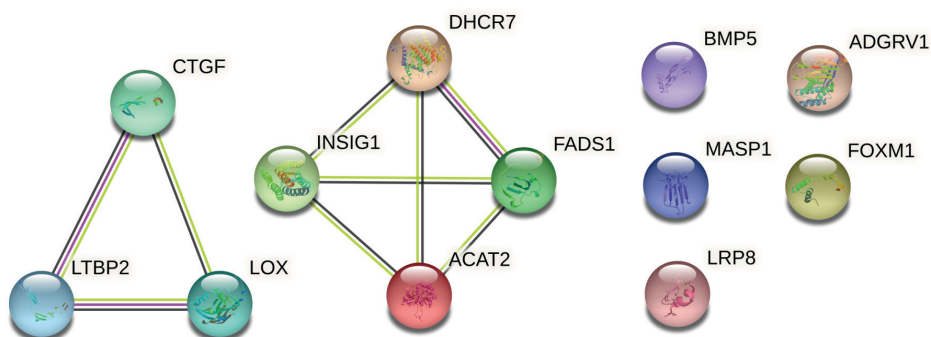


**Figure 2 | Protein-Protein interaction network in STRING of proteins encoded by differentially expressed genes.** Differentially expressed genes between 65%MS and 65%MS+IOP cartilage of osteochondral explants show two connected gene groups with high interactions

### **Comparison between IOP responsive and OA responsive genes.**

To investigate to what extent the DEGs coincide with OA pathophysiology, we compared DEGs (DEG<sub>IOP</sub>) with previously identified DEGs between preserved and lesioned OA cartilage (DEG<sub>OA</sub>) [4]. Of the 12 DEGs, three were also involved in OA pathophysiology (**Table 3**). Notable are *ADGRV15726*, encoding for the calcium binding transmembrane receptor adhesion g protein-coupled receptor V1, and *FOXM1*, encoding for the transcription factor forkhead box protein M1, a known inducer of cell proliferation and key mediator of inflammatory signalling [24], since they mark OA pathophysiology [4] and are being counteracted by IOP treatment (**Table 3**). *DHCR7*, a vital enzyme for cholesterol and vitamin D production [25], was upregulated in both OA pathophysiology and in response to IOP treatment. In addition, we investigated if any of the here identified DEGs are also seen as OA susceptibility risk genes and identified that for *BMP5* several polymorphisms have been associated with OA [26,27].

**Table 3 | Investigation of the 12 FDR significant genes in OA pathophysiology.**

Gene	65%MS+IOP vs 65%MS			OA pathophysiology <sup>b</sup>		
	FC	P-value	FDR <sup>a</sup>	FC	P-value	FDR <sup>a</sup>
<i>INSIG1</i>	3.25	6.12x10 <sup>-6</sup>	2.24x10 <sup>-2</sup>	1.04	NS	NS
<i>DHCR7</i>	2.92	1.47x10 <sup>-5</sup>	3.28x10 <sup>-2</sup>	1.28	1.21x10 <sup>-3</sup>	1.56x10 <sup>-2</sup>
<i>FADS1</i>	2.91	1.88x10 <sup>-5</sup>	3.28x10 <sup>-2</sup>	1.00	NS	NS
<i>LRP8</i>	2.87	3.75x10 <sup>-5</sup>	4.58x10 <sup>-2</sup>	1.15	3.00x10 <sup>-2</sup>	NS
<i>ACAT2</i>	2.25	1.55x10 <sup>-5</sup>	3.28x10 <sup>-2</sup>	1.19	3.00x10 <sup>-2</sup>	NS
<i>LTBP2</i>	0.43	2.01x10 <sup>-5</sup>	3.28x10 <sup>-2</sup>	1.06	NS	NS
<i>CTGF</i>	0.35	3.78x10 <sup>-6</sup>	2.24x10 <sup>-2</sup>	1.18	1.00x10 <sup>-2</sup>	NS
<i>BMP5</i>	0.29	2.47x10 <sup>-5</sup>	3.29x10 <sup>-2</sup>	0.74	NS	NS
<i>LOX</i>	0.23	4.14x10 <sup>-6</sup>	2.24x10 <sup>-2</sup>	1.13	NS	NS
<i>ADGRV1</i>	0.21	4.66x10 <sup>-6</sup>	2.24x10 <sup>-2</sup>	1.72	2.87x10 <sup>-3</sup>	2.92x10 <sup>-2</sup>
<i>FOXM1</i>	0.16	1.74x10 <sup>-5</sup>	3.28x10 <sup>-2</sup>	1.40	2.31x10 <sup>-3</sup>	2.50x10 <sup>-2</sup>
<i>MASP1</i>	0.13	2.27x10 <sup>-5</sup>	3.29x10 <sup>-2</sup>	0.89	NS	NS

<sup>a</sup>To correct for multiple testing, the Benjamini-Hochberg method was applied to P-values and reported as the false discovery rate (FDR). <sup>b</sup>Gene expression changes measured in RNA-sequencing data between preserved and lesioned OA articular cartilage, with preserved as reference [4]. Legend: FC=fold change; FDR=false discovery rate; OA=osteoarthritis; 65%MS=65% mechanical stress; NS=not significant; IOP=iopanoic acid.

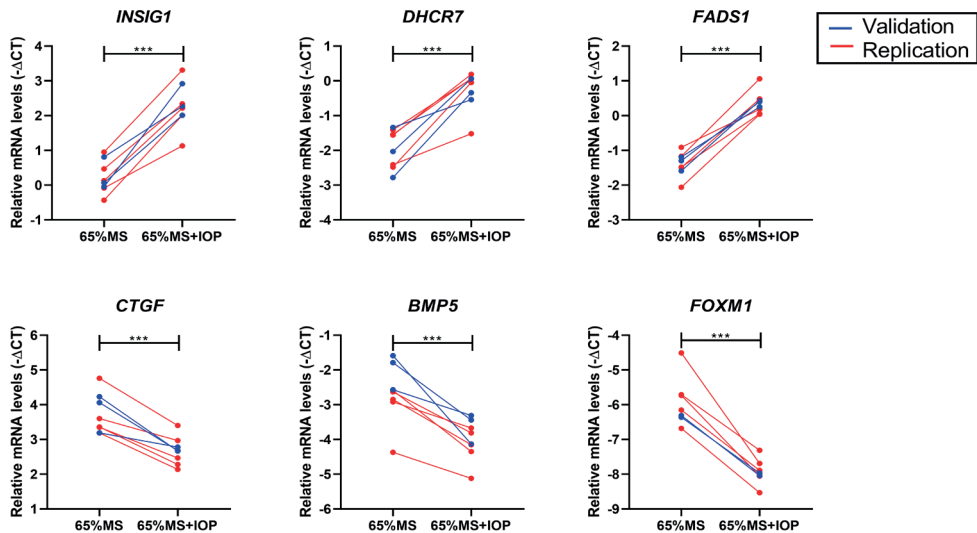


**Figure 3 | Technical and biological validation of the highest up- and downregulated genes was performed using RT-qPCR.** Expression of three upregulated (*INSIG1*, *DHCR7*, *FADS1*) and three downregulated (*CTGF*, *BMP5*, *FOXM1*) genes was validated (blue; n=3 pairs) and replicated (red; n=5 pairs) in cartilage samples by RT-qPCR. Figures show connected paired samples and  $-\Delta\text{CT}$  of each independent sample is depicted by black dots in the graphs. Statistical differences between gene expression in 65%MS and IOP treated 65%MS cartilage (65%MS+IOP) was determined with a linear generalized estimation equation (GEE) with mRNA level as dependent variable. \*\*\*P $\leq$ 0.001. Legend: 65%MS: 65% mechanical stress; RT-qPCR: reverse transcriptase-quantitative PCR; IOP=iopanoic acid.

## Validation of DEGs

For technical validation (n=3 pairs) and biological replication (n=5 pairs) of the DEGs identified in this study, RT-qPCR was performed for three upregulated (*INSIG1*, *DHCR7*, *FADS1*) and three downregulated (*CTGF*, *BMP5*, *FOXM1*) genes. For all genes a significant difference was confirmed between 65%MS and 65%MS+IOP treated cartilage (**Figure 3**), with the same direction and size of effects, confirming robustness of our RNA sequencing results.

## Discussion

In the current study we explored possible beneficial effects of inhibiting D2 activity by adding the anti-deiodinase agent IOP to our previously established aged human osteochondral explant model. Herein detrimental effects were initiated by the OA-relevant trigger injurious mechanical stress (65%MS) [15]. To allow further translation of our results we additionally studied effects of prolonged IOP release from nanoparticles. Our results confirmed that treatment with IOP reduced the majority of detrimental 65%MS-induced chondrocyte signalling and even reduced some of its long-term effects on cartilage integrity. Finally, RNA-sequencing was performed on 65%MS cartilage with and without IOP treatment, which enable us to identify its mode of action.

We identified 12 DEGs of which the majority are involved in metabolic processes (e.g. *INSIG1*, *DHCR7*, *FADS2* and *ACAT2*) and cell proliferation and differentiation (e.g. *CTGF*, *BMP5* and *FOXM1*), indicating IOP is reducing metabolic activity of chondrocytes possibly towards a healthy resting state. This is in line with previous studies showing that adult chondrocytes and the extracellular cartilage matrix benefitted from maintaining a low metabolic maturation-arrested state, while activation of aged chondrocytes results in proliferation, recapitulation of endochondral ossification and eventually cell death [4,28].

We here show that treatment with free IOP in the medium efficiently reduced cartilage degradation of human aged osteochondral explants subjected to injurious mechanical stress. These effects were however less pronounced when we administered PLGA NP(IOP). A possible explanation for the reduced effectiveness of IOP released from NPs, could be that the pharmacological agent is not released in a high enough doses to counteract the detrimental induction. This is further exacerbated by the fact that IOP released slowly from the NP is subjected to a half-life of 1-2 days [29], whereas IOP in the medium was refreshed every 3-4 days. On the other hand, the relatively low concentration of 10  $\mu$ M encapsulated IOP was based on pilot experiments and the underlying thought that NP are being taken up by chondrocytes (**Supplementary Fig 2A**), and thus acting locally and more efficiently. In any case, given that PLGA NP(IOP) appeared less effective, the exact concentration of PLGA NP(IOP) requires further optimization. Moreover, delivery of the NPs can be further optimized, e.g. by modifying charge of the NP to increase retention in the synovial cavity or binding to negatively charged sGAGs. Other factors that need to be considered before performing *in vivo* studies are the effects of tissue disease state, synovial fluid, and NP accumulation as these may modify retention, delivery efficiency and drug efficacy.

To investigate the mode of action of IOP, transcriptome-wide differences between cartilage of osteochondral explants subjected to injurious mechanical stress with and without IOP was determined showing 12 FDR significant genes with suggested high protein-protein

connectivity (**Figure 2**). Notably, these genes appeared to be primarily involved in metabolic processes, such as *INSIG1* (FC=3.25; FDR=2.24x10<sup>-2</sup>) encoding a membrane protein that limits lipogenesis and cell differentiation [20]. Another notable gene in this respect was *BMP5* (FC=0.29; FDR=3.29x10<sup>-2</sup>). BMP5 is a ligand of the TGF-beta superfamily involved in activation of SMAD, ERK and p38 induced gene expression, negatively affecting cartilage homeostasis [30]. On the other hand, *BMP5* silencing reduced OA progression in mice [31]. Together these data suggest that IOP may have reduced detrimental effects of injurious mechanical stress via lowering BMP5 activation. Of interest is the identification of the transcription factor, *FOXM1* (FC=0.16; FDR=1.74x10<sup>-5</sup>), coinciding with genes involved in OA pathophysiology (**Table 3**) and a key mediator of the inflammatory response inducing OA degeneration [24]. The herein observed downregulation of *FOXM1* suggests that IOP could protect chondrocytes from an inflammatory response upon external stimuli. Finally, because IOP is an inhibitor of thyroid signalling, we compared the 12 DEGs to a consensome meta-analysis of thyroid manipulation studies [32]. Nine (75%) genes were confirmed to be involved in thyroid signalling and among them we identified important genes such as *INSIG1*, *DHCR7*, *FADS1* and *ACAT2* involved in the metabolic process of cholesterol biosynthetic processes (**Supplementary Table S5**). To conclude, genome-wide changes of IOP show its ability to reduce the metabolic activity of chondrocytes as observed by the response of genes involved in metabolic processes and cell proliferation and differentiation.

Although the model used in our study is prone to OA pathophysiology, as it consists of physiologically relevant human aged preserved articular cartilage and subchondral bone, the model is inherently subject to heterogeneity. Nonetheless, in general our results were robustly reflected in multiple donors, giving validity to the observed effects. The RNA-sequencing was performed in a low number of samples, resulting in limited power to identify DEGs with a lower effect. However, by comparing RT-qPCR results with the RNA-sequencing results we show the validity of the results of the RNA-sequencing, as observed by similar effect sizes and *P*-values. Altogether, by combining treatment testing of a genetically based (repurposed) drug in an established human aged biomimetic osteochondral explant model of mechanical injury [15,33], we generated multiple reliable biological replicates on how abrogation of thyroid signalling in cartilage is beneficial for cartilage homeostasis. As such, our approach created reliable data that are highly translatable to the *in vivo* human situation while contributing to the societal need for animal study reduction. In this study we focussed on measuring chondrocyte signalling on the gene expression level since thyroid hormone primarily affects metabolic processes via binding to the thyroid receptor, which regulates downstream gene expression. Additionally, we believe gene expression to be a measurement reflecting detrimental chondrocyte homeostasis prior to any detrimental effects observed in the extracellular matrix.

In this study, we have shown that treatment with the anti-deiodinase IOP reduced detrimental changes induced by injurious mechanical stress. In addition, by performing RNA-sequencing we identified that its mode of action mainly encompassed metabolic processes, cell proliferation and differentiation and also important OA-associated genes, such as *BMP5*, *CTGF* and *FOXM1*. Since in general a lower metabolism has been shown to be beneficial for chondrocytes, we advocate use of IOP is a potential pharmacological treatment agent for OA.

## **Funding**

This work was supported by the Dutch Scientific Research council NWO/ZonMW VICI scheme (nr 91816631/528) and the Dutch Arthritis Society/ReumaNederland (15-4-401).

## **Acknowledgments**

We thank all the participants of the RAAK study. The LUMC has and is supporting the RAAK study. We also thank Enrike van der Linden, Robert van der Wal, Peter van Schie, Anika Rabelink-Hoogenstraaten, Shaho Hasan, Maartje Meijer, Daisy Latijnhouwers and Geert Spierenburg for collecting surgical waste material. Data is generated within the scope of the Medical Delta Programs Regenerative Medicine 4D: Generating complex tissues with stem cells and printing technology and Improving Mobility with Technology.

## **Competing interest**

The authors declare that they have no competing interests.

## **Ethics**

Our study complies with the Declaration of Helsinki. Furthermore, the RAAK study has been approved by the medical ethical committee of the Leiden University Medical Center (P08.239/P19.013) and informed consent was obtained from subjects.

## **Data availability statement**

Data are available on reasonable request. RNA sequencing data underlying this article are available in the European Genome-phenome Archive (EGA) at <https://ega-archive.org/> and can be accessed with EGAS00001006242.

## **REFERENCES**

1. Bijlsma JW, Berenbaum F, Lafeber FP. Osteoarthritis: an update with relevance for clinical practice. *Lancet*. 2011;377(9783):2115-26.
2. Drissi H, Zuscik M, Rosier R, et al. Transcriptional regulation of chondrocyte maturation: potential involvement of transcription factors in OA pathogenesis. *Mol Aspects Med*. 2005;26(3):169-79.
3. Felson DT. Developments in the clinical understanding of osteoarthritis. *Arthritis Res Ther*. 2009;11(1):203.
4. Coutinho de Almeida R, Ramos YFM, Mahfouz A, et al. RNA sequencing data integration reveals an miRNA interactome of osteoarthritis cartilage. *Annals of the rheumatic diseases*. 2019;78(2):270-7.
5. den Hollander W, Ramos YF, Bomer N, et al. Transcriptional associations of osteoarthritis-mediated loss of epigenetic control in articular cartilage. *Arthritis & rheumatology (Hoboken, NJ)*. 2015;67(8):2108-16.

6. Nelson MR, Tipney H, Painter JL, et al. The support of human genetic evidence for approved drug indications. *Nat Genet.* 2015;47(8):856-60.
7. Meulenkamp I, Min JL, Bos S, et al. Identification of DIO2 as a new susceptibility locus for symptomatic osteoarthritis. *Hum Mol Genet.* 2008;17(12):1867-75.
8. Gereben B, Zavacki AM, Ribich S, et al. Cellular and molecular basis of deiodinase-regulated thyroid hormone signaling. *Endocr Rev.* 2008;29(7):898-938.
9. Bos SD, Bovee JV, Duijnisveld BJ, et al. Increased type II deiodinase protein in OA-affected cartilage and allelic imbalance of OA risk polymorphism rs225014 at DIO2 in human OA joint tissues. *Annals of the rheumatic diseases.* 2012;71(7):1254-8.
10. Ijiri K, Zerbini LF, Peng H, et al. Differential expression of GADD45beta in normal and osteoarthritic cartilage: potential role in homeostasis of articular chondrocytes. *Arthritis Rheum.* 2008;58(7):2075-87.
11. Bomer N, Cornelis FM, Ramos YF, et al. The effect of forced exercise on knee joints in Dio2(-/-) mice: type II iodothyronine deiodinase-deficient mice are less prone to develop OA-like cartilage damage upon excessive mechanical stress. *Annals of the rheumatic diseases.* 2016;75(3):571-7.
12. Bomer N, den Hollander W, Ramos YF, et al. Underlying molecular mechanisms of DIO2 susceptibility in symptomatic osteoarthritis. *Annals of the rheumatic diseases.* 2015;74(8):1571-9.
13. Nagase H, Nagasawa Y, Tachida Y, et al. Deiodinase 2 upregulation demonstrated in osteoarthritis patients cartilage causes cartilage destruction in tissue-specific transgenic rats. *Osteoarthritis and cartilage.* 2013;21(3):514-23.
14. Tyer NM, Kim TY, Martinez DS. Review of Oral Cholecystographic Agents for the Management of Hyperthyroidism. *Endocr Pract.* 2014;20(10):1084-92.
15. Houtman E, van Hoofter M, Lakenberg N, et al. Human Osteochondral Explants: Reliable Biomimetic Models to Investigate Disease Mechanisms and Develop Personalized Treatments for Osteoarthritis. *Rheumatol Ther.* 2021;8(1):499-515.
16. Ramos YF, den Hollander W, Bovee JV, et al. Genes involved in the osteoarthritis process identified through genome wide expression analysis in articular cartilage; the RAAK study. *PLoS One.* 2014;9(7):e103056.
17. Love MI, Huber W, Anders S. Moderated estimation of fold change and dispersion for RNA-seq data with DESeq2. *Genome Biol.* 2014;15(12):550.
18. Szklarczyk D, Gable AL, Lyon D, et al. STRING v11: protein-protein association networks with increased coverage, supporting functional discovery in genome-wide experimental datasets. *Nucleic Acids Res.* 2019;47(D1):D607-D13.
19. Diggle P, Liang K-Y, Zeger SL. Analysis of longitudinal data. Oxford New York: Clarendon Press; Oxford University Press; 1994. xi, 253 p. p.
20. Li J, Takaishi K, Cook W, et al. Insig-1 "brakes" lipogenesis in adipocytes and inhibits differentiation of preadipocytes. *Proc Natl Acad Sci U S A.* 2003;100(16):9476-81.21.
21. Degen SE, Jensen L, Hansen AG, et al. Mannan-binding lectin-associated serine protease (MASP)-1 is crucial for lectin pathway activation in human serum, whereas neither MASP-1 nor MASP-3 is required for alternative pathway function. *J Immunol.* 2012;189(8):3957-69.
22. Mailhot G, Yang M, Mason-Savas A, et al. BMP-5 expression increases during chondrocyte differentiation in vivo and in vitro and promotes proliferation and cartilage matrix synthesis in primary chondrocyte cultures. *J Cell Physiol.* 2008;214(1):56-64.
23. Ivkovic S, Yoon BS, Popoff SN, et al. Connective tissue growth factor coordinates chondrogenesis and angiogenesis during skeletal development. *Development.* 2003;130(12):2779-91.
24. Zeng RM, Lu XH, Lin J, et al. Knockdown of FOXM1 attenuates inflammatory response in human osteoarthritis chondrocytes. *Int Immunopharmacol.* 2019;68:74-80.
25. Prabhu AV, Luu W, Li D, et al. DHCR7: A vital enzyme switch between cholesterol and vitamin D production. *Prog Lipid Res.* 2016;64:138-51.
26. Southam L, Dowling B, Ferreira A, et al. Microsatellite association mapping of a primary osteoarthritis susceptibility locus on chromosome 6p12.3-q13. *Arthritis Rheum.* 2004;50(12):3910-4.
27. Tachmazidou I, Hatzikotoulas K, Southam L, et al. Identification of new therapeutic targets for osteoarthritis through genome-wide analyses of UK Biobank data. *Nat Genet.* 2019;51(2):230-6.

28. Sandell LJ, Aigner T. Articular cartilage and changes in arthritis. An introduction: cell biology of osteoarthritis. *Arthritis Res.* 2001;3(2):107-13.
29. Eason CT, Frampton CM. The plasma pharmacokinetics of iophenoxic and iopanoic acids in goat. *Xenobiotica.* 1992;22(2):185-9.
30. Snelling SJ, Hulley PA, Loughlin J. BMP5 activates multiple signaling pathways and promotes chondrogenic differentiation in the ATDC5 growth plate model. *Growth Factors.* 2010;28(4):268-79.
31. Shao Y, Zhao C, Pan J, et al. BMP5 silencing inhibits chondrocyte senescence and apoptosis as well as osteoarthritis progression in mice. *Aging (Albany NY).* 2021;13(7):9646-64.
32. Ochsner SA, McKenna NJ. No Dataset Left Behind: Mechanistic Insights into Thyroid Receptor Signaling Through Transcriptomic Consensus Meta-Analysis. *Thyroid.* 2020;30(4):621-39.
33. Houtman E, Tuerlings M, Riechelmann J, et al. Elucidating mechano-pathology of osteoarthritis: transcriptome-wide differences in mechanically stressed aged human cartilage explants. *Arthritis Res Ther.* 2021;23(1):215.

## Supplementary Files

### *List of content:*

#### ***Supplementary Tables***

**Supplementary Table S1.** Baseline information of the donors included in this study.

**Supplementary Table S2.** Primer sequences used in RT-qPCR.

**Supplementary Table S3.** Summary of the different outcome parameters in response to perturbation with 65% mechanical stress (65%MS), 65%MS+IOP and 65%MS+PLGA NP(IOP) compared to unperturbed controls.

**Supplementary Table S4.** Gene expression measured by RT-qPCR and RNA sequencing between 65%MS+IOP in comparison to 65%MS.

**Supplementary Table S5.** Investigation of the 12 FDR significant genes in a consensome of thyroid signalling.

#### ***Supplementary Materials and Methods***

#### ***Supplementary Figures***

**Supplementary Figure S1.** Schematic representation of study setup.

**Supplementary Figure S2.** Characterization of PLGA-PEG nanoparticles.

## Supplementary Tables

**Supplementary Table S1 | Baseline information of the donors included in this study.**

Characteristic	Average±SD [Range]
Age	67.1±9.8 [52-85]
Sex	4M, 12F (75% F)
BMI	30.8±4.7 [24.6-39.2]

The table represents the age, sex, and BMI of donors used in this study. Legend: F=Females, M=Males; age given in years)

**Supplementary Table S2 | Primer sequences used in RT-qPCR.**

Gene	Forward primer (5'- 3')	Reverse primer (5'- 3')
<i>SDHA</i>	TGGAGCTGCAGAACCTGATG	TGTAGTCTTCCCTGGCATGC
<i>YWHAZ</i>	CTGAGGTTGCAGCTGGTGATGACA	AGCAGGCTTTCTCAGGGGAGTTCA
<i>MMP13</i>	TTGAGCTGGACTCATGTGTCG	GGAGCCTCTCAGTCATGGAG
<i>ADAMTS5</i>	TGGCTCACGAAATCGGACAT	GCGCTTATCTTCTGTGGAACC
<i>EPAS1</i>	ACAGGTGGAGCTAACAGGAC	CCGTGCACTTCATCCTCATG
<i>COL2A1</i>	CTACCCCAATCCAGCAAACGT	AGGTGATGTTCTGGGAGCCTT
<i>ACAN</i>	AGAGACTCACAGTCGAAACAGC	CTATGTTACAGTGCTCGCCAGTG
<i>COL1A1</i>	GTGCTAAAGGTGCCAATGGT	ACCAGGTTACCCGCTGTTAC
<i>COL10A1</i>	GGCAACAGCATTATGACCCA	TGAGATCGATGATGGCACTCC
<i>ALPL</i>	CAAAGGCTTCTTCTTGCTGGTG	CCTGCTTGGCTTTTCCTTCA
<i>INSIG1</i>	GCTGCAGATCCAGAGGAATGT	GTGACTGTCGATACAGGGGT
<i>DHCR7</i>	ACAGAACCGCATCTCAAGGG	AGCTGTACTGGTCACAAGCC
<i>FADS1</i>	AGCTTTGAGCCACCAAGAA	CATCCAGCAGCAAGATGTGC
<i>CTGF</i>	CCGTACTCCAAAATCTCCA	ATGTCTTCATGCTGGTGCAG
<i>BMP5</i>	ACTCTATGTGAGCTTCCGGG	CAGCGTATCCTTCTGGTGCT
<i>FOXM1</i>	TCACAGCAGAAACGACCGAA	TCACCGGGAAGTGGATAGGT

**Supplementary Table S3 | Summary of the different outcome parameters in response to perturbation with 65% mechanical stress (65%MS), 65%MS+IOP and 65%MS+PLGA NP(IOP) compared to unperturbed controls.**

Outcome measure	65%MS+IOP vs control		65%MS+NP(IOP) vs control	
	FC <sup>a</sup>	P-value <sup>§</sup>	FC <sup>a</sup>	P-value <sup>§</sup>
Gene expression				
Catabolism				
<i>MMP13</i>	0.60	NS	2.05	NS
<i>ADAMTS5</i>	0.12	1.99X10 <sup>-2</sup>	1.05	NS
<i>EPAS1</i>	2.06	1.71X10 <sup>-3</sup>	2.11	1.17X10 <sup>-9</sup>
Anabolism				
<i>ACAN</i>	0.68	NS	0.99	NS
<i>COL2A1</i>	1.79	NS	0.85	NS
Hyperthrophy				
<i>COL1A1</i>	0.14	4.02X10 <sup>-2</sup>	0.48	NS
<i>COL10A1</i>	0.22	3.06X10 <sup>-2</sup>	1.55	NS
<i>ALPL</i>	0.11	6.20X10 <sup>-2</sup>	0.53	NS
Outcome Measure	65%MS+IOP vs control		65%MS+NP(IOP) vs control	
	Beta <sup>b</sup>	P-value <sup>§</sup>	Beta <sup>b</sup>	P-value <sup>§</sup>
Histology				
Mankin score	0.32	NS	0.55	NS
<i>Cartilage structure</i>	0.07	NS	0.39	NS
<i>Cellularity</i>	0.37	NS	0.04	NS
<i>Toluidine blue</i>	-0.08	NS	0.12	NS
<i>Tidemark integrity</i>	0.01	NS	-0.03	NS
sGAG				
Medium	13.86	NS	29.74	4.07X10 <sup>-2</sup>

<sup>a</sup>FC is determined by the 2<sup>-ΔΔCT</sup> method and compared to its respective control. FC>1 is upregulation and FC<1 is downregulation. <sup>b</sup>Beta is determined by the GEE during the modelling and represents the difference between the perturbation and control group. <sup>§</sup> Significance of mean difference in gene expression between controls and treated explants were estimated by generalized estimating equation (GEE) with robust variance estimators to account for donor effects. Legend: FC=Fold change; IOP=iopanoic acid; NP=nanoparticle; MS=Mechanical stress; NS=Not significant; sGAG=sulphated glycosaminoglycans.

**Supplementary Table S4 | Gene expression measured by RT-qPCR and RNA sequencing between 65%MS+IOP in comparison to 65%MS.**

Gene	RT-qPCR		RNA-seq	
	FC	P-value	FC	P-value
<i>MMP13</i>	0.10	1.73x10 <sup>-4</sup>	0.06	9.00x10 <sup>-3</sup>
<i>ADAMTS5</i>	0.43	2.16x10 <sup>-2</sup>	0.84	NS
<i>EPAS1</i>	1.32	NS	1.01	NS
<i>COL2A1</i>	3.58	3.71x10 <sup>-5</sup>	2.52	NS
<i>ACAN</i>	1.29	NS	1.06	NS
<i>COL1A1</i>	0.11	5.29x10 <sup>-2</sup>	0.02	4.72x10 <sup>-4</sup>
<i>COL10A1</i>	0.23	1.05x10 <sup>-3</sup>	0.18	6.36x10 <sup>-2</sup>
<i>ALPL</i>	0.03	5.71x10 <sup>-2</sup>	0.01	3.65x10 <sup>-3</sup>

FC was calculated by the 2<sup>-ddCT</sup> method in the RT-qPCR between 65%MS+IOP (n=11) and 65%MS (n=24). P-value in RT-qPCR was determined by performing a GEE. FC was calculated by DeSEQ for RNA-sequencing data between 65%MS+IOP (n=7) and 65%MS (n=14). P-value in the RNA-seq was determined by DESeq2 using a general linear model assuming a negative binomial distribution followed by a Wald-test. Legend: FC=Fold Change, RT-qPCR=real-time quantitative polymerase chain reaction; RNA-seq=RNA sequencing, NS=not significant.

**Supplementary Table S5 | Investigation of the 12 FDR significant genes in a consensome of thyroid signalling.**

Gene	65%MS+IOP vs 65%MS			Thyroid signalling <sup>b</sup>	
	FC	P-value	FDR <sup>a</sup>	GMFC	CPV
<i>INSIG1</i>	3.25	6.12x10 <sup>-6</sup>	2.24x10 <sup>-2</sup>	1.20	1.59x10 <sup>-4</sup>
<i>DHCR7</i>	2.92	1.47x10 <sup>-5</sup>	3.28x10 <sup>-2</sup>	1.27	1.42x10 <sup>-11</sup>
<i>FADS1</i>	2.91	1.88x10 <sup>-5</sup>	3.28x10 <sup>-2</sup>	1.15	8.03x10 <sup>-6</sup>
<i>LRP8</i>	2.87	3.75x10 <sup>-5</sup>	4.58x10 <sup>-2</sup>	1.13	5.15x10 <sup>-3</sup>
<i>ACAT2</i>	2.25	1.55x10 <sup>-5</sup>	3.28x10 <sup>-2</sup>	1.17	1.91x10 <sup>-5</sup>
<i>LTBP2</i>	0.43	2.01x10 <sup>-5</sup>	3.28x10 <sup>-2</sup>	1.12	NS
<i>CTGF</i>	0.35	3.78x10 <sup>-6</sup>	2.24x10 <sup>-2</sup>	1.38	1.46x10 <sup>-7</sup>
<i>BMP5</i>	0.29	2.47x10 <sup>-5</sup>	3.29x10 <sup>-2</sup>	1.10	NS
<i>LOX</i>	0.23	4.14x10 <sup>-6</sup>	2.24x10 <sup>-2</sup>	1.26	1.17x10 <sup>-2</sup>
<i>ADGRV1</i>	0.21	4.66x10 <sup>-6</sup>	2.24x10 <sup>-2</sup>	1.09	NS
<i>FOXM1</i>	0.16	1.74x10 <sup>-5</sup>	3.28x10 <sup>-2</sup>	1.15	3.28x10 <sup>-5</sup>
<i>MASP1</i>	0.13	2.27x10 <sup>-5</sup>	3.29x10 <sup>-2</sup>	1.16	1.36x10 <sup>-2</sup>

<sup>a</sup>To correct for multiple testing, the Benjamini-Hochberg method was applied to p-values and reported as the false discovery rate (FDR). <sup>b</sup>A consensome meta-analysis of thyroid manipulation studies summarizes genes involved in thyroid signalling [1]. Legend: FC=fold change; FDR= false discovery rate; GMFC= Geometric mean fold change; CPV=Consensome P-value.

## Supplementary Materials and Methods

### 1.1 Study design and patient participation

Osteochondral explants were obtained from knee joints included in the Research in Articular Osteoarthritis Cartilage (RAAK) study [2]. The RAAK study has been approved by the medical ethical committee of the Leiden University Medical Center (Po8.239/P19.013) and informed consent was obtained from subjects. Osteochondral explants were punched from the macroscopically preserved load bearing area of the femoral condyle of human OA knee joints and maintained in serum-free chondrogenic differentiation medium (DMEM, supplemented with Ascorbic acid (50 µg/ml; Sigma-Aldrich; Zwijndrecht, The Netherlands), L-Proline (40 µg/ml; Sigma-Aldrich), Sodium Pyruvate (100 µg/ml; Sigma-Aldrich), Dexamethasone (0.1 µM; Sigma-Aldrich), ITS+ and antibiotics (100 U/ml penicillin; 100 µg/ml streptomycin) in a 5% (v/v) CO<sub>2</sub> incubator at 37°C [3]. Medium was refreshed every three to four days. In total 83 osteochondral explants were obtained from 16 donors for this study and divided over the treatment groups: control (n=30), injurious mechanical stress (65%MS; n=25), injurious mechanical stress treated with IOP (65%MS+IOP; n=11) and injurious mechanical stress treated with IOP encapsulated in PLGA NPs (65%MS+NP(IOP); n=17). Donor characteristics are summarized in **Supplementary Table 1**.

Patients and public were involved in the design, reporting and dissemination of the research via the patient, participation osteoArthritis Leiden (PPA-Leiden). PPA-Leiden consists of scientists of our research team and osteoarthritis patients that meet every 3 months. During meetings there is mutual exchange of information, reporting on progress, new research applications and discussions on research priorities. Reach out to broader public is via Facebook and Twitter. Dissemination of PPA-Leiden meetings is established by summary reports of meetings. As members of the PPA-Leiden are actively involved in other patient organizations such as poly-osteoarthritis society and the Dutch Arthritis Foundation this additionally allowed us to reach out to a broader OA patient population

### 1.2 RNA isolation, Reverse Transcription and quantitative Real-Time PCR

Cartilage RNA was extracted by pulverizing the tissue using a Mixer mill 200 (Retch, Germany) and homogenizing in TRIzol reagent (Invitrogen, San Diego, CA). RNA was extracted with chloroform, precipitated with ethanol, and purified using the RNeasy Mini Kit (Qiagen, GmbH, Hilden, Germany). Genomic DNA was removed by DNase (Qiagen, GmbH, Hilden, Germany) digestion and quantity of the RNA was assessed using a Nanodrop spectrophotometer (Thermo Fischer Scientific Inc., Wilmington, USA). Synthesis of cDNA was performed using 200 ng of total mRNA with the First Strand cDNA Synthesis Kit (Roche Applied Science, Almere, The Netherlands) according to the manufacturer's protocol. Subsequently, pre-amplification was performed and gene expression was determined with the Roche Lightcycler 480 II (Roche Applied Science) using Fast Start Sybr Green Master mix (Roche Applied Science). To measure changes in chondrocyte signalling upon perturbations, we measured gene expression levels by RT-qPCR. Primer sequences used are listed in **Supplementary Table 2**. Fold changes (FC) were determined using the  $2^{-\Delta\Delta CT}$  method, in which cyclic threshold (CT) levels were adjusted

for the housekeeping gene *SDHA* ( $-\Delta\text{ACT}$ ) and subsequently for control samples ( $-\Delta\Delta\text{ACT}$ ). A  $\text{FC} > 1$  represents an upregulation, while  $\text{FC} < 1$  depicts a downregulation. This endogenous reference genes were chosen based on literature stating the stability of this gene in response to mechanical stress [4,5].

### **1.3 RNA-sequencing**

#### **1.3.1 Quality control of sequencing data**

Paired-end 2x150 base pair RNA sequencing (Illumina TruSeq mRNA Library Prep Kit, Illumina HiSeq X ten) was performed. Strand specific RNA-sequencing libraries were generated which yielded on average 14 million reads per sample. Data from the Illumina platform was analysed with an in-house pipeline as previously described [6]. The adapters were clipped using Cutadapt v1.1. RNA-seq reads were then aligned using GSNAP against GRCh38 [7]. Read abundances per sample were estimated using HTSeq count v0.11.1 [8] with Ensembl gene annotation version 94. Only uniquely mapping reads were used for estimating expression. The quality of the raw reads and initial processing for RNA-sequencing was checked using MultiQC v1.7 [9]. Samples containing  $> 50\%$  genes with zero values and average read count  $< 10$  were removed from further analysis. To identify outliers, principal component analysis (PCA) was applied and identified two clusters which were independent of treatment and hence analysis was performed with corrections for principal component 1.

#### **1.3.2. Differential expression analysis and protein-protein interactions**

Differential expression analysis was performed in 65%MS+IOP cartilage compared to 65%MS cartilage obtained from osteochondral explants using DESeq2 R package version 1.24 [10] on 14,668 protein-coding genes. A general linear model assuming a negative binomial distribution was applied and followed by a Wald-test between 65%MS+IOP and 65%MS samples with correction for principal component 1. In all analyses, 65%MS samples were set as reference. To correct for multiple testing the Benjamini-Hochberg method was used, as indicated by the false discovery rate (FDR) in which a significant cut-off value of 0.05 was used. For protein-protein interactions, analysis was performed using the online tool STRING version 11.0 [11].

#### **1.3.3 RNA-sequencing validation by Real-time quantitative PCR (RT-qPCR)**

For validation and replication a total of 8 paired samples were selected. 200 ng of RNA was processed into cDNA using the First Strand cDNA Synthesis Kit (Roche Applied Science, Almere, The Netherlands). Real-Time qPCR was performed and normalized as described above to determine gene expression of *INSIG1*, *DHCR7*, *FADS1*, *CTGF*, *BMP5* and *FOXM1*. Primer sequences are listed in **Supplementary Table 2**.

## **1.4 Determining cartilage integrity**

### **1.4.1 Sulphated glycosaminoglycan (sGAGs) measurement**

Sulphated glycosaminoglycans (sGAGs) concentration was measured in conditioned media of explants on day 13 following extraction with the photometric 1,9 dimethylene blue (DMMB; Sigma-Aldrich) dye method [12]. Shark chondroitin sulfate (Sigma-Aldrich) was used as the reference standard. To measure concentrations, 100µl of medium or digested cartilage was mixed with 200µl of DMMB solution and the absorbance at 525nm and 595nm was measured in a microplate reader (Synergy HT; BioTek, Winooski, USA).

### **1.4.2 Histology**

Osteochondral explants were fixed in 4% formaldehyde for one week and decalcified using EDTA (12,5%, pH=7.4) for two weeks at 4°C. Subsequently, samples were dehydrated with an automated tissue processing apparatus and embedded in paraffin. Tissue sections of 5 µm were stained with Hematoxylin and Eosin (H&E) or toluidine blue (Sigma-Aldrich) and mounted with Pertex (Sigma-Aldrich). Quantification of OA related cartilage damage was scored according to Mankin *et al* [13].

## **1.5 Preparation and characterization of nanoparticles (NPs)**

### **1.5.1 Preparation of PLGA-PEG NPs**

PLGA NPs with entrapped iopanoic acid (IOP) and near-infrared fluorescent labels was prepared using an o/w emulsion and solvent evaporation-extraction method [14]. In brief, 100 mg of PLGA in 3 mL of DCM containing IOP (2mg; Sigma Aldrich) and Indocyanine green (1mg; ICG) was added dropwise to 25 mL of aqueous 2% (w/v) PVA in distilled water and emulsified for 90 seconds using a sonicator (Branson, sonofier 250). A lipid mPEG 2000 PE (20 mg) was dissolved in DCM and added to the vial. The DCM was removed by a stream of nitrogen gas. Subsequently, the emulsion was rapidly added to the vial containing the lipids and the solution was homogenized during 30 seconds using a sonicator. Following overnight evaporation of the solvent at 4°C, the PLGA NPs were collected by centrifugation at 10,000 g for 10 min, washed three times with distilled water and lyophilized.

### **1.5.2 Encapsulation Efficiency Analysis**

In order to determine the encapsulating efficiency (EE) and the loading content of the IOP and near infrared dye (ICG), the lyophilized NPs were dissolved in 0.8 M NaOH. Separately, 5 mg of PLGA NPs were dissolved in in 0.5 mL 0.8 M NaOH overnight at 37°C. Afterwards, the basic solutions of all the NPs were centrifuge at 13.8 g, at RT for 20 min and the supernatants were collected. The IOP content was determined by RP-HPLC and the ICG dye content was then measured using Odyssey Infrared Imager 9120 (LI-COR) scanner with a 800nm scan. NIR dye encapsulation efficiency was calculated following a previously described [15] formula as following:

$$EE = \frac{\text{Amount of drug in formulation}}{\text{Amount of drug used for formulation}} \times 100$$

*Amount of drug in formulation* is the amount of IOP and ICG loaded in the PLGA NPs. The values were obtained as previously described. *Amount of drug used for formulation* is the amount of IOP and NIR added in the preparation of NPs.

### 1.5.3 Particles size and charge surface

The average size and polydispersity index (PDI) of the PLGA NPs were determined by Dynamic Light Scattering (DLS) (Zetasizer Nano S90, Malvern Instruments, Worcestershire, UK). PLGA NPs were dissolved in MilliQ water and the measurement was performed at 25 °C at an angle of 90°. The values presented are averages and standard deviations of triplicate measurements. The stability and the aggregation in a dispersion NPs was determined by Zeta potential (Zetasizer Nano S90, Malvern Instruments, Worcestershire, UK) (**Table 1**).

**Table 1 | Characterization of PLGA nanoparticles used in this study.**

Nanoparticles	Particles size (nm±stdev)	Polydispersity	Zeta potential (mV)	EE% (ICG)	EE% (IOP)
1-PLGA-NP-(ICG)-PEG	256 ± 0.85	0.176 ± 0.08	-12.2	8.8	29.6
2-PLGA-NP-(IOP)-PEG	265 ± 0.67	0.185 ± 0.06	-14.6	9.4	31.0

PLGA NPs size, polydispersity, zeta potential, fluorescent dye and drug encapsulation efficiency (EE) of PLGA NPs

### 1.5.4. Release of IOP from NPs

Release of IOP from NPs was measured by maintaining 150µl of 5mg/ml NP at 21°C or 37°C under slight shaking. On each time point, NPs were centrifuged (12.000 rpm) for 10 minutes and PBS was carefully taken for subsequent IOP concentrations measurement using a Nanodrop spectrophotometer (Thermo Fischer Scientific Inc., Wilmington, USA) at 310nm (**Supplementary Figure S1C**).

## 1.6 In vitro experiments.

### 1.6.1 Cell culture.

Human primary chondrocytes were cultured in DMEM (High glucose) supplemented with 10% fetal calf serum (FBS; Gibco, Bleiswijk, The Netherlands), 0.5 ng/ml FGF-2 (PreproTech, Heerhugowaard, The Netherlands) and antibiotics (100U/ml penicillin; 100µg/ml streptomycin; Gibco) in a 5% (v/v) CO<sub>2</sub> incubator at 37°C.

### 1.6.2 NP uptake study.

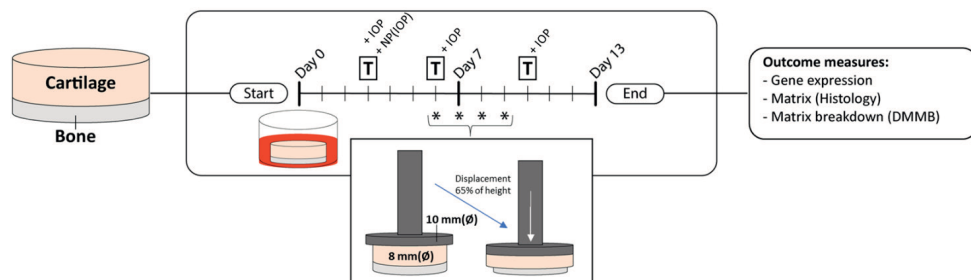
Subsequently, cells were seeded in a 96-well cell culture microplate (Greiner Bio-One B.V. Alphen aan den Rijn, The Netherlands) (1x10<sup>6</sup> cells/well) and incubated with 1.6 µl of 5mg/ml Indocyanine green (ICG) loaded PLGA-PEG NPs for 1h, 4h and 24h. In short, after incubation, cells were washed twice with PBS, fixed for 15 minutes with 1% paraformaldehyde, washed

with PBS and subsequently, stained with TO-PRO<sup>®</sup>-3 iodide dye (ThermoFisher, Marietta, OH, USA) to stain cell nucleus at 700 nm. Uptake of NPs by cells was measured using an Odyssey Infrared Imager 9120 (LI-COR, Lincoln, NE, USA) scanner at 800 nm and 700 nm intensity to visualize the NPs and cells, respectively (**Supplementary Figure S2A**). This experiment was performed in triplicate (n=3).

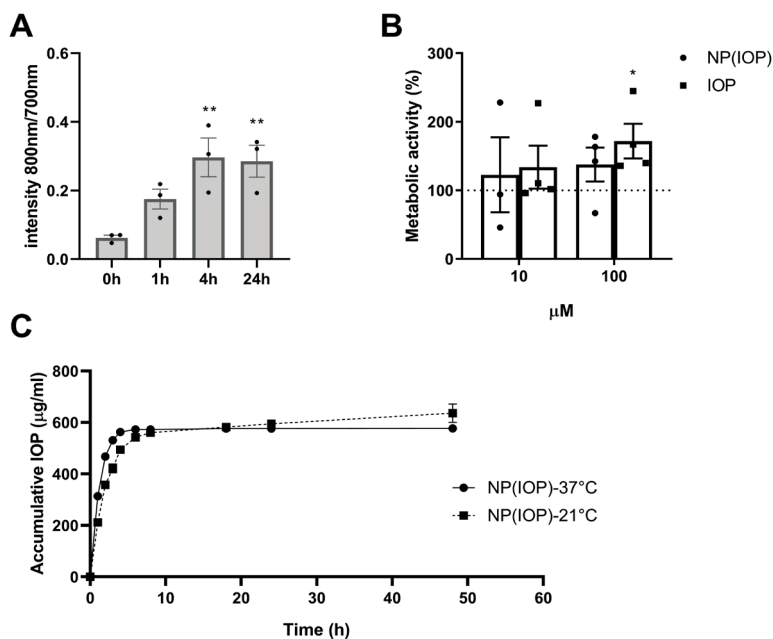
### **1.6.3 Cell viability assay.**

Effects of 8 and 80 µg/ml NP(IOP) and 10µM and 100µM IOP on cell metabolism was investigated using a chondrosarcoma cell line CH2879 (**Supplementary Figure S2B**) [16,17]. CH2879 cells were cultured in RPMI 1640 (HEPES, L-glutamine, Gibco) supplemented with 10% fetal calf serum (FBS; Gibco) and antibiotics (100U/ml penicillin; 100µg/ml streptomycin; Gibco). Cells were seeded (16,000 cells/well) in a 96 well cell culture microplate (Greiner Bio-One B.V. Alphen aan den Rijn, The Netherlands). 24hrs after seeding cells, respective treatments were added. Subsequently, 24hrs after treatment, Alamar Blue (Invitrogen) was added to the wells at a final concentration of 10% and incubated for 4hr in a 5% (v/v) CO<sub>2</sub> incubator at 37°C. Fluorescence was measured using an excitation of 544nm and emission of 590nm with a spectrometer (PerkinElmer). This experiment was performed in quadruplicate (n=4).

## Supplementary Figures



**Supplementary Figure S1 | Schematic representation of study setup.** Osteochondral explants were punched from the still macroscopically preserved looking knee condyle area and taken into culture. Explants were treated with IOP (100 $\mu$ M) or PLGA NP-IOP from day 3 onwards. Asterix depicts days explants received mechanical stresses at a strain of 65% for 10 min per day. Media was collected on the with T indicated days and subsequently each explant received fresh media. Finally, on day 13, a sagittal section was fixed in 4% formaldehyde for histology, while for the remaining explant cartilage and bone was separated, snap frozen and stored at -80C for downstream analyses. Legend: NP=Nanoparticles, IOP=iopanoic acid, DMMB=Dimethylmethylene Blue Assay.



**Supplementary Figure S2 | Characterization of PLGA-PEG nanoparticles.** [A] *In vitro* cellular uptake of PLGA-PEG nanoparticles of primary chondrocytes characterized by Odyssey. Bars represent the mean  $\pm$  s.e.m and n=3. [B] Metabolic activity upon 24h treatment with 10 $\mu$ M or 100 $\mu$ M of IOP in nanoparticles and free IOP was measured using Alamar Blue assays in CH2874 cell lines. Viability of untreated controls is depicted by the dashed line and was set to represent 100% cell viability. Bars represent the mean  $\pm$  s.e.m. [C] Release of IOP from nanoparticles over time measured at 21°C and 37°C. Asterisks represent significant differences as measured by one way ANOVA. \*p<0.05; \*\*p<0.01. n=3 or n=4. Legend: IOP=iopanoic acid; NP=nanoparticles

## REFERENCES

1. Ochsner SA, McKenna NJ. No Dataset Left Behind: Mechanistic Insights into Thyroid Receptor Signaling Through Transcriptomic Consensus Meta-Analysis. *Thyroid*. 2020;30(4):621-39.
2. Ramos YF, den Hollander W, Bovee JV, et al. Genes involved in the osteoarthritis process identified through genome wide expression analysis in articular cartilage; the RAAK study. *PLoS One*. 2014;9(7):e103056.
3. Houtman E, van Hoolwerff M, Lakenberg N, et al. Human Osteochondral Explants: Reliable Biomimetic Models to Investigate Disease Mechanisms and Develop Personalized Treatments for Osteoarthritis. *Rheumatol Ther*. 2021;8(1):499-515.
4. Al-Sabah A, Stadnik P, Gilbert SJ, et al. Importance of reference gene selection for articular cartilage mechanobiology studies. *Osteoarthritis Cartilage*. 2016;24(4):719-30.
5. McCulloch RS, Ashwell MS, O'Nan AT, et al. Identification of stable normalization genes for quantitative real-time PCR in porcine articular cartilage. *J Anim Sci Biotechnol*. 2012;3(1):36.
6. Coutinho de Almeida R, Ramos YFM, Mahfouz A, et al. RNA sequencing data integration reveals an miRNA interactome of osteoarthritis cartilage. *Ann Rheum Dis*. 2019;78(2):270-7.
7. Wu TD, Watanabe CK. GMAP: a genomic mapping and alignment program for mRNA and EST sequences. *Bioinformatics*. 2005;21(9):1859-75.
8. Anders S, Pyl PT, Huber W. HTSeq—a Python framework to work with high-throughput sequencing data. *Bioinformatics*. 2015;31(2):166-9.
9. Ewels P, Magnusson M, Lundin S, et al. MultiQC: summarize analysis results for multiple tools and samples in a single report. *Bioinformatics*. 2016;32(19):3047-8.
10. Love MI, Huber W, Anders S. Moderated estimation of fold change and dispersion for RNA-seq data with DESeq2. *Genome Biol*. 2014;15(12):550.
11. Szklarczyk D, Gable AL, Lyon D, et al. STRING v11: protein-protein association networks with increased coverage, supporting functional discovery in genome-wide experimental datasets. *Nucleic Acids Res*. 2019;47(D1):D607-D13.
12. Farndale RW, Buttle DJ, Barrett AJ. Improved quantitation and discrimination of sulphated glycosaminoglycans by use of dimethylmethylene blue. *Biochim Biophys Acta*. 1986;883(2):173-7.
13. Mankin HJ, Dorfman H, Lippiello L, et al. Biochemical and metabolic abnormalities in articular cartilage from osteo-arthritic human hips. II. Correlation of morphology with biochemical and metabolic data. *J Bone Joint Surg Am*. 1971;53(3):523-37.
14. Cruz LJ, Tacke PJ, Fokkink R, et al. Targeted PLGA nano- but not microparticles specifically deliver antigen to human dendritic cells via DC-SIGN in vitro. *J Control Release*. 2010;144(2):118-26.
15. Rosalia RA, Cruz LJ, van Duikeren S, et al. CD40-targeted dendritic cell delivery of PLGA-nanoparticle vaccines induce potent anti-tumor responses. *Biomaterials*. 2015;40:88-97.
16. Gil-Benso R, Lopez-Gines C, Lopez-Guerrero JA, et al. Establishment and characterization of a continuous human chondrosarcoma cell line, ch-2879: comparative histologic and genetic studies with its tumor of origin. *Lab Invest*. 2003;83(6):877-87.
17. van Oosterwijk JG, Herpers B, Meijer D, et al. Restoration of chemosensitivity for doxorubicin and cisplatin in chondrosarcoma in vitro: BCL-2 family members cause chemoresistance. *Ann Oncol*. 2012;23(6):1617-26.





# Chapter 6

**General discussion and  
future perspectives**

Translating biomedical research from *in vitro* and *in vivo* animal models to clinical applications has critical challenges and shortcomings that need to be addressed in order to advance drug development for osteoarthritis patients. Thus far, pre-clinical models are typically limited to either relatively young animals subjected to hyper-physiological stimuli or to 2D and 3D *in vitro* cell culture models of neo-cartilage from (aged) human primary chondrocytes or stem cells. Nonetheless, these human models do not reliably represent the osteochondral compartment nor do they capture aspects of human aging of articular joint matrix which is prone to initiate OA upon disease relevant triggers. In addition, the use of animals for pre-clinical models is less desirable as they do not support the societal 3R-principle of replacement, reduction and refinement of animal research. Henceforth advancement of clinical development in the OA field requires models reliably mimicking aged human tissue that ideally would allow for transcriptional and biochemical output in response to relevant perturbations initiating OA related tissue damage.

This thesis aimed to bridge the gap between biomedical data and clinical translation by developing reliable biomimetic *ex vivo* human osteochondral explant models. These models focussed on the impact of OA relevant triggers in humans and as such allowed for in depth studies of human OA pathophysiology in interaction with genetic factors. For that matter, in **chapter 2** our human aged OA joint tissue model was set up with taking into account different pathophysiological modalities triggering OA related damage being inflammation, hypertrophy of cartilage and injurious mechanical stress. The model was exploited to obtain insight into underlying disease mechanisms in response to injurious mechanical stress in **chapter 3**, whereas in **chapter 4** we explored it in interaction with the strong OA risk gene *MGP*. Finally, in **chapter 5**, a proof of concept pre-clinical study was performed on the chondroprotective effect of iopanoic acid, a pharmacological agent that acts via downregulating thyroid signaling, on mechanically induced OA related cartilage damage.

### ***Development of a reliable human biomimetic joint tissue OA model***

In **chapter 2**, a reliable human biomimetic tissue model was set up that captured age-related human articular joint changes prone to initiate OA upon disease relevant triggers. Our established model has several advantages relative to other models. First, to circumvent the need for species translation, we chose to use human tissues in our model. Second, it is extremely difficult to recreate native articular cartilage due to its complexity and presence of multiple dedicated layers. Therefore, to mimic cartilage to the best of our abilities we took macroscopically normal plugs of *ex vivo* tissue from human knee condyles of OA patients undergoing joint replacement surgery. Notable, within these samples several degrees OA changes are present. Third, our model takes ageing into account, given the age related changes that occur in articular cartilage and chondrocytes [1-6]. Finally, an important aspect which makes our model more representative of the human (OA) joint is that we retained the bone-cartilage interface. The rationale for this is that in recent years the perspective from OA as a cartilage disease has shifted towards a multi-tissue disease. This is reflected by the identification of many risk genes (e.g. *TNC*, *MGP*, *IL11*) in OA that have a function in both bone and cartilage [7]. However, limitation of using aged human osteochondral explants are scalability and dependency on surgery. The latter became more obvious during the COVID19 pandemic when the number of joint replacement surgeries decreased and even came to a hold. With respect to scalability, it should be noted that the number of explants that can be

taken from a joint is dependent on size of joint and degree of OA damage. Moreover, donor differences with respect to age-related changes or extent of OA pathophysiology in the preserved cartilage brings about heterogeneity, that need to be taken into account during analysis. On the other hand, such diversity contributes to a more realistic situation, since the OA patient population is very heterogenous as well, and will not comply to an “one medicine fits all patients” approach. To accommodate higher throughput, an option could be to confirm findings of *ex vivo* models in *in vitro* chondrogenesis models of primary cells such as human chondrocytes. Although, in such a model interaction with the bone compartment is often missing. Even though our aged human biomimetic model closely resembles the human joint, other joint tissues can be added to further complete this model. For that matter, the synovial component could be added by inflammatory stimulation or addition of synovial fluid, synovium explants and/or exosomes from synovial cells. To accommodate throughput as well as multiple tissue interaction, a joint-on-a-chip can be a good alternative model, in which genetic manipulation and co-culture of cartilage and bone is possible. Herein, both cartilage and bone can be cultured separated by a semi-permeable membrane, facilitating crosstalk and allowing for straightforward manipulation. Another advantage of this model is that infinite cell types such as induced pluripotent stem cells (iPSCs) can be used, increasing scalability and reducing heterogeneity of this model. Moreover, such *in vitro* cell models are compatible with genetic engineering technologies such as CRISPR/Cas that allows introduction of additional genetic factors contributing to OA susceptibility.

### ***Relevant triggers for OA like damage in the ex vivo explant model***

#### ***Inflammation***

Inflammation is considered an important trigger to OA related damage and widely applied. Therefore, in **chapter 2** we used the pro-inflammatory IL-1 $\beta$  to induce detrimental catabolic and inflammatory response in human aged articular cartilage. Our observations were in line with many other studies that previously investigated detrimental effects of a similar or higher IL-1 $\beta$  or other inflammatory cytokine stimulation. These studies showed that above a concentration of 10ng/ml, IL-1 $\beta$  consistently increased cartilage degradation, inflammation and MMP13 levels in explants of different species, but lower levels (0.5ng/ml) could not consistently induce cartilage degradation [8-11]. Nonetheless, there are several limitations of this OA model. First, the levels necessary to induce this response are not physiological, in human synovial fluids only very low levels (<1pM) of IL-1 have been measured in some OA patients [12]. Second, this inflammatory response is not typically observed in OA and the inflammatory response is not found as a key pathway in large transcriptomic and genomic studies [13-15]. Evidence from pre-clinical animal studies have determined a conflicting role of IL-1 in OA, with both protection and detrimental effects observed in different species [16-19]. Recently, several large human clinical studies targeting IL-1 have failed to reach the primary endpoint in hand and knee OA, further reducing the fields enthusiasm for IL-1 as target to combat OA [20-23]. Therefore, we advocate that IL-1 and other pro-inflammatory cytokines are not the most promising targets for treatment of OA and focus should shift to other approaches that are preferably based on key pathways involved in OA pathophysiology.

## ***Hypertrophy***

Next we investigated the effect on the induction of hypertrophy by perturbation with the active thyroid hormone, triiodothyronine (T<sub>3</sub>). In this aged human osteochondral explant model we observed mainly upregulation of hypertrophic and mineralization markers such as *COL10A1*, *MMP13*, *COL1A1* and *ALPL*, similarly to upregulation of these markers in the process of OA [24-28]. In addition, two critical and detrimental transcription factors, *RUNX2* and *EPAS1*, were slightly upregulated after perturbation with T<sub>3</sub>, indicating that they are possibly downstream of T<sub>3</sub>. We also measured upregulation of *COL2A1* expression after T<sub>3</sub> treatment, possibly as a response to initiate cartilage repair or remodeling. Similar studies into the effects of T<sub>4</sub> and/or T<sub>3</sub> have measured increased collagen production in the absence of hypertrophic markers [29,30]. Conversely, other studies did observe that T<sub>3</sub> induced terminal differentiation by initiating hypertrophic morphology in chondrocytes and expression of molecular hypertrophy markers without proliferation [31-33]. Chen-An et al [34] determined effects of treatment with T<sub>3</sub> in (relative young) bovine articular cartilage explants and observed increased expression of hypertrophic markers, such as *ALPL* and *IHH* and increased size of lacunas indicating hypertrophy without affecting cell viability. These difference between the above mentioned studies and what our study found could be due to differences in cell type, model, species or T<sub>3</sub> concentrations used. These diverse results are not unexpected as the effects of T<sub>3</sub> are known to be time and tissue specific partially due to expression of the different deiodinases (D1, D2 and D3) that control intracellular concentrations [35]. Taken together, our results indicated that treatment of aged human osteochondral explants with T<sub>3</sub> induced hypertrophy and that this is not necessarily detrimental to cartilage matrix in our timeframe as cartilage matrix integrity was not affected. Nonetheless, this model can be used to investigate the potential of hypertrophy inhibitors in the treatment of OA.

## ***Mechanical loading***

Overloading conditions in a joint are considered a major trigger in the initiation of OA. Nonetheless, little knowledge exists on the chondrocyte signaling response in aged human cartilage triggering OA onset. Therefore in **chapter 2** we demonstrated that mechanical stress at a strain of 65% of cartilage height induced detrimental changes that affected cartilage integrity of aged human osteochondral explants whereas in **chapter 3** we performed genome-wide differentially expressed mRNAs in articular cartilage following repeated exposure to 65% mechanical stress using our human *ex vivo* osteochondral explant model. Our results gave insights into how injurious mechanical strain on the short term affects signalling in aged human articular chondrocytes that could enlighten how these cells lose their matured state and converse towards the OA disease state. Our data indicated that the short term response to injurious mechanical stress of aged human cartilage involves pathways such as IGF I and II binding, cellular senescence and focal adhesion. In addition, amongst the highly upregulated genes we identified *MMP13* and *IGFBP5* as early markers of injurious stress. Strikingly, both genes are not found to be responsive in OA pathophysiology, i.e. differentially expressed between preserved and lesioned OA cartilage [13], and might therefore reflect the initial unbeneficial response to injurious loading rather than the ongoing OA disease process. Though other collagenases exist and are involved in cartilage degradation, *MMP13* has been observed to have the highest affinity for cleaving collagen II and to a lesser extent other collagens, aggrecan, osteonectin and perlecan [36,37]. In addition, knockout of *MMP13* in

mice reduced cartilage damage [38]. Conversely, cartilage specific overexpression of *MMP13* induced OA-related joint pathologies and increased collagen II breakdown [39]. Knockout of other MMPs, such as *MMP3*, actually increased cartilage degradation and catabolic enzyme production instead of protecting the joints [18]. This suggests that *MMP3* might play a more essential role in healthy cartilage remodeling while *MMP13* is more involved in the (early) pathophysiological OA processes and therefore a good marker of detrimental underlying processes.

Next to providing knowledge to facilitate clinical development of counteracting unbeneficial chondrocyte signalling upon injurious stress, we advocate that a set of the here identified response key genes, such as *MMP13*, *IGFBP4/5* and *TNC*, can be used to distinguish between beneficial and unbeneficial mechanical stress in different age categories. Such experiments could entail submitting explants from different age categories to different strains and velocity of loading, while subsequently measuring upon which type of loading these unbeneficial markers start responding. Given the known age related changes occurring in cartilage [1,40,41] and the fact that immobilisation is unbeneficial for joint health [42], increasing our understanding of which personal circumstances, for example weight, movement speed or age, exercise is preventive or even curative can develop scientifically founded OA therapies in elderly. This need for more knowledge on physical activity and exercise therapy was recently reviewed by Nissen et al [43]. Many clinicians have limited knowledge into exercise and movement as a therapy and they recommend a multitude of exercises based on their “experience of feeling knees”, basically based on the presence of effusion and synovitis [43]. In addition, biomarkers could be used in human *in vivo* studies to determine if injurious stress has occurred and thus the long term and almost irreversible degradation of cartilage could be prevented by for example changing to a lighter exercise regime. The most direct biomarkers are those excreted by chondrocytes or other joint tissues into the synovial space. However, insufficient accessibility and invasiveness limits utility for (early) diagnostic biomarker development based on synovial fluid. Blood plasma, serum and urine overcome this obstacle and hold great potential as a biomarker to reflect joint tissue status.

### ***Insight into pathophysiological aspects of the OA risk gene MGP***

A reliable human biomimetic model capturing age-related OA development in human articular joints is useful in gathering knowledge on disease mechanisms as well as interactions with OA risk genes. In **chapter 4** we exploited a RNA sequencing dataset of preserved and lesioned articular cartilage and subchondral bone, or 3D *in vitro* cartilage model of primary human chondrocytes as well as our ex vivo explant model with mechanical loading as trigger to induce OA related damage. As such we gather data to strengthen causality of risk SNPs and their effector gene and clarify the direction of effects. For this purpose, *MGP* expression as function of the OA risk allele rs1800801-T was measured. We determined that carriers of the risk allele had inherent lower expression of *MGP* in articular cartilage and subchondral bone and that its expression is upregulated during OA pathophysiology, specifically in carriers of the rs1800801-T risk allele. Our results suggest that to counteract the low inherent *MGP* levels in OA tissues, chondrocytes increase *MGP* expression, but this is still not enough to reach the same level as those measured in reference allele carriers. In addition, by measuring *MGP* expression as function of rs1800801 in our biomimetic model, we determined that risk allele carriers do not have a dynamic response. This paints a complex picture of action and

response of *MGP* expression that is different in carriers of the OA risk allele rs1800801-T when compared to reference allele carriers, suggesting that besides lifelong lower expression of *MGP* also its inability to change expression in response to a trigger are likely responsible for increased OA risk (**Figure 1**).

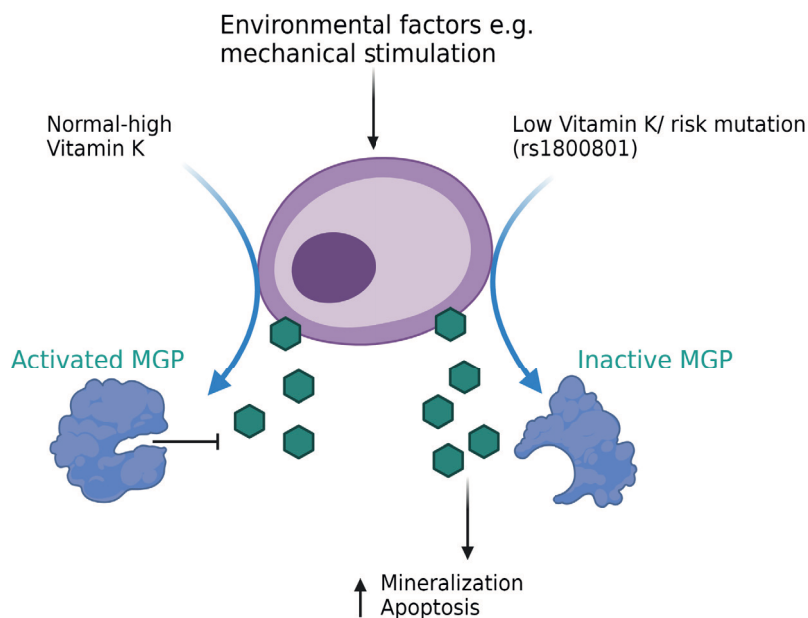


**Figure 1 | Suggested mechanism of low vitamin K or risk mutations on decreased activated MGP levels.** In response to an external trigger, upon sufficient vitamin K levels, MGP excreted by cells can be carboxylated into its active form and inhibit mineralization. When there are low vitamin K levels or reduced MGP expression, there are insufficient activated MGP levels to completely inhibit mineralization, eventually resulting in apoptosis of cells, induced by an external trigger.

Upon confirming *MGP*, encoding an inhibitor of ectopic calcifications, as strong OA risk gene, it was hypothesized that the OA risk was conferred via calcification of cartilage tissue [10, 11]. Moreover, as *MGP* protein is activated by vitamin K dependent  $\gamma$ -carboxylation (c-MGP) our findings underscored the relevance of previous found associations between OA and low vitamin K status for OA prevention and treatment [44,45]. We demonstrated that exposure of human osteochondral explants to the vitamin K inhibitor warfarin, provoked unbeneficial chondrocyte signaling towards hypertrophy, reduced bone formation and altered bone remodeling together likely resulting in bone loss [46,47]. Future studies should further explore the influence of rs1800801 genotype on the response of cells to warfarin. Two recent studies, one from the Rotterdam study [48] and one case-control study from the UK [49], showed a strong association between vitamin K dependent blood anticoagulant use and incidence and progression of knee and hip OA. In light of our combined result, we advocate that non-vitamin K antagonist should be preferred as anticoagulants to reduce the risk of evoking OA [50], especially in carriers of the rs1800801-T *MGP* risk allele. In addition, to overcome reduced active MGP levels, supplementation with vitamin K could be a potential novel OA-modifying treatment option in an appropriate subset of patients. Until now, only one clinical trial on vitamin K supplementation was performed. Although the study contained a relatively small

number of patients with low vitamin K levels at baseline, beneficial effects on OA progression in individuals were observed in these individuals [51]. Another reasons to consider vitamin K supplementation as OA treatment, is the correlation between low dietary vitamin K and increased progression of knee OA [52] and the increased uncarboxylated MGP and GRP proteins levels in OA cartilage [53,54]. Altogether and given the evidence from genetic risk genes and clinical patient data, there is a strong rationale to undertake further clinical trials to address treatment of vitamin K supplementation in a subgroup of OA patients with low vitamin K levels and/or carriers of the rs1800801-T OA risk allele.

### ***Opportunities to address effects of OA risk genes with the ex vivo osteochondral model***

To explore the direction of effect of high potential risk SNPs such as rs34195470 (*WWP2*), or rs4252548 (*IL11*) in OA, a similar strategy as performed in **chapter 4** could be undertaken. Expression of its effector gene as function of its OA risk allele in articular cartilage, subchondral bone and our human biomimetic models can help determine their therapeutic potential. Exploration of risk SNP's like rs34195470 (associated with effector gene *WWP2* involved in skeletal development) can be performed. Styrkarsdottir et al. [55] reported on reduced *WWP2* expression in carriers of the risk allele of a proxy SNP rs4985453 ( $R^2=0.79$ ) in adipose tissue. Conversely in GTEX[56], rs34195470-G was associated to increased *WWP2* expression in arteries while another proxy SNP (rs1052429 ( $R^2=0.77$ )) increased *WWP2* expression in four different tissues. This underscores that further research is necessary, preferably in OA relevant tissues, to investigate expression levels of OA risk genes and alleles prior to determining direction of effects.

Another example of an interesting gene which can be further validated in our biomimetic model is *IL11*. Multiple independent GWAS studies have found the risk allele rs4252548-T [15,55,57] in *IL11* and it was one of the highest upregulated genes in both articular cartilage [13] and subchondral bone [7] with OA pathophysiology. The IL-11 protein has a well-established role in osteoclast development and bone turnover and mice lacking this protein had impaired bone formation [58]. One study showed that rs4252548-T reduced IL-11 stability, however changes implied by this low frequency SNP on gene expression level have not been identified [59]. Since a large response is observed in both cartilage and subchondral bone and it is likely a genetic risk factor for OA, modulating IL-11 levels is a promising therapeutical target in OA. More investigation on the effects of decreased and increased IL11 levels could be performed in our relevant human aged biomimetic model to unravel its role in OA and the implications of rs4252548 in both tissues.

### ***Proof of concept pre-clinical study to explore effects of IOP as chondroprotective agent against mechanical induced OA related damage***

#### ***IOP, a chondroprotective pharmacological agent***

In **chapter 5**, a drug based clinical target in an OA relevant model was investigated to determine if this could be an effective treatment strategy. For the OA risk gene *DIO2* [60], encoding for the type II iodothyronine deiodinase D2 enzyme, previous *in vitro* and *in vivo* research

demonstrated causality in OA and beneficial effects were observed in the absence of *Dio2* or with *DIO2* inhibition using iopanoic acid (IOP) [61,62]. However, evidence of efficacy of IOP in a relevant human aged model subjected to a relevant trigger was essential to complement the line of evidence. The *ex vivo* aged human osteochondral explant model was chosen for this purpose because they retain aged chondrocytes in their native extracellular matrix, they are derived from human tissue, and they can be subjected to OA relevant perturbations such as mechanical stress. Our results show that the deiodinase inhibitor IOP reduced mechanical induced detrimental chondrocyte signaling, likely by reducing metabolic activity of cells, thereby confirming potential for treatment with IOP. However to advance IOP towards clinical trials, appropriate *in vivo* mice studies are deemed necessary as evidence. If the research field wants to increase complying to the 3Rs (replacement, reduction and refinement) of laboratory animals, an option could be to perform efficacy studies first in relevant *in vitro* human models prior to human clinical studies.

### ***The road from translation to clinical application***

The European Medicines Agency (EMA) states that a variety of toxicity and safety testing of a drug *in vivo* animal studies are required prior to the initiation of human clinical trials. Therefore, animal and human clinical trials are often performed concurrently, which gives the impression that many clinical trials are not based on efficacy animal study results and also suggests that animal studies do not give required information and are even often ignored [63-65]. For example, only recently a study reported that the anti-ADAMTS5 drug GLPG1972 reduced cartilage damage and bone sclerosis in mice and rat OA models [66], while recruitment for a clinical phase II trial on efficacy and safety already started in 2018 and finished in 2020 [67]. The additional rationale and benefits of this animal study are unclear and unfortunately several additional examples of studies simultaneously performed in animals and humans exist [63-65]. In addition, translational success rates from animal-to-human range from 0 to 100%, suggesting that success is partially unpredictable and these could not be explained by species, study size, field or year of publication [68]. However, as unfortunately a lot of animal studies are still not of sufficient quality, partially due to study design, and animal to human translation is unpredictable, pre-clinical animal studies are unable to completely predict safety and efficacy in humans. This erratic safety and efficacy translation is still the main reason why many phase I-III trials fail [69-71]. Another review compared methodology of trials in animal and human studies of methotrexate, a rheumatoid arthritis drug, and found large differences dependent on sex and how power calculations and statistics were performed [72]. This misalignment of designs is problematic as it decreases the animal to human translation and validity. Therefore, to improve translatable conclusions, more often relevant *in vitro* models should be taken into consideration for drug efficacy testing. In addition, with the increasing computational modeling power, more reliable predictions can be made with respect to expected toxicity of drugs *in vivo* [73]. Both *in vitro* and *in silico* models can further reduce the need for extensive *in vivo* animal studies.

The potential of OA therapies based on genetics underlying development of OA pathophysiology would be an important improvement in the treatment of OA. Many of the current clinical trials are hypothesis driven, however similar to candidate gene studies such hypothesis driven targets may not cover risk factors that have the highest impact on development or progression of OA. Two examples of recently failed clinical trials based on hypothesis driven targets are

the ADAMTS5-inhibitor GLPG1972 and the IL-1 targeting Anakinra and Lutikizumab [20-23]. In both cases, clinical trials were based mainly on hypothesis driven OA pathways, but the selected targets are not present as OA risk alleles in large GWAS studies. Neither could be substantiated that they have a large impact on OA pathophysiology, i.e. these genes are not among those highly differentially expressed between healthy, preserved and lesioned OA cartilage or subchondral bone [7,13]. In retrospect, AstraZeneca published a report that variables such as genetically supported data or a stronger evidence of the target in the disease etiology contribute to success rate of clinical trials and increase efficacy [69]. In addition, they concluded that targeting molecules with a genetic link to the disease increased successfulness of projects in Phase II to 70%. These findings are supported by other studies showing a doubling in clinical success rate when genetically supported drug targets are chosen [74,75].

### ***Opportunities for (pre-)clinical studies based on OA risk SNPs and their direction of effect***

Recently, a concise list of potential OA therapeutical drugs targeting established risk genes was published in Cell [15]. For a portion of these drugs experimental research in OA has been performed while others are investigated in other diseases. Some notable examples of genes on the list that have experimentally been investigated in relation to OA are: vitamin D receptor (*VDR*), insulin-like growth factor 1 receptor (*IGF1R*) and carbohydrate sulfotransferase 3 (*CHST3*). Supplement with vitamin D has given mixed results on OA symptoms and progression, but suggests a small benefit in individuals with insufficient vitamin D levels [76-80]. Another example is Mecasermin, an agonist of the OA risk gene *IGF1R*, reducing apoptosis and increasing matrix production of OA chondrocytes [81,82]. Finally, thalidomide, an agonist of *CHST3*, was effective in early OA development in a DMM mouse model likely via a *VEGF* dependent mechanism [83]. Interestingly, this list also mentions the widely used hyperthyroidism anti-thyroid agent carbimazole, to target thyroid peroxidase (*TPO*), as potential drug. Its active component, methimazole, is a competitive inhibitor of TPO, preventing iodination of thyroglobulin and thereby thyroid hormone (T4 and T3) production. Though its mode of action is different from the in **Chapter 5** used pharmacological anti-thyroid agent IOP, it supports the potential of anti-thyroid hormone drugs in the treatment of OA.

Information often omitted in describing OA risk SNPs and their effector genes is the expected direction of effect on the gene expression, while knowledge on this is important when identifying therapeutical targets. Boer et al [15] recently reported a list of genes identified in a large GWAS of over 800,000 subjects with different OA phenotypes. For some genes on this list the direction of effect has been determined previously by expression quantitative trait loci (eQTL) or allelic expression imbalance (AEI) analyses and is also available in a large eQTL database GTEx, though this database lacks joint tissues [56]. In **Table 1**, direction of effects based on previous research or online databases has been added to the list OA risk genes.

**Table 1 | Leading risk SNPs with their effector gene adapted from Boer et al [15].**

Lead OA SNP	EA	EAF	eQTL dir	eQTL	eQTL/AI	OA pathophysiology		Bone	Expected dir effect
			GTEx (dn/up)	(GTEx/OA tissue)	OA tissues	Cartilage			
						Gene	Protein	Gene	
rs3740129	A	0.46	<i>CHST3</i> (2/6)	<i>CHST3</i> (8/1)	AC(-)	<i>CHST3</i> (+)			<i>CHST3</i> (-)
rs12908498	C	0.54	<i>SMAD3</i> (1/1)	<i>SMAD3</i> (2/0)	AC(0), FP(0), SY(0)	<i>SMAD3</i> (-)			Unclear
rs143384	A	0.59	<i>GDF5</i> (10/1)	<i>GDF5</i> (11/2)	AC(-),SY(-)	<i>GDF5</i> (+)			<i>GDF5</i> (-)
rs67924081	A	0.74	<i>LTBP3</i> (0/8)	<i>LTBP3</i> (8/0)			<i>LTBP3</i> (+)		<i>LTBP3</i> (+)
rs7294636	A	0.37	<i>MGP</i> (5/0)	<i>MGP</i> (5/4)	AC(-),SB(-), FP(-),SY(-)	<i>MGP</i> (+)		<i>MGP</i> (+)	<i>MGP</i> (-)
rs1530586	T	0.8	<i>FGFR3</i> (16/0)	<i>FGFR3</i> (16/0)		<i>FGFR3</i> (-)			<i>FGFR3</i> (-)
rs17615906	T	0.84	<i>FBN2</i> (5/1)	<i>FBN2</i> (6/0)				<i>FBN2</i> (+)	<i>FBN2</i> (-)
rs62578126	T	0.37	<i>LMX1B</i> (5/0)	<i>LMX1B</i> (5/0)					<i>LMX1B</i> (-)
rs1149620	A	0.44	<i>TSKU</i> (9/0)	<i>TSKU</i> (9/0)		<i>TSKU</i> (-)			<i>TSKU</i> (-)
rs7967762	T	0.16	<i>COL2A1</i> (2/0)	<i>COL2A1</i> (2/1)	AC(-)	<i>COL2A1</i> (-)			<i>COL2A1</i> (-)
rs7967762	T	0.16	<i>PFKM</i> (0/5)	<i>PFKM</i> (5/0)			<i>PFKM</i> (-)		<i>PFKM</i> (+)

The column 'eQTL dir GTEx(up/dn)' describes in how many tissues and in which direction the lead OA SNP is associated with gene expression in GTEx. The column 'eQTL (GTEx/OA tissue)' describes the number of different tissues in GTEx and OA relevant tissues with eQTL findings for this SNP. The column 'eQTL/AI OA tissues' describes associations between SNP and eQTL and/or AI in OA relevant joint tissues. The column 'OA pathophysiology' describes if a changed gene or protein expression was found between preserved vs lesioned OA cartilage or bone. In columns 'eQTL OA tissues', 'cartilage', 'bone' and 'expected direction of effect': - represents the SNP associates with a downregulation of expression of corresponding gene, + represents the SNP associates with an upregulation of expression of corresponding gene, o represents that the SNP was associated with no change of expression of corresponding gene. Legend: Lead OA SNP, rs number of the lead variant; EA, effect allele; EAF, effect allele frequency; eQTL, expression quantitative trait loci; dir, direction; GTEx, The Genotype-Tissue Expression project; OA, osteoarthritis; AC, articular cartilage; SB, subchondral bone; FP, Fat pad; SY, synovium.

### Future perspectives in OA research

To further improve OA research the work performed in this thesis is to emphasize that there is a need for good biomimetic models of OA in the aged population. The latter should be a prerequisite for showing treatment modalities and can give a solid genetic basis for druggable targets. The use of pharmacological agents based on genetic risk genes or pathways in combination with testing of these drugs in appropriate relevant disease models will greatly benefit clinical drug development in OA. Another important factor to be taken into account in clinical trials of OA targets is patient selection. Due to the heterogeneity of the disease it is extremely unlikely that there will be a 'one drug fits all' treatment option.

In 2011, Freedman et al [84] proposed a good systematic strategy to follow up on risk loci, however there is more to it. For future purpose we propose to follow the path that could be

taken for a druggable target stemming from genetic risk alleles in **Figure 2**. A first early step when the causal risk SNP has been identified is to investigate if it affects expression of a nearby gene. This can be done *in silico* by looking up the risk SNP and/or its proxy SNPs in an online database, such as GTEx[56], or in published papers describing OA relevant tissues, such as articular cartilage [85]. If an effect of the SNP on gene expression is identified, additional *in silico* databases (UCSC Genome Browser, HaploReg, ENCODE, etc.) can be explored to identify if the risk SNP is in a regulatory region such as a promoter or enhancer. Another factor that increases rational of a risk SNP is if the associated gene is involved in OA pathophysiology, i.e. differentially expressed between healthy, preserved and/or lesioned OA relevant tissues. A final *in silico* step that strengthens causality is if the gene has been linked to a disorder or a musculoskeletal phenotype in humans or mice databases (OMIM, Mouse Genome Informatics (MGI), Knockout mouse project (KOMP), etc.).

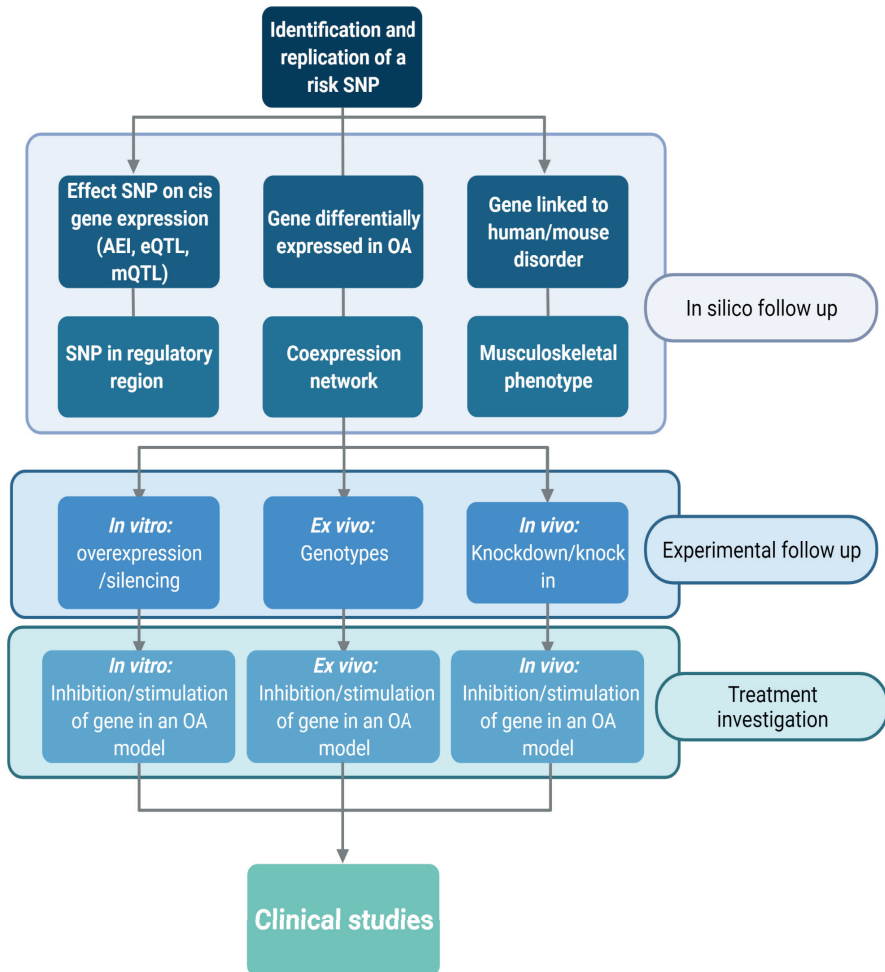


**Figure 2** | Proposed example of an investigation scheme to go from identification of a risk SNP to treatment.

When involvement of a gene is shown *in silico*, follow up experiments can consist of either *in vitro* silencing/overexpression in human aged relevant cells, stratified *ex vivo* human tissues based on genotypes or *in vivo* knockdown/knock-in in animals. This can increase causality of the risk SNP and/or gene and gives a rationale to start investigating it as a possible treatment. To investigate toxicity and efficacy of treatments, inhibition or stimulation of a gene or its pathway in *in vivo* OA animal models can be performed. In addition, to improve translation to human, efficacy of this treatment should also be proven in a relevant human aged *in vitro* and/or *ex vivo* OA model. Hopefully by using such a strategy, the OA field can reduce the number of animal studies and failing clinical trials that are based on ineffective targets.

The aged human biomimetic model described in this thesis mimics the human joint quite well, however addition of other joint components, such as the synovium, could further add to its completion. In addition, other *in vitro* models such as the joint-on-a-chip are taking off in the OA field. These models can simulate the joint environment plus enable genetic manipulation, are more scalable and have reduced heterogeneity. As mentioned in this thesis, the biomimetic human OA models can be exploited for several applications. One of them is the development of biomarkers for what is “healthy physical activity” in elderly, as current guidelines are not based on empirical data, while “healthy physical activity” could be of great benefit for managing healthy joints in OA patients. Another example our model can be used for is to (further) clarify or confirm the direction of effect of other OA risk SNPs (**Table 1**).

With the increase of reliable models for OA it is important that the legislation on when human clinical trials are approved should be revisited. With the high number of clinical trials failing, we should reconsider giving less credit to results from *in vivo* (small) animal studies. With this thesis we show an alternative to animal models and demonstrate different applications of this biomimetic *ex vivo* human aged osteochondral model. Our research group has the benefit of access to end-stage osteoarthritic human joints coming from joint replacement surgeries in the Research in Articular Osteoarthritis Cartilage (RAAK) biobank [86]. However, when this is not possible, other human models such as iPSCs and joint-on-a-chip have further increased research possibilities in the OA field in recent years. Finally, an important side note for clinical application of many drugs is the need to further develop safe and effective methods for local intra-articular delivery in patients, thereby reducing the need for repeated injections and hopefully increasing drug retention and efficacy.

## REFERENCES

1. Armstrong CG, Mow VC. Variations in the intrinsic mechanical properties of human articular cartilage with age, degeneration, and water content. *J Bone Joint Surg Am.* 1982;64(1):88-94.
2. Vignon E, Arlot M, Patricot LM, et al. The cell density of human femoral head cartilage. *Clin Orthop Relat Res.* 1976(121):303-8.
3. Mitrovic D, Quintero M, Stankovic A, et al. Cell density of adult human femoral condylar articular cartilage. Joints with normal and fibrillated surfaces. *Lab Invest.* 1983;49(3):309-16.
4. Martin JA, Ellerbroek SM, Buckwalter JA. Age-related decline in chondrocyte response to insulin-like growth factor-I: the role of growth factor binding proteins. *J Orthop Res.* 1997;15(4):491-8.
5. Loeser RF, Shanker G, Carlson CS, et al. Reduction in the chondrocyte response to insulin-like growth factor 1 in aging and osteoarthritis: studies in a non-human primate model of naturally occurring disease. *Arthritis Rheum.* 2000;43(9):2110-20.
6. Loeser RF. Aging and osteoarthritis: the role of chondrocyte senescence and aging changes in the cartilage matrix. *Osteoarthritis Cartilage.* 2009;17(8):971-9.

7. Tuerlings M, van Hoolwerff M, Houtman E, et al. RNA Sequencing Reveals Interacting Key Determinants of Osteoarthritis Acting in Subchondral Bone and Articular Cartilage: Identification of IL11 and CHADL as Attractive Treatment Targets. *Arthritis Rheumatol.* 2021;73(5):789-99.
8. Byron CR, Trahan RA. Comparison of the Effects of Interleukin-1 on Equine Articular Cartilage Explants and Cocultures of Osteochondral and Synovial Explants. *Front Vet Sci.* 2017;4:152.
9. Bird JL, Wells T, Platt D, et al. IL-1 beta induces the degradation of equine articular cartilage by a mechanism that is not mediated by nitric oxide. *Biochem Biophys Res Commun.* 1997;238(1):81-5.
10. Clutterbuck AL, Mobasheri A, Shakibaei M, et al. Interleukin-1beta-induced extracellular matrix degradation and glycosaminoglycan release is inhibited by curcumin in an explant model of cartilage inflammation. *Ann NY Acad Sci.* 2009;1171:428-35.
11. Geurts J, Juric D, Muller M, et al. Novel Ex Vivo Human Osteochondral Explant Model of Knee and Spine Osteoarthritis Enables Assessment of Inflammatory and Drug Treatment Responses. *Int J Mol Sci.* 2018;19(5):1314.
12. Moldovan F, Pelletier JP, Jolicoeur FC, et al. Diacerein and rhein reduce the ICE-induced IL-1beta and IL-18 activation in human osteoarthritic cartilage. *Osteoarthritis Cartilage.* 2000;8(3):186-96.
13. Coutinho de Almeida R, Ramos YFM, Mahfouz A, et al. RNA sequencing data integration reveals an miRNA interactome of osteoarthritis cartilage. *Ann Rheum Dis.* 2019;78(2):270-7.
14. Ji Q, Zheng Y, Zhang G, et al. Single-cell RNA-seq analysis reveals the progression of human osteoarthritis. *Annals of the rheumatic diseases.* 2019;78(1):100-10.
15. Boer CG, Hatzikotoulas K, Southam L, et al. Deciphering osteoarthritis genetics across 826,690 individuals from 9 populations. *Cell.* 2021;184(18):4784-818 e17.
16. Caron JP, Fernandes JC, Martel-Pelletier J, et al. Chondroprotective effect of intraarticular injections of interleukin-1 receptor antagonist in experimental osteoarthritis. Suppression of collagenase-1 expression. *Arthritis Rheum.* 1996;39(9):1535-44.
17. Elsaid KA, Ubhe A, Shaman Z, et al. Intra-articular interleukin-1 receptor antagonist (IL1-ra) microspheres for posttraumatic osteoarthritis: in vitro biological activity and in vivo disease modifying effect. *J Exp Orthop.* 2016;3(1):18.
18. Clements KM, Price JS, Chambers MG, et al. Gene deletion of either interleukin-1beta, interleukin-1beta-converting enzyme, inducible nitric oxide synthase, or stromelysin 1 accelerates the development of knee osteoarthritis in mice after surgical transection of the medial collateral ligament and partial medial meniscectomy. *Arthritis Rheum.* 2003;48(12):3452-63.
19. Nasi S, Ea HK, So A, et al. Revisiting the Role of Interleukin-1 Pathway in Osteoarthritis: Interleukin-1alpha and -1beta, and NLRP3 Inflammasome Are Not Involved in the Pathological Features of the Murine Meniscectomy Model of Osteoarthritis. *Front Pharmacol.* 2017;8:282.
20. Kloppenburg M, Peterfy C, Haugen IK, et al. Phase IIa, placebo-controlled, randomised study of lutikizumab, an anti-interleukin-1alpha and anti-interleukin-1beta dual variable domain immunoglobulin, in patients with erosive hand osteoarthritis. *Ann Rheum Dis.* 2019;78(3):413-20.
21. Fleischmann RM, Bliddal H, Blanco FJ, et al. A Phase II Trial of Lutikizumab, an Anti-Interleukin-1alpha/beta Dual Variable Domain Immunoglobulin, in Knee Osteoarthritis Patients With Synovitis. *Arthritis Rheumatol.* 2019;71(7):1056-69.
22. Chevalier X, Goupille P, Beaulieu AD, et al. Intraarticular injection of anakinra in osteoarthritis of the knee: a multicenter, randomized, double-blind, placebo-controlled study. *Arthritis Rheum.* 2009;61(3):344-52.
23. Cohen SB, Proudman S, Kivitz AJ, et al. A randomized, double-blind study of AMG 108 (a fully human monoclonal antibody to IL-1R1) in patients with osteoarthritis of the knee. *Arthritis Res Ther.* 2011;13(4):R125.
24. Pfander D, Swoboda B, Kirsch T. Expression of early and late differentiation markers (proliferating cell nuclear antigen, syndecan-3, annexin VI, and alkaline phosphatase) by human osteoarthritic chondrocytes. *Am J Pathol.* 2001;159(5):1777-83.
25. von der Mark K, Kirsch T, Nerlich A, et al. Type X collagen synthesis in human osteoarthritic cartilage. Indication of chondrocyte hypertrophy. *Arthritis Rheum.* 1992;35(7):806-11.
26. Poole AR, Nelson F, Dahlberg L, et al. Proteolysis of the collagen fibril in osteoarthritis. *Biochem Soc Symp.* 2003(70):115-23.
27. Fuerst M, Bertrand J, Lammers L, et al. Calcification of articular cartilage in human osteoarthritis. *Arthritis Rheum.* 2009;60(9):2694-703.
28. Kuhn K, D'Lima DD, Hashimoto S, et al. Cell death in cartilage. *Osteoarthritis Cartilage.* 2004;12(1):1-16.

29. Whitney GA, Kean TJ, Fernandes RJ, et al. Thyroxine Increases Collagen Type II Expression and Accumulation in Scaffold-Free Tissue-Engineered Articular Cartilage. *Tissue Eng Part A*. 2018;24(5-6):369-81.
30. Glade MJ, Kanwar YS, Stern PH. Insulin and thyroid hormones stimulate matrix metabolism in primary cultures of articular chondrocytes from young rabbits independently and in combination. *Connect Tissue Res*. 1994;31(1):37-44.
31. Bohme K, Conscience-Egli M, Tschan T, et al. Induction of proliferation or hypertrophy of chondrocytes in serum-free culture: the role of insulin-like growth factor-I, insulin, or thyroxine. *J Cell Biol*. 1992;116(4):1035-42.
32. Burch WM, Lebovitz HE. Triiodothyronine stimulation of in vitro growth and maturation of embryonic chick cartilage. *Endocrinology*. 1982;111(2):462-8.
33. Ishikawa Y, Genge BR, Wuthier RE, et al. Thyroid hormone inhibits growth and stimulates terminal differentiation of epiphyseal growth plate chondrocytes. *J Bone Miner Res*. 1998;13(9):1398-411.
34. Chen-An P, Andreassen KV, Henriksen K, et al. The inhibitory effect of salmon calcitonin on tri-iodothyronine induction of early hypertrophy in articular cartilage. *PLoS One*. 2012;7(6):e40081.
35. Gereben B, Zavacki AM, Ribich S, et al. Cellular and molecular basis of deiodinase-regulated thyroid hormone signaling. *Endocr Rev*. 2008;29(7):898-938.
36. Mitchell PG, Magna HA, Reeves LM, et al. Cloning, expression, and type II collagenolytic activity of matrix metalloproteinase-13 from human osteoarthritic cartilage. *J Clin Invest*. 1996;97(3):761-8.
37. Shiomi T, Lemaitre V, D'Armiento J, et al. Matrix metalloproteinases, a disintegrin and metalloproteinases, and a disintegrin and metalloproteinases with thrombospondin motifs in non-neoplastic diseases. *Pathol Int*. 2010;60(7):477-96.
38. Little CB, Barai A, Burkhardt D, et al. Matrix metalloproteinase 13-deficient mice are resistant to osteoarthritic cartilage erosion but not chondrocyte hypertrophy or osteophyte development. *Arthritis Rheum*. 2009;60(12):3723-33.
39. Neuhold LA, Killar L, Zhao W, et al. Postnatal expression in hyaline cartilage of constitutively active human collagenase-3 (MMP-13) induces osteoarthritis in mice. *J Clin Invest*. 2001;107(1):35-44.
40. Felson DT, Zhang Y. An update on the epidemiology of knee and hip osteoarthritis with a view to prevention. *Arthritis Rheum*. 1998;41(8):1343-55.
41. Felson DT, Lawrence RC, Dieppe PA, et al. Osteoarthritis: new insights. Part 1: the disease and its risk factors. *Ann Intern Med*. 2000;133(8):635-46.
42. Peeters G, Edwards KL, Brown WJ, et al. Potential Effect Modifiers of the Association Between Physical Activity Patterns and Joint Symptoms in Middle-Aged Women. *Arthritis Care Res (Hoboken)*. 2018;70(7):1012-21.
43. Nissen N, Holm PM, Bricca A, et al. Clinicians' beliefs and attitudes to physical activity and exercise therapy as treatment for knee and/ or hip osteoarthritis: A scoping review. *Osteoarthritis Cartilage*. 2021.
44. Neogi T, Booth SL, Zhang YQ, et al. Low vitamin K status is associated with osteoarthritis in the hand and knee. *Arthritis Rheum*. 2006;54(4):1255-61.
45. Shea MK, Kritchevsky SB, Hsu FC, et al. The association between vitamin K status and knee osteoarthritis features in older adults: the Health, Aging and Body Composition Study. *Osteoarthritis Cartilage*. 2015;23(3):370-8.
46. Bonnet N, Gineys E, Ammann P, et al. Periostin deficiency increases bone damage and impairs injury response to fatigue loading in adult mice. *PLoS One*. 2013;8(10):e78347.
47. Zhang Y, Zhao L, Wang N, et al. Unexpected Role of Matrix Gla Protein in Osteoclasts: Inhibiting Osteoclast Differentiation and Bone Resorption. *Molecular and Cellular Biology*. 2019;39(12):e00012-19.
48. Boer CG, Szilagyi I, Nguyen NL, et al. Vitamin K antagonist anticoagulant usage is associated with increased incidence and progression of osteoarthritis. *Ann Rheum Dis*. 2021;80(5):598-604.
49. Ballal P, Peloquin C, Boer CG, et al. Warfarin use and risk of knee and hip replacements. *Ann Rheum Dis*. 2021;80(5):605-9.
50. Zhu J, Alexander GC, Nazarian S, et al. Trends and Variation in Oral Anticoagulant Choice in Patients with Atrial Fibrillation, 2010-2017. *Pharmacotherapy*. 2018;38(9):907-20.
51. Neogi T, Felson DT, Sarno R, et al. Vitamin K in hand osteoarthritis: results from a randomised clinical trial. *Ann Rheum Dis*. 2008;67(11):1570-3.
52. Horace RW, Roberts M, Lu B, et al. The association between vitamin K and medial tibial-femoral knee osteoarthritis progression: Data from the osteoarthritis initiative. *Osteoarthritis and Cartilage Open*. 2021;3(3):100172.

53. Wallin R, Schurgers LJ, Loeser RF. Biosynthesis of the vitamin K-dependent matrix Gla protein (MGP) in chondrocytes: a fetuin-MGP protein complex is assembled in vesicles shed from normal but not from osteoarthritic chondrocytes. *Osteoarthritis Cartilage*. 2010;18(8):1096-103.
54. Rafael MS, Cavaco S, Viegas CS, et al. Insights into the association of Gla-rich protein and osteoarthritis, novel splice variants and gamma-carboxylation status. *Mol Nutr Food Res*. 2014;58(8):1636-46.
55. Styrkarsdottir U, Lund SH, Thorleifsson G, et al. Meta-analysis of Icelandic and UK data sets identifies missense variants in SMO, IL11, COL11A1 and 13 more new loci associated with osteoarthritis. *Nat Genet*. 2018;50(12):1681-7.
56. The Genotype-Tissue Expression (GTEx) project. *Nat Genet*. 2013;45(6):580-5.
57. Tachmazidou I, Hatzikotoulas K, Southam L, et al. Identification of new therapeutic targets for osteoarthritis through genome-wide analyses of UK Biobank data. *Nat Genet*. 2019;51(2):230-6.
58. Sims NA, Jenkins BJ, Nakamura A, et al. Interleukin-11 receptor signaling is required for normal bone remodeling. *J Bone Miner Res*. 2005;20(7):1093-102.
59. Lokau J, Gottert S, Arnold P, et al. The SNP rs4252548 (R112H) which is associated with reduced human height compromises the stability of IL-11. *Biochim Biophys Acta Mol Cell Res*. 2018;1865(3):496-506.
60. Meulenbelt I, Min JL, Bos S, et al. Identification of DIO2 as a new susceptibility locus for symptomatic osteoarthritis. *Hum Mol Genet*. 2008;17(12):1867-75.
61. Bomer N, den Hollander W, Ramos YF, et al. Underlying molecular mechanisms of DIO2 susceptibility in symptomatic osteoarthritis. *Ann Rheum Dis*. 2015;74(8):1571-9.
62. Bomer N, Cornelis FM, Ramos YF, et al. The effect of forced exercise on knee joints in Dio2(-/-) mice: type II iodothyronine deiodinase-deficient mice are less prone to develop OA-like cartilage damage upon excessive mechanical stress. *Ann Rheum Dis*. 2016;75(3):571-7.
63. Pound P, Nicol CJ. Retrospective harm benefit analysis of pre-clinical animal research for six treatment interventions. *PLoS One*. 2018;13(3):e0193758.
64. Pound P, Ebrahim S, Sandercock P, et al. Where is the evidence that animal research benefits humans? *BMJ*. 2004;328(7438):514-7.
65. Horn J, de Haan RJ, Vermeulen M, et al. Nimodipine in animal model experiments of focal cerebral ischemia: a systematic review. *Stroke*. 2001;32(10):2433-8.
66. Clement-Lacroix P, Little CB, Smith MM, et al. Pharmacological characterization of GLPG1972/S201086, a potent and selective small-molecule inhibitor of ADAMTS5. *Osteoarthritis Cartilage*. 2021.
67. ClinicalTrials.gov. <https://clinicaltrials.gov/ct2/show/NCT03595618>. Visited 2022.
68. Leenaars CHC, Kouwenaar C, Stafleu FR, et al. Animal to human translation: a systematic scoping review of reported concordance rates. *J Transl Med*. 2019;17(1):223.
69. Cook D, Brown D, Alexander R, et al. Lessons learned from the fate of AstraZeneca's drug pipeline: a five-dimensional framework. *Nat Rev Drug Discov*. 2014;13(6):419-31.
70. Harrison RK. Phase II and phase III failures: 2013-2015. *Nat Rev Drug Discov*. 2016;15(12):817-8.
71. Hwang TJ, Carpenter D, Lauffenburger JC, et al. Failure of Investigational Drugs in Late-Stage Clinical Development and Publication of Trial Results. *JAMA Intern Med*. 2016;176(12):1826-33.
72. Leenaars C, Stafleu F, de Jong D, et al. A Systematic Review Comparing Experimental Design of Animal and Human Methotrexate Efficacy Studies for Rheumatoid Arthritis: Lessons for the Translational Value of Animal Studies. *Animals (Basel)*. 2020;10(6).
73. Passini E, Britton OJ, Lu HR, et al. Human In Silico Drug Trials Demonstrate Higher Accuracy than Animal Models in Predicting Clinical Pro-Arrhythmic Cardiotoxicity. *Front Physiol*. 2017;8:668.
74. Nelson MR, Tipney H, Painter JL, et al. The support of human genetic evidence for approved drug indications. *Nat Genet*. 2015;47(8):856-60.
75. King EA, Davis JW, Degner JF. Are drug targets with genetic support twice as likely to be approved? Revised estimates of the impact of genetic support for drug mechanisms on the probability of drug approval. *PLoS Genet*. 2019;15(12):e1008489.
76. Arden NK, Cro S, Sheard S, et al. The effect of vitamin D supplementation on knee osteoarthritis, the VIDEO study: a randomised controlled trial. *Osteoarthritis Cartilage*. 2016;24(11):1858-66.

77. McAlindon T, LaValley M, Schneider E, et al. Effect of vitamin D supplementation on progression of knee pain and cartilage volume loss in patients with symptomatic osteoarthritis: a randomized controlled trial. *JAMA*. 2013;309(2):155-62.
78. Sanghi D, Mishra A, Sharma AC, et al. Does vitamin D improve osteoarthritis of the knee: a randomized controlled pilot trial. *Clin Orthop Relat Res*. 2013;471(11):3556-62.
79. Jin X, Jones G, Cicuttini F, et al. Effect of Vitamin D Supplementation on Tibial Cartilage Volume and Knee Pain Among Patients With Symptomatic Knee Osteoarthritis: A Randomized Clinical Trial. *JAMA*. 2016;315(10):1005-13.
80. Zheng S, Jin X, Cicuttini F, et al. Maintaining Vitamin D Sufficiency Is Associated with Improved Structural and Symptomatic Outcomes in Knee Osteoarthritis. *Am J Med*. 2017;130(10):1211-8.
81. Song Y, Xu K, Yu C, et al. The use of mechano growth factor to prevent cartilage degeneration in knee osteoarthritis. *J Tissue Eng Regen Med*. 2018;12(3):738-49.
82. Zhang L, Smith DW, Gardiner BS, et al. Modeling the Insulin-Like Growth Factor System in Articular Cartilage. *PLoS One*. 2013;8(6):e66870.
83. Song JL, Li L, Fang H, et al. Intraperitoneal injection of thalidomide alleviates early osteoarthritis development by suppressing vascular endothelial growth factor expression in mice. *Mol Med Rep*. 2018;18(1):571-9.
84. Freedman ML, Monteiro AN, Gayther SA, et al. Principles for the post-GWAS functional characterization of cancer risk loci. *Nat Genet*. 2011;43(6):513-8.
85. den Hollander W, Pulyakhina I, Boer C, et al. Annotating Transcriptional Effects of Genetic Variants in Disease-Relevant Tissue: Transcriptome-Wide Allelic Imbalance in Osteoarthritic Cartilage. *Arthritis Rheumatol*. 2019;71(4):561-70.
86. Ramos YF, den Hollander W, Bovee JV, et al. Genes involved in the osteoarthritis process identified through genome wide expression analysis in articular cartilage; the RAAK study. *PLoS One*. 2014;9(7):e103056.





# Appendix

**Nederlandse samenvatting**

**Curriculum Vitae**

**List of publications**

**Dankwoord**

## Nederlandse samenvatting

### *Inleiding*

Osteoartrose, beter bekend als artrose, is de meest voorkomende gewrichtsaandoening met ruim 1.5 miljoen gevallen in Nederland. De verwachting is echter dat het aantal patiënten met artrose de komende jaren sterk zal toenemen door de steeds ouder wordende populatie en toename in mensen met overgewicht. Artrose wordt gekenmerkt door pijn en stijfheid van de gewrichten en leidt tot verminderde mobiliteit. Deze symptomen ontstaan doordat er bij artrose afbraak is van de kraakbeenlaag, dat bij gezonde gewrichten voorkomt dat bot over bot gaat schuren. Ook ontstaan er vaak botuitstulpingen aan de randen van de gewrichten (osteofieten). Artrose kan ontstaan in bijna alle gewrichten, maar komt voornamelijk voor in de handen, heupen en knieën. Bij het ontstaan van artrose spelen zowel de erfelijke genetische factoren als omgevingsfactoren een rol. De meest invloedrijke omgevingsfactoren zijn overbelasting, leeftijd en geslacht. In de afgelopen jaren is er veel onderzoek gedaan in grote patiëntengroepen naar de invloed van genetische factoren op het risico om artrose te krijgen. Om vanuit deze veranderingen in de genetica tot een mogelijk aangrijpingspunt voor medicijnen te komen is het essentieel om eerst in het laboratorium op ziekterelevante weefsels experimenten uit te voeren. Ondanks het feit dat er duidelijke artrose risico genen zijn geïdentificeerd, blijft het vervolgonderzoek achterlopen. Een van de redenen daarvoor is dat er geen goede in vitro modellen zijn die het artrose proces in verouderd menselijk weefsel na kunnen bootsen.

### *Doel van dit proefschrift*

Om het onderzoek verder te brengen is een goed menselijk model nodig. In zo'n model moet bijvoorbeeld rekening gehouden worden dat artrose niet een ziekte is van maar één weefsel, maar eerder van het hele gewricht. Daarnaast is het van belang dat medicijnen worden getest op verouderd weefsel omdat uit veel onderzoek naar voren komt dat oudere kraakbeencellen anders/minder reageren op externe stimulatie. Daarom is het van belang voor de patiënt dat medicijnen en/of medische interventies ook getest worden in een model dat zoveel als mogelijk het menselijk verouderde gewricht representeert. Zo'n model kan dienen om de translatie van artrose risico genen naar ontdekking en het testen van nieuwe aangrijpingspunten voor medicijnen te bevorderen.

### *Het opzetten en onderzoeken van een verouderd humaan kraakbeen-bot model*

Artrose wordt veroorzaakt doordat verouderd kraakbeen en zijn cellen niet in staat zijn om goed te reageren op ontstane schade na bv. een overbelasting. In dit proces spelen ook genetische factoren een rol in de capaciteit om te reageren op zulke belastende factoren. Daarnaast is het artrose proces gelinkt aan een verhoogde metabole activiteit van de kraakbeencellen, wat overeenkomt met groeiplaat-kraakbeencellen die endochondrale verbening ondergaan (het proces waarbij bot wordt aangemaakt vanuit de groeiplaat). Tijdens dit proces gaan de kraakbeencellen vermeerderen (delen), worden groter in volume (hypertrofie) en verhogen productie van specifieke markers zoals *ALPL*, *COL10A1* en *MMP13*. Om de tekortkomingen van de vertaling van preklinische diermodellen naar de mens en tegelijkertijd de noodzaak

voor dierproeven te verminderen, zijn er menselijke modellen nodig die de verschillende aspecten van artrose omvatten. Op het moment bestaan de modellen waarop behandelingen worden gebaseerd bijna allemaal uit overbelaste (jonge) diermodellen of uit onderzoek in 2D of 3D cel modellen waarin nieuw kraakbeen wordt aangemaakt door kraakbeencellen of stamcellen. Echter, veel van deze modellen missen de interactie tussen bot en kraakbeen en/of representeren niet het verouderde gewrichtsweefsel dat gevoeliger is voor schade en moeilijker herstelt. Voor zowel het onderzoeken van ziektemechanismes als het testen van medicijnen is het belangrijk om dit in een model te doen die zo dicht mogelijk bij de natuurlijke situatie blijft.

In **hoofdstuk 2** hebben we ervoor gekozen om de response van de kraakbeencel te onderzoeken in verouderde menselijke biopten bestaand uit kraakbeen met daaronder een stukje bot. Het voordeel van dit model is dat de cel in zijn eigen omgeving blijft en de modellen redelijk simpel en makkelijk zijn op te zetten. Vervolgens is onderzocht wat de gevolgen op kraakbeen zijn van drie belastende factoren waarvan bekend is dat ze betrokken zijn bij het artrose proces, zijnde een ontsteking (door middel van IL-1 $\beta$ ), hypertrofie (door middel van schildklierhormoon(T3)) en overbelasting (65% indentatie kraakbeen). Vervolgens is er gekeken naar kraakbeencel signalering (gen expressie), kraakbeenstructuur en -afbraak, en mechanische eigenschappen van kraakbeen. Hierin vonden we dat alle drie de belastende factoren afbraaksignalen stimuleren in verschillende mate. Naast deze overlap waren er ook specifieke reacties per verstoring te onderscheiden. Zo induceerde de ontstekingsfactor een verlaging van kraakbeen aanmaak genen en werd afbraak van kraakbeen matrix gemeten. In tegenstelling, bij de hypertrofie factor werd met name een verhoogde gen expressie van verbenings geassocieerde eiwitten (*ALPL*, *COL10A1*, *COL1A1*) gemeten. Overbelasting gaf een lagere expressie van kraakbeen aanmaak genen en verlaagde de mechanische eigenschappen van het kraakbeen aanzienlijk. In dit hoofdstuk hebben we laten zien dat het mogelijk is om met artrose relevante belastende factoren in verschillende mate afbraak van kraakbeen te induceren. De kracht van ons model is dat het uitgevoerd is in verouderde, macroscopisch normale, menselijke biopten uit een heterogene artrose patiëntenpopulatie. Ondanks deze heterogene populatie laten we zien dat de uitkomsten per verstoring robuust zijn. Onze studie laat zien dat het mogelijk is persoonlijke menselijke artrose modellen op te zetten die de verschillende relevante aspecten van het ziekteproces omvatten. Daarnaast kunnen de opeenvolgende effecten van de verschillende belastende factoren gebruikt worden in de ontwikkeling van nieuwe specifieke behandelingen die de verschillende aspecten van artrose omvatten.

### ***Gevolgen van mechanische belasting op de kraakbeencel gezondheid***

Om te weten te komen welke specifieke processen in verouderd menselijk kraakbeen een rol spelen in de afbraak na overbelasting, is in **hoofdstuk 3** een genomwijde genexpressie analyse uitgevoerd. Dit wil zeggen dat de hoeveelheid van alle genen van een monster zijn gemeten en vergeleken tussen mechanische overbelaste en niet-overbelaste samples om te onderzoeken welke genen veranderen na een overbelasting. Hierin vonden we dat 156 genen een afwijkend expressiepatroon hebben na overbelasting. Tussen deze genen kwam een aantal kraakbeen afbraak en bekende artrose geassocieerde genen naar voren (zoals *MMP13*, *TNC*, *WISP2*, *FRZB* etc). Om een beeld te krijgen van wat de functie van deze genen in kraakbeen is, is gekeken naar de overlap in functies van deze genen. Hieruit kwamen de volgende processen

naar voren: insuline-achtige groeifactor bindende eiwitten (IGF-1 productie reguleren; *IGFBP6*, *IGFBP5*, en *IGFBP4*), focale adhesie (betrokken bij overdracht van mechanische krachten; *ITGA10*, *TLN2*, and *CAV1*) en cellulaire senescentie (eiwitten betrokken bij stop van cel deling; *GADD45A*, *MYC*, *SERPINE1*, en *FOXO1*). Van senescentie is al langer bekend dat het proces een rol speelt in veel aandoeningen zoals artrose doordat de cellen als het ware op non-actief staan als gevolg van stress en niet meer reageren op stimulering terwijl ze wel factoren uitscheiden die ongunstig zijn voor de omgeving. Met ons onderzoek hebben wij kennis toegevoegd aan de reactie van kraakbeencellen op een overbelasting. Uit ons onderzoek komen een aantal aanknopingspunten die in de toekomst gebruikt kunnen worden om de onomkeerbare schade na een overbelasting tegen te gaan. Daarnaast laten we zien dat de identificatie van overbelastings-specifieke genen, zoals *MMP13*, kunnen functioneren als een sensitieve marker om zo preventieve bewegingstherapieën op te zetten.

### ***Matrix Gla eiwit (MGP) en risico van lage vitamine K***

Zoals eerder genoemd spelen erfelijke factoren een grote rol bij het ontstaan van artrose. Een belangrijk risicogen is het Matrix Gla Eiwit (*MGP*) waarbij het risico variant (rs1800801) voor een lagere gen expressie zorgt in meerdere gewrichtsweefsels, waaronder kraakbeen en bot. *MGP* is een eiwit dat extracellulaire calcium hoeveelheden reguleert door aan ze te binden en zo calcificatie van weefsel voorkomt. Belangrijk is echter dat het eiwit voor zijn functionaliteit afhankelijk is van vitamine K. Bij een verlaging van *MGP* eiwitten is er meer calcificatie van kraakbeen en is er een lagere botdichtheid. Daarnaast zijn te lage vitamine K levels al eerder geassocieerd met het krijgen van artrose.

In **hoofdstuk 4** is in een grotere dataset aangetoond dat het artrose risico variant rs1800801-T associeert met een lagere expressie van *MGP* in zowel kraakbeen als bot. Daarnaast was er een hogere expressie van *MGP* in aangedaan artrose kraakbeen en bot in vergelijking met niet-aangedaan kraakbeen en bot. Deze verhoging van *MGP* komt vooral doordat de expressie meer verhoogd wordt in mensen met het risico variant, maar het expressie level blijft alsnog lager dan die van mensen zonder dit risico variant. Dit suggereert dat mogelijk in reactie op het artrose proces, de kraakbeencellen proberen om calcificatie tegen te gaan en hun productie van *MGP* verhogen. Daarnaast is ook gekeken naar de dynamische verandering van *MGP* expressie tussen dragers en niet-dragers waarna verschillende artrose relevante stimuli gegeven worden. Hier werd gezien dat de expressie van *MGP* omlaag gaat als gevolg van deze stimulatie maar dat dragers van het risico variant nauwelijks reageren. Ten slotte is er nog onderzocht wat de gevolgen zijn voor de 'gezondheid' van kraakbeen- en botcellen na toediening van Warfarine, een veel gebruikt vitamine K verlagend medicijn bij mensen met een verhoogd risico op bloedstolsel. Warfarine zorgde voor een ongunstig signaleringsprofiel richting hypertrofie en calcificatie in kraakbeen en verminderde botformatie in onderliggend bot. Ons onderzoek laat zien dat het rs1800801-T variant het risico op artrose verhoogd doordat het de expressie van *MGP* verlaagd. Hierdoor kan in mensen met dit variant het *MGP* eiwit niet zo efficiënt verhoogd worden wanneer dit nodig is om calcificatie tegen te gaan. Daarnaast zijn er risico's verbonden aan het slikken van vitamine K verminderde medicijnen die vooral in mensen met het rs1800801-T variant voor een nog grotere kans op artrose kunnen zorgen.

## ***Verlaging van schildklierhormoon als mogelijke behandeling in artrose***

De kraakbeencel verliest tijdens het artrose proces zijn volwassen status en zet processen aan die normaal vooral bij botgroei vanuit de groeiplaat gezien worden. Meerdere genen betrokken bij groeiplaat verbening zijn geïdentificeerd als artrose risico genen, zoals bijvoorbeeld DIO2. Het DIO2 gen codeert voor het enzym dat verantwoordelijk is voor de intracellulaire omzetting van inactief (T4) naar actief schildklierhormoon tri-joodthyronine (T3). Van T3 was al bekend dat deze een hele belangrijke rol speelt bij de botgroei vanuit de groeiplaat. In een eerder menselijk 3D model waar kraakbeen wordt gemaakt is aangetoond dat teveel T3 niet goed is voor kraakbeen en dat het verlagen van DIO2 eiwit activiteit juist wel goed is voor kraakbeen. Echter, dit werd onderzocht in een 3D in vitro model van nieuw aangemaakt kraakbeen.

In **hoofdstuk 5** kijken we daarom in verouderd humaan kraakbeen of behandeling met iopanoic acid (IOP), een remmer van DIO2 activiteit, de schade van overbelasting verminderd. Voor toekomstige toepassingen is in dit onderzoek ook gekeken of langzame afgifte van IOP uit zogenaamde nanoparticles, een soort eiwit-kooi wat de IOP beschermt van de omgeving, net zo effectief is. In dit onderzoek zagen we dat IOP in staat was om de kraakbeencel te beschermen van de ‘ongezonde’ gen expressie dat aangezet wordt door overbelasting en dat langzame afgifte van IOP minder efficiënt was. Daarnaast werd ook gemeten dat verlagen van schildklierhormoon de schade aan kraakbeenweefsel geïnduceerd door mechanische belasting verminderde. Om uit te zoeken via welk mechanisme IOP de kraakbeencel beschermt is er een genomwijde genexpressie analyse gedaan op de kraakbeencel. Hieruit kwam naar voren dat een aantal genen betrokken bij metabole processen (INSIG1, DHCR7, FADS1 en ACAT2) en celdeling en cel differentiatie (CTGF, BMP5 en FOXM1) belangrijk zijn voor bescherming door IOP.

## ***Conclusie en toekomstige toepassingen***

In ons onderzoek is een verouderd menselijk model opgezet dat voor vele toepassingen gebruikt kan worden. Dit model is nuttig voor zowel kennisvergaring als voor medicijn onderzoek. Daarnaast kan onze data nu al dienen als een referentie om 3D modellen van het gewricht te avanceren naar een gewricht-op-een-chip. Ook geeft ons model de mogelijkheid voor diepere moleculaire exploratie van verstoord versus niet-verstoord weefsel door bijvoorbeeld RNA-sequencing op celniveau wat weer kan leiden tot identificatie van targets voor medicijnen en/of behandelingen. Ten slotte kunnen de verschillende versturende stimuli en hun variatie in effect helpen bij het opzetten van nieuwe persoonlijke behandelingen die meer gebruik maken van de verschillende subtypes van artrose. Door gebruik te maken van een zoals hier gepresenteerd verouderd menselijk biopt model kan het artroseveld en de farmacie nieuwe zo hoog nodige effectieve medicijnen voor artrose identificeren. Als bewijs van dit principe is in het biopt model onderzocht of verlaging van schildklierhormoon, d.m.v. IOP, de versturende effecten van overbelasting kan tegengaan. Hier werd geobserveerd dat het verlagen van de metabole activiteit van kraakbeencellen een gunstig effect heeft op de ‘gezonde’ gen expressie en kraakbeenafbraak inderdaad deels tegengaat.

Onze studies tonen aan dat er nog veel onbekend is over de moleculaire processen betrokken bij overbelasting in kraakbeen en bot, maar dat hier zeker nog veel kansen voor onderzoek liggen en dat hierbij rekening moet worden gehouden met leeftijd van het weefsel. Hier ligt de

kans om wetenschappelijk gegronde bewegingsbehandelingen te genereren door markers te onderzoeken na overbelasting in bipten van verschillende leeftijdsgroepen. Het mooiste zou zijn als deze markers gekoppeld kunnen worden aan markers die in het bloed of urine gemeten kunnen worden (biomarkers) omdat dit minder invasief en makkelijker af te nemen is.

Ten slotte komt uit onze studies naar voren dat er voorzichtigheid geboden moet zijn bij het gebruik van vitamine K verlagende bloedverdunners, zoals warfarine en coumarines, en dat er overwogen moet worden of er in veel gevallen overgestapt kan worden naar direct werkende orale antistollingsmiddelen (DOAC's). Deze verandering in behandeling is zeker belangrijk voor mensen die dragers zijn van het risico variant in MGP, waardoor ze van zichzelf al minder MGP eiwitten hebben en meer risico op o.a. aderverkalking en artrose. Door een tekort aan vitamine K zal er nog minder functioneel MGP eiwit zijn en meer verkalking van aderen en kraakbeen plaatsvinden. Daarnaast geeft dit onderzoek ook aan dat toedienen van vitamine K bij een subgroep van mensen die weinig vitamine K hebben een mogelijke behandeling kan zijn om artrose tegen te gaan. Dit moet echter nog verder onderzocht worden.



## Curriculum Vitae

Evelyn Houtman was born on the 18th of May 1991 in New Plymouth, New Zealand. She graduated from secondary school in 2009 at the Oranje Nassau College in Zoetermeer. In the same year she started the bachelor Biomedical Sciences at the University of Leiden, the Netherlands. During her bachelor she performed an internship at the Department of Clinical Genetics in the Leids Universitair Medisch Centrum (LUMC) under supervision of Dr. M.Losekoot and Dr. N. van der Stoep. During this internship she learned about analysis of whole exome sequencing (WES) data of families with dysplasia and the further development of a High resolution melting curve (HRMCA) single nucleotide polymorphism (SNP) tests for whole exome sequencing sample identification.

After graduating in 2013 she continued her education by starting the Master Biomedical Sciences with the specialization Research at the University of Leiden, the Netherlands. During her Master her first internship was at the department of Endocrinology under supervision of Prof.Dr. P.C.N. Rensen and Dr. S. Kooijman. Here she investigated the effects of inhibition of inflammation in the brain on the function of brown adipose tissue. For her second internship she performed research at the department of Molecular epidemiology under supervision of Prof.Dr. I. Meulenbelt and Dr. Y.F.M. Ramos. This research project involved the identification of the underlying mechanism of osteoarthritis (OA) in the GARP study using exome sequencing data. The mutations that were identified were further explored in functional studies using microtissue models of chondrogenesis. During her studies, Evelyn was in the Year representative Biomedical Sciences Master committee from 2014 till 2015. After obtaining her Master degree in Biomedical Sciences in 2015, she started applying for PhD positions. While applying for positions, Evelyn worked as a student assistant at ZonMw, department science and innovation in The Hague to find field specialists to review grant applications.

In May 2016 she was given the opportunity to start her PhD at the department of Biomedical Data Sciences, section of Molecular epidemiology under supervision of Prof.Dr. I. Meulenbelt and Dr. Y.F.M. Ramos. During the PhD project focus was on developing an aged human model to mimic different onset triggers of osteoarthritis. In addition, these models were used for genetic risk studies, genome-wide transcriptional (RNA-seq) studies and as a proof of concept inhibition of thyroid signalling was investigated as treatment. In 2019, she was a visiting PhD student at the Skeletal Biology and Engineering Research Center at the KU Leuven in Belgium. Here she performed research under supervision of Prof.Dr. R.J. Lories and Dr. F.M. Cornelis, during a period of 3 Months. The results of the research perform during the projects are described in this thesis.

In 2022, Evelyn started as a Post-doctoral researcher in the group of Prof.dr. I. Meulenbelt to optimize expansion and differentiation of human induced pluripotent derived chondroprogenitors (hiCPCs) towards cartilage using small scale bioreactors.



## List of publications

Tuerlings M, Janssen GMC, Boone I, van Hoolwerff M, Rodriguez Ruiz A, **Houtman E**, Suchiman E, van der Wal R, Nelissen RGHH, Coutinho de Almeida R, van Veelen P, Ramos YFM, Meulenbelt I. WWP2 osteoarthritis risk allele rs1052429-A confers risk by affecting cartilage matrix deposition via hypoxia associated genes. *bioRxiv* 2022.03.31.486523; doi: <https://doi.org/10.1101/2022.03.31.486523>

**Houtman E**, Tuerlings M., Suchiman HED, Lakenberg N., Cornelis FMF, Mei H, Broekhuis D, Nelissen RGHH, Coutinho de Almeida R, Ramos YFM, Lories RJ, Cruz LJ, Meulenbelt I. Inhibiting Thyroid Activation In Aged Human Explants Prevents Mechanical Induced Detrimental Signalling By Mitigating Metabolic Processes. *Rheumatology (Oxford)*. 2022 Apr 5;keac202. doi: 10.1093/rheumatology/keac202

van Vliet NA, Bos MM, Thesing CS, Chaker L, Pietzner M, **Houtman E**, Neville MJ, Li-Gao R, Trompet S, Mustafa R, Ahmadizar F, Beekman M, Bot M, Budde K, Christodoulides C, Dehghan A, Delles C, Elliott P, Evangelou M, Gao H, Ghanbari M, van Herwaarden AE, Ikram MA, Jaeger M, Jukema JW, Karaman I, Karpe F, Kloppenburg M, Meessen JM, Meulenbelt I, Milaneschi Y, Mooijaart SP, Mook-Kanamori DO, Netea MG, Netea-Maier RT, Peeters RP, Penninx BWJH, Sattar N, Slagboom PE, Suchiman HED, Völzke H, Willems van Dijk K, Noordam R, van Heemst D; BBMRI Metabolomics Consortium. Higher thyrotropin leads to unfavorable lipid profile and somewhat higher cardiovascular disease risk: evidence from multi-cohort Mendelian randomization and metabolomic profiling. *BMC Med*. 2021 Nov 3;19(1):266. doi: 10.1186/s12916-021-02130-1. PMID: 34727949; PMCID: PMC8565073.

**Houtman E**, Tuerlings M, Riechelmann J, Suchiman EHED, van der Wal RJP, Nelissen RGHH, Mei H, Ramos YFM, Coutinho de Almeida R, Meulenbelt I. Elucidating mechanopathology of osteoarthritis: transcriptome-wide differences in mechanically stressed aged human cartilage explants. *Arthritis Res Ther*. 2021 Aug 16;23(1):215. doi: 10.1186/s13075-021-02595-8. PMID: 34399844; PMCID: PMC8365911.

**Houtman E**, Coutinho de Almeida R, Tuerlings M, Suchiman HED, Broekhuis D, Nelissen RGHH, Ramos YFM, van Meurs JBJ, Meulenbelt I. Characterization of dynamic changes in Matrix Gla Protein (MGP) gene expression as function of genetic risk alleles, osteoarthritis relevant stimuli, and the vitamin K inhibitor warfarin. *Osteoarthritis Cartilage*. 2021 Aug;29(8):1193-1202. doi: 10.1016/j.joca.2021.05.001. Epub 2021 May 10. PMID: 33984465.

**Houtman E**, van Hoolwerff M, Lakenberg N, Suchiman EHD, van der Linden-van der Zwaag E, Nelissen RGHH, Ramos YFM, Meulenbelt I. Human Osteochondral Explants: Reliable Biomimetic Models to Investigate Disease Mechanisms and Develop Personalized Treatments for Osteoarthritis. *Rheumatol Ther*. 2021 Mar;8(1):499-515. doi: 10.1007/s40744-021-00287-y. Epub 2021 Feb 20. PMID: 33608843; PMCID: PMC7991015.

Tuerlings M, van Hoolwerff M, **Houtman E**, Suchiman EHED, Lakenberg N, Mei H, van der Linden EHMJ, Nelissen RRGHH, Ramos YYFM, Coutinho de Almeida R, Meulenbelt I. RNA Sequencing Reveals Interacting Key Determinants of Osteoarthritis Acting in Subchondral Bone and Articular Cartilage: Identification of IL11 and CHADL as Attractive Treatment Targets. *Arthritis Rheumatol*. 2021 May;73(5):789-799. doi: 10.1002/art.41600. Epub 2021 Mar 21. PMID: 33258547; PMCID: PMC8252798.

Coutinho de Almeida R, Mahfouz A, Mei H, **Houtman E**, den Hollander W, Soul J, Suchiman E, Lakenberg N, Meessen J, Huetink K, Nelissen RGHH, Ramos YFM, Reinders M, Meulenbelt I. Identification and characterization of two consistent osteoarthritis subtypes by transcriptome and clinical data integration. *Rheumatology (Oxford)*. 2021 Mar 2;60(3):1166-1175. doi: 10.1093/rheumatology/keaa391. PMID: 32885253; PMCID: PMC7937023.

Coutinho de Almeida R, Ramos YFM, Mahfouz A, den Hollander W, Lakenberg N, **Houtman E**, van Hoolwerff M, Suchiman HED, Rodríguez Ruiz A, Slagboom PE, Mei H, Kielbasa SM, Nelissen RGHH, Reinders M, Meulenbelt I. RNA sequencing data integration reveals an miRNA interactome of osteoarthritis cartilage. *Ann Rheum Dis*. 2019 Feb;78(2):270-277. doi: 10.1136/annrheumdis-2018-213882. Epub 2018 Dec 1. PMID: 30504444; PMCID: PMC6352405.

Bomer N, den Hollander W, Suchiman H, **Houtman E**, Sliker RC, Heijmans BT, Slagboom PE, Nelissen RG, Ramos YF, Meulenbelt I. Neo-cartilage engineered from primary chondrocytes is epigenetically similar to autologous cartilage, in contrast to using mesenchymal stem cells. *Osteoarthritis Cartilage*. 2016 Aug;24(8):1423-30. doi: 10.1016/j.joca.2016.03.009. Epub 2016 Mar 17. PMID: 26995110.

## Dankwoord

Zo, aan dit promotietraject is na jaren zwoegen een eind gekomen. Dit had ik nooit in mijn eentje kunnen doen en daarom wil ik via dit deel iedereen bedanken die betrokken is geweest en heeft bijgedragen aan het tot stand komen van dit proefschrift.

Professor Meulenbelt, beste Ingrid, bedankt voor het geven van deze kans om mijn promotieonderzoek in de artrose groep te doen. Dankzij jouw geduld, steun en adviezen in onze vele meetings heb ik heel veel geleerd en is het gelukt om het onderzoek in de vorm van manuscripten te krijgen.

Professor Nelissen, beste Rob, bedankt voor jouw adviezen en je zeer belangrijke rol in het opzetten en coördineren van de RAAK. Zonder deze waardevolle studie was dit proefschrift niet tot stand gekomen.

Dr Ramos, beste Yolande, bedankt ook aan jou dat je mij deze kans hebt gegeven. Dankzij jouw begeleiding in het lab, experimentele adviezen en geruststellende woorden, kwam ik weer stapjes verder.

Geachte leden van mijn promotiecommissie: Professor Lories, Professor van Meurs en Professor Kloppenburg. Bedankt dat jullie de gelegenheid hebben genomen om het proefschrift te beoordelen. Geachte Professor Slagboom, beste Eline, bedankt dat je als secretaris in mijn commissie deel wilt nemen en als sectiehoofd zo betrokken bent bij al het werk wat op de afdeling gedaan wordt.

Mijn dank gaat ook uit naar mijn collega's die bijgedragen hebben aan dit proefschrift. Bedankt Eka en Nico voor alle hulp bij het verzamelen van explants en de vele maal sessies. Margo and Rodrigo, thank you for the help with all the RNA-sequencing analysis, I could not have done this without your help. Thank you Alejandro, for all our conversations in and out of the lab, you made the time pass a lot faster. Thanks for being my 'paranimf'. Bedankt Nils voor al het belangrijke (voor)werk dat jij gedaan hebt voor de DIO2 project aanvraag. Mijn dank gaat ook uit naar alle (ex-) collega's van de OA groep, Eka, Ghazaleh, Ilja, Marcella, Mathew, Niek, Noline, Nico, Ritchie, Rick en Wouter, bedankt voor alle discussies over mijn werk tijdens en buiten de meetings om. Mijn dank gaat ook uit naar stagairs, jullie hebben mij nog een hoop op het begeleidende vak geleerd: Elwin, Janne en Lynn.

Beste (ex-)collega's van de MolEpi, bedankt voor alle lunch, lab en borrel gesprekken. Over de jaren heen heb ik veel van jullie kunnen leren en veel met jullie kunnen lachen. Daarnaast is er voor een heleboel andere zaken iemand hard nodig die secretariële zaken in goede banen leidt: bedankt Inge.

Ook wil ik iedereen betrokken bij de RAAK van de orthopedie bedanken: Anika en collega's bedankt voor de logistieke regeling en het klaarzetten van de potjes. Dankzij jullie inzet over de jaren heen is dit proefschrift tot stand gekomen.

Professor Lories en Dr Cornelis, beste Rik en Frederique, bedankt dat ik zo welkom was om bij jullie een tijdje te werken. Ik heb veel nieuwe technieken van jullie en de afdeling mogen leren. Verder wil ik graag de volgende mensen bedanken voor hun waardevolle suggesties in meetings en op manuscripten: Luis, Enrike, Demiën, Robert, Leon, Joyce en Cindy.

Dianne, wat was het fijn om na onze studie samen met jou door deze fase heen te gaan. Na een koffie of lunch pauze samen was ik weer wat opgeladen. En wat ben ik blij dat je als paranimf naast me wilt staan.

Elsbeth, Miriam, Rianne en Wida, dank voor al onze spelletjes avondjes en vakanties. Katja, bedankt voor dat je altijd zo relaxed en vrolijk bent en me weer even een oppepper geeft als we afgesproken hebben. Jennifer, dank voor de spelletjes, film en praat avondjes over de jaren heen. Ik waardeer jullie vriendschappen echt enorm.

Lieve familie, Pap, Mam, Maaik, Martijn, Emma en Fenne, bedankt voor jullie interesse in wat ik zoal uitspook op werk en het 'accepteren' dat ik weer eens te laat was omdat ik nog even wat af moest maken. Bedankt ook voor de steun en dat ik altijd even langs kan komen en me laten inzien dat het allemaal niet zo erg is. Lieve schoonfamilie, An, Maart, Rich en Nadine, ook jullie bedankt voor de interesse in mijn onderzoek over de jaren heen en het (proberen) te begrijpen wat het betekent. Lieve Robbert, bedankt voor jouw steun, liefde en jouw 'down to earth' mentaliteit. Zonder jouw duwtjes was ik nooit zo ver gekomen.